

## =University of Southampton Research Repository

Copyright © and Moral Rights for this thesis and, where applicable, any accompanying data are retained by the author and/or other copyright owners. A copy can be downloaded for personal non-commercial research or study, without prior permission or charge. This thesis and the accompanying data cannot be reproduced or quoted extensively from without first obtaining permission in writing from the copyright holder/s. The content of the thesis and accompanying research data (where applicable) must not be changed in any way or sold commercially in any format or medium without the formal permission of the copyright holder/s.

When referring to this thesis and any accompanying data, full bibliographic details must be given, e.g.

Thesis: Author (Year of Submission) "Full thesis title", University of Southampton, name of the University Faculty or School or Department, PhD Thesis, pagination.

Data: Author (Year) Title. URI [dataset]



# **University of Southampton**

Faculty of Medicine

Human Development and Health

## **Subcutaneous Implantable Cardiac Defibrillator - A Personalised Approach**

by

**Dr Mohamed ElRefai MBBCh, MRCP**

PhD Thesis

13<sup>th</sup> of January 2023



# University of Southampton

## Abstract

Faculty of Medicine

Human Development and Health

### PhD Thesis

Subcutaneous Implantable Cardiac Defibrillator – A Personalised Approach

by

Dr Mohamed ElRefai MBBCh MRCP

Sudden cardiac death (SCD) remains one of the leading causes of death in the modern world with most of these deaths being attributed to ventricular arrhythmias.

Implantable cardiac defibrillators (ICDs) are well established treatment and are recommended by the international guidelines for prevention of sudden cardiac death triggered by ventricular arrhythmias in high-risk populations. But they are not risk-free, and traditional transvenous ICDs are associated with long-term complications with potentially fatal consequences.

The subcutaneous ICD (S-ICD) was designed utilising a totally extra-thoracic approach avoiding the complications which have been associated with transvenous ICDs (TV-ICD). The results of clinical trials demonstrated the efficacy of the S-ICD systems in recognising and treating ventricular arrhythmias with fewer lead-related complications when compared to the TV-ICDs.

However, the downside of the S-ICDs is that unlike TV-ICDs, they are unable to provide bradycardia pacing or Anti-tachycardia pacing (ATP) therapy to terminate ventricular arrhythmias painlessly without the need to deliver a shock. Also, they exhibit a relatively higher rate of inappropriate shocks when compared with TV-ICDs. Most of these shocks can be attributed to T-wave oversensing (TWO), an inherent risk to the sensing mechanism of the S-ICD.

Not all patients are eligible for S-ICDs and mandatory screening of all potential candidates following device manufacturer guidelines helps identify eligible patients based on their underlying ECG morphology. Variable rates of screening success and S-ICD eligibility are reported in the literature.

In this thesis I will start by reporting a retrospective analysis of S-ICD eligibility using current recommended screening practices at a tertiary centre for cardiac devices (University Hospital of Southampton). I will then proceed to suggest adopting a different approach towards screening of S-ICD candidates which considers the dynamicity of the ECG signal. I will explore the role of applying prolonged screening using Holter monitors in a wide range of patients' cohorts and prove there is variation in the S-ICD eligibility overtime which can explain oversensing and inappropriate shocks in S-ICDs despite current screening practices. I will also introduce and explain a novel technique utilising artificial intelligence and deep learning methods which has the potential to be applied to clinical practice to help identify S-ICD eligible patients as well as guide vector selection in S-ICD recipients.

I will justify choosing R:T ratio as the main determinant of S-ICD eligibility and validate the novel deep learning methodology used in my studies by comparing the outcomes to those produced by the "gold standard" S-ICD simulator.

I will then proceed to propose targeting less strict R:T ratios in S-ICD screening in vectors that prove to be stable with prolonged screening. I will then compare the eligibility rates for S-ICD using different R:T ratios, proposing that it is reasonable to revisit the S-ICD Screening thresholds if we adopt prolonged screening approaches.

Afterwards, I will address the inability of S-ICDs to provide pacing therapy and the need to co-implant pacemaker devices to cover pacing therapy when clinically indicated. I will highlight that the effect of pacing on the S-ICD sensing has not been well studied before. I will proceed by first introducing a simple radiological method to define the LP position, then demonstrate that there is no effect of LP position on short- and long-term LPs performances. Afterwards I will show that pacing regardless of the pacing site has a significant effect on the R:T ratio, one of the main determinants of S-ICD eligibility and increases the risk of S-ICD oversensing. However, I will conclude that with adoption of personalised approach towards device therapy, it is theoretically feasible to utilise concomitant device therapies in most patients, without increasing the risk of adverse clinical events.

In summary, I believe that extravascular cardiac devices are soon to establish themselves as the new standard of care to provide defibrillation protection and pacing therapy. Current issues with S-ICDs can be overcome by incorporating efficient artificial intelligence methods to help with more accurate and yet efficient screening for better patient selection. Together with adopting a personalised approach, higher S-ICD eligibility can be achieved, and the risk of inappropriate shocks can be mitigated.







# Table of Contents

<b>Table of Contents</b> .....	<b>i</b>
<b>Table of Tables</b> .....	<b>vii</b>
<b>Table of Figures</b> .....	<b>ix</b>
<b>Research Thesis: Declaration of Authorship</b> .....	<b>xvii</b>
<b>Acknowledgements</b> .....	<b>xix</b>
<b>Definitions and Abbreviations</b> .....	<b>xxi</b>
<b>Chapter 1 Introduction</b> .....	<b>1</b>
1.1 Burden and significance of ventricular arrhythmia.....	1
1.2 Implantable Cardiac Defibrillators .....	5
1.3 Subcutaneous defibrillators .....	5
1.3.1 Mechanism of action of S-ICD .....	7
1.3.1.1 The R:T ratio .....	9
1.3.1.2 SMART pass .....	10
1.3.2 S-ICD screening.....	10
1.3.2.1 Overlay Vs AST screening .....	12
1.3.2.2 Role of Exercise screening.....	14
1.3.3 Inappropriate shocks.....	15
1.3.4 S-ICD Vs TV-ICD indications .....	17
1.4 Specific patients' subgroups.....	18
1.4.1 Heart failure .....	18
1.4.1.1 Epidemiology of Heart failure .....	18
1.4.1.2 SCD in Heart failure .....	19
1.4.1.3 S-ICD in Heart failure .....	19
1.4.2 Adult congenital heart disease.....	20
1.4.2.1 Prevalence of ACHD.....	20
1.4.2.2 Common ACHD .....	21
1.4.2.3 SCD in ACHD .....	23
1.4.2.4 SVT in ACHD.....	23

1.4.2.5	ICDs in ACHD .....	24
1.4.2.6	S-ICD in ACHD.....	26
1.4.3	Hypertrophic cardiomyopathy.....	29
1.4.3.1	Epidemiology of HCM .....	29
1.4.3.2	Clinical course of HCM .....	29
1.4.3.3	Management of HCM.....	30
1.4.3.4	Role of S-ICD in HCM.....	32
1.4.4	Dynamic ECG changes in ARVC .....	36
1.5	Leadless pacemakers .....	37
1.5.1	S-ICDs and pacemakers.....	41
1.6	Artificial Intelligence and Machine learning .....	42
1.6.1	Terminology .....	42
1.6.2	Machine learning .....	42
1.6.2.1	Techniques .....	42
1.6.2.2	Strengths and limitations .....	43
1.6.2.3	Convolutional neural networks .....	43
1.6.3	Use in Cardiology .....	44
1.7	Combined Cardiac rhythm management therapy .....	44
1.8	Aims and objectives .....	45
<b>Chapter 2 Eligibility for the subcutaneous implantable cardiac defibrillator using</b>		
<b>standard screening practice – A real-world experience from a UK centre ...47</b>		
2.1	Introduction .....	47
2.2	Objectives.....	47
2.3	Methods.....	47
2.3.1	Statistical methods .....	48
2.4	Results.....	48
2.5	Discussion.....	56
2.5.1	S-ICD eligibility rates .....	56
2.5.2	S-ICD eligibility in specific patients' subgroups .....	57

2.5.2.1	ACHD population .....	57
2.5.2.2	HCM population .....	58
2.5.3	Insights into the data.....	58
2.5.4	Limitations.....	59
2.6	Conclusion .....	60
<b>Chapter 3 Holter recorded changes in R:T ratio and T wave morphology: an observational study of S-ICD sensing (HEART-TWO) .....</b>		<b>61</b>
3.1	Introduction.....	61
3.2	Objectives.....	62
3.3	Methods .....	63
3.3.1	Patients' subgroups.....	65
3.3.2	Data analysis.....	65
3.3.2.1	Machine learning tool .....	66
3.3.3	Statistical methodology:.....	67
3.4	Results .....	68
3.4.1	Heart failure patients .....	68
3.4.2	ACHD patients .....	72
3.4.3	HCM patients.....	78
3.5	Discussion.....	83
3.5.1	Data analysis.....	84
3.5.2	Clinical relevance and potential applications .....	85
3.5.3	Limitations.....	86
3.6	Conclusion .....	87
<b>Chapter 4 The deep learning methods algorithm .....</b>		<b>88</b>
4.1	Introduction.....	88
4.1.1	Details of collaboration .....	88
4.1.1.1	Role of clinical team, represented by me, Mohamed ElRefai, PhD student and author of this work .....	88

4.1.1.2	Role of Mathematics team, represented by Anthony Dunn, PhD student at UoS, school of mathematics, Stefan Coniglio, Associate Professor of Mathematics at UoS, and Alain Zemkoho, Associate Professor of Mathematics at UoS .....	88
4.2	Artificial intelligence and neural network model .....	89
4.2.1	Phase Space Reconstruction .....	90
4.2.2	CNN training.....	92
4.3	Validation of the tool .....	94
4.3.1	Manual confirmation .....	94
4.3.1.1	Error parameters.....	94
4.3.2	Correlation of the tool outcome.....	95
4.3.2.1	Introduction .....	95
4.3.2.2	Objectives.....	96
4.3.2.3	Methods.....	96
4.3.2.4	Results.....	96
4.3.2.5	Discussion.....	101
4.3.2.6	Conclusion.....	103
<b>Chapter 5</b>	<b>Deep learning-based insights on T:R ratio behaviour during prolonged screening and optimal T:R ratio for S-ICD eligibility .....</b>	<b>104</b>
5.1	Introduction .....	104
5.2	Objectives.....	104
5.3	Methods.....	105
5.3.1	Statistical methods .....	106
5.4	Results.....	106
5.5	Discussion.....	114
5.5.1	Mechanism of action of S-ICD.....	114
5.5.2	Optimal T:R ratio for prolonged screening.....	115
5.5.3	Limitations .....	117
5.6	Conclusion.....	117

<b>Chapter 6</b>	<b>Defining the position of the leadless pacemaker and the effect of the implantation site on the device performance .....</b>	<b>119</b>
6.1	Introduction.....	119
6.2	Objectives.....	119
6.3	Methods .....	120
6.4	Results .....	121
6.5	Discussion.....	123
6.5.1	Why leadless?.....	123
6.5.2	Clinical trials .....	124
6.5.3	Implantation location.....	125
6.5.4	Location and device performance.....	127
6.5.5	Limitations.....	127
6.6	Conclusion .....	128
<b>Chapter 7</b>	<b>The Effect of Leadless Pacemaker Position on the R:T Ratio: An Observational Study Of S-ICD Sensing (PACE HERE).....</b>	<b>129</b>
7.1	Introduction.....	129
7.1.1	S-ICD paired with a pacemaker .....	129
7.1.2	Concerns with the concomitant use of both devices.....	130
7.2	Objectives.....	131
7.3	Methods .....	131
7.3.1	Statistical analysis.....	132
7.4	Results .....	133
7.5	Discussion.....	144
7.5.1	Clinical relevance.....	144
7.5.2	Pacemaker position effect on ECG signals .....	144
7.5.3	Data analysis.....	145
7.5.4	Limitations.....	147
7.6	Conclusion .....	148
<b>Chapter 8</b>	<b>Conclusion .....</b>	<b>149</b>
8.1	Summary of findings.....	149

8.2	Clinical implications .....	150
8.3	Summary of limitations.....	150
8.4	Proposed further work.....	151
8.4.1	Application of the deep learning tool in clinical practice .....	151
8.4.2	Personalised devices therapy .....	152
8.5	Summary .....	152
<b>Appendix A 154</b>		
A.1	Publications arising from work in this thesis .....	154
A.1.1	Abstracts presented.....	154
A.1.2	Peer-reviewed published manuscripts .....	155
<b>Appendix B 156</b>		
B.1	Research Governance, Monitoring, Ethics and Research and Development (R&D) approval .....	156
B.1.1	Approaching Participants:.....	156
B.1.2	Data handling and record keeping.....	156
<b>Bibliography .....</b>		<b>158</b>

## Table of Tables

Table 1 Patients' demographics.....	48
Table 2 Screening outcomes for all vectors combined.....	50
Table 3 Factors influencing number of passing vectors.....	51
Table 4 Screening outcomes for the primary vector .....	53
Table 5 Screening outcomes for the secondary vector. ....	54
Table 6 Screening outcomes for the alternate vector. ....	55
Table 7 S-ICD screening failure rates in previous studies. ....	56
Table 8 Patients' demographics.....	68
Table 9 Patients demographics for the heart failure and structurally normal hearts groups. ....	69
Table 10 Comparison between the parameters of the T:R between both groups.....	70
Table 11 Differences in the "unfavourable" T:R ratios in both groups.....	71
Table 12 Patients' demographics.....	73
Table 13 Mean, median, and SD of the T:R ratios measured in 24 hours for the all the Leads/S-ICD vectors. ....	74
Table 14 Mean, median, and SD of the T:R ratios measured in 24 hours classified according to the S-ICD vector. ....	75
Table 15 Shows the probability of S-ICD screening failure for all the S-ICD vectors. ....	77
Table 16 Patients' demographics.....	78
Table 17 Mean, median, and SD of the T:R ratios measured in 24 hours for the all the Leads/S-ICD vectors. ....	79
Table 18 Mean, median, and SD of the T:R ratios measured in 24 hours classified according to the S-ICD vector. ....	80

Table 19 Probability of each vector passing the screening using standard screening practice in both groups. ....	83
Table 20 Patients' demographics .....	97
Table 21 Results of T:R assessment using the deep learning tool.....	97
Table 22 Outcome of the deep learning tool vs the outcome of the S-ICD simulator. ....	99
Table 23 Patients' demographics. ....	106
Table 24 Shows probability of passing standard S-ICD screening in a 24-hour period based on a T:R of 1:3. ....	107
Table 25 showing S-ICD screening success rates at different thresholds for all patients. ....	108
Table 26 showing S-ICD screening success rates at T:R of 1:3 for each vector separately. ....	109
Table 27 showing S-ICD screening success rates at T:R of 1:2 for each vector separately. ....	110
Table 28 showing S-ICD screening success rates at T:R of 2:3 for each vector separately. ....	111
Table 29 showing S-ICD screening success rates at T:R of 3:4 for each vector separately. ....	112
Table 30 showing S-ICD screening success rates at T:R of 1:1 for each vector separately. ....	112
Table 31 Patients demographics. ....	121
Table 32 Patients' demographics. ....	133
Table 33 Comparison between the R:T ratios at different pacing sites and with no pacing.....	134
Table 34 post-hoc subgroup analyses for the R:T ratio for different pacing sites .....	135
Table 35 Comparison between the R:T ratios at different pacing sites. ....	135
Table 36 Comparison between the R:T ratio in the three distinct S-ICD vectors.....	136
Table 37 Favourable R:T ratios (>3:1) in the three distinct S-ICD vectors.....	137
Table 38 R:T ratios on the individual scale. ....	138



## Table of Figures

Figure 1	12 lead ECG showing ventricular tachycardia.....	2
Figure 2	12 lead ECG showing Ventricular fibrillation. ....	2
Figure 3	S-ICD sensing electrodes and vectors. An implanted S-ICD showing the location of the pulse generator, the proximal (Pr) and distal (D) sensing electrodes and the shocking coil. Image (prior to annotation) © Boston Scientific Corporation or its affiliates. Annotations on the image produced by Dr. Benedict Wiles. Reproduced with permission.....	6
Figure 4	Surface ECG, intracardiac signal and S-ICD sensing vectors. Image © Boston Scientific Corporation or its affiliates. Reproduced with permission. ....	7
Figure 5	Illustrates how fixed sensitivity could lead to under sensing of ventricular fibrillation with potentially fatal consequences. Original image prior to annotations produced by Dr. Benedict Wiles, reproduced with permission.....	8
Figure 6	illustrates adjustable sensitivity of the S-ICD system. S = sensed event and T=tachycardia detected. Original image prior to annotations produced by Dr. Benedict Wiles, reproduced with permission. ....	9
Figure 7	Surface ECG electrodes positioning; LL: left leg lead, placed at the 5th intercostal space along the mid-axillary line to represent the intended location of the pulse generator. LA: left arm lead, placed 1 cm left and lateral of the xiphoid to represent the intended location of the proximal sensing node of the implanted subcutaneous electrode. RA: right arm lead, should be placed 14 cm superior to the ECG Electrode LA, to represent the intended position of the distal sensing tip of the implanted subcutaneous electrode. The right leg lead (RL) is a neutral lead which is not shown, it is usually placed on the right side of the chest wall. Image (prior to annotation) © Boston Scientific Corporation or its affiliates. Reproduced with permission.....	11
Figure 8	S-ICD screening tool. The recorded QRST morphology is then compared to the templates. The template is aligned to the isoelectric line of the ECG, and the QRST complexes are viewed through the appropriately sized template. The R wave peak of the ECG must be placed within either hashed box of any template. A vector passes screening if the remainder of the QRST complex sits entirely	

within the template. Image reproduced with permission from Boston Scientific  
 ..... 12

Figure 9 Classification of congenital heart diseases.<sup>54</sup> ..... 22

Figure 10 Risk of Ventricular arrhythmias and SCD.<sup>54</sup> ..... 24

Figure 11 ESC guidelines on ICD implantation in ACHD population.<sup>54</sup> ..... 25

Figure 12 Distribution of the congenital heart diseases in the meta-analysis.<sup>54</sup> ..... 26

Figure 13 Predictive variables for the HCM Risk-SCD model..... 31

Figure 14 Score calculation for the HCM Risk-SCD model.<sup>63</sup> ..... 31

Figure 15 Flow Chart guiding decision for implanting ICD in HCM patients.<sup>63</sup> ..... 32

Figure 16 Showing the typical S-ICD vectors. Image prior to annotation © Boston Scientific Corporation or its affiliates. Annotations on the figure originally produced by Dr. Benedict Wiles, reproduced with permission. .... 63

Figure 17 shows the Holter® surface ECG positions..... 64

Figure 18 Variation of the predicted TR ratio over the 24-hour screening period for each lead. Leads A, B and C correspond to primary, alternate, and secondary vectors of an S-ICD respectively.<sup>120</sup> ..... 67

Figure 19 Histogram of the T:R ratio over the 24-hour screening period for each lead. Leads A, B and C correspond to primary, alternate, and secondary vectors of an S-ICD respectively.<sup>120</sup> ..... 67

Figure 20 Box plots for the Mean ( $p < 0.001$ ) and standard deviation ( $p = 0.02$ ) of the T:R ratio over 24 hours screening period in the studied subgroups (Heart failure patients undergoing diuresis vs healthy volunteers with structurally normal hearts). Leads A, B and C correspond to primary, alternate, and secondary vectors of an S-ICD respectively. .... 70

Figure 21 An example of the T:R ratio fluctuating overtime crossing the S-ICD screening threshold for the T:R ratio (0.33 or 1:3) on multiple occasions over the 24-hour period. The histogram illustrates the exact number of 10-second segments at each T:R ratio throughout the 24-hour recording. The above example represents the alternate vector for one of the patients who was recruited to the HF subgroup. .... 72

Figure 22	Mean, median, and SD of the T:R ratios measured in 24 hours for the all the Leads/S-ICD vectors in ACHD and healthy volunteers with normal hearts subgroups. ....	74
Figure 23	Mean T:R ratios measured in 24 hours classified according to the S-ICD vector. ....	76
Figure 24	Median T:R ratios measured in 24 hours classified according to the S-ICD vector. ....	76
Figure 25	Standard deviation (SD) of the T:R ratios measured in 24 hours classified according to the S-ICD vector. ....	77
Figure 26	Mean, median, and SD of the T:R ratios measured in 24 hours for the all the Leads/S-ICD vectors in HCM and healthy volunteers with normal hearts groups. ....	79
Figure 27	Mean T:R ratios measured in 24 hours classified according to the S-ICD vector. ....	81
Figure 28	Median T:R ratios measured in 24 hours classified according to the S-ICD vector. ....	81
Figure 29	Standard deviation (SD) of the T:R ratios measured in 24 hours classified according to the S-ICD vector. ....	82
Figure 30	An example of how the tool can help select the most suitable vector for programming the S-ICD. The analysis of the Holter recording for one of the patient recruited in the HF subgroup: All the 3 leads had acceptable T:R ratios at some stage of the 24-hour recordings, however, while the T:R ratios for Leads A and B (corresponding to the primary and alternate vectors) showed significant fluctuations over the 24-hours recording and crossed the screening threshold multiple times, T:R ratio for Lead C (secondary vector) was stable in comparison and didn't cross the threshold throughout the 24-hours posing the least risk of TWO. ....	86
Figure 31	Shows an example of a 10-second ECG segment; (a) pre-filtering, and (b) after the application of filtering. R wave and T wave peaks are shown in red and blue, respectively. <sup>120</sup> ....	89
Figure 32	Illustrates how a PSR image of the sine wave is created. As the sine wave has a repeated behaviour, the sine wave signal could have any length and the phase space points generated from this signal would continuously trace and retrace the resulting circle figure which represents the PSR image of the sine wave. Original image prior to annotations produced by Mr Anthony Dunn, reproduced with permission. ....	90

Figure 33 Visualisation of the data from 10-second ECG segments. <sup>120</sup> .....	92
Figure 34 One example of the results of vector analysis produced by the tool.....	94
Figure 35 Mean T:R ratio + standard deviation of T:R (x-axis) in correlation with mean vector score + standard deviation of mean vector score(y-axis) using spearman's rank correlation test. Rho= 0.636 (p<0.001) denoting strong correlation.....	100
Figure 36 Mean T:R ratio + standard deviation of T:R (x-axis) in correlation with eligible vector time (EVT)(y-axis) using spearman's rank correlation test. Rho= 0.668 (p<0.001) denoting strong correlation. ....	101
Figure 37 Favourable ratio time (x-axis) in correlation with eligible vector time (EVT)(y-axis) using spearman's rank correlation test. Rho= 0.652 (p<0.001) denoting strong correlation.....	101
Figure 38 Shows the S-ICD vectors screening pass rates for each S-ICD vector, for all the proposed thresholds and for all the underlying aetiologies that were represented in the analysis. ....	114
Figure 39 Demonstrates how slightly changing the threshold can impact the outcome of S-ICD screening. It shows the results of a recorded 24-hour ECG signal corresponding to the alternate vector of an S-ICD from one of the patients from the HCM subgroup in the study as analysed by the tool. There is a clear demonstration of T:R ratio fluctuation along the recorded 24 hours. The top half of the figure shows how the T:R ratio crosses the proposed T: R threshold of 1:3 on 20 occasions- convincingly failing the screening-, while the bottom half shows how the T:R ratio never crossed the proposed T: R threshold of 1:2, effectively passing the screening if this threshold was adopted.....	116
Figure 40 Criteria used for classification of device position:.....	120
Figure 41 Clustered Error Bars mean of parameters by the validated positions. ....	123
Figure 42 Comparison of leadless pacemaker deployment sites between UHS and the trans-catheter pacing system (TPS) worldwide post-approval registry. ....	126
Figure 43 Fluoroscopic images in the left anterior oblique (top row) and right anterior oblique (bottom row) views showing the pacing catheter placed at four different sites in the right ventricle corresponding to the potential implantation sites for the leadless pacemaker. ....	132

Figure 44 Boxplot comparing between different pacing sites and the "no pacing" group. Significant decrease was noticed in the R:T ratio when pacing in any of the selected sites. Multiple outliers were detected in all the pacing sites with nearly isoelectric T waves. Vectors A, B, and C correspond to Primary, alternate, and secondary vectors of an S-ICD, respectively. ....134

Figure 45 R:T ratios on the individual scale for the primary vector. The R:T ratios are plotted on the y-axis against the individual study ID. No refers to no pacing, A, AS, MS, and OF refers to Apical, apical septum, mid septum, and outflow tract pacing respectively.....140

Figure 46 R:T ratios on the individual scale for the secondary vector. The R:T ratios are plotted on the y-axis against the individual study ID. No refers to no pacing, A, AS, MS, and OF refers to Apical, apical septum, mid septum, and outflow tract pacing respectively.....141

Figure 47 R:T ratios on the individual scale for the alternate vector. The R:T ratios are plotted on the y-axis against the individual study ID. No refers to no pacing, A, AS, MS, and OF refers to Apical, apical septum, mid septum, and outflow tract pacing respectively.....142

Figure 48 Vectors with favourable R:T ratios on the individual scale. The study ID is plotted on the y-axis against the number of favourable R:T ratios on the x-axis. ....143

Figure 49 An example of the effect of pacing as well as changing the pacing site on the morphology of the Holter traces corresponding to the S-ICD vectors. A, B, and C correspond to primary, alternate, and secondary vectors respectively. ....146









# Research Thesis: Declaration of Authorship

Print name: Mohamed Hassan ElRefai

Title of thesis: Subcutaneous Implantable Cardiac Defibrillators – A Personalised Approach

I declare that this thesis and the work presented in it are my own and has been generated by me as the result of my own original research.

I confirm that:

1. This work was done wholly or mainly while in candidature for a research degree at this University.
2. Where any part of this thesis has previously been submitted for a degree or any other qualification at this University or any other institution, this has been clearly stated.
3. Where I have consulted the published work of others, this is always clearly attributed.
4. Where I have quoted from the work of others, the source is always given. With the exception of such quotations, this thesis is entirely my own work.
5. I have acknowledged all main sources of help.
6. Where the thesis is based on work done by myself jointly with others, I have made clear exactly what was done by others and what I have contributed myself.
7. Parts of this work have been published as: -
  - M Elrefai, C Menexi, P Roberts, Leadless pacemakers: where is the device? EP Europace, Volume 23, Issue Supplement\_3, May 2021, euab116.375, <https://doi.org/10.1093/europace/euab116.375>
  - C Menexi, M Elrefai, M Abouelasaad, P Roberts, Leadless pacemakers: does location matter? EP Europace, Volume 23, Issue Supplement\_3, May 2021, euab116.376, <https://doi.org/10.1093/europace/euab116.376>
  - Abstract 10370: Personalised Approach is the Key When it Comes to Pacing a Patient with an S-ICD. Circulation. 2021;144: A10370. [https://www.ahajournals.org/doi/10.1161/circ.144.suppl\\_1.10370](https://www.ahajournals.org/doi/10.1161/circ.144.suppl_1.10370)
  - Abstract 9203: Role of Artificial Intelligence and Utilisation of Deep Learning Methods in Screening for Subcutaneous Implantable Cardioverter Defibrillator Eligibility. Circulation. 2021;144: A9203. [https://www.ahajournals.org/doi/10.1161/circ.144.suppl\\_1.9203](https://www.ahajournals.org/doi/10.1161/circ.144.suppl_1.9203)
  - Eligibility for the subcutaneous implantable cardiac defibrillator therapy using standard screening practice – our experience. European Journal of Arrhythmia & Electrophysiology.

2021;7(Suppl. 1): abstr67. <https://www.touchcardio.com/devices/journal-articles/67-eligibility-for-the-subcutaneous-implantable-cardiac-defibrillator-therapy-using-standard-screening-practice-our-experience/>

- Anthony J. Dunn, Mohamed H. ElRefai, Paul R. Roberts, Stefano Coniglio, Benedict M. Wiles, Alain B. Zemkoho, Deep learning methods for screening patients' S-ICD implantation eligibility, *Artificial Intelligence in Medicine*, Volume 119, 2021, 102139, ISSN 0933-3657, <https://doi.org/10.1016/j.artmed.2021.102139>.
- ElRefai, M., Abouelasaad, M., Menexi, C. et al. Impact of right ventricular pacing site on the subcutaneous ICD sensing—a step towards personalised device therapy? *J Interv Card Electrophysiol* (2022). <https://doi.org/10.1007/s10840-022-01218-9>
- ElRefai, M., Abouelasaad, M., Wiles, B.M. et al. Deep learning-based insights on T:R ratio behaviour during prolonged screening for S-ICD eligibility. *J Interv Card Electrophysiol* (2022). <https://doi.org/10.1007/s10840-022-01245-6>
- M Elrefai, M Abouelasaad, I Conibear, B Wiles, A Dunn, S Coniglio, A Zemkoho, P Roberts, The use of artificial intelligence and deep learning methods in subcutaneous implantable cardioverter defibrillator screening to optimise selection in special patient populations, *EP Europace*, Volume 24, Issue Supplement\_1, May 2022, euac053.448, <https://doi.org/10.1093/europace/euac053.448>
- M Elrefai, M Abouelasaad, A Dunn, S Coniglio, A Zemkoho, B Wiles, P Roberts, Eligibility for subcutaneous implantable cardiac defibrillator utilising artificial intelligence and deep learning methods for prolonged screening: where is the cut-off, *EP Europace*, Volume 24, Issue Supplement\_1, May 2022, euac053.447, <https://doi.org/10.1093/europace/euac053.447>
- ElRefai M, Menexi C, Abouelasaad M, Tsoi V, Roberts PR. Insights on subcutaneous implantable cardiac defibrillator eligibility using standard screening practices. *J Interv Card Electrophysiol*. 2022 Dec 16. doi: 10.1007/s10840-022-01453-0. Epub ahead of print. PMID: 36525169.
- ElRefai M, Abouelasaad M, Wiles BM, Dunn AJ, Coniglio S, Zemkoho AB, Morgan JM, Roberts PR. Role of deep learning methods in screening for subcutaneous implantable cardioverter defibrillator in heart failure. *Ann Noninvasive Electrocardiol*. 2022 Dec 16:e13028. doi: 10.1111/anec.13028. Epub ahead of print. PMID: 36524869.

Signature: Mohamed ElRefai

Date: October 2022

## Acknowledgements

I am extremely grateful to my supervisors Professor Paul Roberts and Professor John Morgan, first, for giving me the opportunity and having the faith in me to assign me to this amazing research program at University Hospital of Southampton. I would also like to thank them for their ongoing guidance and support on this project.

I want to thank Dr. John Paisey for his ongoing guidance when it comes to my professional career as a cardiologist. He encouraged me to pursue this research adventure, for which I will remain grateful.

Thank you to my colleague, friend, and predecessor Dr Benedict Wiles for pointing me in the right direction from the outset and for his ongoing collaboration and support with this project.

I would like to thank the outstanding Cardiac Rhythm Management Research Department and all the cardiac physiologists at University Hospital Southampton NHS Foundation Trust. In particular: Elizabeth Greenwood, Sarah Earles and Lisa Fletcher who were an invaluable source of knowledge and support throughout the whole process.

I would like to thank Mr. Anthony Dunn, Associate Professor Stefano Coniglio, and Associate Professor Alain Zemkoho from the school of Mathematical sciences at the University of Southampton for their collaboration. Their expertise in the field of data analysis using deep learning methods has been an invaluable resource for this project.

I wish to acknowledge the financial assistance that was provided by Boston Scientific in the form of an unrestricted research grant that provided the backbone funding for this project.

This project could not have been possible without the numerous patients and volunteers who generously agreed to participate in my research.

I would also like to thank my cardiology colleague, and my friend Dr Lavinia Gabara with whom I shared this research adventure. I would also like to thank my cardiology colleague and my friend Dr. Ahmed ElSerwey for always having the time to listen over a cup of coffee. Thank you also to my colleague and my friend Dr Mohamed Abouelasaad who provided invaluable statistical support to the whole project.

I would like to thank my uncle and my mentor Professor Medhat ElRefai- whom I aspire to emulate as a clinician and a cardiologist – for his unwavering support and encouragement. I would like to thank my parents and my sister for their unconditional support. Finally, I offer the most

## Acknowledgements

sincere and heartfelt thanks to my colleague, best friend, and wife Dr. Christina Menexi. Thank you for being you, this work is dedicated to you.

## Definitions and Abbreviations

ACHD	adult congenital heart disease
AIIRB	angiotensin II receptor blocker
ARVC	arrhythmogenic right ventricular cardiomyopathy
ASCII	American Standard Code for Information Interchange
AST	automated screening tool
ATP	anti-tachycardia pacing
AV	atrio-ventricular
AVNRT	atrio-ventricular nodal re-entrant tachycardia
AVRT	atrio-ventricular reciprocating tachycardia
BBB	bundle branch block
BMI	body mass index
bpm	beats per minute
CABG	coronary artery bypass graft
CI	confidence interval
cm	centimetre
CRT	cardiac resynchronisation therapy
CRT-D	cardiac resynchronisation therapy defibrillator
CRT-P	cardiac resynchronisation therapy pacemaker
D	S-ICD distal sensing electrode
ECG	electrocardiogram
EF	ejection fraction

eGFR	estimated glomerular filtration rate
EPS	electrophysiology study
ESC	European Society of Cardiology
FDA	United States Food and Drug Administration
HEART-TWO	Holter recorded changes in R: T ratio and T wave morphology: an observational study of S-ICD sensing
HCM	hypertrophic cardiomyopathy
HRA	Health Research Authority
Hz	Hertz
ICD	implantable cardioverter defibrillator
IDE	Investigational Device Exemption (clinical trial)
ISHNE	International Society for Holter and Non-invasive Electrocardiology
J	Joules
LA	left atrium
LBBB	left bundle branch block
LL	left leg lead / electrode (ECG acquisition)
LQTS	long QT syndrome
LV	left ventricle or left ventricular
MADIT	Multicentre Automatic Defibrillator Implantation Trial (clinical trial)
mm	millimetre
MRI	magnetic resonance imaging
ms	milliseconds
mV	millivolts

NSVT	non-sustained ventricular tachycardia
NYHA	New York Heart Association
Pr	proximal sensing electrode
pT	time from onset of QRS complex to peak of T wave
pTc	pT, corrected for heart rate
PTSD	post-traumatic stress disorder
QT	time from onset of QRS complex to end of T wave
QTc	QT, corrected for heart rate
RA	right atrium or right atrial or right arm lead / electrode (ECG acquisition)
RBBB	right bundle branch block
REC	Research and Ethics Committee
RL	right leg lead / electrode (ECG acquisition)
R: T	amplitude ratio of R wave to T wave
RV	right ventricle or right ventricular
s	seconds
S	secondary vector
SA	sinoatrial
SCD	sudden cardiac death
SCD-HeFT	Sudden Cardiac Death in Heart Failure Trial (clinical trial)
S-ICD	subcutaneous implantable cardioverter defibrillator
SVT	supraventricular tachycardia
TV-ICD	transvenous implantable cardioverter defibrillator
TWOS	T wave over sensing

UHS	University Hospital Southampton NHS Foundation Trust
$\mu\text{V}$	microvolts
V	volts
VF	ventricular fibrillation
VT	ventricular tachycardia



# Chapter 1 Introduction

## 1.1 Burden and significance of ventricular arrhythmia

Cardiovascular disease is the leading cause of death worldwide. In 2017 alone 17.8 million lives were lost because of cardiovascular disease.<sup>1</sup> Sudden cardiac death (SCD) is the cause of more than 60% of all deaths from cardiovascular disease.<sup>2</sup> Sudden cardiac death is defined as the unexpected death that occurs within one hour of the symptoms when death is witnessed, most of which can be attributed to cardiac arrhythmias.<sup>3</sup> In most cases, SCD is thought to be the consequence of ventricular tachycardia, degenerating to ventricular fibrillation and subsequent asystole.<sup>3</sup>

Sudden cardiac death (SCD) remains a significant public health problem and is one of the leading causes of death in the modern world with an annual incidence ranging between 50-100 per 100,000 population.<sup>4</sup> Most people who suffer SCD have coronary heart disease and in 50% of the time, SCD is the first manifestation of heart disease.<sup>5</sup> Risk factors for ischaemic heart disease such as, old age, male sex, smoking, hypertension, diabetes mellitus, high cholesterol and family history of coronary heart disease have all been associated with an increased risk of SCD.<sup>6-10</sup> Other risk factors for SCD include heart failure (SCD accounts for 30–50% of all deaths in patients with heart failure)<sup>11</sup>, left ventricular hypertrophy, and poor functional status among others.<sup>3</sup> Although SCD frequently affects individuals who are known to have cardiovascular disease such as coronary artery disease or cardiomyopathy, it can also impact seemingly healthy individuals. Up to 80% of sudden cardiac deaths can be attributed to ventricular arrhythmia.<sup>4</sup>

Ventricular arrhythmias (VA) are rapid abnormal heart rhythms that originate in the ventricles and can result in hemodynamic compromise, collapse, and sudden cardiac death (SCD). The annual global mortality burden attributed to ventricular arrhythmias is approximately 6 million.<sup>12</sup> SCD patients rarely survive. The key to survival is adequate CPR and early defibrillation where literally every minute counts, as every minute of delayed defibrillation reduces the chance of survival by around 10%.<sup>3</sup> Ventricular arrhythmia patients could be rescued if ventricular defibrillators were used in timely manner.<sup>5</sup>

Ventricular arrhythmias can present either as ventricular tachycardia (VT), see Figure 1 or ventricular fibrillation (VF), see Figure 2. When compared with VF, VT is more organised with discrete QRS complexes, thus must be differentiated from fast sinus rhythm and other benign

arrhythmias. VT presents with palpitations, long lasting tachycardia associated with dyspnoea, chest pain, hypotension, syncope, and may also present with sudden cardiac death. It is of note that despite established criteria, differentiating between life threatening ventricular tachycardia and other relatively benign arrhythmias remains a challenge. There is a need for an accurate, noncomplex solution for this and with the current advances in technology, there is a great potential in developing robust devices in analysing ECG signals.



Figure 1 12 lead ECG showing ventricular tachycardia.

VF is a life-threatening rhythm disturbance that is characterised by rapid and chaotic electrical activity. It is defined electrocardiographically by rapid irregular QRS complexes of varying morphology and amplitude.

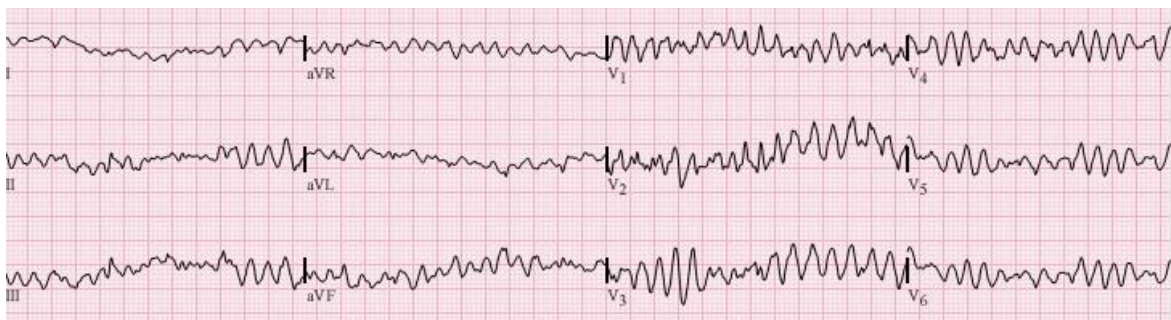


Figure 2 12 lead ECG showing Ventricular fibrillation.

In the UK, it is estimated that 60,000 out of hospital cardiac arrests occur each year.<sup>13,14</sup> In these individuals, prompt defibrillation is the most important determinant of survival. With every

minute that passes after cardiac arrest without defibrillation, survival decreases by around 7–10% (without CPR), and by 3–4% (With CPR). After 10min without defibrillation, only 5% of the patients survive.<sup>15</sup>

Due to the serious consequences of VA, international guidelines recommend the use of implantable cardioverter-defibrillators (ICDs) for secondary prevention of sudden cardiac death triggered by ventricular arrhythmias as well as for primary prevention of sudden cardiac death due to ventricular arrhythmias in high-risk populations.<sup>16</sup>The efficacy of ICDs is well established and is superior to medical treatment for primary and secondary prevention of SCD.<sup>17–20</sup>



## 1.2 Implantable Cardiac Defibrillators

Implantable cardioverter-defibrillators (ICD) are implanted in those considered to have an elevated risk of SCD following the current practice guidelines.<sup>16</sup> A traditional ICD consists of a generator implanted subcutaneously on the upper chest and transvenous leads implanted into the right ventricle ( $\pm$  the right atrium). If a pathological ventricular arrhythmia is sensed by the lead, the ICD will attempt to treat the arrhythmia by overdrive pacing or by delivering a high voltage shock. The efficacy of ICDs is well established and is superior to medical treatment for primary and secondary prevention of SCD.<sup>17–20</sup>

The traditional transvenous ICDs employ transvenous (intracardiac) leads for rhythm discrimination and delivery of defibrillation shock therapy, and as such are associated with potential complications which can be characterised into complications related to invasion of the vascular space. The complications can occur at the time of implant such as pneumothorax and cardiac tamponade due to traumatic placement of the lead(s), and long-term complications such as infection of the device which may progress into sepsis and/or infective endocarditis with potentially fatal consequences.<sup>21,22</sup>

TV-ICD lead longevity is also a significant issue with the annual rate of transvenous ICD lead defects requiring intervention increasing with time and reaching 20% in 10-year-old leads.<sup>21</sup> Estimated TV-ICD lead survival at 5 and 8 years is just 85% and 60% respectively.<sup>21</sup> Additionally, ICD leads that remain in the vasculature for many years may, ultimately, compromise flow or cause obstruction.

## 1.3 Subcutaneous defibrillators

The subcutaneous implantable cardiac defibrillator (S-ICD) represents an entirely new strategy in defibrillator therapy. It was designed to avoid complications of the TV-ICD by utilising a totally extra-thoracic approach. It comprises an electrically active can and a single subcutaneous lead containing two sensing electrodes: primary and distal. During implantation, the proximal electrode (Pr) is sited 1cm inferior to the xiphisternum, fixated to the underlying muscle. The distal electrode (D) is tunnelled to its final location, 14cm superior to the proximal electrode. The electrically active can creates a third sensing point. The S-ICD senses electrocardiogram (ECG)

signals and by measuring the voltage differences between these sensing points, it creates three different sensing vectors; primary (P) - proximal electrode to can, secondary (S) – distal electrode to can, and alternate (A) – distal to proximal electrode, see Figure 3.

The S-ICD was FDA approved in 2012 for use in the United States to address some of the complications of the TV-ICD. These devices do not enter the heart or vascular system and are not exposed to the hostile environment of the vessels or the repetitive contractions of the ventricle. While the S-ICD leads are more exposed to the musculoskeletal movements than the transvenous leads, however, they are larger and therefore more robust than the transvenous leads. S-ICD therapy therefore avoids many of the complications which have been associated with TV-ICD.<sup>23,24</sup> This has been demonstrated through early S-ICD registry data.<sup>25</sup> S-ICDs are therefore particularly useful in patients with no appropriate venous access, in younger patients who will require decades of device therapy and in patients at high risk of infective endocarditis.

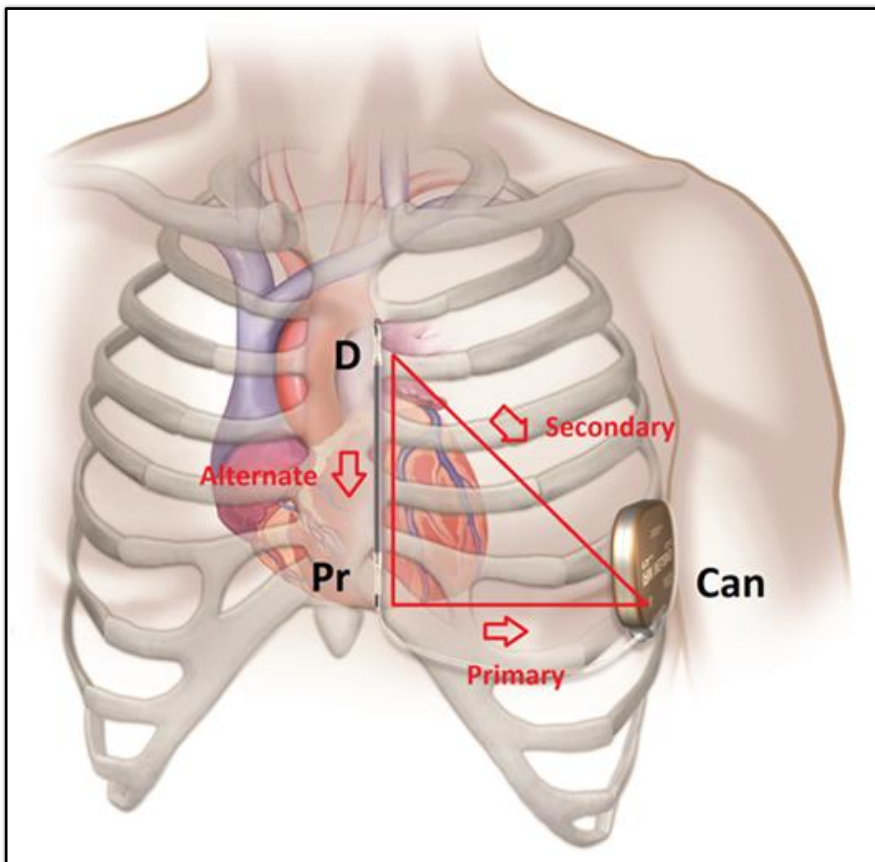


Figure 3 S-ICD sensing electrodes and vectors. An implanted S-ICD showing the location of the pulse generator, the proximal (Pr) and distal (D) sensing electrodes and the shocking coil. Image (prior to

annotation) © Boston Scientific Corporation or its affiliates. Annotations on the image produced by Dr. Benedict Wiles. Reproduced with permission.

### 1.3.1 Mechanism of action of S-ICD

The vectors sensed by the S-ICD strongly resemble a surface ECG and the individual ECG components (R wave, T wave) can be easily visually identified. This is different from the electrograms which are recorded in a TV-ICD system, see Figure 4.

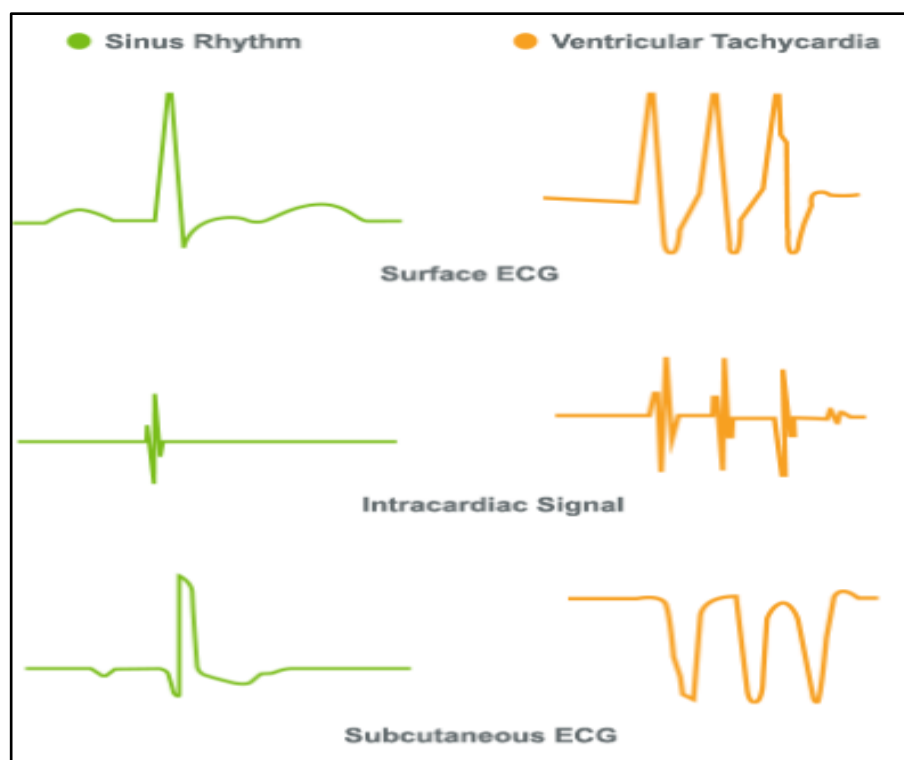


Figure 4 Surface ECG, intracardiac signal and S-ICD sensing vectors. Image © Boston Scientific Corporation or its affiliates. Reproduced with permission.

S-ICD treatment strategies can be primarily determined by heart rate. Different treatment strategies can be applied to variable heart rate ranges. Shock therapies are only delivered if the heart rate exceeds a pre-programmed threshold. The heart rate is calculated by a continuous assessment of the selected vector amplitude using a pre-programmed sensitivity level. Amplitudes above the sensitivity level are identified as R waves (representing ventricular depolarisation) whilst amplitudes below this level are ignored. The heart rate is calculated using the average of four consecutive R to R intervals. After each R wave detection, the S-ICD employs a

blanking period, when no sensing occurs. This is to prevent double counting of a “wide” R wave with more than one peak, this is often seen in the presence of ventricular conduction disease. The length of this blanking period varies from 160ms-200ms depending on the preceding R-R intervals.

The sensitivity level must be high enough to prevent over-sensing. This can happen when other components of the ECG signal, such as T waves are mistakenly counted as R waves. Over-sensing can also occur in the case of interference from background noise or myopotentials from skeletal muscle. The sensitivity level must also be low enough to prevent under-sensing of R waves, which can vary slightly in amplitude from beat to beat.

Fixed sensitivity is inappropriate for an ICD as it can lead to under-sensing of ventricular fibrillation which is characterised by rapidly fluctuating amplitudes. This can have fatal consequences, if appropriate therapy is not delivered and defies the very purpose of implanting an ICD in the first place. The widely utilised solution to this problem is ‘auto adjusting sensitivity,’ whereby the sensitivity level of the device falls gradually after the detection of a R wave, before being rapidly increased to a percentage value of the next sensed R wave. This adjustment of sensitivity is designed to prevent under-sensing of VF, see Figure 5, Figure 6.

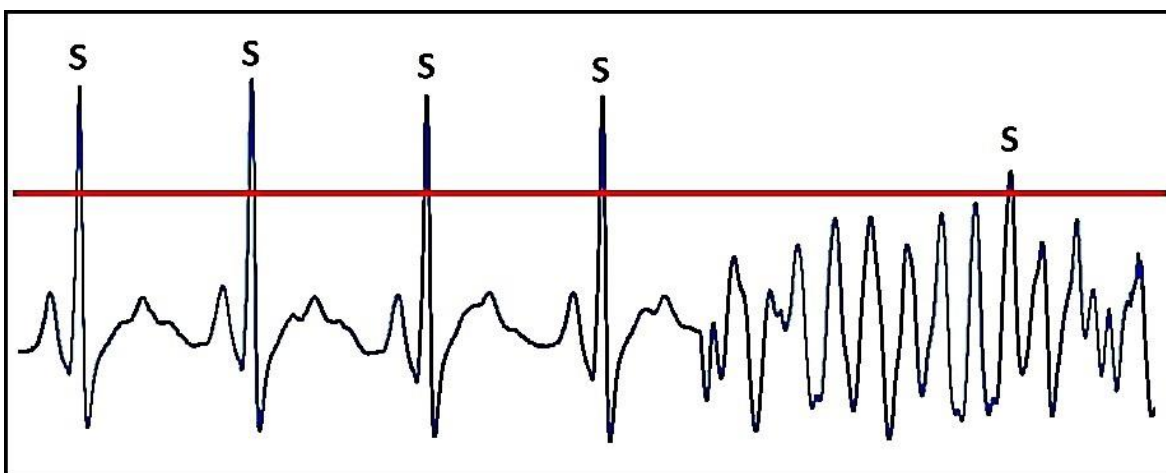


Figure 5 Illustrates how fixed sensitivity could lead to under sensing of ventricular fibrillation with potentially fatal consequences. Original image prior to annotations produced by Dr. Benedict Wiles, reproduced with permission.



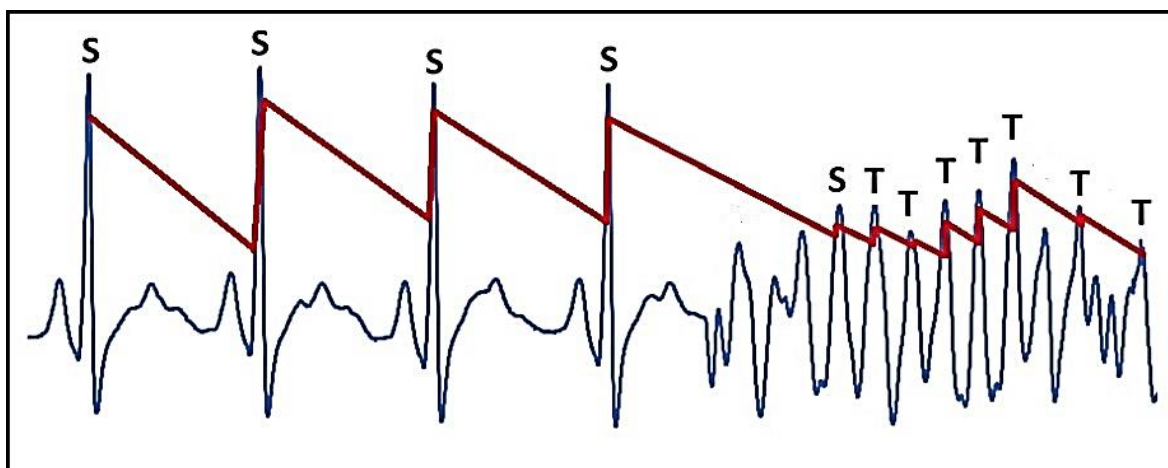


Figure 6 illustrates adjustable sensitivity of the S-ICD system. S = sensed event and T=tachycardia detected. Original image prior to annotations produced by Dr. Benedict Wiles, reproduced with permission.

The sensing mechanism of the S-ICD has been shown to be equally effective to the TV-ICD systems.<sup>26</sup> However, the consequence of this programming is an inherent risk of T wave oversensing (TWO), whereby the T wave following a QRS is interpreted as a second R wave. TWO can lead to inappropriate shocks or can go undetected (silent oversensing) with no record of an event. Due to memory constraints, the S-ICD is designed to save episodes with a long enough duration that lead to capacitor charging. Consequently, if a TWO episode is not long enough to cause the capacitor to charge, it is not stored in the device memory. As such, the real incidence of T wave oversensing in the S-ICD population remains a mystery. These relatively “silent” episodes of T wave oversensing may represent a risk factor for the development of clinically relevant oversensing, manifesting in inappropriate shocks.

### 1.3.1.1 The R:T ratio

The ECG signal is made up of several component parts. The QRS complex is the combination of all the electrical wave fronts which occur during depolarisation of the three-dimensional ventricles. Similarly, the T wave represents the combined repolarisation of the myocardium. In ECG recording, a wave of electrical activity (either depolarisation or repolarisation) that travels towards an electrode, results in a positive deflection on the ECG. Whilst a wave of electrical activity that travels away from an electrode produces a negative deflection.

The R:T ratio is determined by the position from which an electrocardiogram is recorded as varying the angle of recording alters the amplitude of both R wave and T wave. This can be seen on any standard twelve lead ECG, as patients will have different R:T ratios in each of their six standard limb leads, as each looks at the heart from a different angle. Likewise, the S-ICD has three sensing vectors, each with a unique R:T ratio, and the vector with the greatest R:T ratio usually selected for clinical use.

It is important to note that in normal hearts the intrinsic R and T wave axis are often very similar. In hearts with underlying pathology however, the intrinsic axes can be markedly different, Where the R and T wave axis are substantially different, changes in angle of observation should result in marked variations in R:T ratio.

### **1.3.1.2 SMART pass**

The SMART Pass filter (SP; Boston Scientific Corporation, Natick, MA) is a relatively novel filter that was first approved in 2016. This filter is integrated into the S-ICD system, and it aims to reduce inappropriate sensing by the S-ICD. SMART pass works by reducing the amplitude of lower frequency signals such as T-waves, by applying an additional high Pass filter which lets higher frequency signals, such as R waves as well as VT and VF amplitudes, to “pass” through largely unchanged. The introduction of the SMART pass filter led to a significant reduction of inappropriate shocks by the S-ICD without a negative effect on its efficacy in delivering appropriate shocks.<sup>27</sup>

### **1.3.2 S-ICD screening**

Not all patients are eligible for S-ICD therapy. The eligibility for S-ICD is identified during a mandatory pre-implant screening process that is undertaken in all potential S-ICD recipients using guidelines by the device manufacturer. For screening purposes, clinicians use surface ECG recordings as a surrogate marker of future S-ICD vectors to be able to non-invasively assess vector morphology and determine S-ICD eligibility. This allows screening to be performed inexpensively and non-invasively, using equipment that is widely available. Patients with an ECG morphology that does not meet the screening criteria are deemed to be at such high risk of TWO that they are ineligible for an S-ICD.

Pre-implant S-ICD screening was historically undertaken using the “overlay” technique. This required surface ECGs to be done in multiple postures, for example sitting and lying positions. These ECGs were obtained by placing the surface ECG electrodes on the chest wall using the same anatomical landmarks that would guide future S-ICD implantation, see Figure 7. As such, the surface ECGs function as non-invasive surrogates of future S-ICD vector morphology. The ECGs were then compared to a series of acceptable templates provided by the device manufacturer on a transparent ruler, see Figure 8. To be eligible for an S-ICD a patient required a single vector to pass screening in at least two postural positions at the same amplitude.

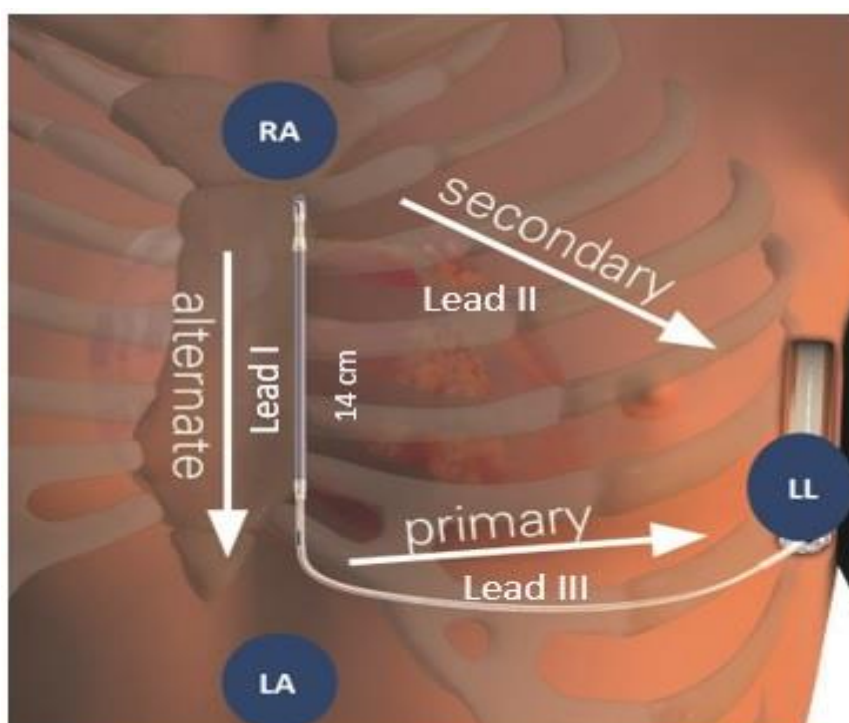


Figure 7 Surface ECG electrodes positioning; LL: left leg lead, placed at the 5th intercostal space along the mid-axillary line to represent the intended location of the pulse generator. LA: left arm lead, placed 1 cm left and lateral of the xiphoid to represent the intended location of the proximal sensing node of the implanted subcutaneous electrode. RA: right arm lead, should be placed 14 cm superior to the ECG Electrode LA, to represent the intended position of the distal sensing tip of the implanted subcutaneous electrode. The right leg lead (RL) is a neutral lead which is not shown, it is usually placed on the right side of the chest wall. Image (prior to annotation) © Boston Scientific Corporation or its affiliates. Reproduced with permission.

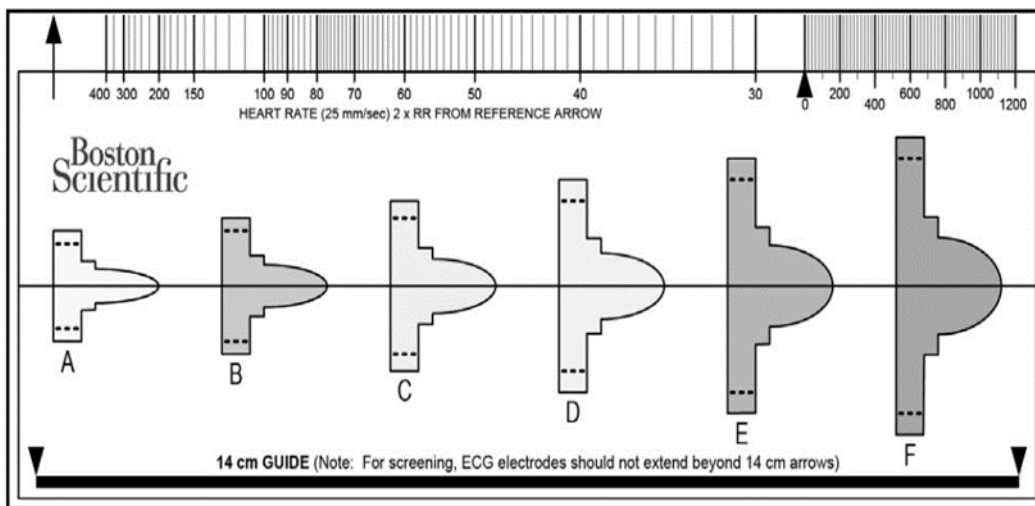


Figure 8 S-ICD screening tool. The recorded QRST morphology is then compared to the templates. The template is aligned to the isoelectric line of the ECG, and the QRST complexes are viewed through the appropriately sized template. The R wave peak of the ECG must be placed within either hashed box of any template. A vector passes screening if the remainder of the QRST complex sits entirely within the template. Image reproduced with permission from Boston Scientific

The overlay technique has widely been replaced by the Automated Screening Tool (AST), a software program that is integrated into the S-ICD programmer which is a specialised device that can communicate wirelessly with the S-ICD. It is utilised in screening, device interrogation and programming. The programmer has external ECG cables which can acquire ECG signal via the application of skin electrodes. The ECG electrodes are placed on the chest wall using the same principles as in the “overlay” technique.

The AST can perform surface ECG analysis allowing vector eligibility to be automatically determined. A major predictor of eligibility of a vector is the R:T ratio. Vectors with higher R:T ratios are more likely to pass the screening. To a clinician a vector that passes is safe for clinical use, whilst a vector that fails cannot be used in clinical practice. After implantation, the most favourable vector from a morphological perspective, is selected for clinical use which can subsequently be changed if problems are identified as a result of baseline ECG changes in the device recipient, or where inappropriate sensing has been detected.

### 1.3.2.1 Overlay Vs AST screening

The manual screening is performed by placing the ECG machine Left Arm (LA) electrode at the intended proximal sensing electrode, placing the Right Arm (RA) electrode at the expected position of the distal sensing electrode, and placing the Left Leg (LL) at the intended S-ICD device site, see Figure 7. 10-second ECG strips at a speed of 25mm/sec are printed out and then assessed

using the manual screening tool described in Figure 8. At least one of the three sensing configurations should be acceptable with QRS complex fit within the screening template in both supine and sitting or standing positions. For the AST, the electrodes are placed in a similar manner to the manual screening technique, but rather than connecting the electrodes to the ECG machine, the electrodes are connected to the manufacturer programmer with the AST built in. AST applies the Vector Select algorithm that is used by the S-ICD to sense the cardiac signal and is designed to represent S-ICD device performance. Data from the manufacturer showed that AST has 24% more likely to predict the performance of a vector than the manual screening tool with more tolerance of large T-waves. There is no published work on the rates of inappropriate shocks between these two screening methods<sup>28</sup>

Chang et al screened patients for S-ICD eligibility using both the manufacturer programmer (AST) as well as manual screening for all the patients. 69 patients were recruited, mean age of  $53.3 \pm 14.7$  years, 51 male (74%). Primary prevention for cardiomyopathy and secondary prevention for prior ventricular fibrillation (VF) in the setting of cardiomyopathy or coronary artery disease were the most common indications for ICD placement (39% and 25%, respectively). A total of 414 of screening leads were assessed using the device programmer as well as the overlay technique. Overall, 285 of 414 (69%) leads assessed by the programmer and 302 of 414 (73%) leads assessed using overlay technique passed the screening ( $P = 0.096$ ). There was discordance in 6.5% (27/414) of corresponding leads between the two different screening methods, five (19%) passed using the programmer and failed the overlay technique and 22 (81%) passed using the overlay technique but failed using the programmer ( $P < 0.001$ ). Overall, there were four subjects who failed the automated screening but passed using the overlay technique. There were no subjects who passed the automated screening while concomitantly failing the overlay screening. The study authors concluded that there can be occasional disagreement between AST And overlay screening, and overall, more subjects are likely to pass screening using the overlay method over the AST screening.<sup>29</sup>

The tools that are being used for S-ICD screening reflect the device's sensitivity, which is not static, but decreases in value after detection of an R wave. This is a programming technique used in defibrillator sensing to ensure that low amplitude ventricular fibrillation is not under-sensed. The consequence of this programming is a risk of T wave over sensing (TWO), whereby a T wave

following a QRS is interpreted as another R wave (double counting). This 'double counting' can result in inappropriate diagnosis of ventricular tachycardia and subsequently activation of shock therapy. Patients with an ECG morphology that does not meet the screening tool criteria are deemed to be at high risk of TWO and ineligible for an S-ICD altogether. This is important as inappropriate shock therapies can have detrimental effects on the quality of life, psychological wellbeing and can even result in the induction of ventricular arrhythmias.<sup>30</sup>

### **1.3.2.2 Role of Exercise screening**

TWO during exercise has been reported as a possible cause of inappropriate shocks in S-ICD patients.<sup>31</sup> Several studies looked at the effect of exercise stress testing on S-ICD eligibility. Francia et al assessed S-ICD eligibility in 47 HCM patients, mean age 52 ±18, 68% male. 33 of these patients underwent S-ICD screening at rest as well as after symptom-limited bicycle exercise test. Overall, 5 patients (15%) were ineligible, 2 (6%) were already ineligible at baseline and 3 patients who had a single eligible S-ICD vector at the baseline, became ineligible during exercise. The study authors concluded that exercise may unmask S-ICD ineligible patients formerly thought to be eligible after S-ICD screening at rest and that exercise screening should be performed in HCM patients.<sup>32</sup>

In another study, Afzal et al conducted a prospective analysis of routine treadmill testing in consecutive patients soon after implantation of an S-ICD to assess the utility of routine treadmill exercise post S-ICD implantation. A total of 87 patients underwent S-ICD screening during a treadmill exercise test. There was no significant difference between R-wave or T wave amplitudes at rest and at peak exercise and they reported no TWO events during exercise in any of the patients. The study authors did not recommend routine ECG exercise testing after S-ICD implantation based on their findings.<sup>33</sup>

In another study by Srinivasan et al, 131 HCM patients (age, 50±16 years; 92 males and 39 females) with ≥1 HCM risk factor for sudden death underwent S-ICD ECG screening at rest and on exercise. In their cohort, 50 patients failed S-ICD screening, 45 (90%) failed screening at rest, while 5 (10%) failed on exercise screening.<sup>34</sup>

Dayal et al performed exercise testing in 47 S-ICD patients who were previously found eligible for S-ICD based on S-ICD screening at rest. 4 S-ICD patients (8.5%) required a change of their programmed S-ICD vector following exercise testing, 2 for TWO and 2 for myopotential oversensing. However, there was no association between the need for change of the programmed vector and rates of inappropriate shocks. Based on their findings, the authors highlighted the potential utility of exercise testing in S-ICD screening.<sup>35</sup>

In another study looking specifically into S-ICD eligibility in Brugada patients, Tachibana et al looked into S-ICD eligibility in 110 Brugada patients, mean age  $54 \pm 13$  years, 98% men at rest and exercise. 89 patients (81%) were found S-ICD eligible at rest screening. 45 patients underwent treadmill stress testing, and 11 of those patients (24%) showed ineligibility for S-ICD during exercise. The study authors concluded that exercise screening should be considered before S-ICD implantation.<sup>36</sup>

Garside et al found no significant differences between S-ICD eligibility during resting ECG and exercise ECG in 14 ACHD S-ICD patients. Only one patient failed to maintain eligibility following their cardiopulmonary exercise test, highlighting the small impact of exercise screening on the eligibility in patients with ACHD.<sup>37</sup>

All the above studies demonstrated variable findings regards the utility of applying routine exercise testing prior to S-ICD implantation. Some clinicians might opt to perform exercise testing prior to S-ICD implantation in selected patients. However, the validity of extending the eligibility for S-ICD implantation to include exercise screening in all S-ICD candidates remains an unresolved issue.<sup>38</sup>

### 1.3.3 Inappropriate shocks

Despite the screening process, the commonest cause of inappropriate shocks in the S-ICD population remains TWO.<sup>39-44</sup> This occurs because T wave morphology and R:T ratio are not fixed in an individual. T wave morphology is in fact dynamic and can alter with position, exercise, electrolyte disturbance, progression of myocardial diseases and changes in autonomic function.

EFFORTLESS, an international S-ICD registry, revealed the rates of inappropriate shocks in the first three years after S-ICD implantation. The rates were 11.4% for dual zone and 13.5% for single zone. The most common reason for inappropriate shocks was T-wave oversensing.<sup>45</sup>

PRAETORIAN is a published international randomised trial involving 849 patients with an indication for an ICD without an indication for pacing. The patients were recruited across 39 centres in the US and Europe between March 2011 and January 2017. Patients received either a conventional TV-ICD (426 patients) or S-ICD (423 patients) and were followed up for 4 years. The composite primary end point of the study was the rate of device related complications and inappropriate shocks. The primary end point occurred in 68 patients in the subcutaneous ICD group and in 68 patients in the transvenous ICD group at 15.1% and 15.7%, respectively (hazard ratio, 0.99; 95% confidence interval [CI], 0.71 to 1.39;  $P=0.01$  for noninferiority;  $P=0.95$  for

superiority). Overall, this trial demonstrated the non-inferiority of the S-ICD to the TV-ICD with respect to the total of device related complications and inappropriate shocks.<sup>46</sup>

Each of the primary end points of the study were also assessed separately. Device-related complications occurred in 31 patients in the subcutaneous ICD group and in 44 patients in the transvenous ICD group (with cumulative incidence of 5.9% and 9.8%, respectively, hazard ratio, 0.69; 95% CI, 0.44 to 1.09). The incidence of complications within the first 30 days was 3.8% in the subcutaneous ICD group and 4.7% in the transvenous ICD group. The incidence of complications related to the ICD lead was lower in the subcutaneous ICD group than in the transvenous ICD group (1.4% vs. 6.6%). However, inappropriate shocks occurred in 41 patients in the subcutaneous ICD group and in 29 patients in the transvenous ICD group (cumulative incidence, 9.7% and 7.3%, respectively, (hazard ratio, 1.43; 95% CI, 0.89 to 2.30). Inappropriate shocks in the subcutaneous ICD group were most frequently caused by cardiac oversensing (in 58.5% of the patients with an inappropriate shock).<sup>46</sup>

The UNTOUCHED trial (Understanding Outcomes With the S-ICD in Primary Prevention Patients with Low Ejection Fraction) is a published prospective, multinational study among primary prevention patients with a reduced ejection fraction. It is the first S-ICD trial to evaluate standardized programming to evaluate rhythm discrimination to high rates (250 bpm) using contemporary electrogram filtering and algorithms to evaluate the inappropriate shocks rate in a more typical ICD patients implanted with the S-ICD. Primary prevention patients with left ventricular ejection fraction  $\leq 35\%$  and no pacing indications were included. Patients were followed for 18 months. The primary end point of the study was freedom of inappropriate shocks. 1111 patients were included in post S-ICD implant follow-up analysis. Mean age of patients  $55.8 \pm 12.4$  years, 25.6% were women, 23.4% were Black, 53.5% had ischemic heart disease, 87.7% had symptomatic heart failure, and the mean left ventricular ejection fraction was  $26.4 \pm 5.8\%$ . Eighteen-month freedom from inappropriate shocks was 95.9% (lower confidence limit, 94.8%). Conversion success rate for appropriate, discrete episodes was 98.4%. Patients receiving a shock for cardiac oversensing included 18 (1.6%) because of T-waves, 4 (0.4%) because of oversensing during a VT/ventricular fibrillation arrhythmia below the rate zone (2 because of double-counting QRS and 2 because of over sensed T-waves), and 10 (0.9%) because of other sources of cardiac oversensing. Sixteen patients (1.4%) received shocks for noncardiac oversensing: 2 patients (0.2%) were shocked because of sensing myopotentials, and 14 patients (1.3%) were shocked from other sources of noncardiac oversensing. Overall, the study demonstrated low inappropriate shock rates and high success rates for termination of ventricular arrhythmias. This highlights the importance of appropriate programming of the device to achieve the optimal balance between minimising the risk of inappropriate shocks, however without compromising on patient safety



through undermining VT detection ability of the S-ICD. The authors of the study concluded that the S-ICD can be considered in all primary prevention patients without pacing indications regardless of underlying heart disease or left ventricular function.<sup>47</sup>

The Achilles heel of the S-ICD to date remains the relatively high rate of inappropriate shocks when compared with conventional TV-ICDs. T-wave oversensing is still the most common cause of inappropriate shock delivery.<sup>46</sup>

#### **1.3.4 S-ICD Vs TV-ICD indications**

The S-ICD is typically implanted in patients with prior device infection or at an increased risk for an infection, younger patients, or patients with difficult venous access.

According to the AHA/ACC/HRS Guidelines for Ventricular Arrhythmia and SCD, there is a Class I recommendation for S-ICD implantation in patients who are at a high risk for infection or are without appropriate venous access and have no indication for bradycardia or biventricular pacing and/or anti-tachycardia pacing (ATP).<sup>48</sup>

A major reason to deny patients S-ICD therapy is the expected benefit of ATP therapy as it provides a painless and successful therapy modality to end sustained ventricular arrhythmia episodes.

While it is straightforward to identify patients with an indication for pacing, it remains challenging to accurately identify patients without a potential benefit of ATP therapy before device implantation because predictors of who will benefit from ATP remain largely unidentified.

In a recent retrospective study published in 2017, Quast et al explored the clinical parameters that would aid in the selection of either a S-ICD or a TV-ICD by assessing incidence and predictors of anti-tachycardia paced (ATP) ventricular arrhythmias. De novo TV-ICD patients implanted between March 2011 and December 2015 were included. Ventricular arrhythmias terminated by ATP without shock therapies were considered successful ATP interventions. Cox proportional hazard analysis was used to assess the adjusted effect of multiple predictors for appropriate ATP and shock therapy. 431 patients were included with a median follow-up of 26 months. 23% of the patients received appropriate ATP therapy, which terminated the arrhythmia in 67%. A history of NSVT or monomorphic VT was the only predictor of appropriate ATP therapy (hazard ratio [HR] 2.73,  $P < 0.001$ ). Sixty-five of 221 patients with a history of NSVT received appropriate ATP (29%) versus 24 patients (11%) without a history NSVT ( $P < 0.001$ ).

This study concluded that a prior history of non-sustained ventricular tachycardia (NSVT) or monomorphic ventricular tachycardia was the only predictor of ATP. Patients with these features may not be good candidates for the S-ICD. No predictive value for successful ATP therapy is found in other patient characteristics such as underlying cardiac disease or prevention indication.<sup>49</sup>

In the absence of the need for ATP, S-ICD therapy could be more beneficially compared with TV-ICD therapy by avoiding transvenous lead complications. A patient tailored device selection, factoring in patients' choices, weighs the benefit of arrhythmia termination with ATP versus risks associated with transvenous leads. Shared decision making should be encouraged when it comes to selecting which defibrillation therapy to offer to patients who are found to be S-ICD eligible.

## **1.4 Specific patients' subgroups**

### **1.4.1 Heart failure**

#### **1.4.1.1 Epidemiology of Heart failure**

Heart failure (HF) is a global cardiovascular disease with an estimated prevalence of more than 37.7 million patients world-wide. It is estimated to affect 1-2% of adults in developed countries.<sup>50</sup> HF by the definition of the European Society of Cardiology (ESC) is a clinical syndrome characterized by typical symptoms (e.g. breathlessness, ankle swelling and fatigue) that may be accompanied by signs (e.g. elevated jugular venous pressure, pulmonary crackles and peripheral oedema) caused by a structural and/or functional cardiac abnormality, resulting in a reduced cardiac output and/ or elevated intracardiac pressures at rest or during stress.<sup>51</sup> It is commonly divided into two subcategories: heart failure with reduced ejection fraction (HFrEF) and heart failure with preserved ejection fraction (HFpEF). HFrEF is defined as an ejection fraction  $\leq 40\%$ , whereas HFpEF is defined as an ejection fraction  $\geq 50\%$ . Patients with an ejection fraction between 40-49% are considered to be in the "grey area" as per the ESC guidelines.<sup>51</sup>

Heart failure, regardless of its underlying aetiology, has a staggering effect on the quality of life, functioning and prognosis of patients while imposing heavy costs on the health care systems worldwide. For example, In the US alone, the total medical cost for patients with Heart failure was US\$20.9 billion in 2012 with a projected rise of cost up to \$53.1 billion by 2030.<sup>52</sup>

Despite increasing levels of care, and the use of evidence based pharmacological therapies as well as device therapies when indicated, heart failure runs a progressive course characterised by functional status declines resulting in multiple admissions to hospitals for heart failure. Acute HF is associated with a poor medium-term prognosis. The ESC-HF Pilot study was conducted in 136 Cardiology Centres in 12 European countries and included 5118 patients with heart failure. 1892 (37%) were admitted for acute HF and 3226 (63%) patients had chronic HF and were managed in outpatient settings. The all-cause mortality rate at 1 year was 17.4% in patients with acute HF and 7.2% in chronic HF. One-year hospitalization rates were 43.9% and 31.9%, in acute and chronic HF patients, respectively.<sup>53</sup>

#### **1.4.1.2 SCD in Heart failure**

A high proportion of deaths among patients with HF occur suddenly and unexpectedly. Many of these deaths can be attributed to ventricular arrhythmias. As such, many international guidelines recommend using ICDs to reduce the risk of sudden death in patients with heart failure. In the published 2016 ESC guidelines : An intracardiac defibrillator (ICD) is recommended as a secondary prevention measure to reduce the risk of sudden death and all-cause mortality in heart failure patients who have recovered from a ventricular arrhythmia (Class IA indication). In addition, an ICD is recommended to reduce the risk of sudden death and all-cause mortality in patients with symptomatic HF (NYHA Class II–III), and an LVEF  $\leq 35\%$  despite  $\geq 3$  months of optimal medical therapy (Class IA and IB indications in patients with ischaemic heart disease and patients with dilated cardiomyopathy respectively).<sup>51</sup>

Transvenous ICDS are associated with potential complications which can be characterised into complications that can occur at the time of implant, such as pneumothorax and cardiac tamponade due to traumatic placement of the lead(s), and long-term complications such as infection of the device which may progress into sepsis and/or infective endocarditis with potentially fatal consequences.<sup>22,54,55</sup>

#### **1.4.1.3 S-ICD in Heart failure**

The S-ICD offers an alternative solution to the traditional TV-ICD in treatment and prevention of sudden cardiac death in patients with heart failure. Studies have confirmed comparable efficacy

to TV-ICDS in the treatment of ventricular arrhythmias and it avoids many of the complications which have been associated with TV-ICD and is particularly useful in patients with no appropriate venous access or in patients at high risk of infective endocarditis.<sup>56</sup>

According to the AHA/ACC/HRS Guidelines for Ventricular Arrhythmia and Sudden cardiac death, there is a Class I recommendation for S-ICD implantation in patients (heart failure patients included) who are at a high risk for infection or are without appropriate venous access and have no indication for bradycardia or biventricular pacing and/or anti-tachycardia pacing (ATP).<sup>57</sup>

It is important to note that temporal variations in R wave and T wave amplitudes in the same individual are frequently observed on ECG recordings. As a consequence, the R:T ratio, a major predictor of S-ICD eligibility, is not fixed in the same individual. Different factors such as changes in posture and heart rate can influence the ECG parameters. Also, changes in electrolytes concentrations, body weight, fluid shifts, lungs congestion and/or pleural effusions can cause detectable dynamic changes on surface ECG recordings.<sup>58-63</sup> Heart failure patients share a lot of these factors that cause variation in the ECG components. This is particularly relevant in patients with significant changes in their weights and shifting of their body fluid status over short time such as heart failure patients undergoing diuresis. The mere presence of LV dysfunction is a standalone factor contributing to the variation of ECG parameters over time.<sup>64</sup>

## **1.4.2 Adult congenital heart disease**

### **1.4.2.1 Prevalence of ACHD**

While the prevalence of severe congenital heart defects is declining in many developed countries, owing to foetal screening, the overall prevalence is increasing globally with a current prevalence of 9 per 1000 new-borns albeit with substantial geographic variation.<sup>65</sup> Due to medical and surgical advances, >90% of individuals who are born with congenital heart defects survive into adulthood.<sup>65</sup> As a result, the prevalence of adult congenital heart disease (ACHD) in the community has increased.

### **1.4.2.2 Common ACHD**

ACHDs can be classified into mild, moderate, and severe according to their complexity, see Figure 9 below.

## Classification of congenital heart disease complexity

**MILD:**

Isolated congenital aortic valve disease and bicuspid aortic disease  
 Isolated congenital mitral valve disease (except parachute valve, cleft leaflet)  
 Mild isolated pulmonary stenosis (infundibular, valvular, supra-ventricular)  
 Isolated small ASD, VSD, or PDA  
 Repaired secundum ASD, sinus venosus defect, VSD, or PDA without residua or sequelae, such as chamber enlargement, ventricular dysfunction, or elevated PAP.

**MODERATE:** (Repaired or unrepaired where not specified; alphabetical order)

Anomalous pulmonary venous connection (partial or total)  
 Anomalous coronary artery arising from the PA  
 Anomalous coronary artery arising from the opposite sinus  
 Aortic stenosis - subvalvular or supra-ventricular  
 AVSD, partial or complete, including primum ASD (excluding pulmonary vascular disease)  
 ASD secundum, moderate or large unrepaired (excluding pulmonary vascular disease)  
 Coarctation of the aorta  
 Double chambered right ventricle  
 Ebstein anomaly  
 Marfan syndrome and related HTAD, Turner Syndrome  
 PDA, moderate or large unrepaired (excluding pulmonary vascular disease)  
 Peripheral pulmonary stenosis  
 Pulmonary stenosis (infundibular, valvular, supra-ventricular), moderate or severe  
 Sinus of Valsalva aneurysm/fistula  
 Sinus venosus defect  
 Tetralogy of Fallot – repaired  
 Transposition of the great arteries after arterial switch operation  
 VSD with associated abnormalities (excluding pulmonary vascular disease) and/or moderate or greater shunt.

**SEVERE:** (Repaired or unrepaired where not specified; alphabetical order)

Any CHD (repaired or unrepaired) associated with pulmonary vascular disease (including Eisenmenger syndrome)  
 Any cyanotic CHD (unoperated or palliated)  
 Double-outlet ventricle  
 Fontan circulation  
 Interrupted aortic arch  
 Pulmonary atresia (all forms)  
 Transposition of the great arteries (except for patients with arterial switch operation)  
 Univentricular heart (including double inlet left/right ventricle, tricuspid/mitral atresia, hypoplastic left heart syndrome, any other anatomic abnormality with a functionally single ventricle)  
 Truncus arteriosus  
 Other complex abnormalities of AV and ventriculoarterial connection (i.e. crisscross heart, heterotaxy syndromes, ventricular inversion).

ASD = atrial septal defect; AV = atrioventricular; AVSD = atrioventricular septal defect; CHD = congenital heart disease; HTAD = heritable thoracic aortic disease; LV = left ventricle/ventricular; PA = pulmonary artery; PAP = pulmonary artery pressure; PDA = patent ductus arteriosus; VSD = ventricular septal defect.

Figure 9 Classification of congenital heart diseases.<sup>65</sup>

### 1.4.2.3 SCD in ACHD

Sudden cardiac death (SCD) is a major cause of mortality in ACHD patients, accounting for 19-26% of all deaths in ACHD patients and is mostly caused by ventricular arrhythmias.<sup>65</sup> The overall SCD incidence in ACHD patients is higher than in the age-matched population without congenital heart disease.<sup>66</sup> As more patients with congenital heart disease survive to adulthood, rates of SCD are expected to rise as longer life expectancy increases the prevalence of arrhythmias owing to structural remodelling. However, not all patients with ACHD have the same risk, as the risk of ventricular arrhythmias and SCD are found to be higher in certain types of congenital heart disease, see Figure 10.

### 1.4.2.4 SVT in ACHD

Supraventricular tachycardias (SVTs) are quite common in ACHD. In some studies, SVTs occurred in up to 38 % in 50-year-old patients with ACHD. Surgical intervention during childhood in ACHD patients lead to the formation of myocardial scars that can act as substrates for SVTs. In addition, some forms of ACHD such as Ebstein's anomaly and congenitally corrected transposition of great arteries (TGA) are associated with high prevalence of AV pathways and accessory connections, also acting as substrates for SVTs.<sup>67</sup>

Most SVTs manifest as narrow complex tachycardias (QRS duration <120 ms), However SVTs can present as wide complex tachycardias (QRS duration >120 ms), such as in SVT with bundle-branch block (BBB) aberration or conduction over an accessory pathway. This is relevant because this can potentially lead to misinterpreting of these SVTs as VTs by an ICD and delivering inappropriate shock therapy.

Type of CHD	Sustained VT	SCD
Secundum ASD		
Superior sinus venosus defect		
AVSD/primum ASD	(+)	
VSD	+	(+) <sup>a</sup>
Ebstein anomaly	(+)	++ <sup>b</sup>
TOF	++	++
TGA		
Atrial switch	+++ <sup>c</sup>	+++ <sup>b</sup>
Arterial switch	+ <sup>c</sup>	(+)
ccTGA	(+)	++ <sup>b</sup>
Fontan operation		
Atriopulmonary connection		+ <sup>b</sup>
Intracardiac lateral tunnel		+ <sup>b</sup>
Extracardiac conduit		+ <sup>b</sup>
Eisenmenger physiology Incompletely palliated CHD		++ <sup>d</sup>

Figure 10 Risk of Ventricular arrhythmias and SCD, (+), +, ++, +++ denotes minimal, mild, moderate, and severe risk respectively.<sup>65</sup>

#### 1.4.2.5 ICDs in ACHD

While the decision to implant ICDs for secondary prevention is relatively straight forward, the decision to implant ICD for primary prevention in ACHD can be more challenging due to the lack of robust evidence in the ACHD population, see Figure 11.



Implantable cardiac defibrillator		
ICD implantation is indicated in adults with CHD who are survivors of an aborted cardiac arrest due to VF or haemodynamically intolerated VT after evaluation to define the cause of the event and exclusion of reversible causes.	I	C
ICD implantation is indicated in adults with CHD and sustained VT after haemodynamic evaluation and repair when indicated. EP evaluation is required to identify patients in whom catheter ablation or surgical ablation may be beneficial as adjunctive treatment or in whom it may offer a reasonable alternative.	I	C
ICD implantation should be considered in adults with CHD with biventricular physiology and a systemic LV presenting with symptomatic heart failure (NYHA II/III) and EF $\leq$ 35% despite $\geq$ 3 months of optimal medical treatment, provided they are expected to survive substantially longer than one year with good functional status. <sup>c</sup>	IIa	C
ICD implantation should be considered in patients with CHD and unexplained syncope and suspicion for arrhythmia aetiology and either advanced ventricular dysfunction or inducible VT/VF at programmed electrical stimulation.	IIa	C
ICD implantation should be considered in selected TOF patients with multiple risk factors for SCD, including LV dysfunction, non-sustained, symptomatic VT, QRS duration $\geq$ 180 ms, extensive RV scarring on CMR, or inducible VT at programmed electrical stimulation.	IIa	C
ICD implantation may be considered in patients with advanced single or systemic RV dysfunction (EF systemic RV $<$ 35%) in the presence of additional risk factors. <sup>d</sup>	IIb	C

Figure 11 ESC guidelines on ICD implantation in ACHD population.<sup>65</sup>

Vehmeijer et al reviewed the available literature on ICD indications, efficacy, and ICD-related complications in ACHD patients and published their meta-analysis on the use of ICD in the ACHD population in the European Heart Journal in 2016. A total of 2162 ACHD patients, who underwent ICD implantation (transvenous ICD in 96.1%) were included in the meta-analysis from 24 different studies, see Figure 12. The mean follow-up for the analysis was 3.7+0.9 years. More than half of all the implants (53.2%, (43.5–62.7)) were for primary prevention. The decision for implanting an ICD for primary prevention was guided by the presence or absence of multiple risk factors: non sustained VT, impaired systemic ventricular function, inducible VT, and syncope being the most prevalent. 220 patients had secondary prevention ICDs following sustained VT in 61% and cardiac arrest in 39%.<sup>68</sup>

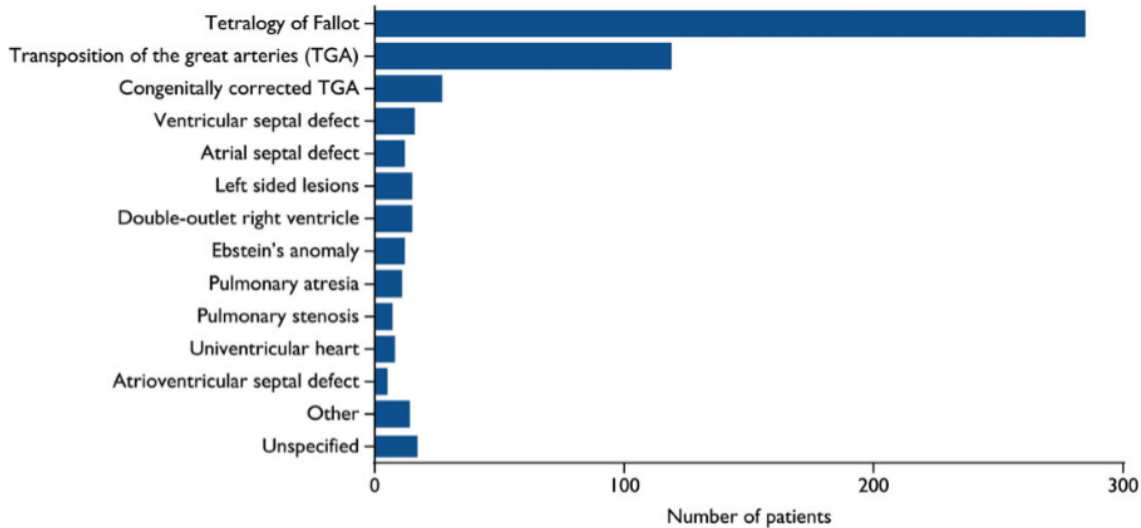


Figure 12 Distribution of the congenital heart diseases in the meta-analysis.<sup>65</sup>

The proportion of patients who received one or more appropriate ICD shocks was 23.3% (18.6–31.3) which is similar to the 22.3% experienced by the conventional ICD population of ischaemic and non-ischaemic cardiomyopathy patients of the Sudden Cardiac Death in Heart Failure Trial (SCD-HeFT). Over one in four patients (25.6%, 18.9–33.6) experienced ICD-related complications and 76% of those complications involved lead or generator-related issues. A total of 390 inappropriate shocks, caused predominantly by SVT, were delivered to 76 patients. This meta-analysis demonstrated that the rates of inappropriate shocks and ICD-related complications were higher (26%) in the ACHD population when compared with those of the conventional ICD population included in the SCD-HeFT trial (14%) for the same duration of follow up of 3.8 years.<sup>65</sup>

#### 1.4.2.6 S-ICD in ACHD

The S-ICD may especially be valuable for ACHD patients as potential anatomical challenges of transvenous lead implantation in ACHD patients can be overcome with a subcutaneous approach. Adult congenital heart disease patients are also younger and require several generator replacements during their lifetime increasing the risk of potential complications associated with TV-ICDs making them less appealing.

D'Souza et al conducted a pooled analysis of patients in the EFFORTLESS S-ICD registry and the U.S. IDE study. Patients with a diagnosis of moderate to complex structural congenital heart disease were compared to patients without ACHD. The analysis included 865 patients, 19 with ACHD and 846 without. Median follow-up was 567 days and 639 days for ACHD and non-ACHD groups, respectively.

There were no deaths and no appropriate shocks for ventricular tachycardia/ventricular fibrillation in the CHD cohort, versus 26 deaths (3.1%,  $p = 0.42$ ) and 111 appropriate shocks in 59 patients (7.1%) in the non-ACHD cohort ( $p = 0.23$ ). Successful defibrillation testing at 80J was comparable for the CHD versus non-CHD groups (100% vs. 98.5%) The overall complication rates were similar in the ACHD and non-ACHD groups (10.5% vs. 9.6%,  $p=0.89$ ), with inappropriate shocks for T-wave oversensing being the only complication in the ACHD group ( $N=2$ ). The rate of inappropriate shocks due to any cause was similar for both groups (10.5% in patients with ACHD vs. 10.9% in patients without ACHD,  $p=0.96$ ). The rate of T-wave oversensing was higher (10.5%, (2.9%, 31.4%)) in ACHD patients when compared with non-ACHD patients (4.4%, (3.2%, 6.0%)), however it didn't reach statistical significance ( $p=0.2$ )

This was the first reported analysis comparing use of the S-ICD in patients with and without ACHD. It showed that the S-ICD is a safe option for patients with ACHD deemed to be at high risk for SCD without having pacing indications. Although the overall complication rates were comparable in both groups, the overall incidence of T-wave oversensing was greater in the ACHD group.<sup>69</sup>

#### 1.4.2.6.1 Screening for S-ICD in ACHD

Literature concerning the eligibility for subcutaneous defibrillator (S-ICD) in patients with adult congenital heart disease is scarce with only a handful of published studies with varying results available.

Alonso et al conducted a study to test S-ICD eligibility specifically in ACHD patients at high risk of SCD to determine the proportion of those patients who would be eligible for S-ICD using standard screening methods. A patient was considered eligible for a S-ICD when at least one sensing vector was considered appropriate in all QRS-T complexes of the ECG strip in both supine and seated position at the same gain. Their analysis was performed on 175 patients, 102 (58%) with Tetralogy of Fallot (ToF), 33 (19%) with systemic RV, and they had 40 patients (23%) in the non-congenital heart disease (control) group. Khairy score calculated for ToF patients showed a mean score of  $2.4 \pm 0.2$ . Using a score of  $\geq 3$  (intermediate to high risk) as the cut-off point, 33 patients (33%) were identified as being at significant risk of SCD. The remaining 69 patients (67%) were deemed to have low SCD risk. 69 patients (68%) of all patients with Tetralogy of Fallot and only 44% of the significant-risk subgroup were eligible for a S-ICD and 26 (80%) patients with systemic RV were deemed eligible for a S-ICD. In contrast, in the control (non-congenital heart disease) group, 37 patients (92%) were deemed eligible for S-ICD after screening ( $p= .03$ ). Predictive factors for failing screening obtained by univariate analysis included QRS duration, QT duration, and ToF. By

multivariate analysis, however, the only independent predictor of conventional screening failure was QRS width (OR = 1.06, CI95 1.03–1.1;  $p = .001$ ). The study concluded that S-ICD eligibility is low in ToF patients at significant risk of SCD.<sup>70</sup>

In another study by Wang et al, ACHD outpatients ( $n = 101$ ; age  $42 \pm 14$  years; 52% female; 85% white; left ventricular ejection fraction [LVEF]  $56\% \pm 9\%$ ) were enrolled in a prospective study to determine eligibility of S-ICD in ACHD Patients. ECG morphologies in standing and supine positions were evaluated using a digitized version of the Boston Scientific EMBLEM S-ICD Patient Screening tool by two different investigators. A sensing vector passed screening if maximum QRS amplitudes crossed the dotted line for the screening tool and all QRS complexes and T waves fit within a profile in all beats, in both standing and supine 10-second recording at 5–20 mm/mV gain.

Forty percent of participants were ineligible for S-ICD. Female participants had greater odds of eligibility (adjusted odds ratio [OR] 5.9; 95% confidence interval [CI] 1.6–21.7;  $P = .008$ ). Sixty-one participants (60%) passed screening; while no patients had all their 3 S-ICD vectors deemed eligible. Less than half of the patients had 2 eligible vectors, whereas nearly one-quarter of participants failed all 3 vectors..<sup>71</sup>

Garside et al conducted a prospective analysis of S-ICD eligibility for 102 ACHD (TOF, Fontan, Transposition of the great arteries (TGA)) patients at a large quaternary specialist ACHD centre (Queen Elizabeth Hospital, United Kingdom). The screening ECG was carried out and analysed according to the S-ICD manufacturer's protocol, using the manufacturer manual screening tool. Mean age for the patients was 30.7 ( $\pm 1.19$ ) years and 54 (53.0%) patients were female. In addition to their primary diagnosis, five (4.9%) patients also had dextrocardia and 61 (59.8%) had a bundle branch block, of which 83.6% were right bundle branch block (RBBB). A total of 77 (75.4%) patients were deemed eligible for an S-ICD with at least one suitable vector. The primary vector was the most common suitable vector found in 48 (62%) participants who had appropriate sensing vectors. Out of eligible patients, 36 (47%) had 2 eligible vectors, whereas only 12 (16%) had all three acceptable vectors and 29 (38%) had only one suitable vector.

Twenty-five (24.5%) patients had no eligible vectors and subsequently failed the S-ICD screening criteria. Only one Fontan patient was deemed ineligible ( $p = 0.01$ ). While 36% of patients with TOF were ineligible ( $p = 0.001$ ). R:T ratio was significantly smaller in the ineligible group ( $p = 0.03$ ), with a mean value of 1.8 for the ineligible group and 2.9 for the eligible group, respectively.<sup>37</sup>

All the above-mentioned studies, acknowledging the high variability of their outcomes, demonstrated higher ineligibility rates in the ACHD population when compared with general population. This may be due to abnormal T-wave morphology, resulting from the unique anatomical and physiological features that characterizes ACHD, such as cardiac chamber enlargement, abnormal cardiac orientation, mechanical strain, and augmented repolarization patterns. ACHD patients who pass the current S-ICD screening are also more likely to suffer inappropriate shocks from their S-ICD when compared to S-ICD recipients without congenital heart disease as demonstrated in the analysis of ACHD in the EFFORTLESS S-ICD registry and the U.S. IDE study.<sup>69</sup>

### **1.4.3 Hypertrophic cardiomyopathy**

#### **1.4.3.1 Epidemiology of HCM**

Hypertrophic cardiomyopathy (HCM) is the most common inherited cardiovascular disorder.<sup>72</sup> It affects 1 in 500 individuals worldwide<sup>72</sup> and remains the most common cause of sudden cardiac death (SCD) in the young, mainly due to fatal arrhythmic events.<sup>73</sup>

In most cases, it is caused by mutations in cardiac sarcomere protein genes and is inherited in an autosomal dominant fashion.<sup>74</sup> It is characterised by a wall thickness  $\geq 15$  mm in one or more Left ventricular segments. The ESC defines HCM by the presence of increased left ventricular wall thickness that is not solely explained by abnormal loading conditions.<sup>74</sup>

#### **1.4.3.2 Clinical course of HCM**

Clinical manifestations resulting from HCM include diastolic dysfunction, left ventricular outflow tract obstruction, mitral regurgitation, microvascular ischaemia, atrial fibrillation, ventricular arrhythmia, and sudden cardiac death. The most recorded fatal arrhythmic event is spontaneous ventricular fibrillation.<sup>74</sup>

Most recent series of adult patients with HCM report an annual incidence for cardiovascular death of 1–2%, with SCD, heart failure and thromboembolism being the main causes of death. However, most patients will have normal life expectancy, owing to widespread adoption of

pharmacological therapy, family screening for affected individuals, risk stratification and implantation of ICDs for high-risk patients.<sup>74</sup>

### 1.4.3.3 Management of HCM

Patients with HCM should be advised against participation in competitive sports and discouraged from intense physical activity, especially when they have risk factors for SCD.<sup>74</sup>

Pharmacological therapy aims to improve functional capacity, reduce symptoms, and prevent disease progression. In patients who have evidence of outflow tract obstruction, the aim is to reduce symptoms using drugs such as B-blockers and non-dihydropyridine calcium channel blockers, surgical myomectomy, septal ablation, or pacing. Therapy in patients without obstruction focuses on managing arrhythmia, reducing LV filling pressures, and treatment of angina. Patients with progressive LV dysfunction refractory to medical therapy may be candidates for cardiac transplantation.<sup>74</sup>

Estimation of SCD risk is essential in the management of HCM and patients at high risk of SCD need to be identified so they can be offered potentially life-saving treatment. Interestingly, until recently there were no randomized trials or statistically validated prospective prediction models that could be used to estimate the risk of SCD and guide ICD implantation in patients with HCM. Recommendations were instead based on observational, retrospective studies that have outlined the relationship between some clinical characteristics in HCM and prognosis.<sup>74</sup>

In 2014, “HCM Risk-SCD”, a novel clinical risk prediction model for sudden cardiac death in hypertrophic cardiomyopathy was designed and validated. This model was derived from a large, diverse, and well characterized population of patients followed at 6 different European centres. This was the first validated risk prediction model for SCD in patients with HCM, and it was adopted by the ESC guidelines in 2014. This clinical risk prediction model uses readily available clinical parameters, see Figure 13, and relies on complex mathematical and statistical modelling, see Figure 14, to produce a score that stratifies 3 groups of risk: low, intermediate, and high risk, according to the estimated 5-year risk of SCD (<4%, 4%–6%, and ≥6%, respectively). While this

new model has been widely incorporated into practice, clinical decisions in intermediate-risk patients remains challenging.<sup>7374</sup>

Predictor variable	Definition	Coding
Age	Age at evaluation.	Continuous, years
Family history of SCD	History of sudden cardiac death in 1 or more first degree relatives under 40 years of age or SCD in a first degree relative with confirmed HCM at any age (post- or ante-mortem diagnosis).	Binary (yes = 1/ no = 0)
Maximal wall thickness	The greatest thickness in the anterior septum, posterior septum, lateral wall, and posterior wall of the LV, measured at the level of the mitral valve, papillary muscles, and apex using parasternal short-axis plane using 2-D echocardiography at time of evaluation	Continuous, mm
Fractional shortening	(LV end-diastolic dimension-LV end-systolic dimension)/ LV end-diastolic dimension measured by M-Mode or 2D echocardiography at time of evaluation	Continuous, %
Left atrial diameter	Left atrial diameter determined by M-Mode or 2D echocardiography in the parasternal long axis plane at time of evaluation	Continuous, mm
Maximal left ventricular outflow tract gradients	The maximum LV outflow gradient determined at rest and with Valsalva provocation (irrespective of concurrent medical treatment) using pulsed and continuous wave Doppler from the apical three- and five-chamber views. Peak outflow tract gradients were determined using the modified Bernouilli equation: Gradient = $4V^2$ , where V is the peak aortic outflow velocity	Continuous, mmHg
Non-sustained ventricular tachycardia	$\geq 3$ consecutive ventricular beats at a rate of $\geq 120$ bpm and $< 30$ s in duration on Holter monitoring (minimum duration 24 hours) at or prior to evaluation.	Binary (yes = 1/ no = 0)
Unexplained syncope	History of unexplained syncope at or prior to evaluation.	Binary (yes = 1/ no = 0)

Figure 13 Predictive variables for the HCM Risk-SCD model.

$$\hat{P}_{\text{SCD at 5 years}} = 1 - 0.998^{\text{exp(Prognostic Index)}}$$

where Prognostic Index =  $0.15939858 * \text{Maximal wall thickness (mm)} - 0.00294271 * \text{Maximal wall thickness}^2 \text{ (mm}^2\text{)} + 0.0259082 * \text{Left atrial diameter (mm)} + 0.00446131 * \text{Maximal left ventricular outflow tract gradient (mmHg)} + 0.4583082 * \text{Family history SCD} + 0.82639195 * \text{NSVT} + 0.71650361 * \text{Unexplained syncope} - 0.01799934 * \text{Age at clinical evaluation (years)}$ .

Figure 14 Score calculation for the HCM Risk-SCD model.<sup>74</sup>

There are no randomized, controlled data to support the use of antiarrhythmics for the prevention of SCD in HCM. Guidelines recommend the use of ICD in preventing SCD due to arrhythmia in HCM. Patients with HCM who survive VF or sustained ventricular tachycardia are at very high risk of subsequent lethal cardiac arrhythmias and should receive an ICD (Secondary prophylaxis). Risk prediction models such as the widely adopted “HCM Risk-SCD” can be used to stratify risk of SCD and guide clinicians to identify HCM patients who would likely benefit from having an ICD as a primary prophylaxis, see Figure 15. In all cases, and prior to implantation,

patients should be counselled, using a shared decision approach, on the risk of inappropriate shocks, implant complications, and the social and occupational implications (including driving restrictions) of having an ICD.<sup>74</sup>

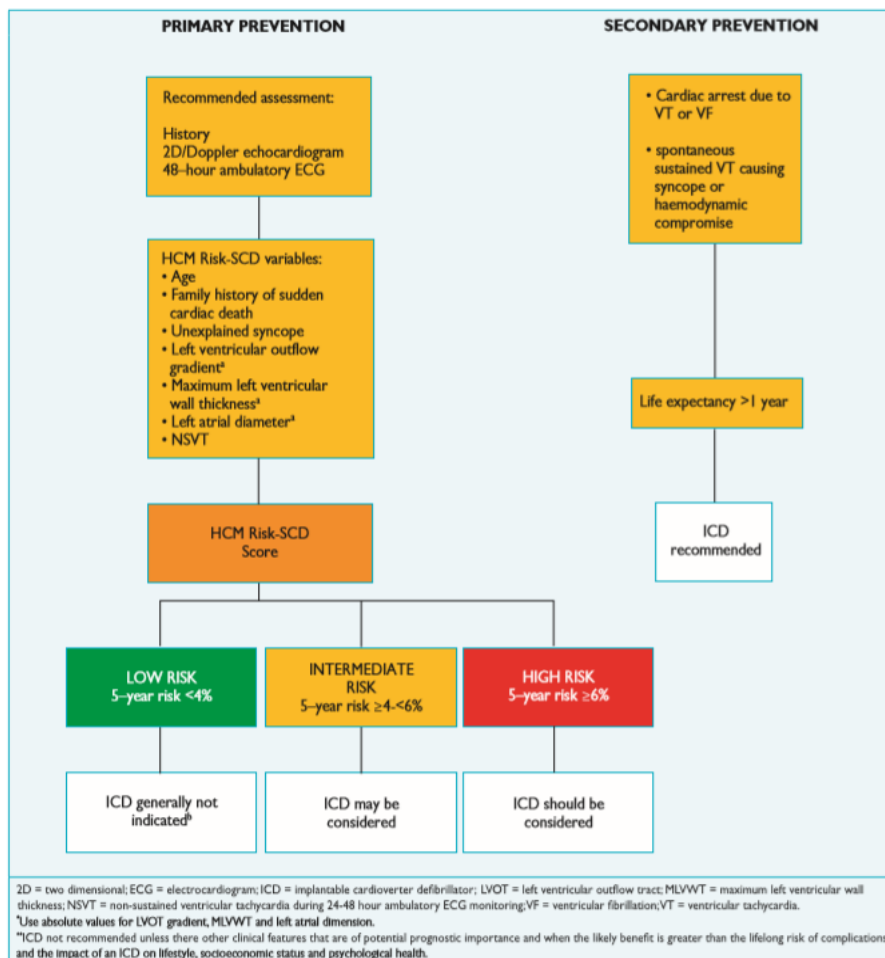


Figure 15 Flow Chart guiding decision for implanting ICD in HCM patients.<sup>74</sup>

#### 1.4.3.4 Role of S-ICD in HCM

HCM patients can be young and require longer ongoing protection from sudden cardiac death (SCD). The risk of transvenous ICD lead failure increases over time. In a TV-ICD, lead failure rates range from 5-15% and may be as high as 40% at 8 years accounting for additional morbidity and mortality because of the need for additional transvenous leads, with or without lead extraction.<sup>75</sup>

One of the key advantages of the S-ICD is the avoidance of lead complications. The S-ICD lead is not subject to the same environment as a transvenous lead. Also, the absence of a lumen in the S-ICD lead reduces the risk of lead failure. Therefore, survival of an S-ICD lead can be expected to be



longer than a transvenous lead, making it a particularly good option for the young individual. Moreover, the consequences of lead failure or infection are far less serious with an S-ICD compared to a transvenous system because removal of an S-ICD lead is of much lower risk compared to a transvenous lead. It seems reasonable that the subcutaneous ICD may be considered in HCM patients who have no indication for pacing.

In one large study published in 2016, Lambiase et al compared the outcomes of patients with HCM implanted with S-ICD to those of non-HCM S-ICD recipients using pooled data from a total of 872 subjects enrolled in the EFFORTLESS Registry and US IDE study. The cohort included 99 HCM (75% male) and 773 non-HCM (72% male) patients with a median follow up of 637 days. The HCM group were younger and more likely to receive a primary prophylaxis S-ICD (88.5% vs 67.5%,  $P < 0.001$ ). At the time of the implant, successful defibrillation was achieved in 98.9% of HCM and 98.5% of non-HCM patients. One-year post-implant complication-free rates were similar: 92.7% in HCM (No lead complications requiring intervention) versus 89.5% in non- HCM. Overall shock conversion efficacy was 100% in HCM versus 98% non-HCM. Inappropriate shocks occurred in 12.5% HCM patients and 10.3% non-HCM patients. In HCM, inappropriate shocks (10.4% of patients) were mostly caused by oversensing issues particularly due to TWO versus 7.2% T wave oversensing in the non-HCM patients.<sup>76</sup>

Overall, that analysis of S-ICD performance in the HCM population showed that the S-ICD could safely and effectively convert ventricular tachyarrhythmias. The rate of inappropriate shocks was comparable to patients without HCM treated with the S-ICD and to patients with HCM treated with a transvenous ICD. These data support the continued use of the S-ICD in the HCM population with the application of careful pre-operative screening and device programming to minimise inappropriate shocks.<sup>76</sup>

#### **1.4.3.4.1 Screening for S-ICD in HCM**

Currently, an S-ICD system may be considered in HCM patients with no indication for pacing (Class IIb, level of Evidence C) according to published ESC guidelines for HCM. The ESC guidelines also recommend that each patient should have more than one ECG vector that passes screening, to allow alternative programming if oversensing does occur.<sup>74</sup>

Although most patients with HCM have no pacing requirement<sup>74</sup>. Previous studies in a mixed SCD risk cohort have suggested that HCM is an independent risk factor for S-ICD screening failure.<sup>77</sup> In HCM, the cardiac frontal axis is increasingly shifted towards the left owing to left ventricular hypertrophy. This can shift the major depolarizing and repolarizing vectors parallel to the primary screening vector, producing large QRS and T waves which are more likely to fail screening. Interestingly, one study reported that the alternate sensing vector was the most compatible in their cohort of HCM patients which is contrary to the findings in non-HCM cohort where the alternate vector is the least likely to pass S-ICD screening.<sup>78</sup>

Studies looking specifically into the proportion of HCM patients who satisfy the S-ICD screening criteria reported highly varying eligibility rates. Francia et al reported eligibility rates of 85 – 93% after selectively screening<sup>79</sup> HCM patients for S-ICD eligibility and found a failure rate of 7% at rest using the standard supine and standing screening method. 15% of patients failed the screening after exercise testing. Maurizi et al screened 165 patients with HCM and reported a 16% screening failure rate. However, they did not screen these patients after exercise.<sup>78</sup> Lambiase et al conducted a study to assess the proportion of HCM patients with risk factors for SCD (41% high risk and 18% intermediate ESC score risk for SCD) without pacing indications who would be eligible for an S-ICD based on screening at rest and on exercise. A total of 131 HCM patients with  $\geq 1$  risk factor for SCD were screened for eligibility for S-ICD between July 2014 and September 2015. In total, 50 (38%) patients were ineligible for the S-ICD with 1-vector safety and 71% were ineligible with  $\geq 2$ -vector safety. Most importantly, younger patients and patients with higher 5-year risk of SCD were more likely to fail the screening in that study.<sup>80</sup> In all those studies, high T-wave voltages were the main cause of screening failure. This is consistent with the high rate of inappropriate shocks due to TWOs in HCM patients.<sup>76</sup>

#### **1.4.3.4.2 Inappropriate shocks in HCM**

S-ICD patients with HCM are at increased risk for inappropriate shocks due to either the occurrence of SVT or cardiac oversensing due to T-wave oversensing with increasing T-wave amplitudes particularly during exercise.<sup>81</sup> Since cardiac oversensing usually occurs during increased heart rates, oversensing can be minimized by screening HCM patients for S-ICD eligibility at rest and after exercise.

In a study by Lambiase et al, the outcomes of patients with HCM implanted with S-ICD were compared to non- HCM S-ICD recipients using pooled data from a total of 872 subjects enrolled in the EFFORTLESS Registry and US IDE study. The cohort included 99 HCM and 773 non-HCM patients with a median follow up of 637 days. There was no significant difference in the incidence of inappropriate shocks in both HCM and non- HCM patients. However, in HCM, the majority of inappropriate shocks (10.4% of patients) were caused by TWO versus 7.2% TWO in the non-HCM patients.<sup>76</sup>

The long-term outcomes from the EFFORTLESS study have been recently published by Lambiase et al. 984 S-ICD patients with diverse diagnoses were followed up for a median of 5.1 (4.7-5.5) years. 155 patients experienced 328 inappropriate shocks, with the commonest cause of inappropriate shocks of cardiac oversensing in 106 patients (68.3%). Interestingly, the annual inappropriate shocks rate dropped to 2.1% in years 2–5 after an initial 8.7% in year 1, but the main cause of inappropriate shocks was TWO. This highlights the importance of optimising the programming of S-ICDs which has the potential to markedly reduce the risk of inappropriate shocks due to TWO.<sup>82</sup>

76

#### **1.4.3.4.3 Progressive ECG changes in HCM**

In HCM, there is progressive hypertrophy and remodelling of the ventricles over time. This translates into dynamic changes on the surface ECG where R wave amplitude and T wave morphology can vary significantly over time. In one study by McKenna et al, the natural history of electrocardiographic left ventricular hypertrophy was assessed in relation to clinical features, treatment, and prognosis in 100 patients with hypertrophic cardiomyopathy who were followed for a mean of 8(5-20) years. At the initial diagnosis, the voltage measurement from S wave in V1 + R wave in V5 was 37 +/- 20 mm, the R wave in lead aVL was 12 +/- 6 mm and the mean frontal plane voltage was 15 +/- 10 mm. After 5 years, these values were increased to 43 +/- 22 mm (p <0.0002), 14 +/- 6 mm (p < 0.003) and 17 +/- 10 mm (p< 0.01), respectively. In addition, 20% of cases developed >10mm increase in R wave amplitude over 20 years follow-up. The authors concluded that in HCM, there is electrocardiographic evidence of progressive

hypertrophy.<sup>83</sup> These ongoing changes can be detrimental to the functioning of the S-ICD because the device sensing functions are currently entirely dependent on the surface ECG.

Therefore, it is arguable that there is a need to carefully monitor these patients to ensure that the evolution in ECG morphology with disease progression does not alter device sensing. This is particularly relevant in lower-risk younger HCM cohorts where screening failure is low and clinicians may favour to implant an S-ICD, given the lower risk of long-term complications. Such patients will benefit from monitoring their ECGs on follow-up, and if significant changes develop, the S-ICD can be optimized to avoid any inappropriate therapies.

These dynamic QRS-T wave changes also emphasise the importance of further scrutinising the screening process in these often-young HCM patients prior to implant to ensure adequate patient selection and to optimise S-ICD vector selection to avoid future oversensing issues and inappropriate shocks.

#### **1.4.4 Dynamic ECG changes in ARVC**

Arrhythmogenic right ventricular cardiomyopathy (ARVC) is an inherited cardiomyopathy which is characterised by electrical instability which can potentially lead to ventricular arrhythmias and sudden cardiac death.

Negative T waves in right precordial leads (V1 to V3) are observed in up to 80% of ARVC patients. Zorzi et al, assessed the ECG changes that occur during exercise testing of 35 ARVC patients with negative T waves in the precordial leads at the baseline. There was a complete normalization of right precordial negative T waves with exercise in 34% of patients and a trend toward normalization (i.e., either normalization or partial reversal) in 91% of patients.<sup>84</sup>

Although the electrophysiologic mechanisms underlying these significant ECG changes upon exercise in ARVC are unknown, these ECG changes has important clinical implications. ARVC patients are often young and are at risk of ventricular arrhythmias and sudden cardiac death. As such, they require many years of defibrillator therapy making S-ICD therapy an appealing option for these patients. However, in view of the dynamicity of the ECG in these patients during exercise, this may result in the lack of consistency of appropriate S-ICD sensing vectors during S-

ICD screenings both at resting and during exercise or inappropriate S-ICD sensing and delivery of inappropriate therapy in S-ICD recipients.

## 1.5 Leadless pacemakers

While transvenous pacemakers are well established solutions for management of bradycardia, it has been shown that almost 90% of their complications are related to the presence of endovascular leads and device pocket issues, such as erosion and infection.<sup>85–87</sup> Occasionally, it can sometimes be difficult to do transvenous pacing due to access issues such as difficult underlying anatomy or vascular occlusions. Also, in some cases transvenous pacing poses a high risk of infection particularly in patients with prior history of device related infections.

Improvements in battery technology and advanced electrical circuitry helped in the development of leadless pacemakers (LP). LPs are much smaller self-contained intracardiac single-chamber pacemakers delivered in the right ventricle through a percutaneous transfemoral catheter-based approach. They are screwed (Nanostim<sup>®</sup>, Abbott Medical Sylmar, CA, USA) or anchored (Micra<sup>®</sup>, Medtronic, Minneapolis, MN, USA) with tines into the endocardium of the right ventricle.

The first leadless pacemaker (Nanostim<sup>®</sup>) was implanted in a patient in December 2012.<sup>88</sup> In December 2013, the first-in-human implantation of Micra<sup>®</sup>, another leadless pacemaker developed by Medtronic™ was performed at the Kepler University Hospital in Linz, Austria.<sup>89</sup> Both leadless pacing systems shared a few similarities. Both systems were delivered through a wide bore sheath inserted through the femoral vein. Also, both of them incorporated motion sensors and rate response algorithms. Both had steroid eluting tips to help reduce inflammation and maintain low thresholds. In addition, both devices have been designed to recapture the system for repositioning or retrieval if need be.

Implantation is performed in the Catheter laboratory, under fluoroscopy, through a venous femoral approach, under local anaesthesia. A dedicated deflectable delivery catheter with the pacemaker housed in its distal part is advanced through the inferior vena cava and the right atrium, across the tricuspid valve and into the right ventricle. Once inside the right ventricle, the catheter with the pacemaker is placed against the apex or the septum. Once adequate position is confirmed, the pacemaker is screwed (Nanostim<sup>®</sup>) or anchored (Micra<sup>®</sup>) with tines into the

endocardium of the right ventricle and the pacemaker is liberated from the delivery catheter, although it still maintains a connection to it by a tethering mechanism. This allows pacemaker thresholds, sensing, and impedance as well as stability to be tested. If sensing and pacing parameters are not satisfactory, the pacemaker may be repositioned to an alternative position before final release from the delivery catheter. Otherwise, after adequate parameters are confirmed, the pacemaker is released, and the catheter system is removed. Later, the leadless pacemakers become encapsulated into the cardiac tissue, in the same way that parts of pacing leads of transvenous systems can. LPs are, theoretically, unlikely to be retrievable at the end of battery life due to encapsulation. At the end of the battery life, a leadless pacemaker can be turned off and a new pacemaker implanted (Leadless or traditional) if clinically indicated.

The main differences between the 2 systems are (a) Mechanism of fixation, (b) Programming systems, and (c) Size. Micra<sup>®</sup> is 26 mm in length, 7 mm in width, and 0.8 cm<sup>3</sup> in volume. Compared to the Nanostim<sup>®</sup>, Micra<sup>®</sup> is considerably shorter but approximately 1 mm thicker, therefore requiring a 23F sheath (27F outer diameter) for implantation. The fixation mechanism is also significantly different, Micra<sup>®</sup> attaches to the right ventricle myocardium via four linear self-expanding nitinol tines, while Nanostim<sup>®</sup> attaches via an active screw-in helix and secondarily via three nitinol tines angled perpendicularly to the helix. The estimated battery longevity is approximately 10 years for both devices which is comparable to standard transvenous pacemakers. Overall, both systems have demonstrated a high implant success rate and low serious adverse event rate.<sup>90</sup>

Complications may occur during the procedure, which may be related to femoral vein access which may be minimised by using ultrasound guidance to gain access. There is also the risk of cardiac perforation with subsequent pericardial effusion. This can be minimised by preferentially implanting the pacemaker into the septal wall avoiding the free wall of the right ventricle. Furthermore, pacing from the septum might result into narrower QRS complexes leading to less desynchrony. Heparin is administered during the procedure to prevent the development of thrombosis.

Clinical data of two leadless pacing systems are available: Nanostim<sup>®</sup> leadless cardiac pacemaker (LCP; Abbott Inc., Abbott Park, IL, USA) and Micra<sup>®</sup> transcatheter pacing system (TPS; Medtronic Inc., Minneapolis, MN, USA).

The LEADLESS trial (Assessing safety and performance of Nanostim) demonstrated that leadless pacing is feasible and safe.<sup>91</sup> This was followed by LEADLESS II trial that involved significantly higher number of patients in comparison to LEADLESS trial. It showed that the leadless pacemaker Nanostim was successfully implanted in 504 of the 526 patients (95.8%). The primary efficacy end point was met in 270 of the 300 patients (90.0%; 95% confidence interval [CI], 86.0 to 93.2,  $P=0.007$ ), and the primary safety end point was met in 280 of the 300 patients (93.3%; 95% CI, 89.9 to 95.9;  $P<0.001$ ). At 6 months, device-related serious adverse events were observed in only 6.7% of the patients; events included device dislodgement with percutaneous retrieval (in 1.7%), cardiac perforation (in 1.3%), and pacing-threshold elevation requiring percutaneous retrieval and device replacement (in 1.3%).<sup>92</sup>

However, premature battery failure has been identified in 34 out of 1423 implanted Nanostim devices, more than what was initially expected. This occurred approximately 3 years after implantation. In some of the patients, the device could not be interrogated, and the battery depletion caused loss of pacing. Consequently, the Nanostim<sup>®</sup> was withdrawn from the market and is currently not commercially available.<sup>93</sup>

The safety and efficacy of the Micra<sup>®</sup> device was evaluated in a prospective study (Micra Transcatheter Pacing Study) concluding that the leadless pacemaker met the specified safety and efficacy goals; demonstrating a safety profile similar to that of traditional pacing whilst providing stable pacing thresholds.<sup>94</sup>

Further evaluation of the safety of the Micra system in a “real – world” setting and the Micra Post-Approval Registry (PAR) was initiated. Enrolment for the registry started in 2015 and finished in March 2018 with a total of 1817 patients enrolled. Analysis of safety and effectiveness data was published with 1 month as well as 12 months of follow-up. The “real-world” data were even better than the results of the Micra Transcatheter Pacing Study. It showed a high implantation success rate (99.1%) and a low rate of major complications (2.7% in 41 patients).<sup>95</sup>

To date, there are no randomized controlled trials planned to compare efficacy and long-term safety between transvenous and leadless pacemakers and further studies comparing both systems on the long-term are needed. There are currently a few published reports with

recommendations for indications for LP therapy as opposed to the traditional transvenous pacing such as the national expert consensus of the Austrian Society of Cardiology<sup>96</sup> and the recommendations of the expert opinion of the working group on leadless pacing of the Polish Cardiac Society.<sup>97</sup> A recently conducted survey by the European Heart Rhythm association (EHRA) provided a contemporary insight into pacemaker implantations across European centres. It was a prospective multicentre study carried out during a consecutive 10-week period between November 2018 and January 2019 across multiple participating European centres. The participating centres were requested to prospectively include consecutive patients implanted with a transvenous or a leadless pacemaker during the 10-week period of the study. The aim of the study was to provide insight into the criteria governing the choice between transvenous and LP implantation in the contemporary European practice.<sup>98</sup>

A total number of 798 patients were implanted with a pacemaker during the period of the study. The main indication for a pacemaker in that survey was symptomatic severe atrioventricular conduction disease in more than two-thirds of patients, with less than one-third of patients implanted for sinus node dysfunction.<sup>98</sup>

The total number of Leadless pacemakers implanted during the survey period was 69 out of the total 798 pacing devices implanted representing around 9%. The distribution of the transvenous devices were as such: CRT pacemaker (n = 79, 10%), Dual chamber pacemaker (n= 528, 66%), and single chamber ventricular pacemaker (n= 122, 15%).<sup>98</sup>

Factors associated with Leadless pacemaker implantation vs. transvenous pacemakers were male sex (74% vs. 58%, P = 0.009), valvular heart disease (45% vs. 35%, P= 0.01), chronic renal failure (28% vs. 16%, P= 0.01) and diabetes (34% vs. 21%, P= 0.01). Overall, with patients who ended up receiving leadless pacing having more co-morbidities than those in the transvenous group (>\_ one comorbidity, 66% vs. 52%, P= 0.02).<sup>98</sup>

No specific factor was overwhelmingly reported to prioritize the choice of leadless pacing in that survey. The most declared reasons favouring LP implantation were old age (38%), anticipated high risk of infection or previous device infection with prior removal (46%), previous or anticipated lead-related complications (19%), or anticipated low rate of ventricular pacing (25%). The most common factors favouring the use of transvenous pacing were the need for resynchronization



therapy (in 100% of CRT devices implantation) and atrial pacing (90% of dual chamber transvenous pacemaker implantations). In addition, advanced age and anticipated high rate of ventricular pacing were also reported to be barriers in 53% and 34% of the single chamber ventricular transvenous pacemaker patients, respectively, for which implanting a leadless pacemaker could have been a potential alternative.<sup>98</sup>

### **1.5.1 S-ICDs and pacemakers**

Occasionally, patients with implanted pacemakers subsequently develop an indication for an ICD. In such cases, one option would be choosing to implant a transvenous ICD lead with or without extracting the existing pacing lead. In some cases, this may not be possible due to the presence of vascular occlusion or stenosis or not desirable due to increased risk of infection. Another option would be the addition of an S-ICD to an existing transvenous pacemaker. However, the impact of ventricular pacing on the qualification for S-ICD is not readily known since ventricular pacing may lead to large QRS amplitudes and may also lead to T-wave oversensing in this scenario.

Conversely, some patients that have an existing S-ICD may develop a pacing indication. In those patients, if standard transvenous approaches are not feasible for pacing, the combination of a leadless S-ICD and leadless pacing might be an attractive option in such a setting.

The effect of pacing on the sensing process of the S-ICD is not well studied. Even though the patient would have passed S-ICD screening, it is possible that QRS double counting or T wave oversensing could occur during paced rhythm. In this case there is a potential risk of inappropriate shock due to oversensing of paced rhythm.

Ip et al explored the proportion of ventricularly paced patients who would qualify for an S-ICD. They evaluated 100 patients who had transvenous pacing devices in situ, including 25 patients with biventricular pacing devices. It was the first study to systematically evaluate S-ICD candidacy based on the screening template in patients who already have existing transvenous pacing devices. The overall S-ICD screening pass rate was 58% among patients who were ventricularly paced. Those who were bi-ventricularly paced were more likely to fulfil screening criteria based on the QRS:T ratio compared to those with RV pacing alone. Furthermore, patients that were

paced from the RV septum were more likely to qualify compared to those paced from the RV apex (67% versus 37%,  $p < 0.01$ ).<sup>99</sup>

## **1.6 Artificial Intelligence and Machine learning**

### **1.6.1 Terminology**

Artificial intelligence (AI) is a broad term that describes the use of algorithms and software which demonstrate human-like intelligence in analysing, interpreting, and understanding complicated data. When machines can extract information from data, improve their function or make predictions about future events, they are referred to as machine learning, a subset of AI. Machine learning comprises a range of sub-branches, such as deep learning and neural networks. An algorithm is simply a set of actions to be followed to get a solution.<sup>100</sup>

### **1.6.2 Machine learning**

Machine learning is a subfield of artificial intelligence, which is broadly defined as the capability of a machine to imitate intelligent human behaviour to perform complex tasks in a way that is similar to how humans solve problems. In other words, machine learning gives computers the ability to learn without explicitly being programmed but rather lets computers learn to program themselves through experience.<sup>101</sup>

#### **1.6.2.1 Techniques**

Machine learning techniques are divided into 4 main categories:

- a) Supervised learning: machine learning models are trained with data sets, pre-labelled by humans. With time, the machine would learn ways to identify the un-labelled data sets on their own. This is the most common technique used.
- b) Unsupervised learning: The machine is trained with either unlabelled data sets or labels only. The machine can then find patterns or trends in data that people aren't explicitly looking for. The machine may not always provide correct output compared to supervised learning.
- c) Reinforcement learning: This is a feedback-based learning technique. Machines learn through trial and error by establishing a reward system. Reinforcement learning can train

machines by telling the machine when it made the right decisions, which helps it learn over time what actions it should take.

- d) Semi-supervised learning: This is an intermediate technique of both supervised and unsupervised learning. It performs actions on datasets having few labels as well as unlabelled data. It requires less time and effort needed for labelling the data when compared to supervised learning. It also increases the accuracy and performance of the machine learning model when compared to the unsupervised learning.<sup>101</sup>

### **1.6.2.2 Strengths and limitations**

Machine learning allows efficient and accurate processing of vast amounts of data. It can identify patterns and trends that might not be apparent to humans. Machine learning is highly effective at data mining, efficiently identifying trends or patterns without compromising on accuracy.

However, machines are trained by humans, and human biases can be incorporated into algorithms. If biased information, or data, is fed to a machine learning program, the program will learn to replicate it. There is also the issue of “explainability”, which is simply when the machines produce outcomes or decisions that cannot be explained even by its designers. Overfitting is another limitation of machine learning, this is where the machines produce overly complex outputs or decisions that have to satisfy all the past training data, even if not relevant to the data at hand.

### **1.6.2.3 Convoluted neural networks**

Neural networks are a specific class of machine learning algorithms. They are designed to mimic the human brain, in which thousands or millions of processing nodes are interconnected and organized into layers. Cells, or nodes, are connected, with each cell processing inputs and producing an output that is sent to other neurons. Data moves through the nodes, or cells, with each cell performing a different function.

Convoluted neural networks or CNN are a specialized kind of neural network for processing data that has a known grid-like topology such as image data, which can be thought of as a 2-D grid of pixels. CNNs employ a mathematical operation called convolution, a specialised kind of linear operation, in place of general matrix multiplication in at least one of their layers. Convolution is a mathematical operation on two functions (f and g) that produces a third function that expresses how the shape of one is modified by the other. The term convolution refers to both the result function and to the process of computing it.<sup>102</sup>

### 1.6.3 Use in Cardiology

The level of efficiency that the use of AI provides will help to lessen the global burden of cardiovascular disease. In cardiology, the most well-researched use of AI is in the realm of the ECG. The application of AI to ECG data can help extract highly accurate projections of the past, present, and future of the health of the patient.<sup>103</sup>

Machine learning methods are already in use for ECG analysis in a variety of applications. They have been used in ECG analysis for classifying heart attacks, atrial fibrillation, and other arrhythmias as well as for predicting blood pressure, as well as predicting the risk of myocardial infarctions.<sup>104–111</sup>

## 1.7 Combined Cardiac rhythm management therapy

The development of a modular cardiac rhythm management system (mCRM) that combines an S-ICD with a leadless pacemaker could provide a viable therapy option for patients who would benefit from ATP therapy after S-ICD implantation. This combined device system represents a novel concept for management of such patients in which device therapy could be further personalized to the current and future patients' needs. This would essentially require reliable device–device communication.

The safety and efficacy of this combined devices system with successful S-ICD/leadless pacemaker device to device communication has been evaluated previously in animal studies and it was first reported in 2016.<sup>112</sup> Since then larger animal studies were published evaluating the pacing and sensing performance of leadless pacing as well as the performance of the mCRM system (S-ICD and leadless pacemaker) altogether in acute as well as chronic (3 months) animal implants. The results of the evaluations were promising showing stable communication thresholds between the devices throughout the 3-month study.<sup>113</sup>

Although animal model evaluations can be a useful surrogate when human evaluation is not feasible or ethical, animal models cannot fully replicate human anatomy. Further studies of the mCRM system are required to evaluate its safety and efficacy in human subjects. Human clinical studies of the EMPOWER™ leadless pacemaker (Boston Scientific) and the mCRM systems started in 2021.<sup>114</sup>

Prospects of the mCRM system are expected to include communicating leadless devices to provide dual chamber pacing therapy or even cardiac resynchronization therapy with the potential of coordination with a co-implanted S-ICD. Several manufacturers are currently working on the development of such systems.

There are only a few sporadic cases published of patients who have leadless pacemakers who would qualify for an S-ICD if they develop an indication for one. <sup>88,89</sup>

## **1.8 Aims and objectives**

There is a growing trend towards the utilisation of sophisticated rhythm management systems. These systems require precise sensing capabilities without direct contact with the cardiovascular tissue (S-ICDs) or direct contact between their individual components (modular CRM systems).

In this thesis I will examine the sensing capabilities of the S-ICDs in the context of different underlying cardiac disease aetiologies. I will also explore the potential interactions between S-ICDs and other rhythm management devices with particular emphasis on the effect of these interactions on the sensing capabilities of the S-ICD systems. In addition, I will also demonstrate how adopting new software technologies can enhance ECG signals processing and subsequently refine patient selection process and management of advanced rhythm management therapies.



## **Chapter 2 Eligibility for the subcutaneous implantable cardiac defibrillator using standard screening practice – A real-world experience from a UK centre**

### **2.1 Introduction**

Studies and registries reported variable rates of S-ICD screening success. Information regarding suitability for S-ICD implantation in specific patients' subgroups such as patients with congenital heart disease and hypertrophic cardiomyopathy have been scarce and published studies reported highly varying eligibility rates.<sup>37,71,115,116</sup>

### **2.2 Objectives**

In this chapter, I present a retrospective analysis of the S-ICD screening eligibility rates from a UK tertiary referral centre for complex cardiac devices. My aim is to report on the experience with S-ICD screening in a diverse real-world population. Special emphasis is given on the screening success rates in respect to the underlying cardiac aetiology. Other factors that could alter the screening outcomes are also highlighted in this chapter.

### **2.3 Methods**

This is a retrospective analysis of S-ICD eligibility in a single UK centre for cardiac devices (University Hospital of Southampton, UK). The analysis was done retrospectively on consecutive patients with an indication for ICD therapy who were referred by their treating clinician for consideration of a subcutaneous ICD and who had undergone screening for S-ICD eligibility between 2014 and 2021. Patients' demographics (age, gender, BMI, underlying cardiac anatomy), indication for ICD therapy, rationale behind referring for S-ICD therapy specifically, and the outcome of S-ICD screenings were obtained from the hospital medical records.

Patients were considered S-ICD eligible if they had at least one vector that passed screening. Initial S-ICD screenings were performed using the overlay technique, which was subsequently replaced with the automated screening tool (AST) at the beginning of 2017. For the overlay technique, the S-ICD vectors were assessed in at least two postures (e.g., supine and standing or

supine and sitting). For the AST screening, S-ICD vectors were assessed in 5 different postures: supine, sitting, standing, supine on the right side, and supine on the left side. For a S-ICD vector to be deemed eligible, it had to pass the screening in all the forementioned postures.

### 2.3.1 Statistical methods

Data was analysed using R program. Parametric data was presented as mean  $\pm$  SD and categorical data as n/N (%). Kruskal-Wallis rank sum, Pearson's Chi-squared, Fisher's exact and Wilcoxon rank sum tests were used to determine the significance of the differences in the patients' characteristics in relation to the outcomes of the screening in the three S-ICD vectors.

## 2.4 Results

A total of 126 patients (mean age  $47 \pm 18$  years, 67% male) had their S-ICD screenings retrospectively analysed in this study. Patients' demographics are shown in Table 1.

Table 1 Patients' demographics.

Demographic	Value
<b>Gender</b>	
Female	42 / 126 (33%)
Male	84 / 126 (67%)
<b>Age(years)</b>	
Mean (SD)	47 (18)
<b>BMI(Kg/m2)</b>	
Mean (SD)	26.9 (6.0)
<b>Underlying anatomy</b>	
Dilated cardiomyopathy	34 / 126 (27%)
Adult congenital heart disease	7 / 126 (5.6%)
	Pulmonary atresia with ventricular septal defect 2/7(28.6%)
	Tetralogy of Fallot 1/7(14.2%)



	Transposition of the great arteries 2/7(28.6%)	
	Others 2/7(28.6%)	
Hypertrophic cardiomyopathy	28 / 126	(22%)
Ischaemic cardiomyopathy	27 / 126	(21%)
Structurally normal heart	28 / 126	(22%)
Arrhythmogenic right ventricle cardiomyopathy	2 / 126	(1.6%)
<b>Screen method</b>		
Automated screening tool	115 / 126	(91%)
Overlay technique	11 / 126	(8.7%)
<b>ICD indication</b>		
Primary prevention	70 / 126	(56%)
Secondary prevention	56 / 126	(44%)
<b>S-ICD indication</b>		
Difficult underlying anatomy	6 / 126	(4.8%)
Patient preference	51 / 126	(40%)
Prior device related infection	9 / 126	(7.1%)
High risk of infection	7 / 126	(5.6%)
Perceived by the treating clinician to be of relatively young age requiring multiple generator replacements in their lifetime	53 / 126	(42%)

Difficult underlying anatomy, as an indication for S-ICD therapy specifically, refers to the presence of anatomical constraints complicating/precluding transvenous leads implantations such as venous obstructions or anomalies. High risk of infection refers to patients who are immunocompromised or receiving immunosuppressants or steroids therapy or patients who have or at high probability of having indwelling vascular catheters, such as end stage renal failure patients on dialysis.

A total of 96.8% of patients fulfilled the S-ICD screening criteria and were deemed eligible for S-ICD therapy. Patients who passed the screening had a mean age of  $47 \pm 18$  versus  $53 \pm 27$  years in patients who didn't pass the screening ( $p=0.7$ ). In addition, patients who passed the screening had

a mean BMI of 26.9  $\pm$ 6 versus 28.3  $\pm$ 5.4 in patients who didn't pass the screening (p=0.6) see Table 2 for the detailed screening outcomes for all the S-ICD vectors combined.

Table 2 Screening outcomes for all vectors combined.

Demographic	N	Screening outcome		p-value <sup>1</sup>
		Fail (4)	Pass (122)	
	12 6			
<b>Gender</b>	12 6			>0.9
Female		1 / 4 (25%)	41 / 122 (34%)	
Male		3 / 4 (75%)	81 / 122 (66%)	
<b>Age(years)</b>	12 6			0.7
Mean (SD)		53 (27)	47 (18)	
<b>BMI</b>	12 6			0.6
Mean (SD)		28.3 (5.4)	26.9 (6.0)	
<b>Underlying anatomy</b>	12 6			0.4
Dilated cardiomyopathy		1 / 4 (25%)	33 / 122 (27%)	
Adult congenital heart disease		1 / 4 (25%)	6 / 122 (4.9%)	
Hypertrophic cardiomyopathy		1 / 4 (25%)	27 / 122 (22%)	
Ischaemic cardiomyopathy		1 / 4 (25%)	26 / 122 (21%)	
Structurally normal heart		0 / 4 (0%)	28 / 122 (23%)	
Arrhythmogenic right ventricle cardiomyopathy		0 / 4 (0%)	2 / 122 (1.6%)	
<b>Screen method</b>	12 6			>0.9
Automated screening tool		4 / 4 (100%)	111 / 122 (91%)	
Overlay technique		0 / 4 (0%)	11 / 122 (9.0%)	
<b>ICD indication</b>	12 6			0.6
Primary prevention		3 / 4 (75%)	67 / 122 (55%)	
Secondary prevention		1 / 4 (25%)	55 / 122 (45%)	
<b>S-ICD indication</b>	12 6			0.2

Difficult underlying anatomy	1 / 4 (25%)	5 / 122 (4.1%)
Patient preference	1 / 4 (25%)	50 / 122 (41%)
Prior device related infection	1 / 4 (25%)	8 / 122 (6.6%)
High risk of infection	0 / 4 (0%)	7 / 122 (5.7%)
Perceived by the treating clinician to be of relatively young age requiring multiple generator replacements in their lifetime	1 / 4 (25%)	52 / 122 (43%)

<sup>1</sup> Fisher's exact test; Wilcoxon rank sum test

A total of 32.5% of all patients had all their 3 (primary, alternate, and secondary) vectors pass the S-ICD screening, 47.6% of patients passed with 2 suitable vectors, and 16.7% had only one passing vector. Mean BMI of patients who passed with 3 vectors was  $25.8 \pm 5.5$ , patients who passed with 2 vectors had an average BMI of  $27.2 \pm 5.9$ , and patients with a single suitable vector had a mean BMI of  $28.1 \pm 7.1$ ,  $p=0.3$ . Patients' age didn't correlate with the number of passing vectors, and there was no statistically significant difference in the numbers of vectors that passed the screening attributed to gender, underlying anatomy, indication for ICD therapy, or screening method, see Table 3.

Table 3 Factors influencing number of passing vectors.

Demographic	N	Number of vectors passed				p-value <sup>1</sup>
		0, N = 4	1, N = 21	2, N = 60	3, N = 41	
<b>Gender</b>	126					0.09
Female	42	1 / 4 (25%)	9 / 21 (43%)	24 / 60 (40%)	8 / 41 (20%)	
Male	84	3 / 4 (75%)	12 / 21 (57%)	36 / 60 (60%)	33 / 41 (80%)	
<b>Age(years)</b>	126					0.2
Mean (SD)		53 (27)	45 (18)	50 (18)	43 (17)	
<b>BMI</b>	126					0.3
Mean (SD)		28.3 (5.4)	28.1 (7.1)	27.2 (5.9)	25.8 (5.5)	
<b>Underlying anatomy</b>	126					0.06
Dilated cardiomyopathy	34	1 / 4 (25%)	9 / 21 (43%)	11 / 60 (18%)	13 / 41 (32%)	
Adult congenital heart disease	7	1 / 4 (25%)	1 / 21 (4.8%)	2 / 60 (3.3%)	3 / 41 (7.3%)	
Hypertrophic cardiomyopathy	28	1 / 4 (25%)	5 / 21 (24%)	15 / 60 (25%)	7 / 41 (17%)	
Ischaemic cardiomyopathy	27	1 / 4 (25%)	5 / 21 (24%)	17 / 60 (28%)	4 / 41 (9.8%)	
Structurally normal heart	28	0 / 4 (0%)	1 / 21 (4.8%)	13 / 60 (22%)	14 / 41 (34%)	

Arrhythmogenic right ventricle cardiomyopathy	2	0 / 4 (0%)	0 / 21 (0%)	2 / 60 (3.3%)	0 / 41 (0%)
<b>Screen method</b>	126				0.7
Automated screening tool	115	4 / 4 (100%)	19 / 21 (90%)	56 / 60 (93%)	36 / 41 (88%)
Overlay technique	11	0 / 4 (0%)	2 / 21 (9.5%)	4 / 60 (6.7%)	5 / 41 (12%)
<b>ICD indication</b>	126				0.4
Primary prevention	70	3 / 4 (75%)	15 / 21 (71%)	31 / 60 (52%)	21 / 41 (51%)
Secondary prevention	56	1 / 4 (25%)	6 / 21 (29%)	29 / 60 (48%)	20 / 41 (49%)
<b>S-ICD indication</b>	126				0.4
Difficult underlying anatomy	6	1 / 4 (25%)	1 / 21 (4.8%)	2 / 60 (3.3%)	2 / 41 (4.9%)
Patient preference	51	1 / 4 (25%)	9 / 21 (43%)	29 / 60 (48%)	12 / 41 (29%)
Prior device related infection	9	1 / 4 (25%)	2 / 21 (9.5%)	4 / 60 (6.7%)	2 / 41 (4.9%)
High risk of infection	7	0 / 4 (0%)	1 / 21 (4.8%)	4 / 60 (6.7%)	2 / 41 (4.9%)
Perceived by the treating clinician to be of relatively young age requiring multiple generator replacements in their lifetime	53	1 / 4 (25%)	8 / 21 (38%)	21 / 60 (35%)	23 / 41 (56%)

<sup>1</sup>Fisher's Exact Test for Count Data with simulated p-value; Kruskal-Wallis rank sum test

Primary vectors were the most likely to pass screening (81%), followed by the secondary (75.4%), then the alternate vectors (53.2%). There was a statistically significant difference associated with gender in the passing rates of the alternate vector; 64.3% of the alternate vectors in male patients passed the screening, in comparison to only 31% in female patients ( $p < 0.001$ ). There were no significant differences in the other two vectors. Patients who were more likely to pass the screening in the alternate vector were younger with mean age of  $43 \pm 19$  years versus  $51 \pm 17$  years in those who failed the screening in the alternate vector ( $p = 0.02$ ), while there were no significant differences in the other two vectors. Patients who passed the screening in the alternate vector also had a lower BMI  $25.6 \pm 5.3$  versus  $28.4 \pm 6.4$  in patients who failed the screening,  $p = 0.01$ . Again, there were no significant differences in the other two vectors. The primary vector passed the screening in 100% of patients with ARVC, 96.4% in patients with structurally normal hearts, 88.9% in ICM patients, 75% in HCM patients, 73.5% in DCM and only 42.9% in ACHD patients ( $p = 0.01$ ). The secondary vector passed the screening in 100% of the

patients with ARVC, 96.4% in patients with structurally normal hearts, 76.5% in DCM, 71.4% in ACHD patients, 64.3% in HCM, and 63% in ICM patients ( $p=0.02$ ). In the alternate vector, the percentage of screening success was less than the two other vectors for all the underlying anatomies except for the ACHD patients who had a higher success rate in the alternate vector in comparison to the other two vectors with a pass rate of 85.7%. The alternate vector passed the screening in 60.7% of HCM patients, 55.9% of DCM patients, 53.6% in structurally normal hearts, 37% in ICM and neither of the two ARVC patients passed the screening in the alternate vector,  $p=0.12$ , see Table 4, Table 5, and Table 6.

Table 4 Screening outcomes for the primary vector

Demographic	N	Primary vector			P-value <sup>1</sup>
		Fail, N = 24	Pass, N = 102	Pass %	
<b>Overall</b>	126			102/126(81%)	
<b>Gender</b>	126				>0.9
Female	42	8 / 24 (33%)	34 / 102 (33%)	34/42(81%)	
Male	84	16 / 24 (67%)	68 / 102 (67%)	68/84(81%)	
<b>Age(years)</b>	126				0.9
Mean (SD)		47 (21)	47 (18)		
<b>BMI(Kg/m<sup>2</sup>)</b>	126				0.8
Mean (SD)		27.0 (6.5)	26.9 (5.9)		
<b>Underlying anatomy</b>	126				0.01
Dilated cardiomyopathy	34	9 / 24 (38%)	25 / 102 (25%)	25/34(73.5%)	
Adult congenital heart disease	7	4 / 24 (17%)	3 / 102 (2.9%)	3/7(42.9%)	
Hypertrophic cardiomyopathy	28	7 / 24 (29%)	21 / 102 (21%)	21/28(75%)	
Ischaemic cardiomyopathy	27	3 / 24 (12%)	24 / 102 (24%)	24/27(88.9%)	
Structurally normal heart	28	1 / 24 (4.2%)	27 / 102 (26%)	27/28(96.4%)	
Arrhythmogenic right ventricle cardiomyopathy	2	0 / 24 (0%)	2 / 102 (2.0%)	2/2(100%)	
<b>Screen method</b>	126				0.4
Automated screening tool	115	21 / 24 (88%)	94 / 102 (92%)	94/115(81.7%)	
Overlay technique	11	3 / 24 (12%)	8 / 102 (7.8%)	8/11(72.7%)	
<b>ICD indication</b>	126				0.4
Primary prevention	70	15 / 24 (62%)	55 / 102 (54%)	55/70(78.6%)	
Secondary prevention	56	9 / 24 (38%)	47 / 102 (46%)	47/56(83.9%)	
<b>S-ICD indication</b>	126				0.2
Difficult underlying anatomy	6	3 / 24 (12%)	3 / 102 (2.9%)	3/6(50%)	

Patient preference	51	8 / 24 (33%)	43 / 102 (42%)	43/51(84.3 %)
Prior device related infection	9	3 / 24 (12%)	6 / 102 (5.9%)	6/9(66.7%)
High risk of infection	7	1 / 24 (4.2%)	6 / 102 (5.9%)	6/7(85.7%)
Perceived by the treating clinician to be of relatively young age requiring multiple generator replacements in their lifetime	53	9 / 24 (38%)	44 / 102 (43%)	44/53(83.0 %)

<sup>1</sup>*Pearson's Chi-squared test; Wilcoxon rank sum test; Fisher's exact test*

Table 5 Screening outcomes for the secondary vector.

Demographic	N	Secondary vector			P-value <sup>1</sup>
		Fail, N = 31	Pass, N = 95	Pass %	
<b>Overall</b>	126			95/126(75.4 %)	
<b>Gender</b>	126				0.3
Female	42	8 / 31 (26%)	34 / 95 (36%)	34/42(81%)	
Male	84	23 / 31 (74%)	61 / 95 (64%)	61/84(72.6 %)	
<b>Age(years)</b>	126				0.6
Mean (SD)		46 (20)	47 (17)		
<b>BMI(Kg/m<sup>2</sup>)</b>	126				>0.9
Mean (SD)		26.7 (5.7)	27.0 (6.1)		
<b>Underlying anatomy</b>	126				0.02
Dilated cardiomyopathy	34	8 / 31 (26%)	26 / 95 (27%)	26/34(76.5 %)	
Adult congenital heart disease	7	2 / 31 (6.5%)	5 / 95 (5.3%)	5/7(71.4%)	
Hypertrophic cardiomyopathy	28	10 / 31 (32%)	18 / 95 (19%)	18/28(64.3 %)	
Ischaemic cardiomyopathy	27	10 / 31 (32%)	17 / 95 (18%)	17/27(63.0 %)	
Structurally normal heart	28	1 / 31 (3.2%)	27 / 95 (28%)	27/28(96.4 %)	
Arrhythmogenic right ventricle cardiomyopathy	2	0 / 31 (0%)	2 / 95 (2.1%)	2/2(100%)	
<b>Screen method</b>	126				>0.9
Automated screening tool	115	28 / 31 (90%)	87 / 95 (92%)	87/115(75.7 %)	
Overlay technique	11	3 / 31 (9.7%)	8 / 95 (8.4%)	8/11(72.7%)	
<b>ICD indication</b>	126				0.05
Primary prevention	70	22 / 31 (71%)	48 / 95 (51%)	48/70(68.6 %)	
Secondary prevention	56	9 / 31 (29%)	47 / 95 (49%)	47/56(83.9 %)	
<b>S-ICD indication</b>	126				0.2
Difficult underlying anatomy	6	2 / 31 (6.5%)	4 / 95 (4.2%)	4/6(66.7%)	
Patient preference	51	11 / 31 (35%)	40 / 95 (42%)	40/51(78.4 %)	

Prior device related infection	9	5 / 31 (16%)	4 / 95 (4.2%)	4/9(44.4%)
High risk of infection	7	1 / 31 (3.2%)	6 / 95 (6.3%)	6/7(85.7%)
Perceived by the treating clinician to be of relatively young age requiring multiple generator replacements in their lifetime	53	12 / 31 (39%)	41 / 95 (43%)	41/53(77.4%)

<sup>1</sup>*Pearson's Chi-squared test; Wilcoxon rank sum test; Fisher's exact test*

Table 6 Screening outcomes for the alternate vector.

Demographic	N	Alternate vector			P-value <sup>1</sup>
		Fail, N = 59	Pass, N = 67	Pass %	
<b>Overall</b>	126			67/126(53.2%)	
<b>Gender</b>	126				<0.001
Female	42	29 / 59 (49%)	13 / 67 (19%)	13/42(31%)	
Male	84	30 / 59 (51%)	54 / 67 (81%)	54/84(64.3%)	
<b>Age(years)</b>	126				0.02
Mean (SD)		51 (17)	43 (19)		
<b>BMI(Kg/m<sup>2</sup>)</b>	126				0.01
Mean (SD)		28.4 (6.4)	25.6 (5.3)		
<b>Underlying anatomy</b>	126				0.12
Dilated cardiomyopathy	34	15 / 59 (25%)	19 / 67 (28%)	19/34(55.9%)	
Adult congenital heart disease	7	1 / 59 (1.7%)	6 / 67 (9.0%)	6/7(85.7%)	
Hypertrophic cardiomyopathy	28	11 / 59 (19%)	17 / 67 (25%)	17/28(60.7%)	
Ischaemic cardiomyopathy	27	17 / 59 (29%)	10 / 67 (15%)	10/27(37.0%)	
Structurally normal heart	28	13 / 59 (22%)	15 / 67 (22%)	15/28(53.6%)	
Arrhythmogenic right ventricle cardiomyopathy	2	2 / 59 (3.4%)	0 / 67 (0%)	0/2 (0%)	
<b>Screen method</b>	126				0.05
Automated screening tool	115	57 / 59 (97%)	58 / 67 (87%)	58/115(50.4%)	
Overlay technique	11	2 / 59 (3.4%)	9 / 67 (13%)	9/11(81.8%)	
<b>ICD indication</b>	126				>0.9
Primary prevention	70	33 / 59 (56%)	37 / 67 (55%)	37/70(52.9%)	
Secondary prevention	56	26 / 59 (44%)	30 / 67 (45%)	30/56(53.6%)	
<b>S-ICD indication</b>	126				0.09
Difficult underlying anatomy	6	2 / 59 (3.4%)	4 / 67 (6.0%)	4/6(66.7%)	
Patient preference	51	31 / 59 (53%)	20 / 67 (30%)	20/51(39.2%)	
Prior device related infection	9	3 / 59 (5.1%)	6 / 67 (9.0%)	6/9(66.7%)	

High risk of infection	7	4 / 59 (6.8%)	3 / 67 (4.5%)	3/7(42.9%)
Perceived by the treating clinician to be of relatively young age requiring multiple generator replacements in their lifetime	53	19 / 59 (32%)	34 / 67 (51%)	34/53(64.2%)

<sup>1</sup>*Pearson's Chi-squared test; Wilcoxon rank sum test; Fisher's exact test*

Only four (3.2%) patients in total who had previously passed the S-ICD screening test had T-wave oversensing during the follow up period. All patients were male and had a BMI>25 kg/m<sup>2</sup>. One patient had a structurally normal heart, one had DCM, one had HCM, and one had ICM. Three of the four patients passed the manual S-ICD screening using the overlay technique and one patient passed the automated screening using the AST.

## 2.5 Discussion

### 2.5.1 S-ICD eligibility rates

Previously published studies reported screening failure rates of 3.6-9% among potential S-ICD candidates, see Table 7.<sup>117-121</sup> However, studies looking into S-ICD eligibility in special patients' populations such as patients with ACHD and patients with hypertrophic cardiomyopathy are scarce and reported highly variable eligibility rates.

Table 7 S-ICD screening failure rates in previous studies.

Authors of the study	Patients' demographics	S-ICD ineligibility rates	Characteristic findings
Olde Nordkamp et al <sup>121</sup>	230 consecutive ICD outpatients (75% male, age 57 ± 15 years)	7.4% of patients, all male	Independent predictors for screening failure were hypertrophic cardiomyopathy (HCM; odds ratio [OR] 12.6), a heavy weight (OR 1.5), a



			prolonged QRS duration (OR 1.5) and a R:T ratio <3 in the lead with the largest T wave on a standard 12-lead surface ECG (OR 14.6).
<b>Randles et al</b> <sup>120</sup>	196 ICD patients, (80.1% male, age 66 years)	3.6% didn't have any qualifying vectors	-No differences with age, gender, height, weight, or underlying aetiology of heart disease  -Primary and secondary vectors satisfied the surface ECG screening template more frequently than the alternate vector
<b>Rudic et al</b> <sup>119</sup>	254 patients (167 men; mean age 45±16 years)	7-8% ineligibility	HCM patients had higher failure rate
<b>Groh et al</b> <sup>118</sup>	100 ICD patients (72% male, age 57 ± 16 years, body mass index 29 ± 6 kg/m <sup>2</sup> )	8% ineligibility	-No differences in patient clinical characteristics -Patients with T-wave inversions in standard ECG leads I, II, and aVF had a 45% chance of failing.
<b>Francia et al</b> <sup>117</sup>	235 consecutive ICD candidates and patients previously implanted with transvenous ICD or S-ICD and no need for permanent pacing (76% male, age 57 ±17 years)	6-9% ineligibility	No differences in the ineligibility rates attributed to the underlying cardiomyopathy

## 2.5.2 S-ICD eligibility in specific patients' subgroups

### 2.5.2.1 ACHD population

The S-ICD may offer added value for congenital heart disease patients. Anatomical challenges of transvenous lead implantation in these patients can be potentially overcome with a subcutaneous approach. This patient population is relatively younger and the concern for future device infection or lead failure necessitating extraction over time makes traditional transvenous systems less appealing. However, the eligibility for S-ICD is reliable on the surface ECG, and patients with ACHD will frequently have grossly abnormal ECGs with either small complexes or large T waves, both of which can be a problem for S-ICD sensing.

Previous studies demonstrated higher ineligibility rates in the ACHD population than in general population.<sup>37,71,122</sup> This may be due to abnormal T-wave morphology resulting from structural and functional disturbances that characterizes ACHD, including cardiac chamber enlargement, abnormal cardiac position, mechanical strain, and augmented repolarization.

### **2.5.2.2 HCM population**

HCM patients are relatively young and require prolonged protection against sudden cardiac death. A S-ICD system may be considered in HCM patients with no indication for pacing (Class IIb, level of Evidence C) in the most recently published ESC guidelines.<sup>74</sup> However, HCM patients will frequently have significant repolarisation changes on their ECGs with characteristically large R waves (and large T waves) that can affect the S-ICD sensing.

Previous studies have suggested that HCM is an independent risk factor for S-ICD screening failure. Studies looking specifically into the proportion of HCM patients who satisfy the S-ICD screening criteria reported highly varying eligibility rates.<sup>115,116</sup>

### **2.5.3 Insights into the data**

The cohort of patients included in this study were relatively young (mean age 47 years), overweight by BMI standards (26.9 kgs/m<sup>2</sup>) and had a wide range of underlying cardiac conditions. The choice of S-ICD specifically was predominantly dictated by the patients' age as well as patients' preference. This might reflect the complications associated with long term therapy using TV-ICDs. Regardless of the underlying aetiology, most of the patients included in this study passed the screening (mostly via the AST) and met the eligibility criteria for a S-ICD.

Due to the very low number of patients who failed the S-ICD screening in this study's cohort, attempting to compare the characteristics of the patients who passed the screening with those of who failed was unlikely to yield any meaningful results of statistical significance. While most of the patients passed the S-ICD screening, only one third of the patients passed the screening in all three vectors and 17% passed the screening with only a single eligible vector. This is significant as it can potentially lead to limited management options in the future if this single eligible vector is

hindered by oversensing issues. Assessing the three S-ICD vectors individually provided some insights into some of the characteristics that impact the screening outcomes.

Vector eligibilities were noted to be different in the subgroups of patients described. For example, the alternate vector was the least likely vector to pass the screening with only 53.2% pass rate for all the underlying aetiologies except for the ACHD group that was more likely to pass the screening in the alternate vectors (85.7%), compared to secondary (71.4%) and primary (42.9%) vectors. This might be a reflection of the unique underlying anatomies that characterise the ACHD population which can alter the axis of the QRS as well as the T waves, and subsequently affecting the vector eligibilities. In addition, patients with higher BMI and female patients, probably due to gender differences in the size of the breast tissue regardless of BMI, were more likely to fail the screening in the alternate vector. Perhaps this is not surprising as higher BMI, as well as gender differences in the breast mass, translate into more tissue between the sensing electrodes embedded in the subcutaneous lead and the electricity impulses generated by the heart. This results in ECG signals of smaller amplitudes, which are particularly pronounced in the case of the alternate vectors, that are more likely to fail the screening. These findings are particularly important, as they cast some concerns on the appropriateness of utilising the surface ECG signals as surrogates for the ultimately subcutaneous S-ICD vectors in patients with higher BMI as well as female patients. Perhaps that these patients' populations could lend themselves to a different approach to S-ICD screening.

#### **2.5.4 Limitations**

It is worthy of noting that despite the high passing rates of S-ICD screening reported in this study, the rates of TWO were low and in keeping with TWO rates reported in literature. Perhaps one explanation for the high passing rates in this study is selection bias. The analysis was done retrospectively on patients who were selectively referred for S-ICD therapy by their treating cardiologists, while other studies reported in literature prospectively recruited consecutive patients referred for ICD therapy generally and not S-ICD specifically. The analysis also was not designed to report on the S-ICD screening success rate in a specific patients' population, but the cohort of patients included in this study is a representation of real-life patient population of various aetiologies referred for S-ICD therapy at a tertiary referral centre for cardiac devices in the UK. Finally, only the outcome of "at rest" screening was considered and the outcome of exercise screening, which was not performed in all patients, was excluded from the analysis.

## 2.6 Conclusion

Most “real-life” patients referred for S-ICD therapy are likely to be deemed S-ICD eligible following current screening practices. Certain patient characteristics such as gender, BMI, and underlying cardiac aetiologies can impact the S-ICD screening outcomes. It is important to highlight that the current screening practices are based on an important fact that the S-ICD can be programmed to one fixed vector at one time. If an advancement in technology allows the dynamic automated shifting from one sensing vector to another, current screening practices and S-ICD eligibility criteria will need to be revisited, with subsequent changes to the S-ICD eligibility rates.

## Chapter 3     Holter recorded changes in R:T ratio and T wave morphology: an observational study of S-ICD sensing (HEART-TWO)

### 3.1     Introduction

In the previous chapter, I have demonstrated through real-world data – in keeping with published literature- that not all patients are eligible for an S-ICD, and that there are many factors that could influence S-ICD eligibility.

A major predictor of eligibility of a vector is the R:T ratio which is unique for every vector as varying the angle of recording alters the amplitude of both R wave and T wave. Vectors with higher R:T ratios are more likely to pass the screening and is safe for clinical use, whilst a vector that fails cannot be used in clinical practice. Patients with vectors that do not meet the screening criteria are at high risk of TWO and deemed ineligible for an S-ICD.

Despite the current screening process, the incidence of inappropriate shocks is greater in S-ICDs when compared with conventional TV-ICDs and the most common reason for inappropriate shocks in S-ICDs is T -wave oversensing.<sup>105,123–130</sup>

It is important to note that temporal variations in R wave and T wave amplitudes in the same individual are frequently observed on ECG recordings and thus, the R:T ratio, a major predictor of S-ICD eligibility, is not fixed in any given individual. Factors such as changes in posture and heart rate can influence ECG parameters. Also changes in electrolytes concentrations, body weight, fluid shifts, and lung congestion can cause detectable dynamic changes on surface ECG recordings.<sup>104,106–111,131–133</sup> These observations are the rationale behind the patient groups selected in this study.

The concept of the potential varying of S-ICD vectors eligibility over time was previously presented in a study by Wiles et al.<sup>134</sup> The study demonstrated that the vector score which determines S-ICD eligibility is in fact dynamic in a real-life ICD population.

In this chapter, I present the findings of HEART TWO study. Through this study, I demonstrate that R:T ratio, one of the integral components of the S-ICD sensing mechanism and a main determinant of S-ICD eligibility, has the tendency to fluctuate overtime, particularly in specific patient populations when compared to patients with structurally normal hearts. I demonstrate that this poses a theoretical risk for TWO and inappropriate shocks in patients who have S-ICDS fitted in after being found S-ICD eligible following the current screening practices.

## 3.2 Objectives

- 1) Quantify and describe the degree of variation R:T ratio observed in different patients' subgroups from an S-ICD vector perspective. The patients' subgroups studied are:
  - Patients with heart failure.
  - Patients with hypertrophic cardiomyopathy.
  - Patients with simple and complex adult congenital heart disease.
  - Healthy volunteers without any known structural heart disease.
  
- 2) Calculate the proportion of patients from each patient subgroup who have favourable R:T ratios that would be eligible for an S-ICD. A R:T ratio eligibility cut-off of 3:1 was chosen for this study based on the manufacturer's guidelines.

Around 5% of S-ICD patients are known to experience inappropriate shocks at some stage due to TWO, however the incidence of silent or subclinical TWO over a short period of time, in a non-S-ICD population could not be easily estimated. I believe that the number of vectors obtained from the recruited participants gives sufficient data to understand the T wave and R:T ratio changes which occur over 24-hour period in the studied subgroups and provides sufficient data for a detailed analysis.

### 3.3 Methods

This study was performed with approvals from the REC (17/SC/0623) and R&D (RHMCAR0528).

This is a prospective observational study on different patients' subgroups. All the participants were asked to wear a seven lead/ three channel Holter® monitors for 24 hours. The leads for the Holters® were positioned so that they mimic and correspond to the three vectors (primary, alternate, and secondary) of an S-ICD, see Figure 16, and Figure 17. Participants were encouraged to pursue their usual daily activities while wearing the Holter monitors.

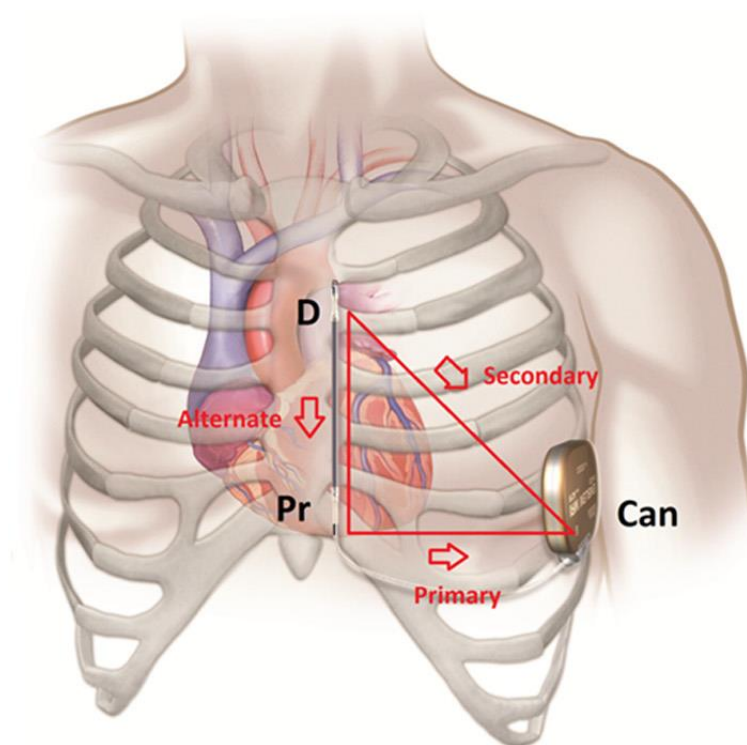


Figure 16 Showing the typical S-ICD vectors. Image prior to annotation © Boston Scientific Corporation or its affiliates. Annotations on the figure originally produced by Dr. Benedict Wiles, reproduced with permission.

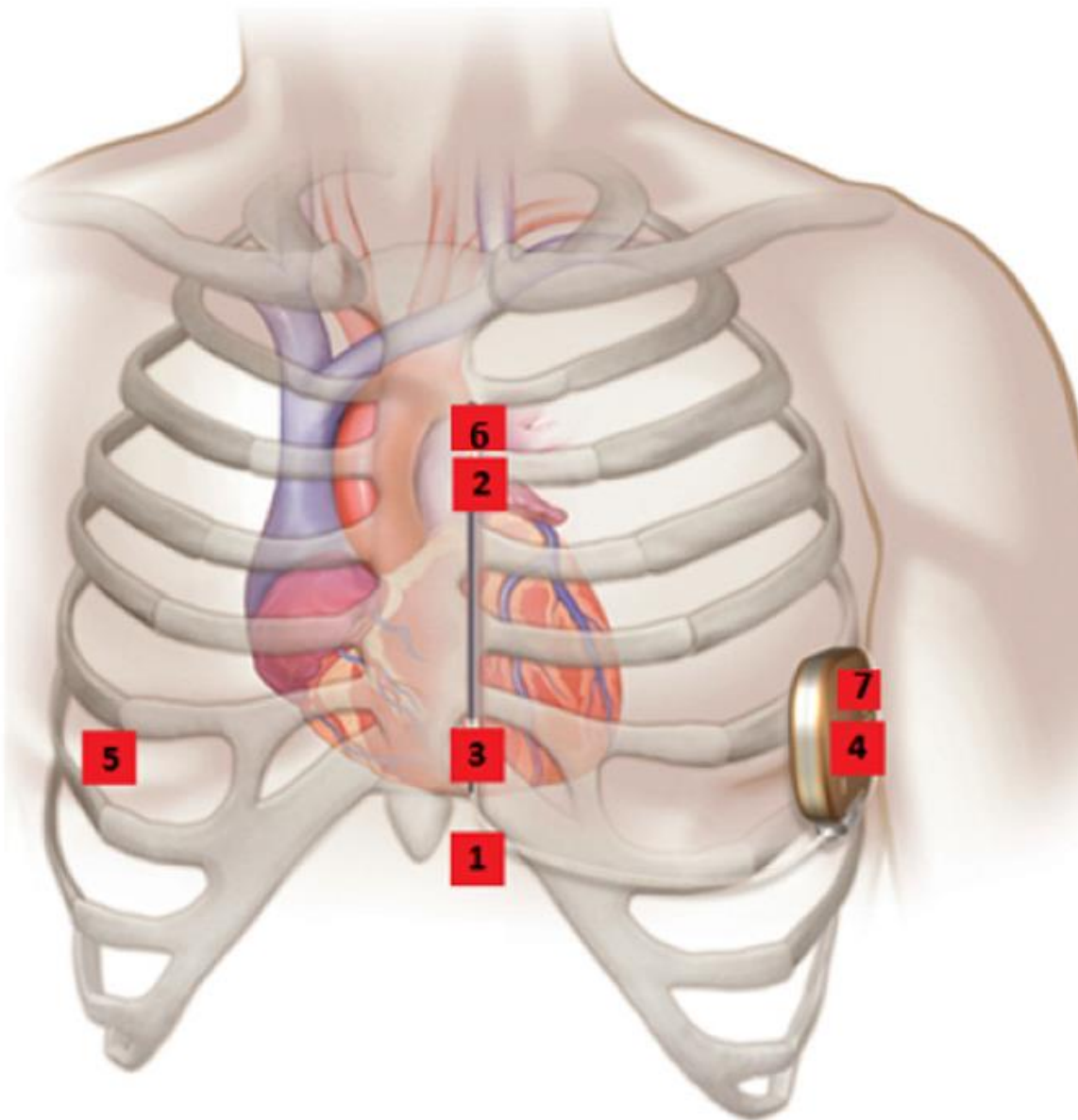


Figure 17 shows the Holter® surface ECG positions

1 = 1cm infero-lateral to the xiphisternum

3 = 5<sup>th</sup> intercostal space, parasternal position

6 = Adjacent to 2

Holter Channel A records between points 1 and 4

Holter Channel B records between points 2 and 3

Holter Channel C records between points 6 and 7 = surrogate of S-ICD secondary vector

5 = 5<sup>th</sup> intercostal space right mid clavicular line = neutral electrode

Image prior to annotation © Boston Scientific Corporation or its affiliates

2 = 14 cm superior to position 1

4 = 6<sup>th</sup> intercostal space left mid axillary line

7 = Adjacent to 4

= surrogate of S-ICD primary vector

= surrogate of S-ICD alternate vector

= surrogate of S-ICD secondary vector



### 3.3.1 Patients' subgroups

- Adult patients receiving high dose intravenous diuretic therapy (equivalent to >120mg furosemide in a 24-hour period) on clinical grounds for the heart failure subgroup.
- Adult patients with underlying adult congenital heart disease ranging from simple pathology such as atrial septal defect or ventricular septal defect (corrected or not) to more complex anatomy such as single ventricle, presence of Fontan circulation or transposition of the great vessels for the adult congenital heart disease subgroup.
- Adult patients with the clinical diagnosis of hypertrophic cardiomyopathy for the cardiomyopathy subgroup.
- Adult patients who have no known structural heart disease for the healthy volunteer's subgroup.

Patients were recruited in the HF subgroup based on having a recorded diagnosis of the clinical syndrome of heart failure regardless of their underlying left ventricular function on the echocardiogram and received intravenous diuretic therapy (at least 120 mg furosemide/24 hours) on clinical grounds under the discretion of their treating physicians. Patients were recruited in the ACHD and HCM subgroups based on having an underlying clinical diagnosis of ACHD and HCM, respectively. Participants with no underlying structural heart disease were recruited to the structurally normal heart/control subgroup.

### 3.3.2 Data analysis

The concept of specifically tracking the R:T ratios in recorded ECG signals is new. As such, there were no dedicated tools readily available for tracking and analysing the R:T ratios for the Holter recordings. In addition, the magnitude of the data prohibited any practical attempts at the manual analysis of the data. A collaboration with the school of Mathematics, University of Southampton resulted in the development of a "machine-learning" tool<sup>135</sup> that was designed specifically to offer a practical, yet accurate solution for the analysis of the data. A brief outline of the use of the tool in the data analysis of this study is explained here. An in-depth review of the tool development, testing and validation is discussed in the next chapter. Holter recordings were securely transferred to the collaborating team at the school of Mathematics at the University of Southampton labelled only with a unique study ID. The school of Mathematics team have no access to further patient details.

### 3.3.2.1 Machine learning tool

It is more common in the literature to use the term R:T ratio to describe the relationship between R wave and T wave amplitudes. However, using R:T ratio is not a suitable parameter for the machine learning tool. As the T wave amplitude approaches zero, very small changes in the T wave amplitude can result in extreme changes in the R:T ratio. This massive variation in R:T ratio for subtle changes in the ECG signals makes R:T ratio inappropriate for use as a label in the regression mathematical problem utilised by the tool. Usually, the R wave is of greater amplitude than the T wave. Because of this, the T:R ratios of a set of ECG segments are well distributed between 0 and 1. For this reason, T:R ratio is a more suitable label/variable to be used in the regression problem.

For the sake of consistency and owing to the methodology used for the data analysis in the form of the machine learning tool as described above. The relationship between R wave and T wave amplitudes will be referred to as T:R ratio thereafter.

Raw data from the Holters were downloaded in ASCII (American Standard Code for Information Interchange) format at a frequency of 500 Hertz (Hz). Then, the data was first split into 10 second segments. Baseline drift correction techniques were then applied, followed by filtering to suppress powerline and high frequency noise. Then Phase Space Reconstruction (PSR), a popular technique in waveform analysis for representing non-linear characteristics of time series set of data using delay maps, was used to convert the ECG signals into compressed 32x32 pixel PSR images, one image for each 10 seconds worth of ECG data.

A Convolutional Neural Network (CNN) model was trained, which is going to be discussed in detail in Chapter 4, to predict the T:R ratio from the PSR images with a high degree of accuracy. The end result is a plot showing the variation of the T:R ratios for each lead/S-ICD vector over the recorded period, see Figure 18. To better examine how the behaviour of the T:R ratio differs between each lead, the tool was also used to plot a histogram of what proportion of the 24-hour screening period the T:R ratio of a particular lead spent in each range of T:R ratios, see Figure 19.

The tool is designed to give the T:R ratio for every 10 seconds of data/ECG signals, equivalent to a standard 12-lead ECG or a standard ECG strip used for current S-ICD screening process, this allowed the assessment of every individual lead/S-ICD vector eligibility for every 10 seconds for the whole 24-hours screening. From there, the probability of each vector failing the current screening methodology if the screenings were done at any time of the day was calculated as follows:

$$\text{Probability of failure} = \frac{\text{number of 10 second segments with unfavourable (>1:3) T:R ratio}}{\text{total number of 10 second segments (8640) in a 24 hour recording}}$$



Figure 18 Variation of the predicted TR ratio over the 24-hour screening period for each lead. Leads A, B and C correspond to primary, alternate, and secondary vectors of an S-ICD respectively.<sup>135</sup>

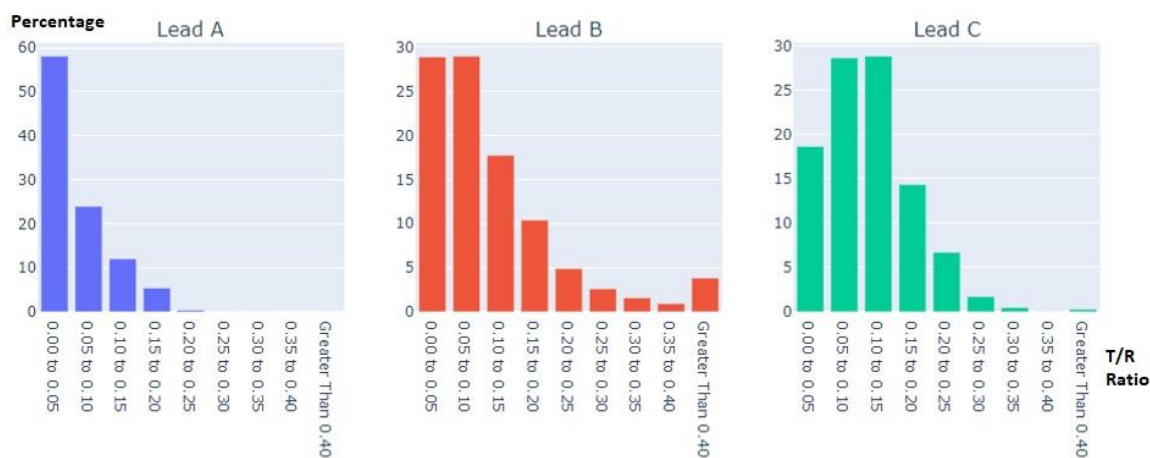


Figure 19 Histogram of the T:R ratio over the 24-hour screening period for each lead. Leads A, B and C correspond to primary, alternate, and secondary vectors of an S-ICD respectively.<sup>135</sup>

### 3.3.3 Statistical methodology:

Data analysis was done using RStudio 1.4.1106 running R 4.0.5. The distribution of the data was identified using histograms, QQ plots, and normality tests. Parametric data was described using

mean  $\pm$  standard deviation (SD), and categorical data as n/N (%). The Welch Two Sample t-test was used to compare the means of parametric data between the groups, and Mann-Whitney U and Wilcoxon rank tests were used to compare the medians of non-parametric data.

### 3.4 Results

A total of 34 patients (mean age  $54.6 \pm 7.0$  years, 64.7% male) were included in the study. The study population presents a mixed cohort of underlying aetiologies; 14 patients had heart failure (HF), 7 HCM, 7 had apparently normal hearts, 6 had adult congenital heart disease (ACHD), see Table 8 for patients' demographics.

The results of the analysis are presented in each subgroup of patients (heart failure, ACHD, HCM) compared to the control group/participants with structurally normal hearts.

<b>Total Number of Participants</b>		<b>n = 34</b>	
<b>Demographics:</b>	Mean age [years $\pm$ 95% CI]	54.6 $\pm$ 7.0	
	Male	22	64.7%
<b>Cardiac co-morbidities:</b>	Heart failure	14	41.2%
	Atrial fibrillation	7	20.6%
	LV diastolic dysfunction	5	14.7%
	Ischaemic heart disease	8	23.5%
	LV systolic dysfunction	14	41.2%
	Hypertrophic Cardiomyopathy	7	20.6%
	Adult Congenital Heart Disease	6	17.6%
	Apparently normal hearts	7	20.6%

Table 8 Patients' demographics.

#### 3.4.1 Heart failure patients

There were 7 patients in the structurally normal heart subgroup and 14 patients in the heart failure subgroup. The mean age was  $58.43 \pm 18.92$  years (62% male), see Table 9. Age and gender were not significantly different for either mean or the standard deviation (SD) of the T:R ratio.

Table 9 Patients demographics for the heart failure and structurally normal hearts subgroups.

<b>Total Number of Participants</b>		<b>N = 21</b>		<b>Heart Failure</b>	<b>Structurally normal heart</b>
				<b>N=14</b>	<b>N=7</b>
<b>Demographics:</b>	<i>Mean age [years ± 95% CI]</i>	58.43 ± 18.92		70 ± 11	36 ± 8
	<i>Male</i>	13	61.9%	10/14 (71%)	3/7 (43%)
<b>Cardiac co-morbidities:</b>	<i>Heart failure</i>	14	66.67%	14	0
	<i>Atrial fibrillation</i>	6	28.57%	6 (42.85%)	0
	<i>LV diastolic dysfunction</i>	4	19.05%	4 (28.57%)	0
	<i>Ischaemic heart disease</i>	6	28.57%	6 (42.85%)	0
	<i>LV systolic dysfunction</i>	10	47.62%	10 (71.43%)	0
				<i>Ejection fraction % =</i> 25.3 ± 6.97 [95% CI]	
	<b>Fluid loss in 24 hours in mls for the HF group</b>			2326.07 ± 1253.18 [95% CI]	
	<b>Furosemide dose in 24 hours in mgs for the HF group</b>			257.86 ± 45.86 [95% CI]	
	<b>Shift in Na levels before and after diuresis [mmol/l] for the HF group</b>			1.93 ± 0.73 [95% CI]	
	<b>Shift in K levels before and after diuresis [mmol/l] for the HF group</b>			0.49 ± 0.27 [0.95 CI]	

Mean T:R ratio was higher in HF patients ( $0.181 \pm 0.084$  versus  $0.104 \pm 0.054$ ,  $p < 0.001$ ), and the SD (a measure of dynamicity) of the T:R ratio was also higher in the HF patients ( $0.093 \pm 0.048$  versus  $0.067 \pm 0.036$ ,  $p = 0.02$ ), see Table 10 and Figure 20. There was no significant difference found in the mean or the SD of the T:R ratio between different leads within the same subgroup.

Table 10 Comparison between the parameters of the T:R between both subgroups.

Parameter	Group		P value
	Heart failure	Structurally normal heart	
Mean T:R ratio	0.181 ± 0.084(95% CI)	0.104 ± 0.054(95% CI)	<0.001 (Welch two sample t-test)
Standard deviation of T:R ratio	0.093 ± 0.048(95% CI)	0.067 ± 0.036(95%CI)	= 0.024 (Welch two sample t-test)

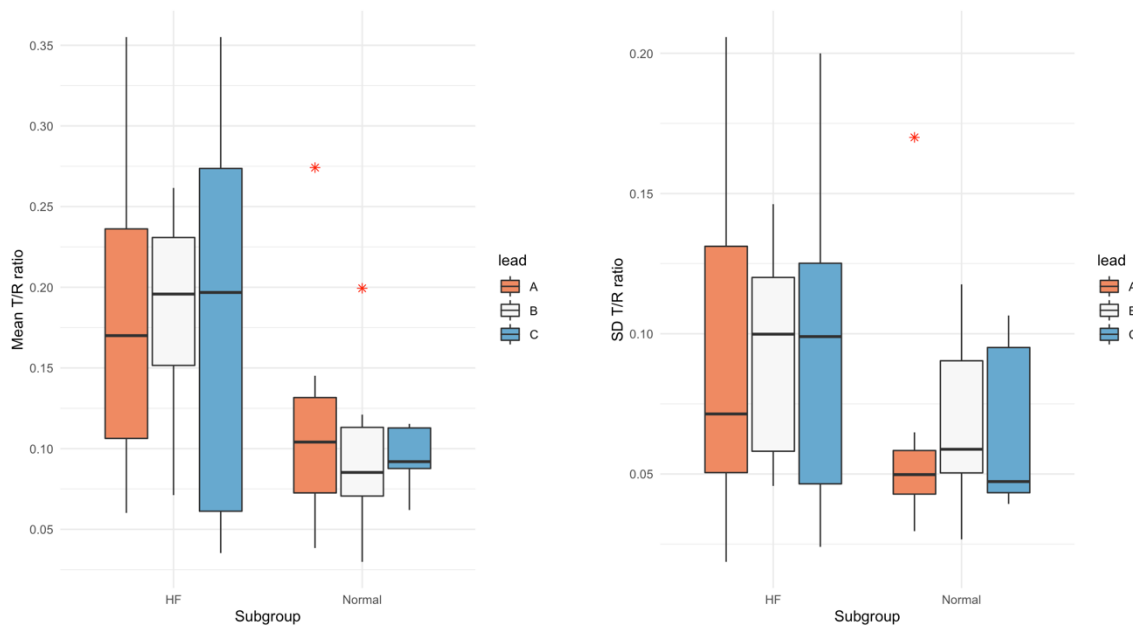


Figure 20 Box plots for the Mean ( $p < 0.001$ ) and standard deviation ( $p = 0.02$ ) of the T:R ratio over 24 hours screening period in the studied subgroups (Heart failure patients undergoing diuresis vs healthy volunteers with structurally normal hearts). Leads A, B and C correspond to primary, alternate, and secondary vectors of an S-ICD respectively.

To highlight the impact of the differences in the mean and SD of T:R between both subgroups; the percentage of time when the T:R ratio was found to be above the screening threshold (1:3) for the T:R ratio (unfavourable) was calculated and compared in both subgroups. Heart failure patients had an unfavourable T:R ratio for significantly longer time in the 24-hour period compared to the healthy volunteers, this was also evident in all the vectors; ( $13.3 \pm 10\%$  versus  $4 \pm 8\%$ ) in the primary vector, ( $9.7 \pm 7.4\%$  versus  $3 \pm 4\%$ ) in the alternate vector, and ( $10.8 \pm 12.8\%$  versus  $<1\%$ ) for the secondary vector, see Table 11 and Figure 21 **Error! Reference source not found.**

Table 11 Differences in the “unfavourable” T:R ratios in both subgroups

ID	Group	Primary Vector		Alternate Vector		Secondary Vector	
		10-second segments of T:R > 1:3 N= 8640	Proportion of the 24 -hour recording (%)	10-second segments > 1:3 N=8640	Proportion of the 24 -hour recording (%)	10-second segments > 1:3 N= 8640	Proportion of the 24 -hour recording (%)
1	Normal	3	<1%	0	0%	23	<1%
2	Normal	2613	30%	19	<1%	0	0%
3	Normal	17	<1%	51	<1%	0	0%
4	Normal	1	<1%	3	<1%	1	<1%
5	Normal	0	0%	452	5%	14	<1%
6	Normal	2	<1%	12	<1%	277	3%
7	Normal	1	<1%	1074	12%	3	<1%
	<b>Mean</b>	377 ±731	4 ± 8 %	230 ±301	3 ± 4 %	45±76	<1%
8	HF	8	<1%	1524	17.6%	NA	NA
9	HF	1024	11.9%	815	9.4%	NA	NA
10	HF	1280	14.8%	219	2.5%	NA	NA
11	HF	0	0%	1828	21.2%	NA	NA
12	HF	2305	26.7%	637	7.4%	NA	NA
13	HF	0	0%	31	<1%	NA	NA
14	HF	1104	12.8%	5	<1%	37	<1%
15	HF	3555	41.1%	4652	53.8%	4054	46.9%
16	HF	389	4.5%	452	5.2%	291	3.4%
17	HF	5562	64.4%	417	4.8%	0	0%
18	HF	13	<1%	400	4.6%	222	2.6%
19	HF	808	9.4%	383	4.4%	2866	33.2%
20	HF	0	0	0	0	0	0
21	HF	2	<1%	406	4.7%	1	<1%
	<b>Mean</b>	1146±862	13.3±10 %	841±640	9.7±7.4%	934±1105	10.8±12.8%

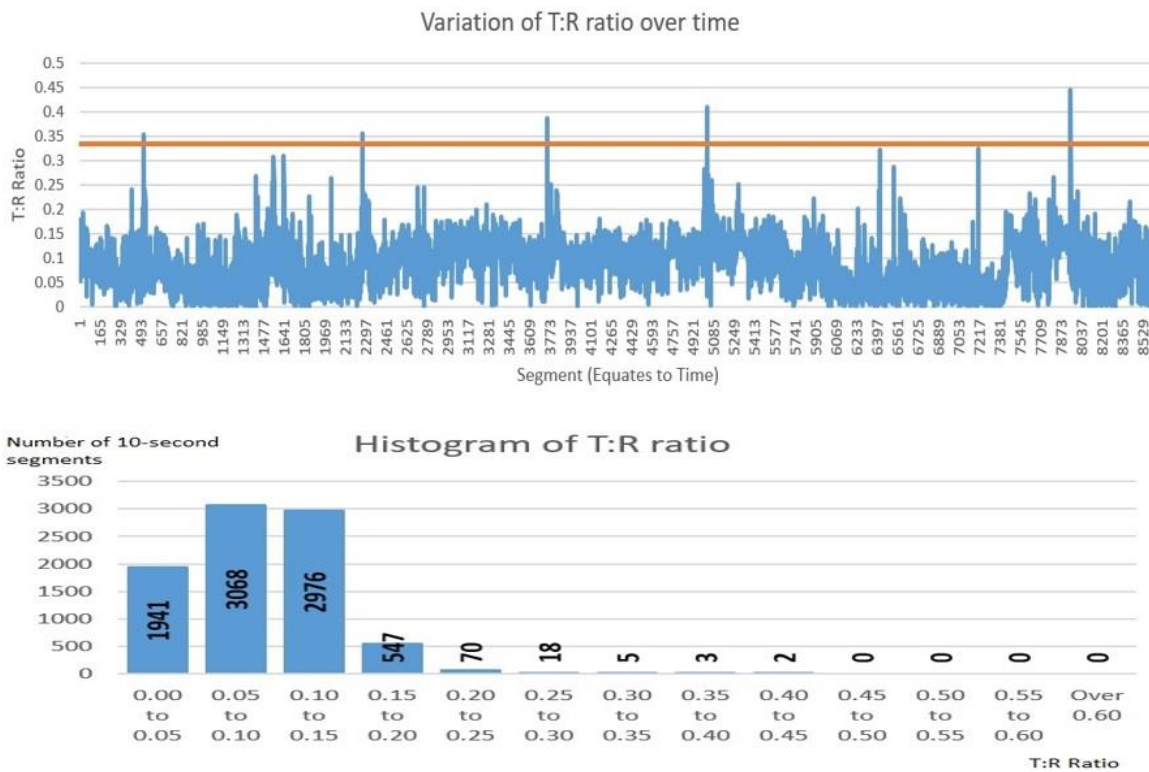


Figure 21 An example of the T:R ratio fluctuating overtime crossing the S-ICD screening threshold for the T:R ratio (0.33 or 1:3) on multiple occasions over the 24-hour period. The histogram illustrates the exact number of 10-second segments at each T:R ratio throughout the 24-hour recording. The above example represents the alternate vector for one of the patients who was recruited to the HF subgroup.

To summarise the results, T:R ratios of S-ICD vectors were higher at the baseline and exhibited more fluctuations in HF patients. This has translated into higher likelihood of unfavourable crossing of the screening threshold in HF patients when compared to the healthy volunteers.

### 3.4.2 ACHD patients

The mean age of the participants was 37.4±7.89 years; there were 8 (61.5%) males and 5(38.5%) females. Patients’ demographics are shown in Table 12.



Table 12 Patients' demographics

<b>Total Number of Participants</b>		<b>N = 13</b>	<b>ACHD subgroup N= 6</b>	<b>Healthy Volunteers N=7</b>
<b>Demographics:</b>	Mean age [years $\pm$ 95% CI]	37.4 $\pm$ 7.89	39 $\pm$ 16.36	36 $\pm$ 6.11
	Male	8 (61.5%)	5(83.3%)	3(42.9%)
<b>Underlying cardiac anatomy:</b>				
	Structurally normal heart		0	7
	Tricuspid atresia and Fontan's procedure		2	0
	Partial atrioventricular defect		1	0
	Double outlet right ventricle, dextrocardia and repaired ventricular septal defect		1	0
	Ventricular septal defect and patent ductus		1	0
	Common arterial trunk with previous complete repair		1	0

When the results from all the leads/S-ICD vectors were combined, there was a statistically significant difference in the mean, median and the standard deviation (SD) of the T:R ratios measured in 24 hours between both subgroups. The mean T:R ratio was higher ACHD patients ( $0.29 \pm 0.18$  versus  $0.1 \pm 0.05$ ,  $p < 0.001$ ). The median T:R was higher in ACHD patients ( $0.29 \pm 0.18$  versus  $0.1 \pm 0.06$ ,  $p < 0.001$ ) and the SD of the T:R ratio was also higher in ACHD patients ( $0.09 \pm 0.05$  versus  $0.06 \pm 0.04$ ,  $p = 0.042$ ). in other words, the T:R ratio was higher and exhibited more tendency to fluctuate (SD) in ACHD patients when compared to the healthy volunteers, see Table 13 and Figure 22.

Table 13 Mean, median, and SD of the T:R ratios measured in 24 hours for the all the Leads/S-ICD vectors.

Parameters	N	Underlying Anatomy		p-value <sup>1</sup>
		ACHD, N = 18	Normal, N = 21	
Mean T: R ratio	39	0.29 (0.18)	0.10 (0.05)	<0.001
SD of T:R ratio	39	0.09 (0.05)	0.06 (0.04)	0.042
Median T: R ratio	39	0.29 (0.18)	0.10 (0.06)	<0.001

<sup>1</sup> Welch Two Sample t-test

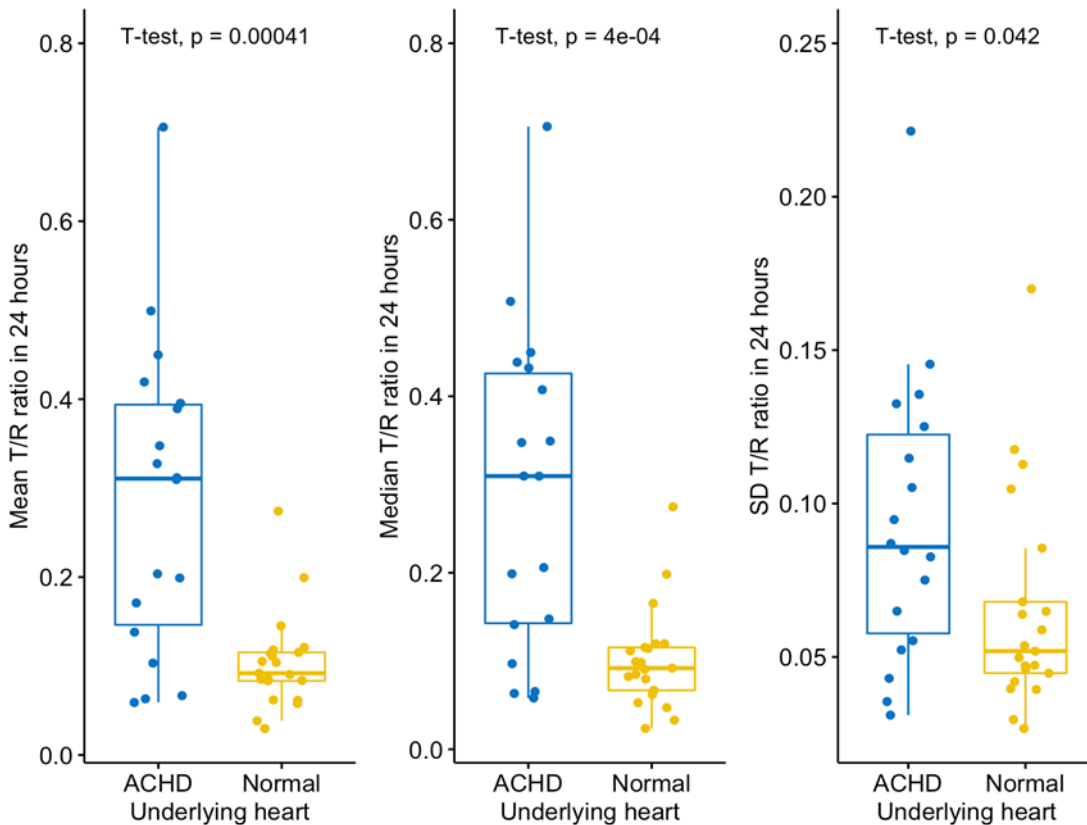


Figure 22 Mean, median, and SD of the T:R ratios measured in 24 hours for the all the Leads/S-ICD vectors in ACHD and healthy volunteers with normal hearts subgroups.

T:R ratios were also assessed in each of the three S-ICD vectors separately. Mean T:R ratios were higher in ACHD patients in all vectors; (0.245 versus 0.118,  $p = 0.11$ ) in the primary vector, (0.346 versus 0.096,  $p = 0.039$ ) in the secondary vector and (0.269 versus 0.097,  $p = 0.051$ ) in the alternate vector. Median T:R ratios were higher in ACHD patients in all vectors; (0.244 versus 0.118,  $p = 0.13$ ) in the primary vector, (0.288 versus 0.088,  $p = 0.02$ ) in the secondary vector and (0.282 versus 0.091,  $p = 0.043$ ) in the alternate vector. The SD of the T:R ratios were also higher in ACHD patients for all vectors; (0.076 versus 0.065,  $p = 0.65$ ) for the primary vector, (0.086 versus 0.061,  $p = 0.15$ ) for the secondary vector and (0.119 versus 0.069,  $p = 0.12$ ) for the alternate

vector. This means that, for the ACHD patients, the secondary vector had the highest T:R ratio (least favourable from S-ICD perspective) at the baseline, followed by the alternate vector then the primary vector. However, T:R ratio demonstrated highest degree of fluctuations in the alternate vector followed by the secondary then the primary vectors in ACHD patients.

Differently, for the healthy volunteers, the primary vector had the highest T:R ratio at the baseline and all the vectors exhibited the same degree of T:R ratio fluctuations, see Table 14, Figure 24 , Figure 25 and Figure 25.

Table 14 Mean, median, and SD of the T:R ratios measured in 24 hours classified according to the S-ICD vector.

<b>Parameters</b>	<b>N</b>	<b>ACHD (N=6)</b>	<b>Normal (N=7)</b>	<b>P-Value</b>	<b>95% CI</b>
<b>Mean T:R Pr. vector</b>	13	0.245	0.118	0.105	(-0.288,0.034)
<b>Mean T:R S. vector</b>	13	0.346	0.096	0.039	(-0.481, -0.019)
<b>Mean T:R Alt. vector</b>	13	0.269	0.097	0.051	(-0.345,0.001)
<b>Median</b>					
<b>Median T:R Pr. Vector</b>	13	0.244	0.118	0.126	(-0.299,0.046)
<b>Median T:R S. vector</b>	13	0.288	0.088	0.021	(-0.354, -0.045)
<b>Median T:R Alt. vector</b>	13	0.282	0.091	0.043	(-0.375, -0.008)
<b>SD</b>					
<b>SD T:R Pr. Vector</b>	13	0.076	0.065	0.649	(-0.065,0.043)
<b>SD T:R S. vector</b>	13	0.086	0.061	0.15	(-0.060,0.011)
<b>SD T:R Alt. vector</b>	13	0.119	0.069	0.119	(-0.116,0.016)

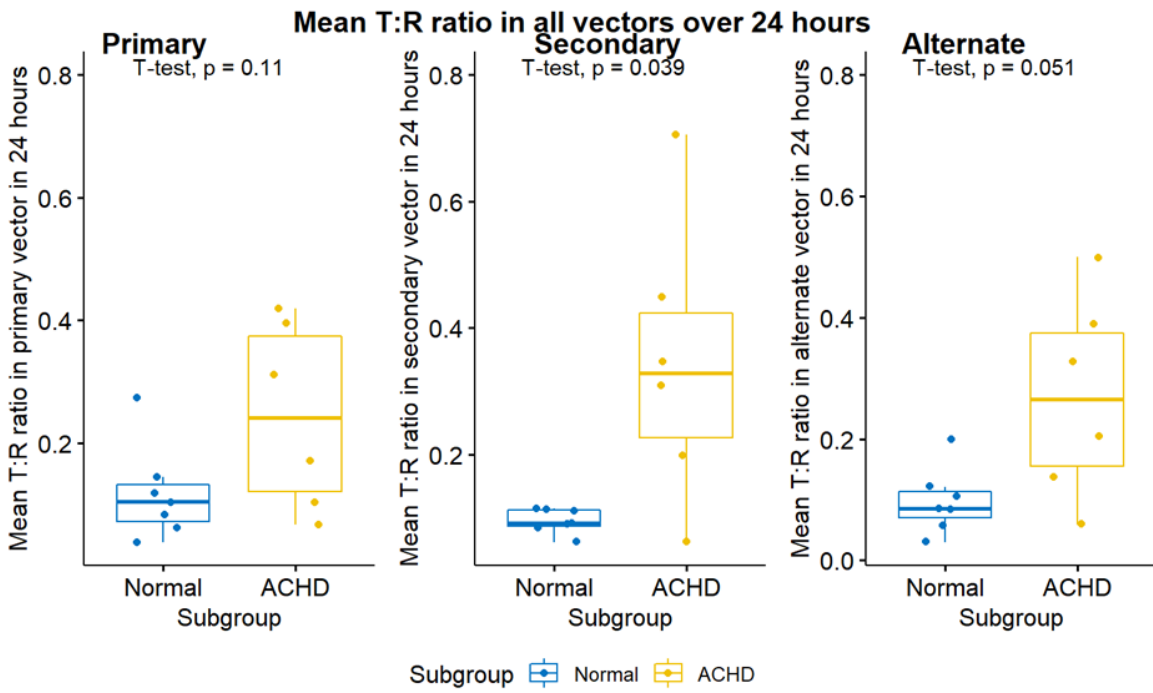


Figure 23 Mean T:R ratios measured in 24 hours classified according to the S-ICD vector.

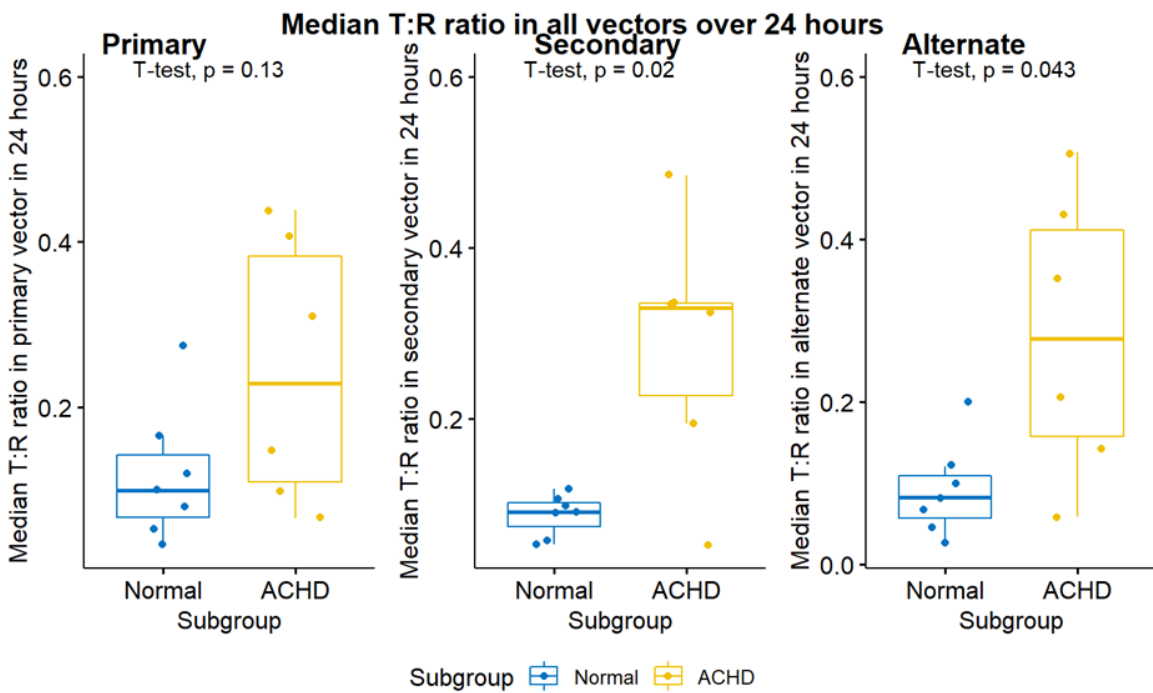


Figure 24 Median T:R ratios measured in 24 hours classified according to the S-ICD vector.

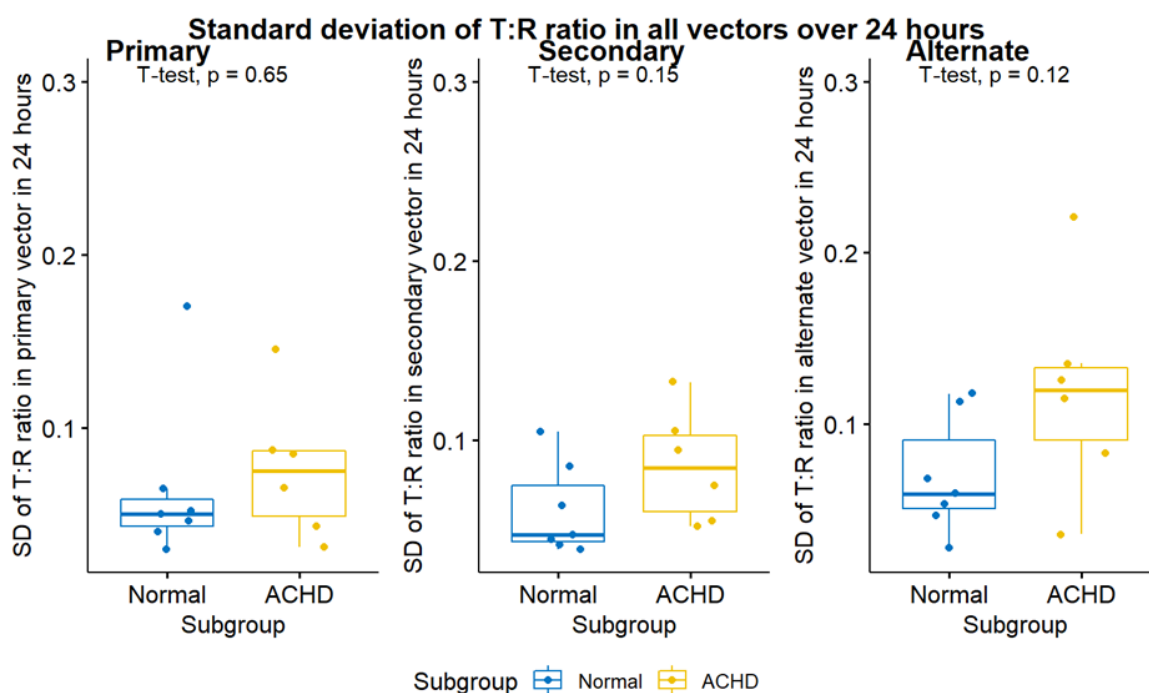


Figure 25 Standard deviation (SD) of the T:R ratios measured in 24 hours classified according to the S-ICD vector.

To highlight the impact of the differences in the mean and SD of T:R between both subgroups; the percentage of time when the T:R ratio was found to be above the screening threshold (1:3) for the T:R ratio (unfavourable) was calculated and compared in both subgroups.

The probability of an S-ICD vector failing the screening for the ACHD cohort averaged at  $36\% \pm 31\%$ ,  $36\% \pm 28\%$ , and  $38\% \pm 25\%$  for the primary, alternate, and secondary vectors, respectively. While the probability of a vector failing the screening in the healthy volunteers was significantly lower at  $4\% \pm 8\%$ ,  $3\% \pm 4\%$ , and  $< 1\%$  for the primary, alternate, and secondary vectors respectively, see Table 15.

Table 15 Shows the probability of S-ICD screening failure for all the S-ICD vectors.

ID	Group	Primary Vector		Alternate Vector		Secondary Vector	
		10-second segments of T:R > 1/3	Probability of failing screening (%)	10-second segments > 1/3	Probability of failing screening (%)	10-second segments > 1/3	Probability of failing screening (%)
1	ACHD	2450	28	1235	14	4364	51
2	ACHD	7106	82	6077	7	6998	81
3	ACHD	0	0	4800	55	4538	52
4	ACHD	7488	87	6573	76	3733	43
5	ACHD	1411	16	34	<1	35	<1
6	ACHD	0	0	1	<1	122	1

<b>Mean</b>		3756±2720	36±31	3120 ±2435	36±28	3298 ±2185	38±25
<b>7</b>	Normal	3	<1	0	0	23	<1
<b>8</b>	Normal	2613	30	19	<1	0	0
<b>9</b>	Normal	17	<1	51	<1	0	0
<b>10</b>	Normal	1	<1	3	<1	1	<1
<b>11</b>	Normal	0	0	452	5	14	<1
<b>12</b>	Normal	2	<1	12	<1	277	3
<b>13</b>	Normal	1	<1	1074	12	3	<1
<b>Mean</b>		377±731	4±8	230±301	3 ±4	45±76	<1

### 3.4.3 HCM patients

The mean age of the participants was 46.3±10.4 years (50% male). 7 of the participants were in the HCM subgroup (mean age 56.6±16.8 years, 57.1% male) and 7 (mean age 36±6.1 years, 42.9% male) in the control group of healthy volunteers. All the healthy volunteers did not have any underlying cardiac conditions, see Table 16.

Table 16 Patients' demographics.

<b>Total Number of Participants</b>		<b>N = 14</b>	<b>HCM group N= 7</b>	<b>Healthy Volunteers N=7</b>
<b>Demographics:</b>	Mean age [years ± 95% CI]	46.3 ±10.4	56.6 ±16.8	36 ±6.1
	Male	7(50%)	4(57.1%)	3(42.9%)
<b>Underlying cardiac anatomy:</b>				
	Structurally normal heart		0	7
	Hypertrophic cardiomyopathy		7	0

When the results from all the leads/S-ICD vectors were combined, there was a statistically significant difference only in the median of the T:R ratios measured in 24 hours between both groups. The mean T:R ratio was higher in HCM patients ( $0.17 \pm 0.11$  versus  $0.1 \pm 0.05$ ,  $p < 0.07$ ). The median T:R was higher in HCM patients ( $0.17 \pm 0.11$  versus  $0.1 \pm 0.06$ ,  $p < 0.04$ ), while the SD of the T:R ratio was only marginally lower in HCM patients ( $0.06 \pm 0.03$  versus  $0.07 \pm 0.04$ ,  $p = 0.3$ ). In other words, the T:R ratio was higher, but exhibited marginally less tendency to fluctuate (SD) in HCM patients when compared to the healthy volunteers, see Table 17, and Figure 26.

Table 17 Mean, median, and SD of the T:R ratios measured in 24 hours for the all the Leads/S-ICD vectors.

Parameters	N	Underlying Anatomy		p-value <sup>1</sup>
		HCM, N = 21	Normal, N = 21	
Mean T: R ratio	42	0.17 (0.11)	0.10 (0.05)	<b>0.07</b>
SD of T:R ratio	42	0.06 (0.03)	0.06 (0.04)	<b>0.3</b>
Median T: R ratio	42	0.17 (0.11)	0.10 (0.06)	<b>0.04</b>

<sup>1</sup> Wilcoxon rank sum exact test

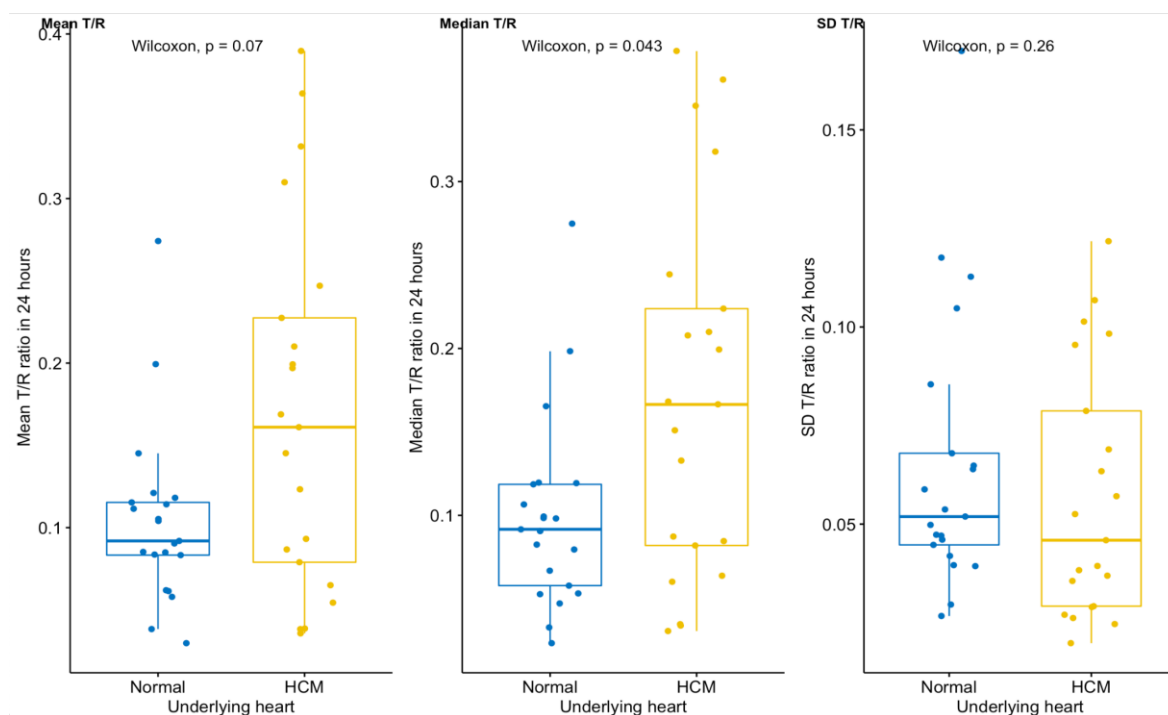


Figure 26 Mean, median, and SD of the T:R ratios measured in 24 hours for the all the Leads/S-ICD vectors in HCM and healthy volunteers with normal hearts groups.

T:R ratios were also assessed in each of the three S-ICD vectors separately. Mean T:R ratios were higher in HCM patients in all vectors; (0.19 versus 0.12,  $p = 0.26$ ) in the primary vector, (0.14 versus 0.10,  $p = 0.8$ ) in the secondary vector and (0.17 versus 0.10,  $p = 0.26$ ) in the alternate vector. Median T:R ratios were higher in HCM in all vectors; (0.2 versus 0.12,  $p = 0.2$ ) in the primary vector, (0.14 versus 0.09,  $p > 0.9$ ) in the secondary vector and (0.17 versus 0.09,  $p = 0.1$ ) in the alternate vector. The SD of the T:R ratios in HCM for all vectors; (0.06 versus 0.07,  $p > 0.9$ ) for the primary vector, (0.04 versus 0.06,  $p = 0.13$ ) for the secondary vector and (0.07 versus 0.07,  $p > 0.9$ ) for the alternate vector. This means that, for HCM patients, the primary vector had the highest T:R ratio (least favourable from S-ICD perspective) at the baseline, followed by the alternate vector then the secondary vector. However, T:R ratio demonstrated highest degree of fluctuations in the alternate vector followed by the primary then the secondary vectors in HCM patients. For the healthy volunteers, the primary vector had the highest T:R ratio at the baseline and all the vectors exhibited, more or less, the same degree of T:R ratio fluctuations, see Table 18, Figure 28, Figure 29, and Figure 29.

Table 18 Mean, median, and SD of the T:R ratios measured in 24 hours classified according to the S-ICD vector.

Parameters	N	HCM (N=7)	Normal (N=7)	P- Value <sup>1</sup>
Mean T:R Pr. vector	14	0.19(0.13)	0.12(0.08)	0.26
Mean T:R S. vector	14	0.14(0.11)	0.10(0.02)	0.8
Mean T:R Alt. vector	14	0.17(0.10)	0.10(0.05)	0.26
Median T:R Pr. Vector	14	0.20(0.13)	0.12(0.08)	0.2
Median T:R S. vector	14	0.14(0.11)	0.09(0.02)	>0.9
Median T:R Alt. vector	14	0.17(0.10)	0.09(0.06)	0.1
SD T:R Pr. Vector	14	0.06(0.03)	0.07(0.05)	>0.9
SD T:R S. vector	14	0.04(0.02)	0.06(0.03)	0.13
SD T:R Alt. vector	14	0.07(0.04)	0.07(0.03)	>0.9

<sup>1</sup> Wilcoxon rank sum exact test

N= Number of patients. Pr. Vector, S. vector, and Alt. vector = Primary, secondary, and alternate vectors respectively.



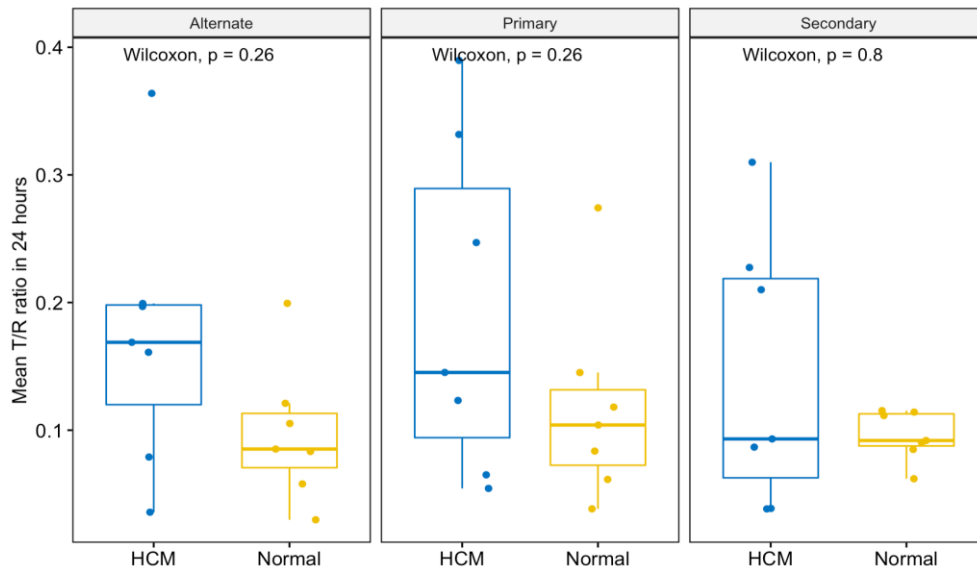


Figure 27 Mean T:R ratios measured in 24 hours classified according to the S-ICD vector.

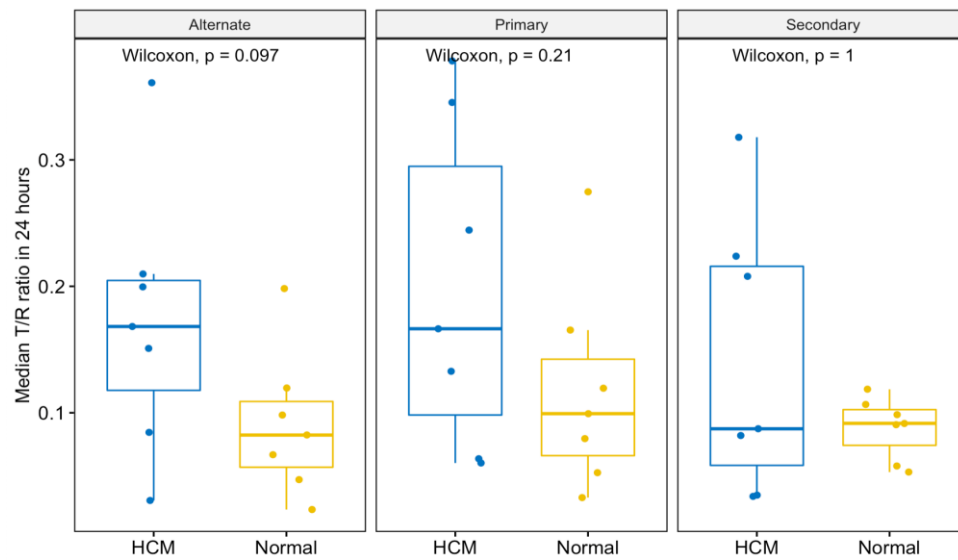


Figure 28 Median T:R ratios measured in 24 hours classified according to the S-ICD vector.

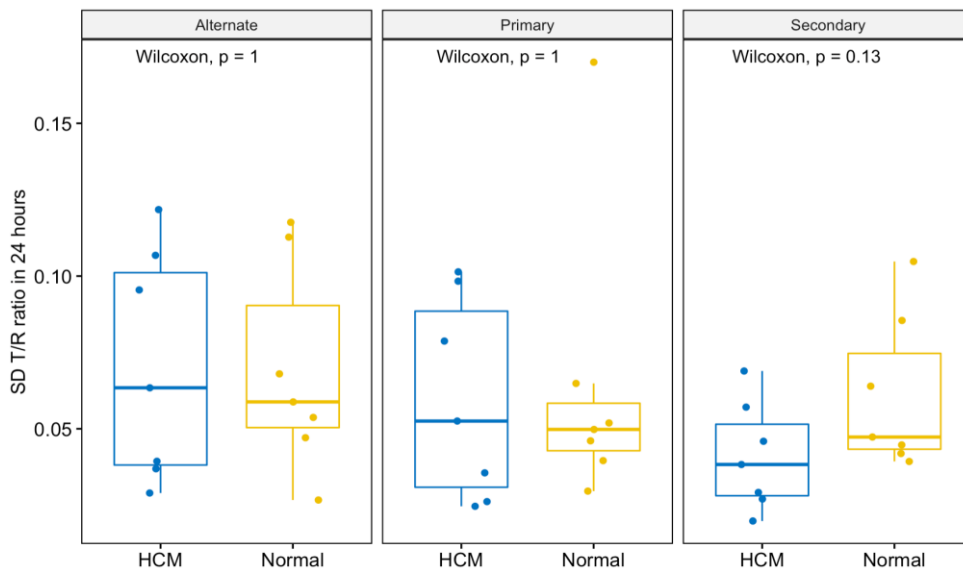


Figure 29 Standard deviation (SD) of the T:R ratios measured in 24 hours classified according to the S-ICD vector.

To highlight the impact of the differences in the mean and SD of T:R between both subgroups; the percentage of time when the T:R ratio was found to be above the screening threshold (1:3) for the T:R ratio (unfavourable) was calculated and compared in both subgroups. The probability of an S-ICD vector failing the screening for the HCM cohort averaged at  $18\% \pm 21\%$ ,  $10\% \pm 16\%$ , and  $5\% \pm 10\%$  for the primary, alternate, and secondary vectors, respectively. While the probability of a vector failing the screening in the healthy volunteers was lower at  $4\% \pm 8\%$ ,  $3\% \pm 4\%$ , and  $< 1\%$  for the primary, alternate, and secondary vectors respectively, see Table 19.

Table 19 Probability of each vector passing the screening using standard screening practice in both subgroups.

ID	Group	Primary Vector		Alternate Vector		Secondary Vector	
		10s segments of T:R > 1/3	Probability of failing screening (%)	10s segments > 1/3	Probability of failing screening (%)	10s segments > 1/3	Probability of failing screening (%)
1	HCM	18	<1	0	0	0	0
2	HCM	0	0	5414	63	1	<1
3	HCM	0	0	100	1	0	0
4	HCM	13	<1	20	<1	16	<1
5	HCM	1	<1	1	<1	0	0
6	HCM	5655	65	403	5	73	1
7	HCM	5262	61	46	<1	3181	37
	Mean	1564.14 ±1826.29	18±21	854.86 ±1382.27	10±16	467.29 ±820.92	5±10
7	Normal	3	<1	0	0	23	<1
8	Normal	2613	30	19	<1	0	0
9	Normal	17	<1	51	<1	0	0
10	Normal	1	<1	3	<1	1	<1
11	Normal	0	0	452	5	14	<1
12	Normal	2	<1	12	<1	277	3
13	Normal	1	<1	1074	12	3	<1
	Mean	377±731	4±8	230±301	3±4	45±76	<1

### 3.5 Discussion

The concept of the potential varying of S-ICD vectors eligibility over time was introduced before in a published study by Wiles et al. That study has demonstrated that the vector score, which determines S-ICD eligibility, is in fact dynamic in real-life ICD population.<sup>134</sup> The clinical significance for this dynamicity is not clear but it sheds the light on the possibility that acquiring screening data over a much longer period than for conventional screening across the three S-ICD vectors

can enable more reliable and descriptive screening of the vectors and can aid patient and vector selection in S-ICD candidates.

### 3.5.1 Data analysis

I have demonstrated through this study that one of the main determinants of S-ICD eligibility, the T:R ratio (or R:T ratio), is dynamic. In this section, I will demonstrate that this dynamicity can be significant with potential clinical implications. This is particularly relevant to the specific patients' populations assessed in this study.

The T:R ratios were unfavourable a priori in HF patients when compared to the healthy volunteers. Importantly T:R ratios were more likely to fluctuate and cross the S-ICD screening threshold in HF patients than in the normal heart patients. The cohort of HF patients in this study shared many of the characteristics, such as rapid fluid and body weight shifts and quick changes in electrolyte concentrations, known to cause dynamic changes in ECG signals.

ACHD is a broad term covering a wide array of underlying anatomical variants. It is as such, expected that there would be a high degree of variability not only of the S-ICD screening passing rate, but also of which of the S-ICD vectors that are likely to pass the screening in the ACHD population. It comes as a no surprise that the probability of S-ICD vectors failing the screening in ACHD patients was much higher than that of the healthy volunteers with structurally normal hearts in this study, which is in line with previously published studies.<sup>37,71</sup> ACHD also had higher T:R ratios at the baseline when compared to participants with normal hearts. Furthermore, T:R ratios were also more likely to fluctuate in ACHD patients when compared to the healthy volunteers. This may be due to abnormal T-wave morphology, resulting from the unique anatomical and physiological features that characterizes ACHD such as cardiac chamber enlargement, abnormal cardiac orientation, mechanical strain, and augmented repolarization patterns.

The T:R ratio fluctuations in the HCM patients were comparable to the control group of structurally normal hearts. However, HCM patients had unfavourable T:R ratios at the baseline when compared to the control group. This has translated to a higher rate of vectors crossing the

S-ICD eligibility screening thresholds for the T:R ratios and higher probabilities of screening failure in HCM patients.

Upon analysing the results down to the individual level, the clinical significance became apparent. These small changes in the T:R ratio parameters can dictate the S-ICD eligibility as dynamic changes in the T:R ratio in some of the vectors that were observed were significant enough in some instances to cause the T:R ratio to cross the threshold for the S-ICD screening, increasing the risk of TWO and inappropriate shocks.

### **3.5.2 Clinical relevance and potential applications**

The cut-off T:R ratio of 1:3 used for current screening practice incorporates a safety margin to accommodate for the fluctuations of the ECG signal amplitudes over time without affecting the sensing of the S-ICD. Currently, patients who do not possess at least a single S-ICD vector meeting this T:R ratio cut-off are deemed ineligible for S-ICD therapy, a significant limitation to their care, particularly in some patients where S-ICD provides a valuable and, in some cases, their only option for defibrillation protection therapy.

The proposed screening approach in this study is novel, where artificial intelligence and deep learning methods are used to screen patients for S-ICD eligibility. Screening data was acquired over a much longer period than for conventional screening approaches and provides an in-depth description of the behaviour of the T:R ratio over that period across the S-ICD vectors. This could enable more reliable assessment of patients' eligibility for S-ICD implantation which potentially eliminates the need to incorporate a "safety-margin" into the eligibility threshold of the T:R ratio. Clinically, this can be translated into higher rates of S-ICD eligibility without having to compromise with a higher risk of TWO and inappropriate shocks. This is important as inappropriate shock therapies can have detrimental effects on the quality of life, psychological wellbeing and can even result in the induction of ventricular arrhythmias.<sup>136</sup>

It is not uncommon for multiple vectors to pass the S-ICD screening. In current practice, the choice of which vector to use for programming is arbitrary since the outcome of the screening is binary (pass or fail) and there are no "degrees" awarded for an S-ICD vector for passing the screening. It is prudent that vector selection for S-ICD programming should be individualised for each patient and this novel screening approach could enable more reliable and descriptive assessment of the S-ICD vectors behaviour over prolonged screening periods. This can guide clinicians to make more informed decisions on vectors selection in S-ICD eligible patients. The most favourable vector would be the most stable or the one that is least

likely to fluctuate and cross the screening threshold during prolonged screening and thus pose the least risk of TWO and inappropriate shock therapy, see Figure 30.

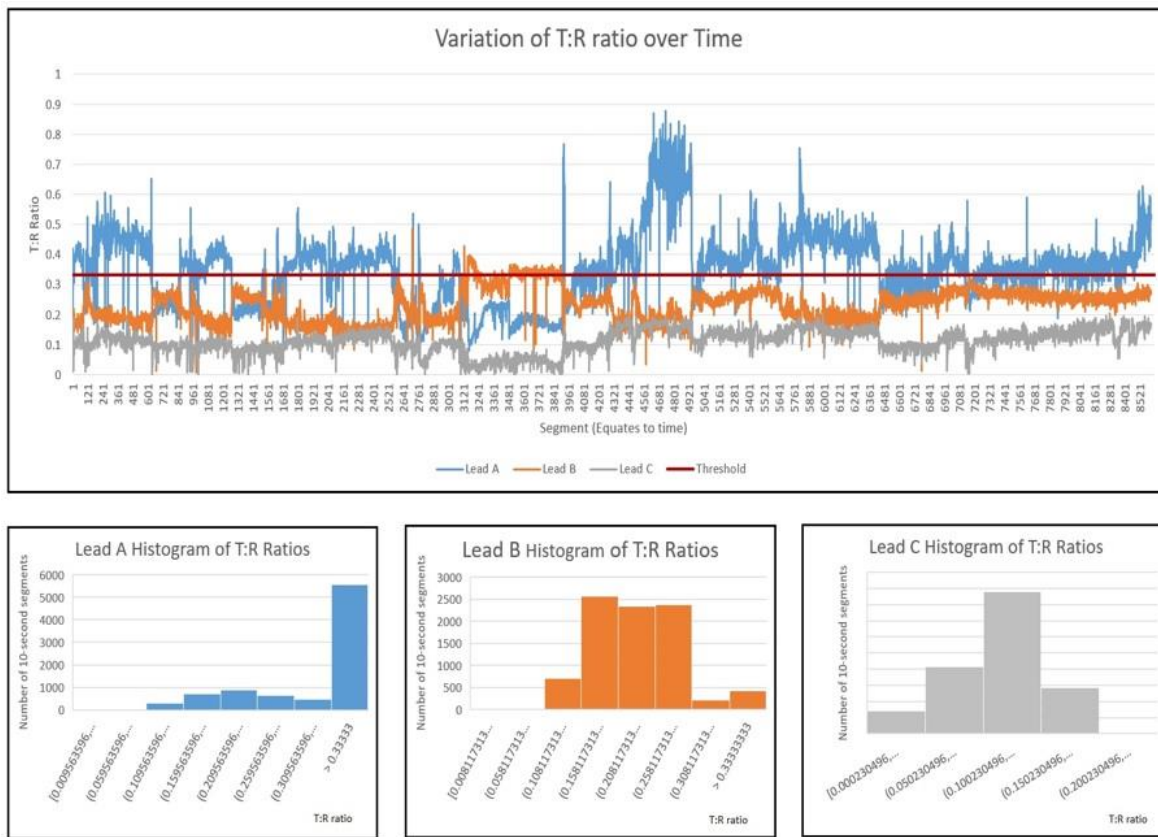


Figure 30 An example of how the tool can help select the most suitable vector for programming the S-ICD. The analysis of the Holter recording for one of the patient recruited in the HF subgroup: All the 3 leads had acceptable T:R ratios at some stage of the 24-hour recordings, however, while the T:R ratios for Leads A and B (corresponding to the primary and alternate vectors) showed significant fluctuations over the 24-hours recording and crossed the screening threshold multiple times, T:R ratio for Lead C (secondary vector) was stable in comparison and didn't cross the threshold throughout the 24-hours posing the least risk of TWO.

### 3.5.3 Limitations

It is important to interpret the results of this study with caution. Firstly, because of the relatively small number of patients involved in the study, though each patient provided significant amount of data on the behaviour of the T:R ratio for the S-ICD vectors for a much longer duration than that currently used in the day-to-day practice. In addition, ACHD is treated as a single entity for the sake of the analysis, when, ACHD covers very different underlying pathologies with various degrees of complexities. Furthermore, none of the patients recruited to the study had S-ICD implants or had an indication for an S-ICD. While it could be argued that the analysis will not apply to real life S-ICD patients, many such S-ICD recipients fall into either of the recruited patients' cohorts. Also, R:T or T:R ratio, despite being a key component in the S-ICD sensing process, is not

the only parameter and other factors that play a role in the S-ICD sensing process such as QRS duration as well as the impact of the relatively newer S-ICD sensing algorithms, i.e., SMART PASS, were not examined in this analysis. It is also important to note that, while theoretically relevant, there is no evidence that the fluctuations in the T:R ratios that were demonstrated in this study would inevitably lead to adverse clinical outcomes such as TWO and inappropriate shocks and further work is needed to appreciate the clinical significance of the findings.

The principles of this study need to be tested in a larger, more diverse patient cohort and the clinical relevance of the findings need to be further investigated before it is possible to apply the proposed screening method to clinical practice. In addition, further prospective studies with real-life S-ICD candidates and long-term follow up will be needed to give insight into the optimal T:R ratio that could be utilised for prolonged screening for S-ICD eligibility.

### **3.6 Conclusion**

R:T or T:R ratio, one of the integral components of the S-ICD sensing mechanism and a main determinant of S-ICD eligibility, is significantly higher in heart failure, ACHD and HCM patients when compared to patients with structurally normal hearts. In addition, this ratio has the tendency to significantly fluctuate overtime, particularly in patients with heart failure and ACHD when compared to patients with structurally normal hearts. This poses a theoretical risk for TWO and inappropriate shocks in patients who have S-ICDS after being found to pass current screening practices. Furthermore, incorporating deep learning methods could enable more accurate and efficient screening and the adoption of novel mathematical approaches for data analysis of longer, data-rich, screening practices to determine patient eligibility for S-ICD implantation seems promising.

## Chapter 4 The deep learning methods algorithm

### 4.1 Introduction

As presented in the previous chapter, the concept of specifically tracking the T:R ratios in recorded ECG signals to assess S-ICD eligibility is novel. There were no readily available practical solutions to aid in analysing the recorded data. A collaboration with the school of Mathematics, University of Southampton resulted in the development of a “machine-learning” tool that was designed specifically to offer a practical, yet accurate solution for the analysis of the data. In this chapter, an in-depth review of the tool development, testing and validation is discussed.

#### 4.1.1 Details of collaboration

##### 4.1.1.1 Role of clinical team, represented by me, Mohamed ElRefai, PhD student and author of this work

- Raising the clinical question, role of prolonged screening in S-ICD eligibility.
- Choosing T:R ratio as the parameter to be examined.
- Recognising that the magnitude of data to be examined needs input from specialists in artificial intelligence methodology and pursuing this collaboration.
- Recruiting the participants, collecting, and anonymising the data.
- Manual annotation of a wide sample of the data, to be used to train the algorithm, also to be used to test the algorithm after training using previously annotated data that were blinded from the algorithm.
- Statistical analysis of the data pre- and post-processing by the algorithm.
- Interpreting the overall results and deducing the conclusions based on the findings.

##### 4.1.1.2 Role of Mathematics team, represented by Anthony Dunn, PhD student at UoS, school of mathematics, Stefan Coniglio, Associate Professor of Mathematics at UoS, and Alain Zemkoho, Associate Professor of Mathematics at UoS

- Choosing Machine learning and more specifically, Phase Space Reconstruction techniques and Convolutional Neural Network models as the most suitable methodology to process the data.
- Creating and coding the DiNovo algorithm.
- Training the algorithm using the data in question.
- 10- fold cross validation of the data.



## 4.2 Artificial intelligence and neural network model

Machine learning methods are already being used in a variety of applications such as the classification and the prediction of various cardiovascular diseases through ECG data analysis.<sup>104–108,125–128</sup> A well-recognized technique for pre-processing ECG data is to create its phase space reconstruction matrix (PSR). Typically, manually selected features such as box counting as well as column and row statistics are extracted from the PSR of the ECG data which then can be used as inputs for a classification model. Convolutional neural networks (CNNs) have been used in ECG analysis for classifying heart attacks, atrial fibrillation, and other arrhythmias as well as for predicting blood pressure.<sup>104–111</sup>

The newly developed tool diverges from standard approaches by using the whole PSR matrix as the input to a CNN model which has not been attempted before. The proposed method is capable of automatically extracting a set of features that are much more descriptive than those that are found manually with more time-consuming methods.

The data (in ASCII format) is first split into 10 second segments. Baseline drift correction is implemented using one dimensional Discrete Wavelet Transformation (DWT). The ECG signal is decomposed at 9 levels, using the Daubechies 8 (db8) wavelet, then reconstructed using only level 9 coefficients. This reconstructed signal is the low frequency component for the ECG signal which is assumed to be the drifting baseline. Subtracting this from the original signal produces ECG signal with a stable baseline. This is followed by adaptive band stop filtering to suppress power-line noise with a frequency of 50 Hz while Butterworth lowpass filter with a cut-off frequency of 40Hz was used to remove the remaining high frequency noise, see Figure 31 below.

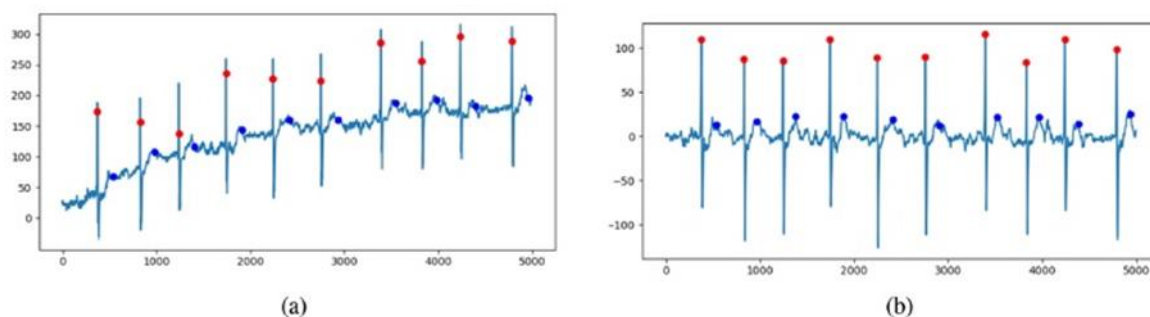


Figure 31 Shows an example of a 10-second ECG segment; (a) pre-filtering, and (b) after the application of filtering. R wave and T wave peaks are shown in red and blue, respectively.<sup>135</sup>

Then, Phase Space Reconstruction (PSR), is utilised to convert the ECG signal into a compressed 32x32 pixel PSR image, one image for each 10 seconds worth of ECG data.

#### 4.2.1 Phase Space Reconstruction

PSR or phase portrait is a popular technique in waveform analysis for representing non-linear characteristics of time series set of data using delay maps. Typically, when a signal is examined, it is plotted against time. To construct the phase space reconstruction or the phase portrait of the signal, a copy of the signal, which is delayed by a given amount of time, is first created. Then the original signal is plotted against the delayed signal. At each time increment, a single point in the phase space reconstruction is created. Each point has an x-axis value equal to the value of the original signal at that time increment and a y-axis value equal to the value of the delayed signal at that time increment. By removing the time axis from this plot, the repetitive behaviours of the signal can be seen.

An example of how a signal can be transformed into its PSR image is illustrated in Figure 32 below.

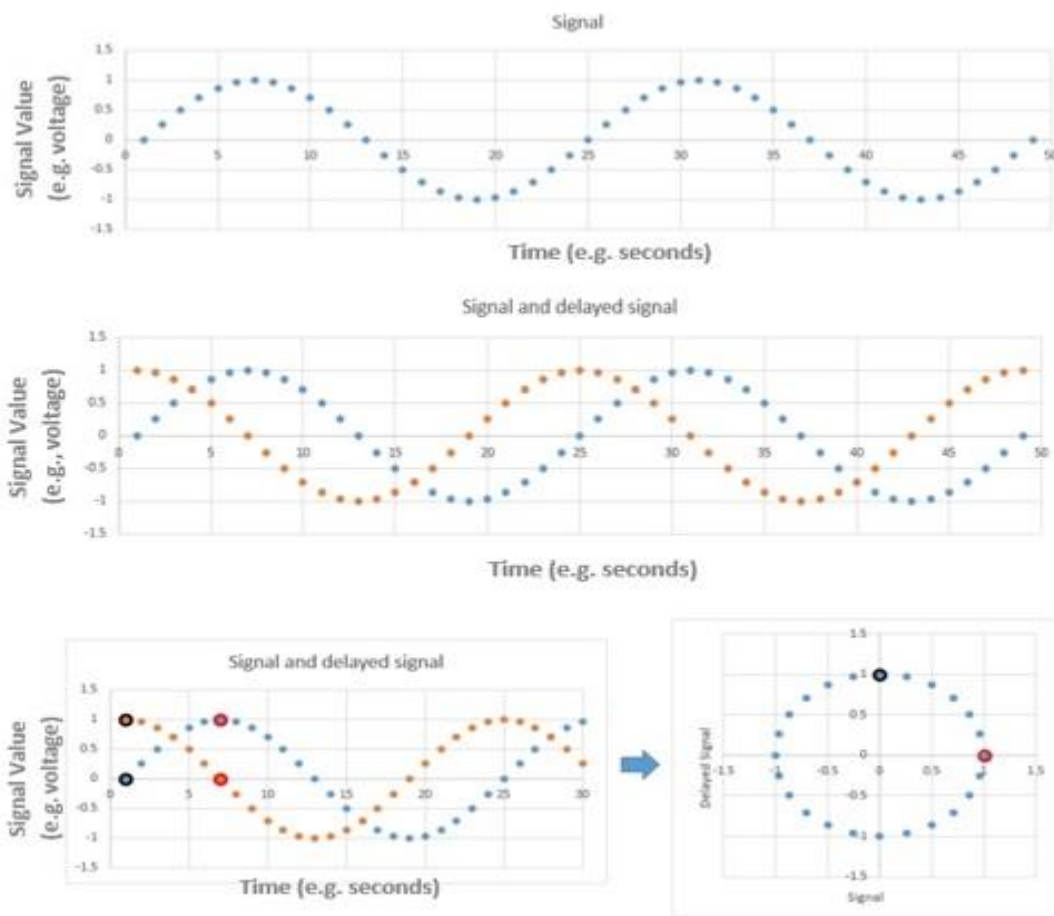


Figure 32 Illustrates how a PSR image of the sine wave is created. As the sine wave has a repeated behaviour, the sine wave signal could have any length and the phase space points generated from this signal would continuously trace and retrace the resulting circle figure which represents the PSR image of

the sine wave. Original image prior to annotations produced by Mr Anthony Dunn, reproduced with permission.

Similarly, the phase space reconstruction of a single heartbeat would trace a particular shape. If the phase space construction of thousands of very similar heartbeats, occurring over a 24-hour period, were to be created, they would all trace roughly the same shape in the phase space. This allows the representation of thousands of heartbeats in a single, small plot. In practice this method can be used to create 32x32pixel images of the phase space reconstruction of 10 seconds of ECG signal. These images provide insight into any repeating behaviours in the signal during that time. The specific morphology of the PSR is dependent on the specific morphology of the ECG it is generated from, therefore, for example, it is expected that a PSR matrix of an ECG with a large R or a large T wave to look different o that of an ECG with a small one.

Several techniques have been used before to analyse PSR or phase portraits. Box counting, where simply the image or the phase space is divided up into a grid and the number of boxes occupied by the image is counted. Also, measuring the area covered by the PSR plot and calculating summary statistics for rows and columns of the PSR matrix.<sup>137,138</sup>

In the algorithm used here, instead of the more rudimentary feature extraction methods, a multi-layered Convoluted Neural Network (CNN) is trained to automatically determine the optimal features to extract from the PSR matrix. This CNN model is then used to predict the T:R ratio from these PSR images without explicitly locating the R or T waves. ECG signals before and after baseline corrections, noise filtering, and transforming the signals into PSR images can be seen in Figure 33.

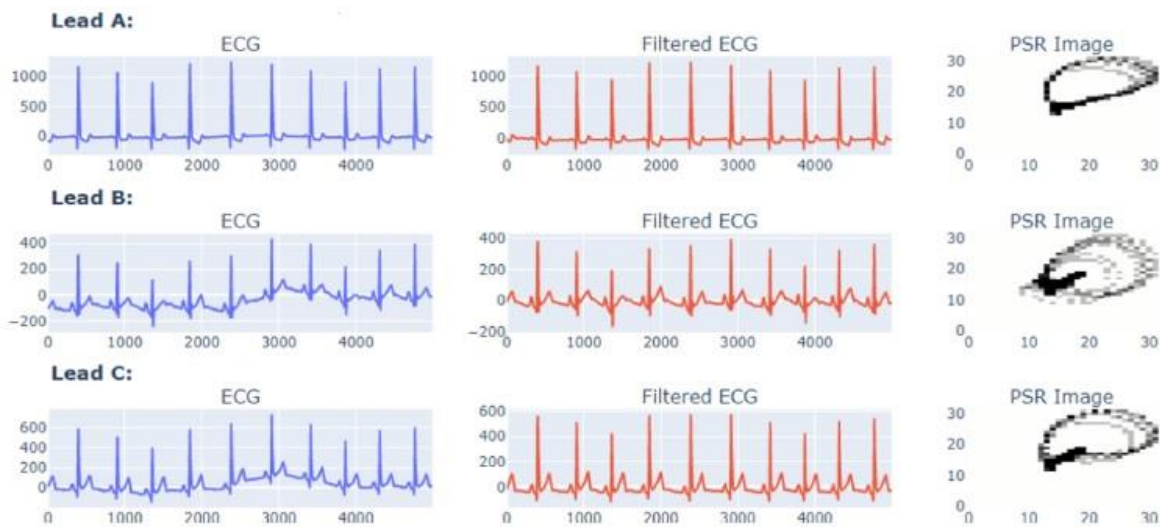


Figure 33 Visualisation of the data from 10-second ECG segments.<sup>135</sup>

#### 4.2.2 CNN training

During training, convolutional layers learn to extract features of the input image (PSR in our model) which are most impactful in accurately determining the model's output. This replaces the need for time consuming feature extractions and produces more descriptive features.

CNNs have been used before to analyse ECGs, but it has been only done using data in which each ECG lead corresponds to a single 1D-ECG signal. For this model, a PSR matrix is generated for each lead that serves as input to a CNN based deep-learning model. In this model calculating T:R ratios by detecting and measuring the amplitude of the R and T waves individually is not attempted. Instead, the T:R ratio is predicted through considering multiple PQRST complexes simultaneously.

The models that comprise the CNN are used predict T:R ratios from  $32 \times 32$ -pixel PSR images. Each model is made up of a number of feature extraction blocks, followed by a regression block. Where the regression block is used by all models to derive the T:R ratio from the extracted features. The outputs from the preceding feature extraction blocks are flattened to a 1D vector and fed into a series of fully connected (dense) layers of neurons to arrive at the final regression output: the T:R ratio.

The first and most basic of the feature-extraction blocks is the Machine learning program (MLP) feature-extraction block. It is comprised of a single layer of fully connected neurons followed by a batch normalisation and activation layer. The input and output of these blocks are 1D. As such, when using these blocks, the images are flattened before the first feature extraction block rather than before the regression block. The basic CNN feature-extraction blocks utilise convolutional

layers, which exploit the 2D structure of the PSR images, as opposed to fully connected layers. These layers are followed by the batch normalisation and activation layers and finally a maximum pooling layer to reduce the size of the output images.

The complex CNN feature-extraction block is based on the basic CNN feature-extraction block. The convolutional layer is replaced by a pair of convolutional layers with smaller kernels. The maximum pooling layer is replaced by an additional convolutional layer with stride equal to 2, which reduces the size of the output whilst continuing to extract features. Finally, addition skip connections, are added over the first two convolutional layers in order to speed up the training.

The Deep CNN feature-extraction block is very similar to the complex CNN feature-extraction block. Before the convolutional layer with stride equal to 2 which is used for pooling, an additional pair of convolutional layers with smaller kernels is included as well as a second skip connection.

At last, to improve the performance of the models used, two techniques were utilised, Firstly, image augmentation, which can strengthen the training of models by randomly introducing small distortions to the training data, thus resulting in models which are more robust to distortions which may occur naturally in the unaltered data. Four image augmentation strategies: shifting, zooming, rotating and shearing were used.

Secondly, 5 ensemble models were used (MLP5, MLP5 small rotation, MLP5 small shear, MLP5 ensemble, and complex CNN5). 20% of the training data was randomly reserved for validation. Models were trained until their accuracy on the validation set was no longer increasing. A different 20% of the training data were reserved for validation for each model, in doing so, while some data were reserved for validation by one model, it was used for training by the remaining 4. The average of these models' predictions was used to obtain a higher prediction accuracy than would be archived by any of the models alone. For further details on the CNN training, refer to the published paper by Dunn et al.<sup>135</sup>

The end result is a plot showing the variation of the T:R ratios for each lead/S-ICD vector over the recorded period, thus making it easy to detect any period where the T:R ratio was consistently high and thus theoretically increased the risk of TWO. To better examine how the behaviour of the T:R ratio differs between each lead, the tool can plot a histogram of what proportion of the 24-hour screening period the T:R ratio of a particular lead spent in each range of T:R ratios, see Figure 34.

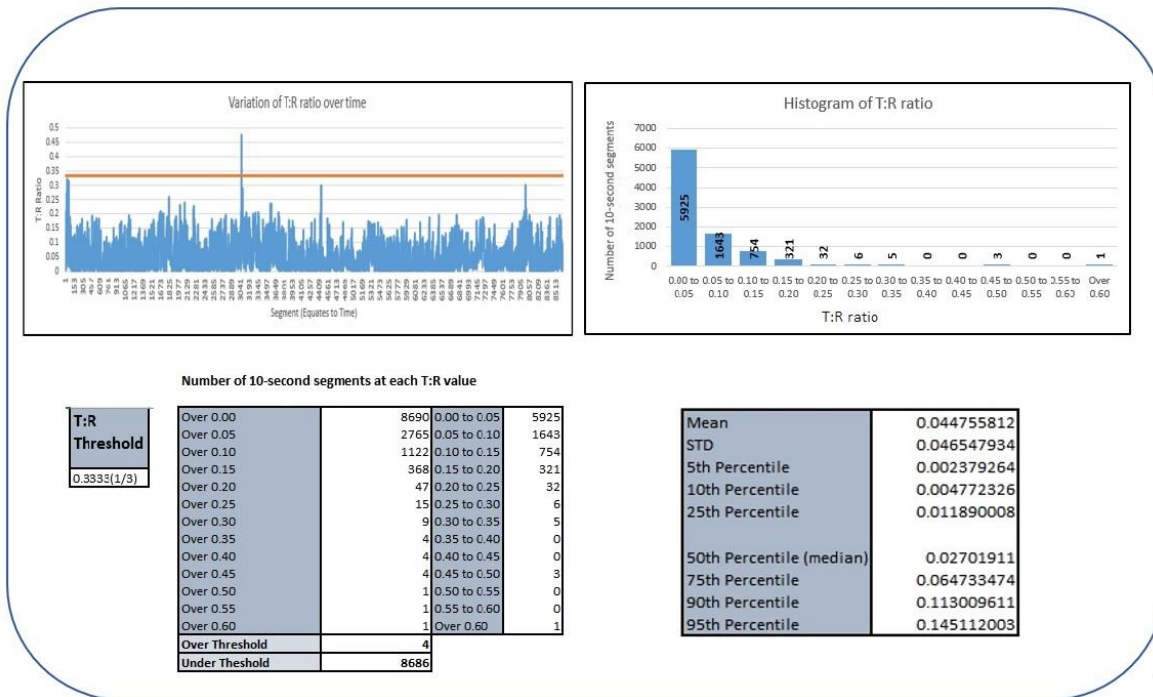


Figure 34 One example of the results of vector analysis produced by the tool.

### 4.3 Validation of the tool

#### 4.3.1 Manual confirmation

The deep learning tool was trained using 10-fold cross validation. ECG segments with pre-determined, manually measured T:R ratios were used to train the tool, while a proportion of the segments were blinded from the tool and were subsequently used for a series of experiments to assess the tool for accuracy. The outcome of the tool (predicted T:R values) was compared to the previously manually measured T:R values. <sup>135</sup>

##### 4.3.1.1 Error parameters

Several standard accuracy parameters were used to assess the accuracy of the tool; Mean squared error (MSE), Root mean squared error (RMSE), and mean absolute error (MAE), see Figure 35.

$$\text{MSE} = \frac{\sum_{i=1}^n (y_i - \hat{y}_i)^2}{n},$$

$$\text{RMSE} = \sqrt{\frac{\sum_{i=1}^n (y_i - \hat{y}_i)^2}{n}},$$

$$\text{MAE} = \frac{\sum_{i=1}^n |y_i - \hat{y}_i|}{n},$$

Figure 35 Showing the equations for the error parameters, where  $y$  are the true T:R ratios,  $\hat{y}$  are the predicted T:R ratios and  $n$  is the number of PSR images.

For our model, the Mean squared error (MSE) = 0.0122, Root mean squared error (RMSE) = 0.0938, and mean absolute error (MAE) = 0.046. Having an MAE of 0.046 means that on average the difference between the tool- predicted T:R ratio and the manually measured T:R was 0.046. The results of these accuracy parameters were very favourable denoting high level of accuracy for the tool.

### 4.3.2 Correlation of the tool outcome

#### 4.3.2.1 Introduction

In a previously published study by Wiles et al<sup>134</sup>, adult ICD patients were asked to wear Holter monitors for 24 hours to record their S-ICD vectors. Then, ECG recordings were analysed using an S-ICD simulator to assess the vector scores automatically at regular intervals. Mean vector scores were analysed and a new concept, Eligible Vector Time (EVT), representing the percentage of all the screening assessments with passing vector scores, was introduced in the study. The study demonstrated that the vector score which determines S-ICD eligibility is in fact dynamic in real-life ICD population. For that study, an S-ICD simulator provided by the device manufacturer was utilised for vector assessment.

### 4.3.2.2 Objectives

In this study, I aim to assess the newly developed tool in screening a cohort of real-life ICD patients for S-ICD vectors eligibility and compare the outcomes against a “gold-standard”, the S-ICD simulator.

### 4.3.2.3 Methods

This is a retrospective correlation study. The same Holter recordings from the previous study by Wiles et al, were first downloaded in ASCII format at a frequency of 500 Hz. Then the recordings were analysed by the deep learning tool. Mean T:R, standard deviation (SD), and the number of 10-second segments that had T:R above a pre-determined threshold for each vector recording were given by the tool. The time that a T:R ratio of a vector was deemed favourable (below the eligibility threshold) was calculated as a percentage of the whole recording (=number of 10-second segments with T:R below eligibility threshold / total number of 10-second segments in the recording x 100). This will be labelled as favourable ratio time or FRT.

$$FRT = \frac{\text{Number of 10 second segments with favourable T: R ratio}}{\text{Total number of 10 second segments in the recording}} \times 100$$

#### 4.3.2.3.1 Statistical analysis

Data analysis was done using RStudio 1.4.1106 running R 4.0.5. Continuous data was presented as mean  $\pm$  SD. The distribution of the data was checked using normality tests and plots, and histograms. The correlation was checked using Spearman's rank coefficient among variables that fit interval, ordinal, or ratio scale, and in paired observations with monotonic relation assumption.

To correlate the outcome of the deep learning tool with that of the S-ICD simulator, the following were compared statistically: (mean vector score + standard deviation of the vector score) and (mean T:R + standard deviation of the T:R), (mean T:R + standard deviation of T:R) and EVT, and finally FRT and EVT.

### 4.3.2.4 Results

#### 4.3.2.4.1 Patients' demographics

A total of 14 patients (mean age 63.7 $\pm$ 5.2 years, 71.4% male) were recruited in the original study.<sup>134</sup> The primary and alternate vectors for each of the patients, amounting to a total of 28 vectors were analysed. A total of 13(92.9%) patients had transvenous ICDs. There was a high



prevalence of ischaemic heart disease (42.9%) and severe LV dysfunction (28.6%) in the recruited cohort. The main indication for ICD therapy was secondary prevention (71.4%). See Table 20 for detailed patients' demographics.

Table 20 Patients' demographics

		<b>n=14</b>	
<b>Demographics:</b>	Mean age (years $\pm$ 95% CI)	63.7( $\pm$ 5.2)	
	Male	10	71.4%
<b>Device:</b>	Primary prevention	4	14%
	Secondary prevention	10	71.4%
	Transvenous ICD	13	92.9%
	Subcutaneous ICD	1	7.1%
<b>Co-morbidities:</b>	Ischaemic heart disease	6	42.9%
	Severe LV systolic dysfunction	4	28.6%
	Previous atrial arrhythmia	3	23.1%
	Hypertension	3	23.1%
	Airway disease	3	23.1%
	Diabetes	2	14.3%
	Valve disease(>mild) or valve surgery	2	14.3%
	Previous CABG	2	14.3%
	Cerebrovascular disease	1	7.1%
	Peripheral vascular disease	1	7.1%
	eGFR<60mls/min/1.73 <sup>2</sup> (n=10)	1	10%
	eGFR<30mls/min/1.73 <sup>2</sup> (n=10)	1	10%

#### 4.3.2.4.2 T:R assessment

Mean T:R was lower in the primary vectors when compared to the alternate vectors ( $0.20 \pm 0.06$  versus  $0.22 \pm 0.06$ , (95% CI),  $p=0.30$ ). Standard deviation of the T:R (a representation of dynamicity) was also lower in the primary vectors ( $0.07 \pm 0.02$  versus  $0.09 \pm 0.02$ , (95% CI),  $p=0.11$ ). This has translated to a higher favourable ratio time (FRT) in the primary vectors when compared to the alternate vectors ( $87.1 \pm 14.13$  versus  $70.4 \pm 16.16$  %, (95% CI),  $p=0.07$ ). However, this was not statistically significant.

Mean T:R for all the 28 vectors combined was  $0.21 \pm 0.11$ , (95% CI), standard deviation for all the 28 vectors combined was  $0.08 \pm 0.04$ , (95% CI), and the FRT for all the vectors combined was  $79 \pm 30$  %.(95% CI). For individual assessment of each vector, see Table 21 below.

Table 21 Results of T:R assessment using the deep learning tool.

Study ID	Vector	Mean T:R	T:R Standard deviation	T:R segments over threshold	T:R segments below threshold	Favourable ratio time (FRT) (%)
----------	--------	----------	------------------------	-----------------------------	------------------------------	---------------------------------

01	Alternate	0.274	0.078	2045	6565	76.25
01	Primary	0.057	0.064	28	8582	99.67
02	Alternate	0.075	0.062	5	8785	99.94
02	Primary	0.175	0.064	84	8706	99.04
03	Alternate	0.045	0.047	4	8686	99.95
03	Primary	0.110	0.107	411	8279	95.27
04	Alternate	0.199	0.138	980	7630	88.62
04	Primary	0.164	0.107	545	8065	93.67
05	Alternate	0.113	0.076	20	8590	99.77
05	Primary	0.102	0.046	10	8600	99.88
06	Alternate	0.363	0.180	4902	3708	43.07
06	Primary	0.187	0.098	414	8196	95.19
07	Alternate	0.297	0.139	4003	4607	53.51
07	Primary	0.479	0.026	8605	5	0.06
08	Alternate	0.382	0.059	6949	1740	20.03
08	Primary	0.311	0.032	1420	7269	83.66
09	Alternate	0.338	0.023	4778	3832	44.51
09	Primary	0.168	0.031	10	8600	99.88
10	Alternate	0.048	0.040	0	8610	100
10	Primary	0.153	0.049	2	8608	99.98
11	Alternate	0.260	0.139	3452	5158	59.91
11	Primary	0.203	0.088	410	8200	95.24
12	Alternate	0.381	0.060	7346	1264	14.68
12	Primary	0.195	0.027	0	8610	100
13	Alternate	0.203	0.107	944	6760	87.75
13	Primary	0.340	0.107	2891	4813	62.47
14	Alternate	0.142	0.070	168	8442	98.05
14	Primary	0.143	0.105	413	8197	95.20
Mean	Primary	0.20±0.06 (95%CI)	0.07±0.02 (95%CI)			87.1±14.13 (95%CI)
Mean	Alternate	0.22±0.06 (95%CI)	0.09 ±0.02 (95%CI)			70.4±16.16 (95%CI)
Mean	Combined	0.21 ± 0.11(95% CI)	0.08 ±0.04(95% CI)			79 ± 30 (95% CI)

#### 4.3.2.4.3 Correlation

Mean vector score was higher in the primary vectors when compared to the alternate vectors (412.6±191 versus 105.6±139.2, (95% CI),  $p=0.008$ ). Standard deviation of vector scores was lower (i.e., more stable vector scores) in the primary vectors when compared to the alternate vectors (95.23±76.17 versus 160.56±60.73, (95% CI),  $p=0.10$ ). However, this was not statistically significant. The EVT was significantly higher in the primary vectors when compared with the alternate vectors (64.55±19.07 versus 13.05±15.34 %, (95% CI),  $p<0.001$ ). Mean vector score for all the vectors combined was 259.09±129.60(95%CI), the standard deviation of the vector score for all the vectors combined was 127.89±49.36(95% CI), and the EVT for all the vectors combined was 38.80±15.45 (95%CI).

There were statistically significant strong correlations between the outcomes of the “gold standard” S-ICD simulator and the deep-learning tool; mean T:R ratio +standard deviation of T:R correlated strongly with mean vector score + standard deviation of mean vector score,  $Rho=0.636$  ( $p<0.001$ ). Mean T:R ratio +standard deviation of T:R correlated strongly with eligible vector time (EVT),  $Rho=0.668$  ( $p<0.001$ ). Favourable ratio time also correlated with eligible vector time (EVT),  $Rho=0.652$  ( $p<0.001$ ). See Table 22 Figure 38, Figure 38, and Figure 38.

Table 22 Outcome of the deep learning tool vs the outcome of the S-ICD simulator.

Study ID	Vector	Deep learning tool			S-ICD simulator		
		Mean T:R	T:R Standard deviation	Favourable ratio time (FRT) (%)	Mean vector scores	Vector scores standard deviation	Eligible vector time (EVT) (%)
01	Alternate	0.274	0.078	76.25	4.6	9.7	0
01	Primary	0.057	0.064	99.67	385.0	76.2	100
02	Alternate	0.075	0.062	99.94	40.9	24.5	2.4
02	Primary	0.175	0.064	99.04	25.6	33.2	2.62
03	Alternate	0.045	0.047	99.95	57.0	40.6	14.32
03	Primary	0.110	0.107	95.27	807.5	522.1	81
04	Alternate	0.199	0.138	88.62	1.0	2.0	0
04	Primary	0.164	0.107	93.67	120.0	137.2	47
05	Alternate	0.113	0.076	99.77	40.7	27.0	2.68
05	Primary	0.102	0.046	99.88	536.6	282.0	100
06	Alternate	0.363	0.180	43.07	0.2	0.9	0
06	Primary	0.187	0.098	95.19	201.0	286.9	43
07	Alternate	0.297	0.139	53.51	5.1	7.7	0.29
07	Primary	0.479	0.026	0.06	3.9	11.8	0.07
08	Alternate	0.382	0.059	20.03	9.6	16.6	0
08	Primary	0.311	0.032	83.66	386.1	217.3	73
09	Alternate	0.338	0.023	44.51	296.5	230.5	57.25
09	Primary	0.168	0.031	99.88	1046.8	262.0	99
10	Alternate	0.048	0.040	100	989.1	218.5	100
10	Primary	0.153	0.049	99.98	453.7	224.1	97
11	Alternate	0.260	0.139	59.91	3.1	4.9	0
11	Primary	0.203	0.088	95.24	314.1	261.8	79
12	Alternate	0.381	0.060	14.68	4.5	4.7	0
12	Primary	0.195	0.027	100	1161.9	211.7	100
13	Alternate	0.203	0.107	87.75	17.7	33.5	5.48
13	Primary	0.340	0.107	62.47	247.3	263.4	61
14	Alternate	0.142	0.070	98.05	7.9	20.2	0.22
14	Primary	0.143	0.105	95.20	87.1	150.0	21

Mean	Primary	0.20±0.06 (95%CI)	0.07±0.02 (95%CI)	87.1±14.13 (95%CI)	412.6 ± 191(95%CI)	95.23±76.17 (95%CI)	64.55 ±19.07 (95%CI)
Mean	Alternate	0.22±0.06 (95%CI)	0.09±0.02 (95%CI)	70.4±16.16 (95%CI)	105.6 ± 139.2 (95%CI)	160.56 ±60.73 (95%CI)	13.05 ±15.34 (95%CI)
Mean	Combined	0.21± 0.11(95% CI)	0.08 ±0.04(95% CI)	79 %±30(95% CI)	259.09 ±129.60 (95%CI)	127.89 ±49.36 (95%CI)	38.80 ±15.45 (95%CI)

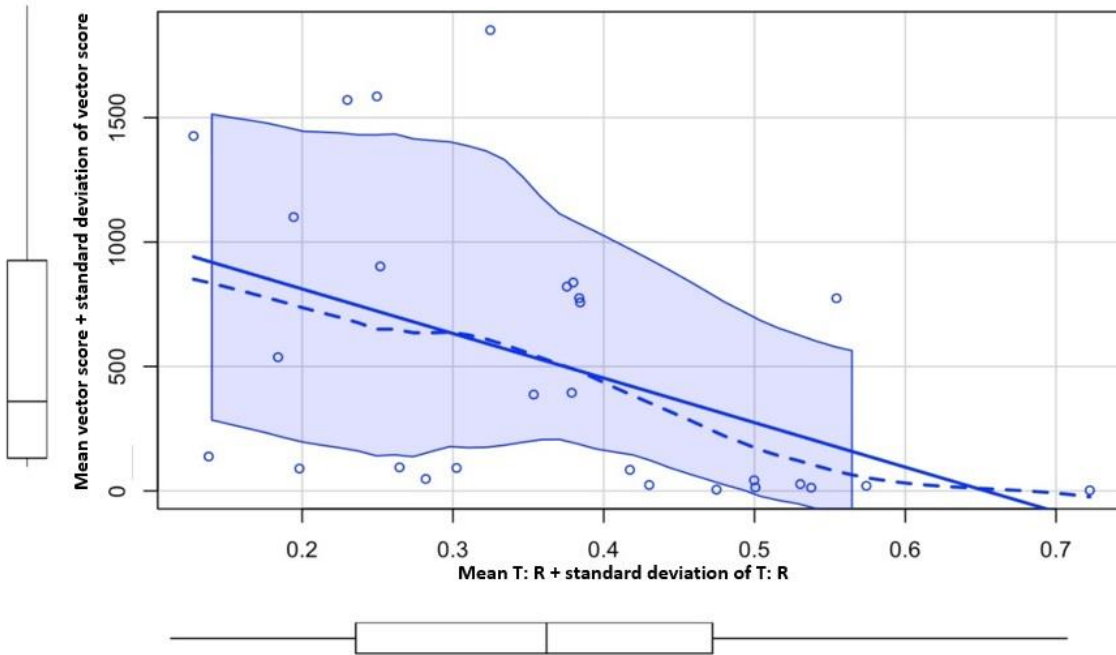


Figure 36 Mean T:R ratio + standard deviation of T:R (x-axis) in correlation with mean vector score + standard deviation of mean vector score(y-axis) using spearman’s rank correlation test. Rho= 0.636 (p<0.001) denoting strong correlation.

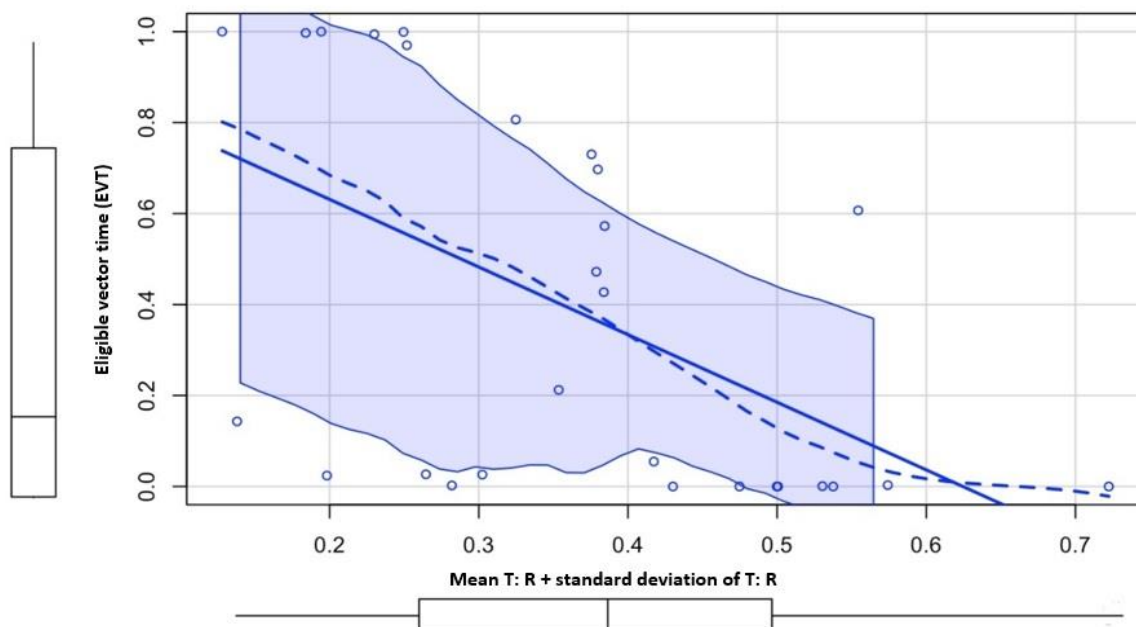


Figure 37 Mean T:R ratio + standard deviation of T:R (x-axis) in correlation with eligible vector time (EVT)(y-axis) using spearman's rank correlation test.  $\rho = 0.668$  ( $p < 0.001$ ) denoting strong correlation.

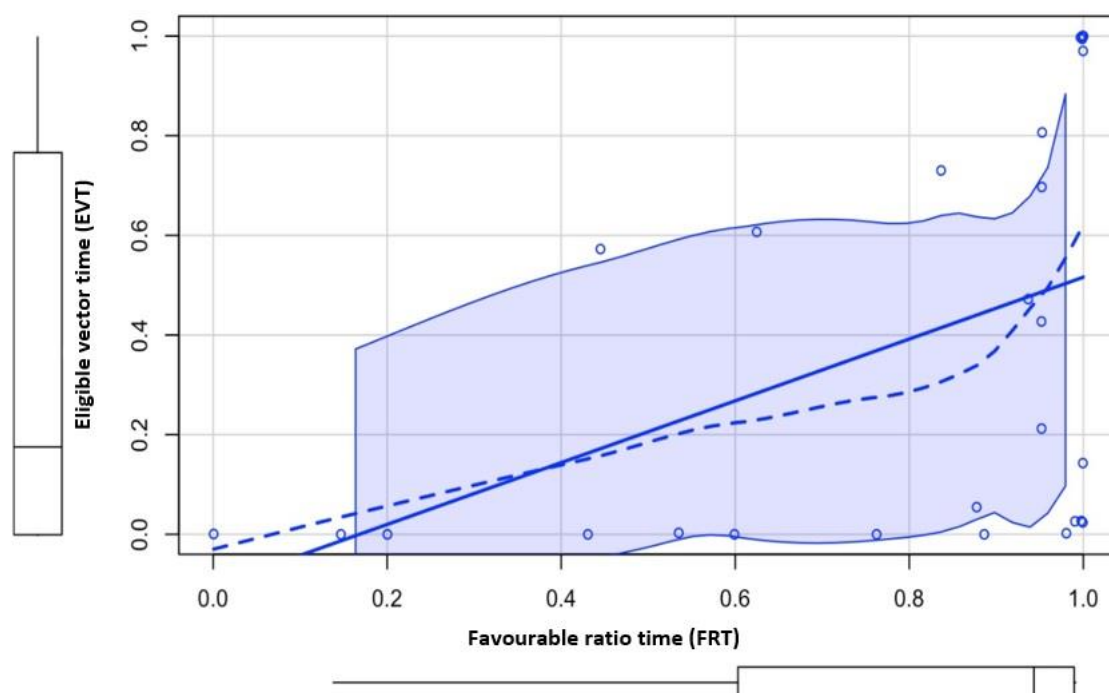


Figure 38 Favourable ratio time (x-axis) in correlation with eligible vector time (EVT)(y-axis) using spearman's rank correlation test.  $\rho = 0.652$  ( $p < 0.001$ ) denoting strong correlation.

#### 4.3.2.5 Discussion

Previous work by Wiles et al<sup>134</sup> utilised a S-ICD simulator- provided by the S-ICD manufacturer- to analyse the vector score over the 24-hour recordings in real-time i.e. It took 24 hours for the S-ICD

simulator to analyse a 24-hour ECG recording (one vector). As the S-ICD simulator essentially replicates the sensing mechanism of a S-ICD in real-time, it can be considered as a “gold-standard” for evaluating various durations of ECG signals representing S-ICD vectors.

The presented correlation study presents some significant findings. This is the first attempt of assessing this deep learning tool outcomes in real-life ICD patients. These patients had their 24-hour ECG signals recordings pre-assessed using a S-ICD simulator which was provided by the manufacturer. It is important to note that these assessments were done for experimental purposes as these prolonged screenings are not standard practice to determine S-ICD eligibility. This simulator emulates what would happen if a standard S-ICD programmer is presented with the ECG signals in real-time. Thus, it is justified to use the outcome of these pre-assessments as a benchmark to compare the outcomes of other screening methodologies against. In this study, I demonstrated that the outcomes of the novel machine learning tool correlate strongly with those of the “gold standard” S-ICD simulator. The findings presented in this study don’t only attest to the potential use of the presented machine learning tool in screening, but they also support the methodology of utilising T:R (or R:T) ratios for S-ICD screening purposes.

The simulator, aside from being not readily available for clinical use, runs in real-time and analyses the S-ICD vectors consecutively, which can be a time-consuming process, particularly if it is required to analyse recordings of even longer durations. The tool is time efficient. It can provide detailed descriptive analysis of the T:R ratios simultaneously for all the vectors across the recordings within a few minutes without compromising on accuracy.

Acquiring screening data for eligibility in S-ICD candidates over a longer period than for conventional screening practices seems like a reasonable approach to minimise the effect of the, at least theoretical, dynamicity of S-ICD eligibility. However, this approach increases the burden of data analysis required to assess S-ICD eligibility. This deep-learning tool represents a practical software solution that could provide detailed data analysis within minutes; thus, facilitating informed decision making and could guide patient selection as well as vector selection in S-ICD candidates.

#### **4.3.2.5.1 Limitations**

There are some limitations to the study; first, is the relatively low number of patients’ vectors analysed in this study. Second, only the primary and alternate vectors were available for analysis, because the Holter that was used to collect the S-ICD vectors was limited to recording only 2 simultaneous channels. Also, the S-ICD simulator analysed the data at 1-minute intervals, while the novel tool provided analysis of the T:R ratios at 10-second intervals. In addition, the role of

the SMART PASS algorithm that could help differentiate between R and T waves based on other characteristics rather than just their amplitudes, was not considered in this study.

#### **4.3.2.6 Conclusion**

T:R ratio, a crucial element in the S-ICD sensing mechanism and a major determinant of S-ICD eligibility, is dynamic in real-life ICD patients. Deep learning methods could provide reliable and time-efficient analysis of T:R ratios. This could help with the S-ICD screening process as well as guide vector selection in S-ICD eligible patients. However, further work is needed before the findings from this study could be translated into clinical practice.

## Chapter 5 Deep learning-based insights on T:R ratio behaviour during prolonged screening and optimal T:R ratio for S-ICD eligibility

### 5.1 Introduction

The eligibility for S-ICD is identified during a mandatory screening process where surface ECGs of few seconds duration done in multiple postures are used as surrogates of S-ICD vectors. The ECGs are then analysed against acceptable templates, now largely done through an automated screening tool, to determine eligibility. At least one vector needs to pass screening in at least two postural positions for the patient to be deemed eligible for an S-ICD. A major predictor of eligibility of a vector is the ratio between the R and T wave amplitudes. It is more common in the literature to use the term R:T ratio to describe the relationship between R wave and T wave amplitudes. However, as explained in previous chapters, using R:T ratio is not a suitable parameter for the machine learning tool and T:R is used instead. For consistency, I will use T:R to refer for the ratio between the amplitudes of the T and R waves of the ECG signal in this chapter.

Tools in current screening practice recommended by the manufacturer propose a T:R ratio of 1:3 as a cut off for S-ICD eligibility. Inappropriate S-ICD shocks due to TWO remain an issue despite current screening practices.<sup>45</sup>The cut-off T:R ratio of 1:3 used for current screening practice incorporates a safety margin to accommodate for the fluctuations of the ECG signal amplitudes over time without affecting the sensing of the S-ICD. Adopting prolonged screening approaches for S-ICD screening for eligibility, utilising deep learning methods as described in the previous chapter, can accurately measure the degree of the T:R ratio fluctuations over the monitoring/screening period, taking away the “guess work”.

### 5.2 Objectives

In this chapter, I will utilise the deep learning tool, that was discussed in detail in the previous chapter, to provide insights on the T:R ratio behaviour during prolonged screening for S-ICD eligibility. Adopting a T:R ratio of 1:3 as a cut-off for eligibility for prolonged screening is likely to unnecessarily exclude a significant number of patients who are otherwise appropriate candidates for S-ICD therapy. Attempting to find the appropriate ratio that identifies patients who are at high risk of TWO and inappropriate shocks while not inappropriately excluding true S-ICD



candidates after prolonged screening has not been examined previously. The purpose of the study presented in this chapter is to provide groundwork for future trials to answer this question.

### 5.3 Methods

The original data of “HEART TWO” study that was previously discussed in chapter three of this thesis was also utilised in this study for further analysis. An additional cohort of patients in the form of patients who have previously experienced inappropriate shock(s) due to TWO via their S-ICD devices, were recruited for this study.

The deep learning tool, which was discussed in detail in the previous chapter, was used to track and analyse the T:R ratios for the leads corresponding to the S-ICD vectors over the 24-hour recordings. The tool was used to predict the T:R ratio for every 10 seconds of data/ECG signals (equivalent to a standard 12-lead ECG or a standard ECG strip used for current S-ICD screening process<sup>115</sup>); this allowed the assessment of the S-ICD screening eligibility for every 10 seconds for the whole 24-hour screening. From there, the probability of each patient passing the screening using the current screening practices if they had their screening done at any time of the day is calculated. The probability equals the number of 10-second segments where at least one Holter lead/S-ICD vector exhibited favourable (<1:3) T: R ratio divided by the total number of 10 second segments (8640) in a 24-hour recording.

$$Probability = \frac{\text{Number of 10 second segments with at least one favourable S – ICD vector}}{\text{Total number of 10 second segments in a 24 hour recording}(8640)}$$

For the proposed prolonged screening methodology, a time interval of 20 consecutive seconds of unfavourable T:R ratio was chosen as a cut off for failing the screening. This is based on the detection, charge, and redetection time of the current S-ICD system. In other words, a TWO episode must be at least this long for the S-ICD system to over sense the T-waves, mistakenly interpret the presenting rhythm as ventricular tachycardia, charge the can, confirm the underlying rhythm, then deliver a shock – an inappropriate one in this case. For the sake of the study, the delivery of a hypothetical inappropriate shock was chosen as a hard cut off criterion for failing the S-ICD screening. It can appear that the S-ICD screening criteria for this proposed methodology is too lax, allowing leads/vectors exhibiting “silent” TWO episodes to pass the screening. However, these proposed criteria are meant to provide a reference point to compare the different S-ICD vectors results against, as a proof of concept. In real life screening, the tool could be adjusted for T:R thresholds as well as time intervals if needed.

Multiple T:R ratio cut-offs were then applied on the whole duration of the recordings (24-hours), identifying the proportion of patients that would be deemed at high risk of inappropriate shocks due to TWO at each of the proposed cut off values (1:3, 1:2, 2:3, 3:4 and 1:1) for the T:R ratio.

The S-ICD can be pre-programmed to sense only one vector at a time, and it doesn't automatically change sensing from one vector to the other. Therefore, with these programming settings in mind, for a patient to pass the screening in this study, they would have to have at least one vector eligible at the proposed T:R threshold throughout the recording.

### 5.3.1 Statistical methods

Data analysis was done using RStudio 1.4.1106 running R 4.0.5. The categorical data were represented as n/N (%) and continuous data as mean (SD). Fisher's exact test was used to analyse the contingency tables given the small sample size and compared continuous non-parametric data using Kruskal-Wallis rank sum test between the different studied groups.

## 5.4 Results

A total of 37 patients (mean age  $54 \pm 21.3$  years, 64.8% male) were included in the study. The study population presents a mixed cohort of underlying aetiologies, see Table 23 for participants demographics.

Table 23 Patients' demographics.

<b>Total Number of Participants</b>		<b>n = 37</b>	
<b>Demographics:</b>	Mean age [years $\pm$ 95% SD]	54.5 $\pm$	21.3
	Male	24	64.8%
<b>Cardiac co-morbidities:</b>	Heart failure	14	37.8%
	Atrial fibrillation	7	18.9%
	LV diastolic dysfunction	5	13.5%
	Ischaemic heart disease	8	21.6%
	LV systolic dysfunction	14	37.8%
	Hypertrophic Cardiomyopathy	7	18.9%
	Adult Congenital Heart Disease	7	18.9%
	S-ICD insitu	3	8.1%
	Apparently normal hearts	7	18.9%

The overall probability of the patient cohort to have passed the screening using the standard screening methods used in current practice based on a T:R ratio of 1:3 is  $0.96 \pm 0.13$  regardless of underlying aetiology. The probabilities are  $0.83 \pm 0.27$ ,  $1.0$ ,  $0.97 \pm 0.1$ ,  $1.0$  for the ACHD, HCM, HF and the normal heart subgroups respectively. Interestingly, the cohort of the three patients who had previously experienced inappropriate S-ICD shocks due to TWO also had a very high probability of passing the standard S-ICD screening ( $0.99 \pm 0.01$ ) ( $p = 0.02$ ), see Table 24 for detailed results.

Table 24 Shows probability of passing standard S-ICD screening in a 24-hour period based on a T:R of 1:3.

Characteristic	Overall, N =	ACHD, N =	HCM, N =	HF, N = 14 <sup>1</sup>	Normal, N =	S-ICD, N =	p-value <sup>2</sup>
	37 <sup>1</sup>	6 <sup>1</sup>	7 <sup>1</sup>		7 <sup>1</sup>	3 <sup>1</sup>	
<b>Outcome</b>	96 (13) %	83 (27) %	100 (0) %	97 (10) %	100 (0) %	99 (1) %	<b>0.02</b>
<b>Age</b>	55 (21)	39 (20)	57 (25)	70 (11)	36 (8)	53 (28)	<b>0.005</b>
<b>Gender</b>							0.62
<b>F</b>	13 / 37 (35%)	1 / 6 (17%)	3 / 7 (43%)	4 / 14 (29%)	4 / 7 (57%)	1 / 3 (33%)	
<b>M</b>	24 / 37 (65%)	5 / 6 (83%)	4 / 7 (57%)	10 / 14 (71%)	3 / 7 (43%)	2 / 3 (67%)	

<sup>1</sup> Mean (SD); n / N (%)

<sup>2</sup> Kruskal-Wallis rank sum test; Fisher's exact test

It is important to highlight that this probability of passing the screening is calculated based upon the current screening practice of having at least a single vector, at any point of time that meets the screening criteria for the short duration of time when the screening is being performed. It is a hypothetical scenario to illustrate the likelihood/probability that a patient would have been deemed S-ICD eligible if this patient had their screening done utilising the current/one point in time screening methods at any time within 24 hours.

These high probabilities can be misleading. One would suspect that the dynamicity of the T:R ratios would make a participant pass at one time in a certain vector and at another in different time; this makes the high probabilities less meaningful, as S-ICDs can only be programmed at a fixed vector at one time and can't automatically change them.

Since S-ICDs can only be programmed at one fixed vector at a time, for the proposed prolonged screening method, using the deep-learning tool, each vector was followed separately throughout the recordings in all the participants, and then based on the pre-defined thresholds, as explained in the methodology section, each vector would be deemed to have passed/failed the screening independently from the other two vectors of the same participant. A patient is deemed to have passed the screening if they exhibited at least one vector that passed the screening throughout. Only 20 (54%) patients, regardless of the underlying aetiology, would have passed the screening if the same T:R ratio of 1:3 was utilised for prolonged screening. All the patients would have passed the screening if a T:R ratio of 1:1 was utilised for prolonged screening. For T:R ratios of 1:2, 2:3 and 3:4, 65%,92% and 95% of the patients would have passed the screening, respectively, see Table 25 Table 30 and Figure 39 for detailed results.

Table 25 showing S-ICD screening success rates at different thresholds for all patients.

Threshold/Subgroup	Overall, N =	ACHD, N =	HCM, N =	HF, N = 14 <sup>1</sup>	Normal, N = 7 <sup>1</sup>	S-ICD, N = 3 <sup>1</sup>	p-value <sup>2</sup>
<b>T:R threshold 1:3 (0.33)</b>	37 <sup>1</sup>	6 <sup>1</sup>	7 <sup>1</sup>				0.022
<b>Fail</b>	17 / 37 (46%)	4 / 6 (67%)	3 / 7 (43%)	7 / 14 (50%)	0 / 7 (0%)	3 / 3 (100%)	
<b>Pass</b>	20 / 37 (54%)	2 / 6 (33%)	4 / 7 (57%)	7 / 14 (50%)	7 / 7 (100%)	0 / 3 (0%)	
<b>T:R threshold 1:2 (0.5)</b>							0.013
<b>Fail</b>	13 / 37 (35%)	2 / 6 (33%)	1 / 7 (14%)	7 / 14 (50%)	0 / 7 (0%)	3 / 3 (100%)	
<b>Pass</b>	24 / 37 (65%)	4 / 6 (67%)	6 / 7 (86%)	7 / 14 (50%)	7 / 7 (100%)	0 / 3 (0%)	
<b>T:R threshold 2:3 (0.66)</b>							0.025

<b>Fail</b>	3 / 37 (8.1%)	0 / 6 (0%)	0 / 7 (0%)	1 / 14 (7.1%)	0 / 7 (0%)	2 / 3 (67%)
<b>Pass</b>	34 / 37 (92%)	6 / 6 (100%)	7 / 7 (100%)	13 / 14 (93%)	7 / 7 (100%)	1 / 3 (33%)
<b>T:R threshold 3:4 (0.75)</b>						<b>0.37</b>
<b>Fail</b>	2 / 37 (5.4%)	0 / 6 (0%)	0 / 7 (0%)	1 / 14 (7.1%)	0 / 7 (0%)	1 / 3 (33%)
<b>Pass</b>	35 / 37 (95%)	6 / 6 (100%)	7 / 7 (100%)	13 / 14 (93%)	7 / 7 (100%)	2 / 3 (67%)
<b>T:R threshold 1:1 (1)</b>						
<b>Pass</b>	37 / 37 (100%)	6 / 6 (100%)	7 / 7 (100%)	14 / 14 (100%)	7 / 7 (100%)	3 / 3 (100%)
<sup>1</sup> n / N (%)						
<sup>2</sup> Fisher's exact test						

Table 26 showing S-ICD screening success rates at T:R of 1:3 for each vector separately.

Threshold/Subgroup	Overall, N = 37 <sup>1</sup>	ACHD, N = 6 <sup>1</sup>	HCM, N = 7 <sup>1</sup>	HF, N = 14 <sup>1</sup>	Normal, N = 7 <sup>1</sup>	S-ICD, N = 3 <sup>1</sup>	p-value <sup>2</sup>
<b>T:R threshold 1:3 (0.33)</b>						<b>0.34</b>	
<b>Primary vector</b>							
<b>Fail</b>	22 / 37 (59%)	4 / 6 (67%)	4 / 7 (57%)	9 / 14 (64%)	2 / 7 (29%)	3 / 3 (100%)	
<b>Pass</b>	15 / 37 (41%)	2 / 6 (33%)	3 / 7 (43%)	5 / 14 (36%)	5 / 7 (71%)	0 / 3 (0%)	
<b>T:R threshold 1:3 (0.33)</b>						<b>0.95</b>	
<b>Alternate vector</b>							
<b>Fail</b>	31 / 37 (84%)	5 / 6 (83%)	5 / 7 (71%)	12 / 14 (86%)	6 / 7 (86%)	3 / 3 (100%)	
<b>Pass</b>	6 / 37 (16%)	1 / 6 (17%)	2 / 7 (29%)	2 / 14 (14%)	1 / 7 (14%)	0 / 3 (0%)	

T:R threshold 1:3 (0.33)							0.1
<b>Secondary vector</b>							
<b>Fail</b>	20 / 31 (65%)	6 / 6 (100%)	3 / 7 (43%)	5 / 8 (62%)	3 / 7 (43%)	3 / 3 (100%)	
<b>Pass</b>	11 / 31 (35%)	0 / 6 (0%)	4 / 7 (57%)	3 / 8 (38%)	4 / 7 (57%)	0 / 3 (0%)	
<sup>1</sup> n / N (%)							
<sup>2</sup> Fisher's exact test							

Table 27 showing S-ICD screening success rates at T:R of 1:2 for each vector separately.

Threshold/Subgroup	Overall, N = 37 <sup>1</sup>	ACHD, N = 6 <sup>1</sup>	HCM, N = 7 <sup>1</sup>	HF, N = 14 <sup>1</sup>	Normal, N = 7 <sup>1</sup>	S-ICD, N = 3 <sup>1</sup>	p-value <sup>2</sup>
<b>T:R threshold 1:2 (0.5)</b>							0.3
<b>Primary vector</b>							
<b>Fail</b>	17 / 37 (46%)	3 / 6 (50%)	2 / 7 (29%)	7 / 14 (50%)	2 / 7 (29%)	3 / 3 (100%)	
<b>Pass</b>	20 / 37 (54%)	3 / 6 (50%)	5 / 7 (71%)	7 / 14 (50%)	5 / 7 (71%)	0 / 3 (0%)	
<b>T:R threshold 1:2 (0.5)</b>							0.29
<b>Alternate vector</b>							
<b>Fail</b>	20 / 37 (54%)	3 / 6 (50%)	3 / 7 (43%)	9 / 14 (64%)	2 / 7 (29%)	3 / 3 (100%)	
<b>Pass</b>	17 / 37 (46%)	3 / 6 (50%)	4 / 7 (57%)	5 / 14 (36%)	5 / 7 (71%)	0 / 3 (0%)	
<b>T:R threshold 1:2 (0.5)</b>							0.091
<b>Secondary vector</b>							
<b>Fail</b>	14 / 31 (45%)	4 / 6 (67%)	1 / 7 (14%)	4 / 8 (50%)	2 / 7 (29%)	3 / 3 (100%)	
<b>Pass</b>	17 / 31 (55%)	2 / 6 (33%)	6 / 7 (86%)	4 / 8 (50%)	5 / 7 (71%)	0 / 3 (0%)	
<sup>1</sup> n / N (%)							

---

 2 Fisher's exact test
 

---

Table 28 showing S-ICD screening success rates at T:R of 2:3 for each vector separately.

Threshold/Subgroup	Overall, N = 37 <sup>1</sup>	ACHD, N = 6 <sup>1</sup>	HCM, N = 7 <sup>1</sup>	HF, N = 14 <sup>1</sup>	Normal, N = 7 <sup>1</sup>	S-ICD, N = 3 <sup>1</sup>	p-value <sup>2</sup>
<b>T:R threshold 2:3 (0.66)</b>							0.11
<b>Primary vector</b>							
<b>Fail</b>	12 / 37 (32%)	2 / 6 (33%)	1 / 7 (14%)	5 / 14 (36%)	1 / 7 (14%)	3 / 3 (100%)	
<b>Pass</b>	25 / 37 (68%)	4 / 6 (67%)	6 / 7 (86%)	9 / 14 (64%)	6 / 7 (86%)	0 / 3 (0%)	
<b>T:R threshold 2:3 (0.66)</b>							0.88
<b>Alternate vector</b>							
<b>Fail</b>	13 / 37 (35%)	2 / 6 (33%)	2 / 7 (29%)	5 / 14 (36%)	2 / 7 (29%)	2 / 3 (67%)	
<b>Pass</b>	24 / 37 (65%)	4 / 6 (67%)	5 / 7 (71%)	9 / 14 (64%)	5 / 7 (71%)	1 / 3 (33%)	
<b>T:R threshold 2:3 (0.66)</b>							<0.001
<b>Secondary vector</b>							
<b>Fail</b>	5 / 31 (16%)	0 / 6 (0%)	0 / 7 (0%)	2 / 8 (25%)	0 / 7 (0%)	3 / 3 (100%)	
<b>Pass</b>	26 / 31 (84%)	6 / 6 (100%)	7 / 7 (100%)	6 / 8 (75%)	7 / 7 (100%)	0 / 3 (0%)	
<sup>1</sup> n / N (%)							
<sup>2</sup> Fisher's exact test							

---

Table 29 showing S-ICD screening success rates at T:R of 3:4 for each vector separately.

Threshold/Subgroup	Overall, N	ACHD, N	HCM, N	HF, N =	Normal, N =	S-ICD, N	p-value <sup>2</sup>
	= 37 <sup>1</sup>	= 6 <sup>1</sup>	= 7 <sup>1</sup>	14 <sup>1</sup>	N = 7 <sup>1</sup>	= 3 <sup>1</sup>	
<b>T:R threshold 3:4 (0.75)</b>							0.39
<b>Primary vector</b>							
<b>Fail</b>	9 / 37 (24%)	2 / 6 (33%)	0 / 7 (0%)	5 / 14 (36%)	1 / 7 (14%)	1 / 3 (33%)	
<b>Pass</b>	28 / 37 (76%)	4 / 6 (67%)	7 / 7 (100%)	9 / 14 (64%)	6 / 7 (86%)	2 / 3 (67%)	
<b>T:R threshold 3:4 (0.75)</b>							0.17
<b>Alternate vector</b>							
<b>Fail</b>	8 / 37 (22%)	2 / 6 (33%)	0 / 7 (0%)	3 / 14 (21%)	1 / 7 (14%)	2 / 3 (67%)	
<b>Pass</b>	29 / 37 (78%)	4 / 6 (67%)	7 / 7 (100%)	11 / 14 (79%)	6 / 7 (86%)	1 / 3 (33%)	
<b>T:R threshold 3:4 (0.75)</b>							<0.001
<b>Secondary vector</b>							
<b>Fail</b>	4 / 31 (13%)	0 / 6 (0%)	0 / 7 (0%)	1 / 8 (12%)	0 / 7 (0%)	3 / 3 (100%)	
<b>Pass</b>	27 / 31 (87%)	6 / 6 (100%)	7 / 7 (100%)	7 / 8 (88%)	7 / 7 (100%)	0 / 3 (0%)	
<b>1 n / N (%)</b>							
<b>2 Fisher's exact test</b>							

Table 30 showing S-ICD screening success rates at T:R of 1:1 for each vector separately.

Threshold/Subgroup	Overall, N	ACHD, N	HCM, N	HF, N =	Normal, N	S-ICD, N	p-value <sup>2</sup>
	= 37 <sup>1</sup>	= 6 <sup>1</sup>	= 7 <sup>1</sup>	14 <sup>1</sup>	= 7 <sup>1</sup>	= 3 <sup>1</sup>	
<b>T:R threshold 1:1 Primary</b>							0.37
<b>vector</b>							
<b>Fail</b>	2 / 37 (5.4%)	0 / 6 (0%)	0 / 7 (0%)	1 / 14 (7.1%)	0 / 7 (0%)	1 / 3 (33%)	



<b>Pass</b>	35 / 37 (95%)	6 / 6 (100%)	7 / 7 (100%)	13 / 14 (93%)	7 / 7 (100%)	2 / 3 (67%)	
<b>T:R threshold 1:1</b>							0.054
<b>Alternate vector</b>							
<b>Fail</b>	2 / 37 (5.4%)	1 / 6 (17%)	0 / 7 (0%)	0 / 14 (0%)	0 / 7 (0%)	1 / 3 (33%)	
<b>Pass</b>	35 / 37 (95%)	5 / 6 (83%)	7 / 7 (100%)	14 / 14 (100%)	7 / 7 (100%)	2 / 3 (67%)	
<b>T:R threshold 1:1</b>							
<b>Secondary vector</b>							>0.99
<b>Fail</b>	1 / 31 (3.2%)	0 / 6 (0%)	0 / 7 (0%)	1 / 8 (12%)	0 / 7 (0%)	0 / 3 (0%)	
<b>Pass</b>	30 / 31 (97%)	6 / 6 (100%)	7 / 7 (100%)	7 / 8 (88%)	7 / 7 (100%)	3 / 3 (100%)	
<sup>1</sup> n / N (%)							
<sup>2</sup> Fisher's exact test							

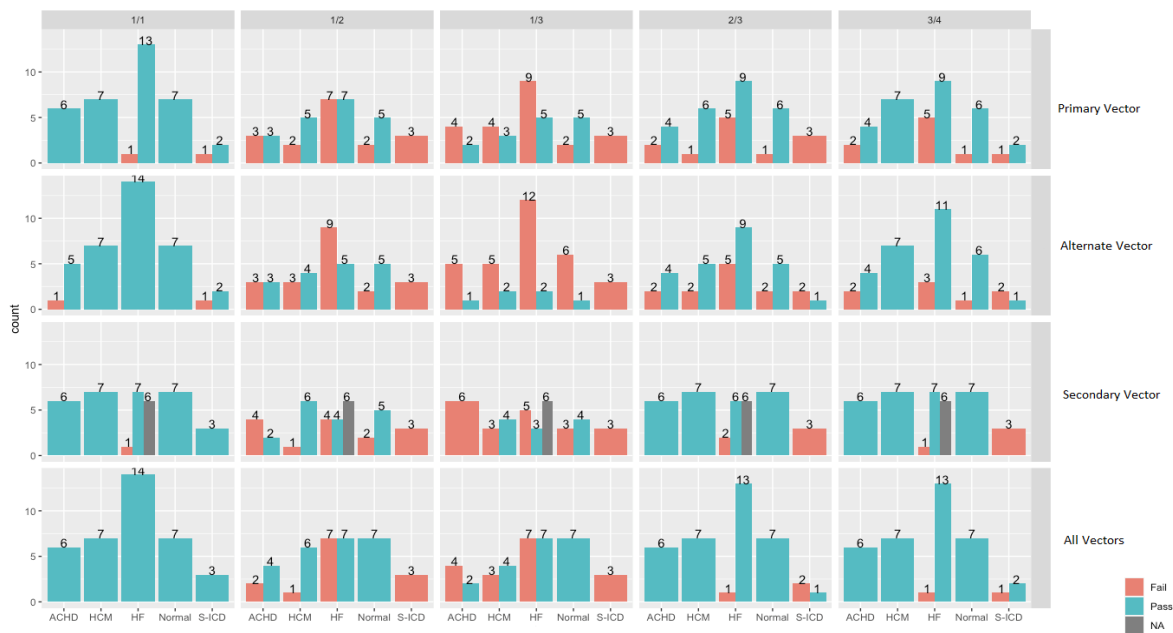


Figure 39 Shows the S-ICD vectors screening pass rates for each S-ICD vector, for all the proposed thresholds and for all the underlying aetiologies that were represented in the analysis.

## 5.5 Discussion

### 5.5.1 Mechanism of action of S-ICD

The sensing mechanism of the S-ICD has been shown to be equally effective to the TV-ICD systems.<sup>26</sup> The problem arises when the device's declining sensitivity level is met with a T-wave with an amplitude that is high enough to be inadvertently sensed by the device and misinterpreted as the next R wave (double counting).

Hypothetically, if the S-ICD did employ fixed sensitivity levels, this would mean that, for a T-wave to be sensed by the device triggering TWO, it must have an equal amplitude to its preceding R wave (in other words a T:R ratio of 1:1). However, smaller ratios should not cause any issues of oversensing provided they are consistent. S-ICDs do not employ fixed but, rather, gradually declining sensitivity levels. This means that, to avoid TWO, T waves must be of an amplitude that is small enough to evade the declining sensitivity levels of their preceding R waves while also allowing for fluctuations of R and T wave amplitudes (safety margin).

### 5.5.2 Optimal T:R ratio for prolonged screening

It is apparent from the results that, if the “standard” T:R of 1:3 was adopted for prolonged screening, 46% of this study’s mixed cohort of patients would have been denied S-ICD therapy if they developed a clinical indication for defibrillation protection and would have likely ended up having a traditional transvenous ICD instead, with all the risks and potential complications that are associated with this. This 46% failure rate is significantly higher than the S-ICD screening failure rates reported in literature using current screening methodology. It is particularly important to point out that all the 37 patients included in this study had a significant proportion of time of the 24-hour recordings (average 96%) when they had at least one lead/S-ICD vector fulfilling the 1:3 ratio. In other words, on average, each patient in the study, regardless of underlying aetiology, had a 96% chance of passing the traditional screening methodology if they turned out on a random time of the day (24 hours) for their screening. This highlights the significant discrepancy in the S-ICD screening pass rates between the current screening process and the proposed method of prolonged screening if the same T:R threshold (1:3) was adopted.

Theoretically there is no point of examining any T:R ratios that are greater than 1:1. If a T:R ratio of 1:1 was adopted as the least strict T:R threshold theoretically feasible even with prolonged screening, all the patients in the study regardless of their underlying aetiology would have passed the screening. A T:R of 1:1 would have been theoretically utilised if the S-ICDs employed fixed sensitivity levels, which they do not. As previously discussed in chapter 1, fixed sensitivity is inappropriate for an ICD. Ventricular fibrillation is characterised by rapidly fluctuating amplitudes. As such, employing fixed sensitivities in an ICD could inadvertently lead to under sensing of VF which can have fatal consequences, if appropriate therapy is not delivered. As such, ICDs are programmed with ‘auto adjusting sensitivity,’ whereby the sensitivity level of the device falls gradually after the detection of a R wave, before being rapidly increased to a percentage value of the next sensed R wave. This is designed to prevent under-sensing of VF. Refer to Figure 5 and Figure 6 for further illustration.

This puts the highest threshold (least strict) of T:R to be considered for the proposed prolonged screening methodology at just below 1:1. Adopting T:R of 1:3 as a reference point was considered because this is the threshold used for current screening practices and it showed in the results that, if this threshold was adopted, 46% of the patients cohort in the study would have not only been at risk of TWO but would have theoretically have had inappropriate shock(s) by their S-ICD

devices potentially within 24 hours of having their S-ICDs implanted (if each of the 24-hour recordings could be considered as a representative of S-ICD vectors signals on an average day). This rate is too high and very far from the inappropriate shock rates due to TWO that occur in real life and are reported by several studies. T:R of 1:3 has proven to be too strict for prolonged screening and would likely inappropriately exclude otherwise S-ICD eligible candidates.

In the presented study, experimentation with a range of T:R ratios ranging between the (standard) 1:3 up to the (least strict but theoretically feasible) 1:1 was done, demonstrating how slightly changing the T:R ratio cut off for eligibility can have a huge impact on the S-ICD eligibility rates specifically for each cohort of patients as well as on the overall eligibility, see Figure 40. The aim of this study was to introduce the concept of prolonged screening for S-ICD eligibility utilising machine learning methods and the need to revisit the current screening parameters if this is to be adopted. A prospective study with real life S-ICD candidates and long term follow up is needed to give insight on the optimal T:R ratio(s) that could be utilised for prolonged screening for S-ICD eligibility.

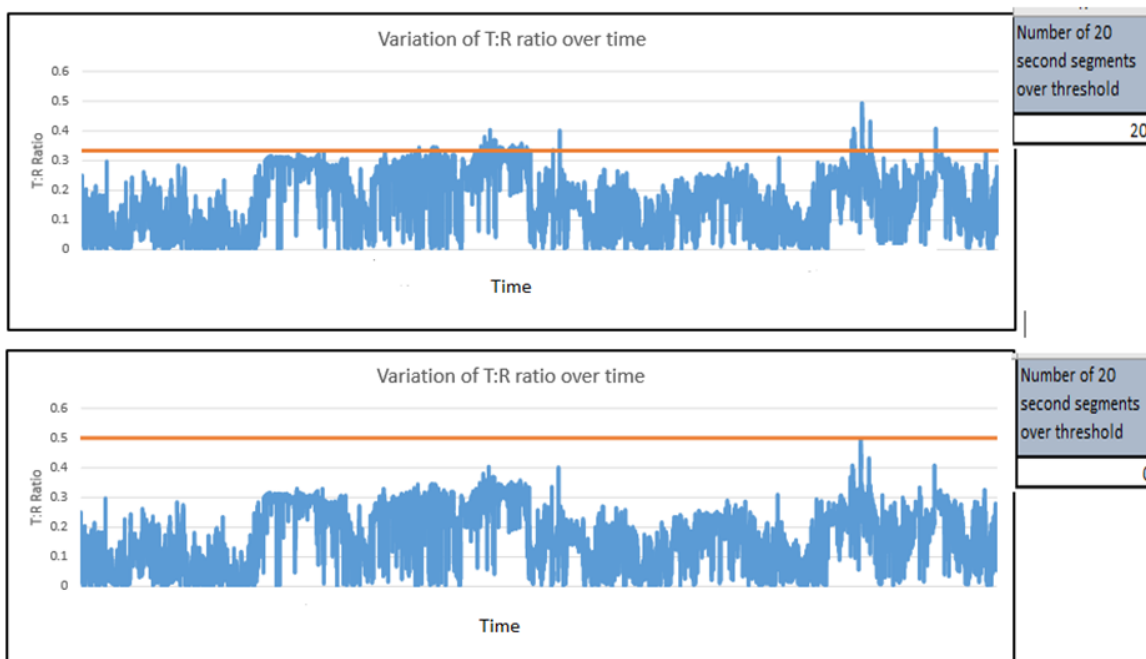


Figure 40 Demonstrates how slightly changing the threshold can impact the outcome of S-ICD screening. It shows the results of a recorded 24-hour ECG signal corresponding to the alternate vector of an S-ICD from one of the patients from the HCM subgroup in the study as analysed by the tool. There is a clear demonstration of T:R ratio fluctuation along the recorded 24 hours. The top half of the figure shows how the T:R ratio crosses the proposed T: R threshold of 1:3 on 20 occasions- convincingly failing the screening-

while the bottom half shows how the T:R ratio never crossed the proposed T: R threshold of 1:2, effectively passing the screening if this threshold was adopted.

### 5.5.3 Limitations

There are several limitations to this study. First, the study focuses on the T:R ratio as the major determinant of S-ICD eligibility, not counting any other parameters which can contribute to the passing or failing of the S-ICD screening. Secondly, the number of the patients recruited in this study is small; as such, results need to be interpreted with caution and larger adequately powered studies are needed to consolidate the findings. In addition, the average heart rates were not incorporated when rejecting a pre-defined ratio, this could be relevant as double counting at a low heart rate is less likely to trigger inappropriate shock therapy than that at a higher rate. It is likely that for future studies, the tool could be adjusted to incorporate this parameter. Moreover, the proposed methodology also does not consider relatively newer algorithms such as SMART PASS that are integrated into the S-ICD that can help it differentiate between R and T waves based on other characteristics rather than just their amplitudes, and potential further work could incorporate new software such as smart pass into the deep learning tool. By choosing a consecutive 20 second periods as cut off for screening, the time needed for the device to deliver a shock is effectively ignoring other potential clinically silent oversensing episodes, allowing those vectors to theoretically pass the screening despite the “silent” oversensing episodes. However, the tool can be adjusted for both the cut off thresholds as well as the time intervals to adapt the screening thresholds as needed. Also, the proposed T:R cut offs are arbitrary but, as mentioned earlier, the aim was not to pinpoint the optimal T:R ratio but, rather, to introduce the concept of prolonged screening and the potential need to revisit the S-ICD screening criteria. Finally, the clinical relevance of the findings of this study is not clear, while the variations in the T:R ratios that is demonstrated in the study is theoretically significant, it is not known for certain if this necessarily translates into adverse clinical events. Further experimental work is needed to consolidate the findings and to incorporate them into clinical practice.

## 5.6 Conclusion

The proposed new methodology, adopting artificial intelligence and deep learning methods, can theoretically help in patient selection for S-ICD therapy while minimising the risk of inappropriate shocks due to cardiac oversensing. The clinical implications of the findings for both screening and

for long term sensing assurance needs further exploring. Whether this proposed methodology, can in fact, reduce TWO in a real-world scenario, with the limitations of having fixed S-ICD sensing vector programming, is yet to be defined. Further work is required, and adequately powered studies are needed to identify the optimal screening thresholds before this can be translated into clinical practice.

## **Chapter 6    Defining the position of the leadless pacemaker and the effect of the implantation site on the device performance**

### **6.1    Introduction**

Patients with an existing subcutaneous implantable cardiac defibrillator (S-ICD) may develop a pacing indication. When transvenous pacing is not feasible, combining an S-ICD and a leadless pacemaker (LP) can be a reasonable option. There are reports of concomitant use of both devices. However, the effect of pacing on the S-ICD sensing is not well studied. The activation pattern produced by pacing has a potential effect on the sensing signals of the S-ICD.

In this chapter, I report on a retrospective analysis done at a tertiary centre for cardiac devices in the UK with a special interest in leadless pacemakers (University Hospital Southampton- UHS). The aim of the retrospective analysis is to, first, demonstrate that leadless pacing has high rate of success and low rate of complications in experienced operators, in real-life populations. Second, to show that there is a variation in the implant sites for the leadless pacemakers, and third, to highlight that the implant site exerts little effect on the short- and long-term performance of the leadless pacemakers. I will use the conclusions from this analysis presented in this chapter as a preamble to the next chapter, where I explore the effect of pacing - with special emphasis on the pacing implant site- on the sensing function of the S-ICD.

### **6.2    Objectives**

Most of the published medical literature describe and characterise the location of the LP implantation site heavily relying on the operator/author assessment of the device location. To be able to reliably compare the devices performance and rate of complications across different implantation sites, a more objective, yet feasible methodology was lacking.

In this study, I propose a feasible, reproducible way of defining the LP location, if widely adopted, can help standardise the assessment of the device location sites across LP implantation centres.

This can prove particularly useful in assessing LP performance across multiple sites such as in multicentre analyses and international registries.

### 6.3 Methods

This is a retrospective analysis of the first 100 leadless pacemakers implanted at a tertiary referral centre for devices (University hospitals of Southampton- UHS) between 2014 and 2021. Two independent observers who didn't implant LPs reviewed the patients' post-implant fluoroscopy images and post-implant CXRs. The reviewers assessed the devices' positions in postero-anterior (PA) and/or right anterior oblique (RAO) views based on conventional fluoroscopic criteria for lead position and conventional practice for LPs positioning. The proposed criteria were used interchangeably on fluoroscopic images and post implant CXRs, see Figure 41. It can prove difficult to reliably differentiate between an implant in the RV free wall and that in the RV mid-septum using only PA and RAO views. As such, the contrast enhanced implant procedure fluoroscopy, clearly demonstrating the characteristic septal trabeculations at the implant sites ruling out free wall placements of the implanted devices, were also retrospectively reviewed.

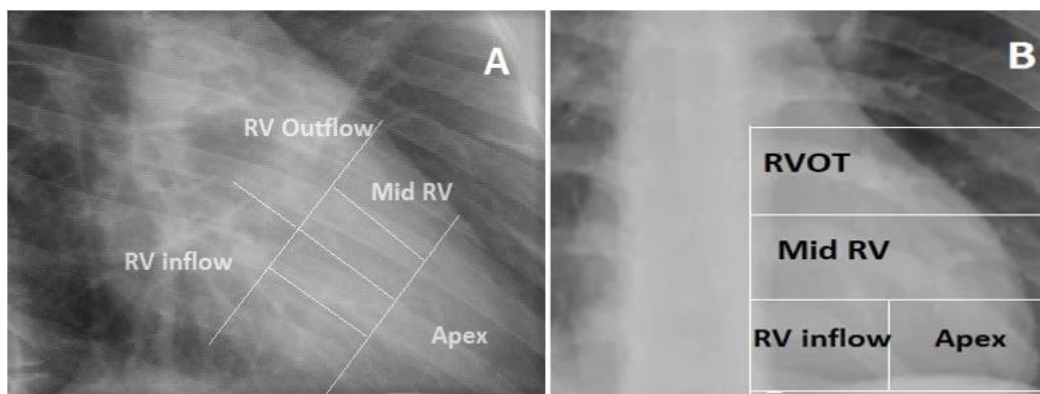


Figure 41 Criteria used for classification of device position:

A: The cardiac silhouette in the RAO view (CXR or Fluoroscopy) was divided evenly by two perpendicular lines into apex, mid RV and the upper-left part of the silhouette was divided into RV outflow / RV inflow. Mid RV was further divided from top to bottom into four quadrants.

B: PA view (CXR or fluoroscopy) The cardiac silhouette from the pulmonary artery bulge above to the inferior border of the cardiac silhouette inferiorly is divided evenly into 3 parts using horizontal lines,



superior third is the RVOT, middle third is mid-RV, and the inferior third is divided into RV inflow and Apex using a vertical line.

To assess the performance of the leadless pacemakers, the implanted devices records at the centre were accessed, and the pacing thresholds, R-wave amplitudes as well as the impedance of the devices at the time of implant and at the latest available routine device follow-up, were recorded. For Statistical analysis, one-way ANOVA testing was used to compare the acute and long-term electrical performance of the devices between different implantation sites.

## 6.4 Results

A total of 100 patients (mean age  $56.6 \pm 22.2$  years, 61% male) were included. 100% of the implants were deemed successful, with no major complications. 88% of the implants required  $\leq 2$  attempts and 70% required one attempt. Refer to Table 31 for patients' demographics.

Table 31 Patients demographics.

Total Number of Participants		n = 100	
<b>Demographics:</b>	Mean age [years $\pm$ 95% CI]	56.6 [ $\pm$ 22.2]	
	Male	61	61.0%
<b>Underlying aetiology:</b>	Normal Heart	74	74%
	Valvular heart disease	5	5.0%
	Adult congenital heart disease	6	6.0%
	Ischaemic heart disease	12	12.0%
	Dilated cardiomyopathy	3	3.0%
<b>Indication for pacing</b>	Symptomatic sick sinus disease	36	36%
	High grade AV block	33	33%
	Bradycardia with associated atrial tachyarrhythmia	27	27%
	Other indications	4	4%
	Presented with syncope	24	24%

The classification of the site of the LPs implants was possible in a total of 90 patients who had fluoroscopic projections or chest x-rays that would allow the classification. The remaining 10 implants could not be reliably categorised based on the available imaging. This is because the post-implant fluoroscopic images were not automatically or manually stored for these patients. A total of 32 implants were in the apex (35.6%). The septal position of the remaining implants was confirmed as the fluoroscopic images with contrast injections clearly showed the characteristic heavy trabeculations of the septal wall at the deployment positions. 28 were in mid-septum (31.1 %), 15 in the apical septum (16.7%), 14 on the septal aspect of the right ventricular inflow (15.5%) and 1 implant (1.1%) in the septum of the RV outflow tract.

Out of the 90 patients with classified device implant locations, 6 patients, whose devices were being followed up at a different center, were excluded from the analysis of the device performance as their devices' electrical parameters at follow up were not available. The follow up period of the 84 patients included in the analysis was  $3.09 \pm 1.97$  years. The first follow ups were scheduled for 6 weeks post implantation, and yearly thereafter. 100% of the LPs had the pacing thresholds  $< 2.0 \text{ V @ } 0.24 \text{ ms}$  at the time of implant. Pacing threshold, R-wave amplitude, and impedance averaged at  $0.67 \pm 0.41 \text{ V}$ ,  $10.86 \pm 5.41 \text{ mV}$ , and  $775 \pm 193.28 \text{ Ohms}$  respectively at the time of implantation and  $0.66 \pm 0.39 \text{ V}$ ,  $14.08 \pm 6.14 \text{ mV}$ , and  $564.29 \pm 96.76 \text{ Ohms}$  at the last device check, see Figure 42. There was no statistically significant difference in either the pacing thresholds or the impedance between implant sites. Post hoc Tukey's analysis (excluding the outflow tract case) demonstrated significant statistical difference in the R-wave amplitudes between implants at the apex and the mid-septum both at the time of implantation ( $12.9 \pm 6.1 \text{ mV}$  and  $8.53 \pm 2.84 \text{ mV}$ ;  $p=0.0196$ ) and at follow up ( $15.97 \pm 5.35 \text{ mV}$  and  $11.52 \pm 5.01 \text{ mV}$ ;  $p=0.0415$ ). There were no differences between other implant sites.

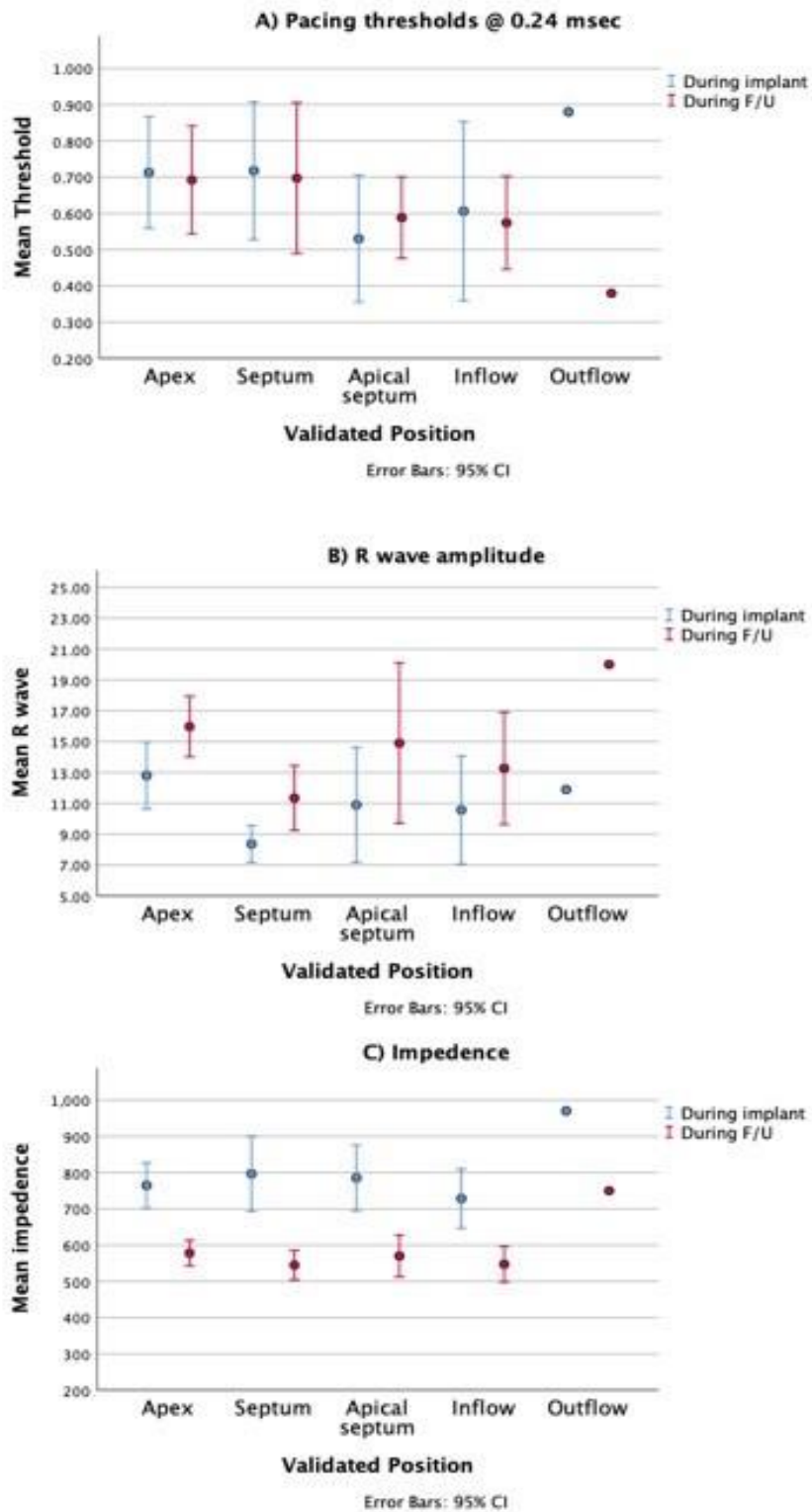


Figure 42 Clustered Error Bars mean of parameters by the validated positions.

## 6.5 Discussion

### 6.5.1 Why leadless?

While transvenous pacemakers are well established solutions for management of bradycardia, it has been shown that almost 90% of their complications are related to the presence of endovascular leads and device pocket issues, such as erosion and infection.<sup>139–141</sup> Transvenous pacing can sometimes be challenging due to access issues such as difficult underlying anatomy or vascular occlusions. Also, in some cases transvenous pacing poses a high risk of infection particularly in patients with prior history of device related infections, haemodialysis<sup>142</sup> or cardiac transplantation<sup>143</sup>. Improvements in battery technology and advanced electrical circuitry helped in the development of leadless pacemakers, much smaller self-contained intracardiac single-chamber pacemakers delivered in the right ventricle through a percutaneous transfemoral catheter-based approach.

To date, there are no randomized controlled trials planned to compare efficacy and long-term safety between transvenous and leadless pacemakers and further studies comparing both systems on the long-term are needed. There are currently few published reports with recommendations for indications for LP therapy as opposed to the traditional transvenous pacing such as the national expert consensus of the Austrian Society of Cardiology<sup>96</sup> and the recommendations of the expert opinion of the working group on leadless pacing of the Polish Cardiac Society.<sup>97</sup>

### 6.5.2 Clinical trials

The Micra<sup>®</sup> safety and efficacy were evaluated in a prospective study (Micra Transcatheter Pacing Study) concluding that the leadless pacemaker system met the specified safety and efficacy goals; demonstrating a safety profile similar to that of traditional pacing, also providing stable pacing thresholds.<sup>144</sup> Further evaluation of the safety of the Micra system in a “real-world” setting was instigated, and the Micra Post-Approval Registry (PAR) was initiated. The “real-world” data were even better than the results of the Micra Transcatheter Pacing Study, it showed high implantation success rate (99%), and a low rate of major complications.<sup>145</sup>

In the Micra TPS international post-approval registry, 795 patients were enrolled from 96 centres in 20 countries, Patients (62.3% male) had a mean age of 75.1 +/- 14.2 years; Indications for implantation were bradyarrhythmia associated with atrial tachyarrhythmia (57.7%), atrioventricular block (14.7%), syncope (14.1%), sinus node dysfunction (8.0%), other indications (3.4%), and unspecified (2.1%). The average follow-up duration was 1.8 +/- 2.9 months. LPs were

successfully implanted in 792 patients (99%). The device was implanted in the septum (52.1%), the apex (39.3%), the right ventricular outflow tract (1.9%), and in other locations including the apical septum (6.3%). 77.3% of the implants required < 2 deployments. The major complication rate was 1.5%. At the time of implant, 97.0% of the patients had a pacing threshold of <2.0 V (mean 0.6 +/- 0.5 V at 0.24 milliseconds). Among the patients with pacing thresholds available at 3 months (n =39) and 6 months (n =25) follow ups, the average pacing thresholds were 0.5 +/- 0.3 V and 0.6 +/- 0.3 V, respectively. The average impedance was 721 +/- 181  $\Omega$  at implant, 634 +/- 143  $\Omega$  at 3 months, and 572 +/- 115  $\Omega$  at 6 months. The mean R-wave amplitude was 11.4 +/- 5.3 mV at implant.<sup>146</sup>

### 6.5.3 Implantation location

Pang et al proposed fluoroscopic criteria to determine ventricular lead position following transvenous device implantation and they assessed their proposed criteria against the gold standard computerised tomography. In their study, fluoroscopic radiographs were recorded in posterior-anterior (PA), and 40° RAO. In the PA view, the area from the pulmonary artery bulge to the inferior border of the cardiac silhouette was divided into three parts by horizontal lines. The uppermost third was the RVOT, the middle third was the middle RV, and the inferior third was divided into the RV inflow and RV apex. A scheme was developed to correlate the RV lead position on the CT images with the RAO fluoroscopy view. In the RAO view, the tricuspid valve formed the left basal border of the RV and was approximated by tricuspid annular calcification or the indentation of the pacing lead by the inferior tricuspid valve. Lead position was classified in the RV long axis as the RVOT, mid-RV, and RV apex. The long-axis position of the lead using the PA and RAO fluoroscopic views were compared to the long-axis CT classification. The conventional PA and proposed RAO criteria had high levels of agreement, specificity, and sensitivity with CT for defining RV apical position. There was high agreement of RAO criteria with CT in distinguishing the middle RV and RVOT (75% and 78%, respectively). Leads in the middle of the fluoroscopic silhouette in the RAO projection were confirmed on CT images to be on the middle of the septum in the short-axis view.<sup>147</sup>

While these criteria were originally introduced to define lead position for transvenous devices, they can be applied to define leadless pacemakers' positions following the same principles. It is difficult to differentiate between an implant in the RV free wall and that in the RV mid-septum using only PA and RAO views, however it is standard procedure to use contrast injections during

implantation procedures to demonstrate the characteristic septal trabeculations at the implant sites to avoid free wall placements of the implanted devices. This is important, as the leadless system requires high tip pressure to deploy the device and ensure good tine activation. If the device is being deployed on the septum, then more pressure can be applied safely without risking perforation which can complicate device deployment on the free wall and true apex.

The proposed method of defining LP position in this study demonstrated that the rate of implants into the true apex was highly comparable to that of the international registry. UHS was involved in the IDE study<sup>148</sup> that originally recommended placement in the RV apex prior to the advice to deploy on the RV septum. It also showed that UHS had lower rates of implants into the mid-septum in favour of apical septum, see Figure 43. There were no pericardial effusions or cardiac perforations resulting from the implant procedures regardless of the site of the implant which is likely a reflection of the experience of UHS operators with LPs implantation procedures. Widely used fluoroscopic and chest x-ray criteria for categorisation of the LPs implantation sites were utilised. The devices positions were not validated using the gold standard CT scans as it was felt that using fluoroscopic and CXR criteria have proven highly correlated to CT images in previous studies.<sup>147</sup> In addition, burdening the available resources and exposing patients enrolled in the study to the high doses of radiation associated with CT scans, could not be justified.

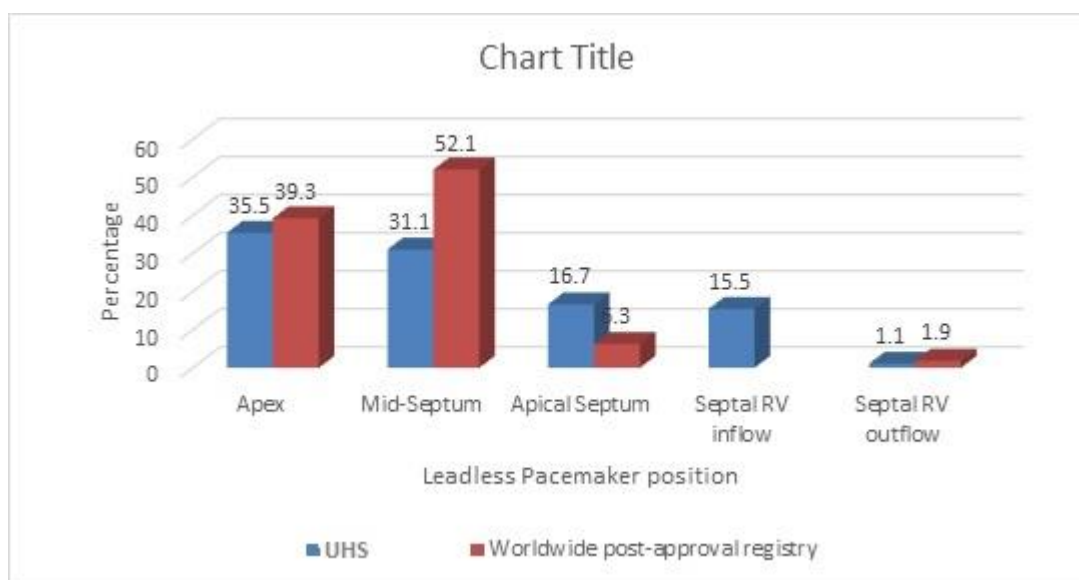


Figure 43 Comparison of leadless pacemaker deployment sites between UHS and the trans-catheter pacing system (TPS) worldwide post-approval registry.

#### 6.5.4 Location and device performance

Garweg et al published their analysis on 133 patients who underwent a leadless pacemaker implantation at the University Hospitals of Leuven. The positions of the leadless devices were assessed on per-procedural ventriculography. The mean follow-up duration for their study was  $13 \pm 11$  months. 45 devices were implanted in the RVOT, 58 in the mid-septum, and 30 at the right ventricular apex. All implant procedures were successful, and they reported two major complications with devices implanted at the apex. Their analysis compared the performance of the devices implanted in the RVOT to the ones implanted at other locations (mid-septum and apex). Pacing impedance was significantly higher in the RVOT ( $946 \pm 292 \Omega$ ) compared to the mid-septal ( $792 \pm 260 \Omega$ ) and apical ( $739 \pm 240 \Omega$ ) positions, ( $P < 0.05$ ). While there were no differences in the pacing thresholds and R-wave amplitudes. Overall, the electrical performance of the devices implanted in the RVOT was comparable to those implanted in mid-septal and apical positions.<sup>149</sup>

Bongiorni et al published their analysis on fifty-two consecutive patients who underwent LP implantation, targeting a non-apical site of delivery when feasible. The mean follow-up period for their analysis was  $13 \pm 9$  months. 60% of their LPs were implanted in a non-apical location without any impact on electrical performance. Pacing threshold remained optimal in most patients (94%) regardless of the site of implantation (apical vs. non-apical location: 0.50 vs. 0.52 V/0.24 ms;  $P = 0.856$ ).<sup>150</sup>

The analysis in this study demonstrated that aside from the difference between the sensed R wave amplitudes between pacemakers implanted at the apex and those implanted at mid-septum, there was no statistically significant difference in the acute or the long-term electrical performance of implanted pacemakers which was satisfactory regardless of the implantation site. This is reassuring and is in keeping with the results of the few previously published analyses.

#### 6.5.5 Limitations

A recognised limitation to the analysis is that the findings regarding the characterisation of the device locations were not validated using other imaging modalities such as echocardiogram or the gold standard cardiac computerised tomography (CT). In addition, PA and RAO views alone are not enough to reliably determine the position of the leadless pacemaker. LAO views are needed to confirm the septal positioning of the leadless pacemaker and to rule out free wall deployment of the device. However, it is standard practice at our centre to only image the RAO and PA views on the post-implant CXRs. Another limitation to the analysis is the relatively low number of the implants included which may have limited the ability to demonstrate differences in the device

performance between implant sites. Also, the analysis included patients from a single centre with a small number of experienced operators and thus the results, particularly the low rate of complications, needs to be interpreted in this context.

## **6.6 Conclusion**

I have demonstrated using simple, reproducible radiological criteria that there is a variation in the implantation sites for leadless pacemakers. Regardless of the deployment site, the rate of complications associated with leadless pacemaker implantations are low in experienced operators. The variation in the implantation site of the pacemakers didn't seem to have any negative effect on the performance of the devices at the time of the implant procedure or during follow up. In the next chapter, I will explore the effect of the variation in the pacemaker implantation locations and the consequent activation patterns on the sensing signals perceived by the S-ICD.



## Chapter 7 The Effect of Leadless Pacemaker Position on the R:T Ratio: An Observational Study Of S-ICD Sensing (PACE HERE)

### 7.1 Introduction

The concomitant use of Leadless pacemakers (LPs) with subcutaneous implantable cardiac defibrillators (S-ICDs) is a tempting option when implanting transvenous leads is not desirable or feasible. However, the effect of pacing on S-ICD sensing has not been studied in detail before. In this chapter, I will examine the potential of oversensing in S-ICD patients who require pacing, and the potential role of individualised device therapy in these patients.

#### 7.1.1 S-ICD paired with a pacemaker

Almost 90% of their complications associated with cardiac implantable devices (CIEDs) are related to the presence of endovascular leads and device pocket issues, such as erosion and infection.<sup>22,151,152</sup> Occasionally, it can sometimes be difficult to implant transvenous CIEDs due to access issues such as difficult underlying anatomy or vascular occlusions. Also, in some cases implanting transvenous devices poses a high risk of infection particularly in patients with prior history of device related infections.

Improvements in battery technology helped in the development of leadless pacemakers. Leadless pacemaker registries demonstrated high implantation success rates (99.1%), and a low rate of major complications of only 2.7% associated with leadless pacing. The overall reliability and safety profile of leadless pacing were comparable to that of traditional pacing.<sup>148,153</sup>

Cardiovascular diseases tend to run a progressive course. As such, patients with an implanted S-ICD might subsequently develop a clinical indication for pacing or vice versa when a patient with a pacemaker in situ develop a clinical need for defibrillation protection. S-ICDs are not suitable to provide reliable pacing. Therefore, the options would be to extract the S-ICD and place a TV-ICD instead for dual function as ICD and a pacemaker or through placing a concomitant pacemaker to act independent from the S-ICD by providing bradycardia pacing therapy to the patient.

It is important to note that patients who have S-ICD implants are likely to share factors that would either preclude them from having a transvenous lead or rendering having a transvenous lead highly undesirable such as high risk of infection, difficult anatomy, difficult venous access, young age with anticipated decades of requirement for defibrillator therapy. This makes the option of extracting S-ICD and placing a TV-ICD less desirable and potentially less viable in real practice than placing a leadless pacemaker which can be an elegant approach to deliver both bradycardia pacing and defibrillation without the need for leads in the vasculature. Prospects of the modular cardiac rhythm management (mCRM) system are expected to include communicating leadless devices to provide dual chamber pacing therapy or even cardiac resynchronization therapy with the potential of coordination with a co-implanted S-ICD. For the time being, leadless pacing systems and S-ICDs act independently. There are a few reports in the literature of the use of leadless pacing with S-ICD.<sup>154,155</sup>

### **7.1.2 Concerns with the concomitant use of both devices**

Previous studies have demonstrated that pacing changes the morphology, and amplitudes of different ECG components. However, the effect of pacing on the sensing process of the S-ICD is not well studied and the effect of pacing specifically on the R:T ratio as perceived by the S-ICD is not currently known. Even though the patient would have passed S-ICD screening, it is possible that QRS double counting or T wave oversensing could occur during paced rhythm. In this case there is a potential risk of inappropriate shock due to oversensing of paced rhythm. This may be particularly relevant in certain pacing circumstances. For example, a patient programmed with hysteresis may see a rapid jump from 40bpm to 90bpm. If there were TWO, this may produce a perceived sudden onset of a heart rate of 180bpm which may be within the detection zone of the programming of the S-ICD. This is important as inappropriate shock therapies can have detrimental effects on the quality of life, psychological wellbeing and can even result in the induction of ventricular arrhythmias.<sup>136</sup>

Through this study, I aim to identify if there could be a benefit in tailoring a leadless pacemaker implant position in patients with concomitant S-ICDs to mitigate any potential adverse outcomes as a consequence of interaction between both devices.

## 7.2 Objectives

This is a prospective observational study to assess the effect of right ventricular pacing on the R:T ratio from the S-ICD perspective. The objectives of the study are:

1. To determine if pacing has a significant impact on the R wave and/or T wave amplitudes and subsequently R:T ratios in the paced beats.
2. To determine if changing the pacing location has a significant impact on the R:T ratios in the paced beats.
3. To quantify the difference in the R:T ratios in the paced beats in different pacing locations.
4. Eventually, to identify the pacemaker positions that would result in the most favourable R:T ratios in the paced beats. Favourable R:T ratios would impose the least risk of T-Wave oversensing by a concomitant S-ICD.

## 7.3 Methods

The study was performed with approvals from the REC (20/NW/0366) and R&D (RHMCAR0582).

Consecutive adult patients (aged 18 years or older) who were undergoing invasive electrophysiological study and/or ablation on clinical grounds were recruited. The invasive electrophysiological procedure includes diagnostic electrophysiological study +/- arrhythmia ablation, pathway ablation, atrioventricular node ablation, implantation of a pacemaker (conventional or leadless), implantation of intracardiac defibrillator (ICD) or a cardiac resynchronisation device (CRT).

Every recruited participant was fitted with a seven-lead, three-channel Holter device prior to their clinical procedure. The leads for the Holter device were placed in a way such as the three recorded channels corresponded to the three distinct sensing vectors of an S-ICD, namely primary (from proximal electrode ring to can), alternate (from distal to proximal electrode) and secondary (from distal electrode ring to can) vectors, see **Error! Reference source not found.**, and Figure 17. At the beginning or towards the end of the clinically indicated electrophysiology procedure, at the discretion of the operator, the right ventricle was paced at four different locations: true apex, apical septum, mid septum, and high septum, for 10 beats at each position at the same rate (10 beats above the resting heart rate) and using the same parameters (8mA/2ms) for all the paced

beats. The positions of the pacing catheter were confirmed by the operator using multiple fluoroscopic views, see Figure 44. The pacing impulses were delivered using a standard conventional pacing catheter to mimic the pacing impulses that would be delivered by a pacemaker. The four different pacing locations that were chosen for the study were based on the most common leadless pacemaker implantation sites reported in the Micra post approval registry.<sup>156</sup>

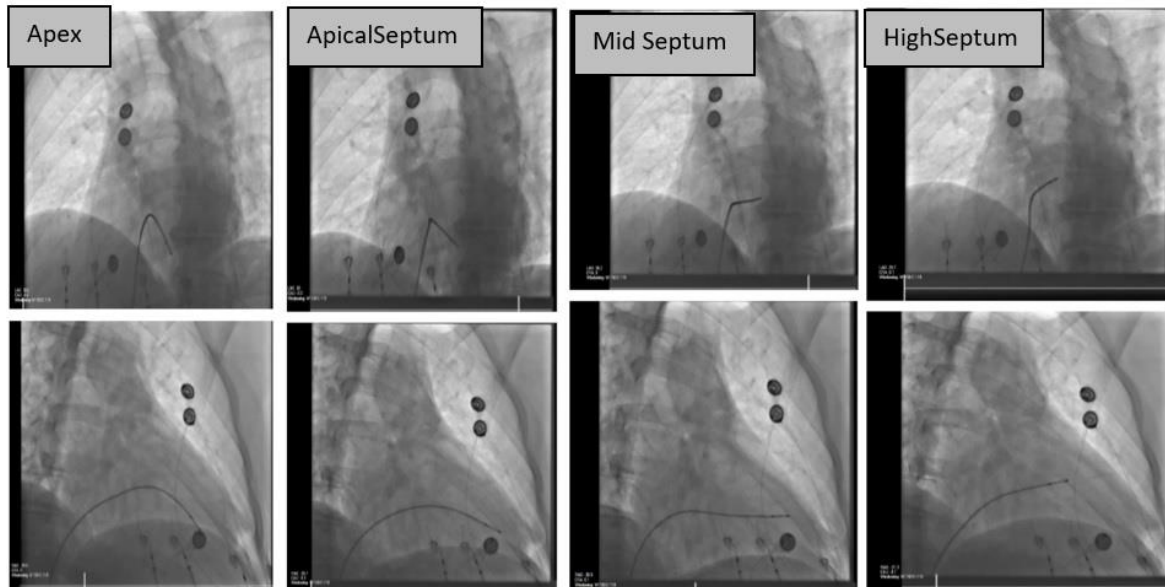


Figure 44 Fluoroscopic images in the left anterior oblique (top row) and right anterior oblique (bottom row) views showing the pacing catheter placed at four different sites in the right ventricle corresponding to the potential implantation sites for the leadless pacemaker.

The Holter data was downloaded and the three channels-corresponding to the three vectors of an S-ICD – were analysed specifically for the R wave and T wave amplitudes in the non-paced beats as well as in the paced beats at the four pre-specified pacing locations using Cardio Calipers™: an on-screen ECG measurement software. An R:T ratio cut-off of 3:1 was chosen following the manufacturer guidelines for the S-ICD screening threshold<sup>157</sup>. R:T ratio of <3:1 was considered unfavourable as they increase the risk of TWO.

### 7.3.1 Statistical analysis

Data was analysed using R program. Normality tests, histograms and boxplots were used to define parametric and non-parametric data. Parametric data was presented as mean  $\pm$  SD and Non-parametric data was presented as median (IQR). Wilcoxon rank sum test was used to compare continuous non-parametric data between different groups. Kruskal-Wallis rank sum and Pearson's

Chi-squared tests were used to determine the significance in the difference between different vectors in the same pacing site and in the non-pacing group. Dunn test was used for subgroup post-hoc analysis with p value adjusted using Bonferroni method.

## 7.4 Results

A total of 47 patients (mean age  $56.0 \pm 16.0$  years, 72% male) were recruited, amounting for 141 vectors for analysis. Refer to Table 32 for patients' demographics. No statistical significance was found when comparing the R:T ratio between different age groups, underlying rhythm, or gender. Patients with structurally normal hearts had statistically significant lower R:T ratios with a median ratio of 2.3 (1.8, 4.0 IQR) when compared with patients with underlying cardiomyopathy, with a median ratio of 2.7 (2.0, 4.1 IQR), ( $P = 0.015$ ).

Table 32 Patients' demographics.

N = 47 <sup>1</sup>	
<b>Sex</b>	
F	13 (28%)
M	34 (72%)
<b>Age(years)</b>	56.02 $\pm$ 16.02
<b>Underlying aetiology</b>	
Adult congenital heart disease	1 (2.1%)
Dilated cardiomyopathy	7 (15%)
Ischaemic cardiomyopathy	1 (2.1%)
Structurally normal heart	38 (81%)
<b>Underlying rhythm</b>	
Atrial fibrillation	15 (32%)
Atrial flutter	3 (6.4%)
Normal sinus rhythm	29 (62%)
<sup>1</sup> n (%); mean $\pm$ SD	

The median R:T ratio for all the vectors combined at the baseline without pacing was 7.8 (4.6,12.0 IQR), significantly higher than the median R:T ratios at different pacing sites; 2.4(1.8,3.2 IQR) pacing at the mid-septum, 2.3(1.9,2.9 IQR) at the septal outflow, 2.0(1.6,2.7 IQR) at the apical septum, and 1.9(1.4,2.6 IQR) at the apex(p<0.001). Pacing-regardless of pacing site- caused significant decrease in the R:T ratio, p <0.0001, see Table 33 and Figure 45.

Table 33 Comparison between the R:T ratios at different pacing sites and with no pacing.

Characteristic	Pacing site					p-value <sup>2</sup>
	Apex, N = 141 <sup>1</sup>	Apical Septum, N = 141 <sup>1</sup>	Mid Septum, N = 141 <sup>1</sup>	No Pacing, N = 141 <sup>1</sup>	Outflow, N = 141 <sup>1</sup>	
<b>R:T ratio</b>	1.9 (1.4, 2.6)	2.0 (1.6, 2.7)	2.4 (1.8, 3.2)	7.8 (4.6, 12.0)	2.3 (1.9, 2.9)	<b>&lt;0.001</b>
<b>Favourable R: T ratio (&gt;3:1)</b>	27 (20%)	23 (17%)	38 (27%)	124 (89%)	32 (23%)	<b>&lt;0.001</b>

<sup>1</sup> Median (IQR); n (%)

<sup>2</sup> Kruskal-Wallis rank sum tests; Pearson's Chi-squared test

**N=141, number of vectors analysed in our study obtained from 47 recruited patients.**

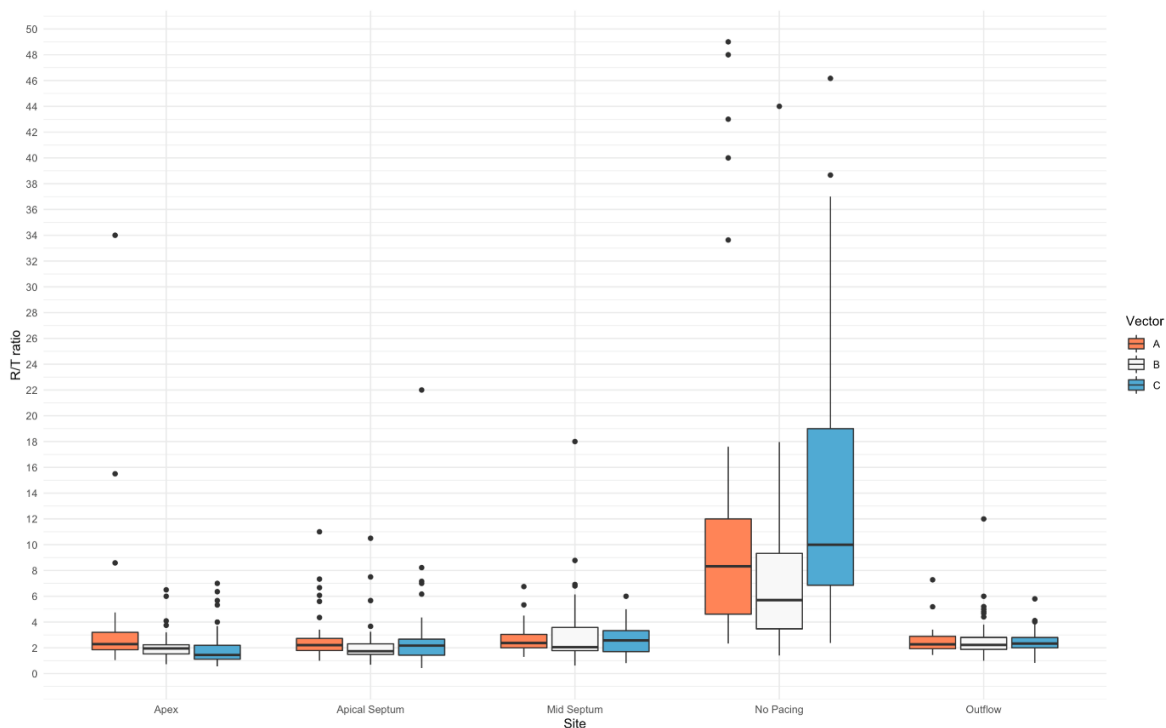


Figure 45 Boxplot comparing between different pacing sites and the "no pacing" group. Significant decrease was noticed in the R:T ratio when pacing in any of the selected sites. Multiple outliers were detected in all

the pacing sites with nearly isoelectric T waves. Vectors A, B, and C correspond to Primary, alternate, and secondary vectors of an S-ICD, respectively.

89% of the vectors exhibited favourable (>3:1) R:T ratios in the absence of pacing, this percentage reduced significantly with pacing; 27% with pacing at the mid-septum, 23% at the septal outflow, 20% at the apex, and 17% at the apical septum( $p<0.001$ ), see Table 33.

There was a statistically significant difference in the median R:T ratios between the different pacing sites. Dunn test was used for subgroup post-hoc analysis. It showed that both outflow and mid-septum pacing sites had higher R:T ratios (2.3 and 2.4 respectively) in comparison with the apical and apical septum (1.9 and 2.0), see Table 34. However, upon comparing the number of cases with favourable R:T ratio (> 3), there was no significant difference between different pacing sites, see Table 35. Table 35

Table 34 post-hoc subgroup analyses for the R:T ratio for different pacing sites

	Apex	Apical septum	Mid-Septum
<b>Apical Septum</b>	-1.068602 0.8557		
<b>Mid Septum</b>	-3.981633 0.0002*	-2.934529 0.0100*	
<b>Outflow</b>	-3.892788 0.0003*	-2.845028 0.0133*	0.089500 1.0000

**Dunn test with Bonferroni adjustment**  
alpha = 0.05  
Reject Ho if  $p \leq \alpha/2$

Table 35 Comparison between the R:T ratios at different pacing sites.

	Site				p-value <sup>2</sup>
	Apex, N = 141 <sup>1</sup>	Apical Septum, N = 141 <sup>1</sup>	Mid Septum, N = 141 <sup>1</sup>	Outflow, N = 141 <sup>1</sup>	
<b>R:T ratio</b>	1.93 (1.43 – 2.60)	2.00 (1.58 – 2.67)	2.36 (1.82 – 3.24)	2.28 (1.94 – 2.85)	<0.001
<b>R:T ratio &gt; 3:1</b>	27 (20)	23 (17)	38 (27)	32 (23)	0.16

<sup>1</sup> Median (IQR); n (%)

<sup>2</sup> Kruskal-Wallis rank sum test; Pearson's Chi-squared test

The median R:T ratios for the primary, alternate, and secondary vectors were also assessed separately; the secondary vector had the highest R:T ratio without pacing (10 (7,19)) followed by the primary vector (8(5,12)) then the alternate vector (6(3,9)),  $p=0.001$ . During pacing at the apex,

the primary vector had the highest R:T ratio (2.29(1.85,3.21)), followed by the alternate vector (1.96(1.53,2.24)) then the secondary vector (1.44(1.12,2.20)),  $p < 0.001$ . Pacing at the apical septum resulted in a highest R:T ratio at the primary vector (2.21(1.80,2.73)), followed by the secondary vector (2.17(1.43,2.67)) then the alternate vector (1.74(1.49,2.31)),  $p = 0.07$ . Mid-septal pacing resulted in the highest R:T ratios at the secondary vector (2.57(1.71,3.33)), followed by the primary vector (2.37(2.00,3.04)) then the alternate vector (2.05(1.79,3.58)),  $p = 0.5$ . There was very little difference between the vectors in the median R:T ratios during pacing at the septal outflow; 2.27(1.93,2.89) in the primary, 2.22(1.88,2.81) in the alternate, and 2.33(2.00,2.80) in the secondary vectors,  $p = 0.9$ , see Table 36.

Table 36 Comparison between the R:T ratio in the three distinct S-ICD vectors.

Site	Vectors (R:T ratio)			p-value <sup>2</sup>
	A(Primary), N = 47 <sup>1</sup>	B(Alternate), N = 47 <sup>1</sup>	C(Secondary), N = 47 <sup>1</sup>	
Apex	2.29 (1.85, 3.21)	1.96 (1.53, 2.24)	1.44 (1.12, 2.20)	<b>&lt;0.001</b>
Apical Septum	2.21 (1.80, 2.73)	1.74 (1.49, 2.31)	2.17 (1.43, 2.67)	0.07
Mid-Septum	2.37 (2.00, 3.04)	2.05 (1.79, 3.58)	2.57 (1.71, 3.33)	0.5
Outflow	2.27 (1.93, 2.89)	2.22 (1.88, 2.81)	2.33 (2.00, 2.80)	0.9
No pacing	8 (5, 12)	6 (3, 9)	10 (7, 19)	<b>0.001</b>
<sup>1</sup> Median (IQR)				
<sup>2</sup> Kruskal-Wallis rank sum tests				

In the absence of pacing, the secondary vector had the highest (96%) probability of exhibiting a favourable (>3:1) R:T ratio, followed by the primary (91%), and then the alternate (78%) vectors,  $p = 0.02$ . Once pacing was instigated, these percentages significantly fall with little difference between the different vectors as follows; during pacing at the apex, the primary vector had the highest percentage of favourable R:T ratios (31%), followed by the secondary (17%), and the alternate (11%) vectors,  $p = 0.057$ . during pacing at the apical septum, the primary vector also had the highest percentage of favourable R:T ratios (20%), followed by the secondary (17%), and the alternate (13%),  $p = 0.7$ . During pacing at the mid-septum, the secondary and the alternate vectors were tied at 28% followed by the primary vector (26%),  $p > 0.9$ . At the septal outflow, the



secondary and the alternate vectors were also tied (23%), followed by the primary vector (22%),  $p > 0.9$ , see Table 37.

Table 37 Favourable R:T ratios (>3:1) in the three distinct S-ICD vectors.

Site	Vectors (R:T ratio > 3:1)			p-value <sup>2</sup>
	A(Primary), N = 47 <sup>1</sup>	B(Alternate), N = 47 <sup>1</sup>	C(Secondary), N = 47 <sup>1</sup>	
Apex	14 (31%)	5 (11%)	8 (17%)	0.057
Apical Septum	9 (20%)	6 (13%)	8 (17%)	0.7
Mid-Septum	12 (26%)	13 (28%)	13 (28%)	>0.9
Outflow	10 (22%)	11 (23%)	11 (23%)	>0.9
No Pacing	43 (91%)	36 (78%)	45 (96%)	<b>0.022</b>
<sup>1</sup> n (%)				
<sup>2</sup> Pearson's Chi-squared tests				

On the individual scale, all the patients recruited in the study had at least one vector which exhibited a favourable R:T ratio in the absence of pacing. While 81% of the patients had at least one vector with a favourable R:T ratio during pacing; 28% had 1 vector, 34% had 2 vectors, 19% had 3 vectors. Only 19% of the patients didn't have any vector that exhibited favourable R:T ratios during pacing regardless of the pacing location, see Table 38 and Figure 46, Figure 48, Figure 49, and Figure 49.

Table 38 R:T ratios on the individual scale.

ID	Primary vector R:T ratio					Alternate vector R:T ratio					Secondary vector R:T ratio					Vectors with favourable (>3:1) R:T ratios	
	No	A	AS	MS	OF	No	A	AS	MS	OF	No	A	AS	MS	OF	Without pacing	During pacing
S01	5.7	1.9	2.0	2.5	2.6	6.2	1.5	2.7	2.3	2.1	4.9	1.3	4.4	2.7	2.1	3	1
S02	8.3	1.7	1.5	1.5	1.5	5.3	2.0	1.7	1.9	2.8	26.2	1.6	1.5	1.7	2.7	3	0
S03	7.7	1.9	1.4	2.0	2.3	10.5	4.1	2.0	2.8	1.9	8.9	2.3	2.0	2.7	2.0	3	1
S04	4.3	NA	2.3	2.0	1.6	5.4	NA	1.5	6.9	1.7	3.5	NA	1.8	3.6	2.0	3	2
S05	9.4	1.9	2.3	3.1	1.7	12.1	NA	1.9	1.9	1.8	26.2	3.7	2.4	2.6	2.3	3	2
S06	10.7	3.5	3.2	2.1	2.0	2.7	1.8	1.5	1.5	1.2	2.4	0.6	0.4	3.3	2.1	1	2
S07	33.6	2.0	1.9	2.1	2.0	NA	NA	NA	NA	NA	46.2	6.4	2.4	2.7	2.7	2	1
S08	7.1	8.6	6.1	3.8	5.2	3.9	2.7	2.4	2.6	1.5	10.7	1.1	1.3	1.0	3.9	3	2
S09	2.4	1.8	2.0	1.8	1.5	2.7	1.7	1.6	4.8	2.7	7.6	2.2	2.3	1.7	1.5	1	1
S10	3.1	3.2	2.7	2.9	7.3	2.1	2.2	2.2	2.1	2.4	2.4	2.4	7.2	2.3	3.5	1	2
S11	3.5	4.0	2.4	2.1	1.7	2.1	1.4	1.4	1.4	2.2	8.9	1.4	1.4	4.7	2.4	2	2
S12	16.5	4.5	4.4	2.8	3.0	8.8	1.7	1.8	3.7	5.0	11.1	0.6	2.2	5.0	4.0	3	3
S13	17.0	3.0	3.0	2.4	2.2	12.0	1.9	1.7	1.9	2.0	26.0	1.2	1.1	3.5	3.1	3	2
S14	40.0	3.3	2.6	2.1	2.8	5.4	1.6	1.7	8.8	1.9	8.2	0.7	1.1	2.7	2.3	3	2
S15	5.3	1.6	1.7	2.8	1.9	3.4	2.0	2.1	1.8	1.9	4.3	5.3	1.9	2.6	2.0	3	1
S16	6.2	2.6	1.9	2.4	2.2	18.0	1.3	1.4	2.4	2.4	11.2	2.0	2.7	2.7	2.1	3	0
S17	3.6	1.9	1.7	1.7	3.1	7.0	1.3	1.4	6.8	2.7	14.0	1.9	2.9	2.0	2.0	3	2
S18	10.7	1.7	1.6	2.4	2.0	3.8	3.2	3.7	2.2	2.0	11.5	3.2	3.5	2.4	1.9	3	2
S19	4.8	2.1	1.8	1.9	2.9	7.2	1.0	3.3	3.8	3.2	12.1	0.9	1.9	2.5	3.2	3	2
S20	11.3	2.6	6.7	6.8	3.1	6.4	2.0	2.9	2.3	2.2	18.0	1.8	2.0	3.9	2.0	3	2
S21	6.2	1.7	1.8	1.8	2.8	7.4	1.3	1.2	1.6	1.8	4.7	0.8	0.6	1.5	2.3	3	0
S22	43.0	2.3	2.1	2.0	3.1	1.5	6.5	1.6	1.9	1.9	8.8	1.0	3.2	2.4	2.5	2	3
S23	9.2	2.9	2.7	3.2	3.2	5.0	1.4	1.5	4.0	2.8	11.8	5.7	2.6	4.8	2.9	3	3
S24	10.0	2.3	2.2	2.3	2.2	14.0	2.6	2.1	2.2	4.8	16.3	1.7	2.4	2.1	5.8	3	2
S25	5.0	3.3	2.9	2.8	3.2	2.0	6.0	3.0	4.0	4.7	24.5	3.3	2.6	2.9	3.6	2	3
S26	10.5	3.1	5.6	3.6	3.2	13.0	2.1	2.8	2.0	6.0	7.0	2.1	7.0	4.8	4.1	3	3
S27	12.0	2.5	2.2	2.6	1.9	1.9	1.7	1.5	1.8	1.6	9.5	1.5	1.3	1.4	2.0	2	0
S28	49.0	4.8	1.4	5.3	2.6	7.0	2.0	1.8	1.9	3.8	22.5	1.7	1.6	1.5	3.6	3	3
S29	3.0	1.9	1.9	2.0	2.8	3.9	0.7	0.8	1.0	1.0	6.8	0.7	2.3	1.2	0.9	3	0
S30	17.6	1.8	2.8	4.2	3.4	12.8	2.0	1.6	2.0	2.3	6.9	1.4	8.2	1.3	0.8	3	2
S31	2.4	2.3	2.3	3.7	2.4	3.8	3.0	10.5	3.3	2.6	9.2	4.0	6.2	4.3	2.5	2	3
S32	48.0	15.5	11.0	4.0	2.3	10.7	2.0	1.7	1.8	1.6	23.0	1.1	1.0	1.0	2.2	3	1
S33	11.3	1.8	2.3	2.4	2.5	9.5	2.3	5.7	1.8	2.1	5.2	1.0	2.4	2.6	2.4	3	1
S34	9.5	2.8	2.4	2.8	2.7	5.4	1.3	1.5	6.1	2.7	6.9	1.3	1.8	3.4	2.6	3	2

<b>S35</b>	2.3	1.4	1.4	1.6	1.4	7.8	1.0	0.7	0.7	1.0	13.5	2.9	2.2	2.2	1.7	2	0
<b>S36</b>	5.3	2.8	2.4	2.0	1.7	6.8	2.1	1.9	1.8	2.1	38.7	1.2	1.6	3.5	2.3	3	1
<b>S37</b>	16.0	1.2	1.0	2.4	2.8	2.7	1.6	1.3	5.5	5.2	11.0	1.4	1.1	4.5	2.1	2	2
<b>S38</b>	7.2	2.0	1.9	1.8	1.9	12.7	1.5	1.3	0.6	4.4	9.2	1.3	0.8	1.9	2.1	3	1
<b>S39</b>	14.0	34.0	7.3	4.5	2.6	8.3	2.0	1.7	18.0	3.3	4.8	1.4	0.8	6.0	3.8	3	3
<b>S40</b>	7.2	3.2	3.4	3.2	3.1	44.0	3.8	3.2	4.3	12.0	37.0	7.0	22.0	2.9	2.6	3	3
<b>S41</b>	12.0	3.9	2.2	4.3	2.2	6.0	2.2	2.3	2.7	2.0	20.0	0.8	2.8	1.7	2.3	3	1
<b>S42</b>	14.7	2.6	2.0	2.3	2.1	4.5	2.4	7.5	1.8	2.3	6.0	2.0	2.8	2.6	2.0	3	1
<b>S43</b>	3.8	NA	NA	NA	NA	3.0	1.7	1.6	1.6	2.2	10.0	1.7	2.3	1.5	1.8	3	0
<b>S44</b>	3.5	1.4	1.3	1.3	1.6	1.4	1.4	1.3	1.3	1.6	3.8	1.4	1.7	1.7	1.7	2	0
<b>S45</b>	9.6	1.9	2.7	2.4	1.6	3.3	2.3	2.2	1.5	1.3	4.3	0.9	0.9	0.8	3.5	3	1
<b>S46</b>	4.4	1.1	2.0	2.1	2.1	12.0	2.0	1.9	2.3	3.8	25.0	1.2	2.4	2.5	1.9	3	1
<b>S47</b>	4.0	2.0	1.7	2.0	2.0	4.9	1.5	1.5	1.5	2.1	24.0	1.3	2.1	2.6	2.4	3	0

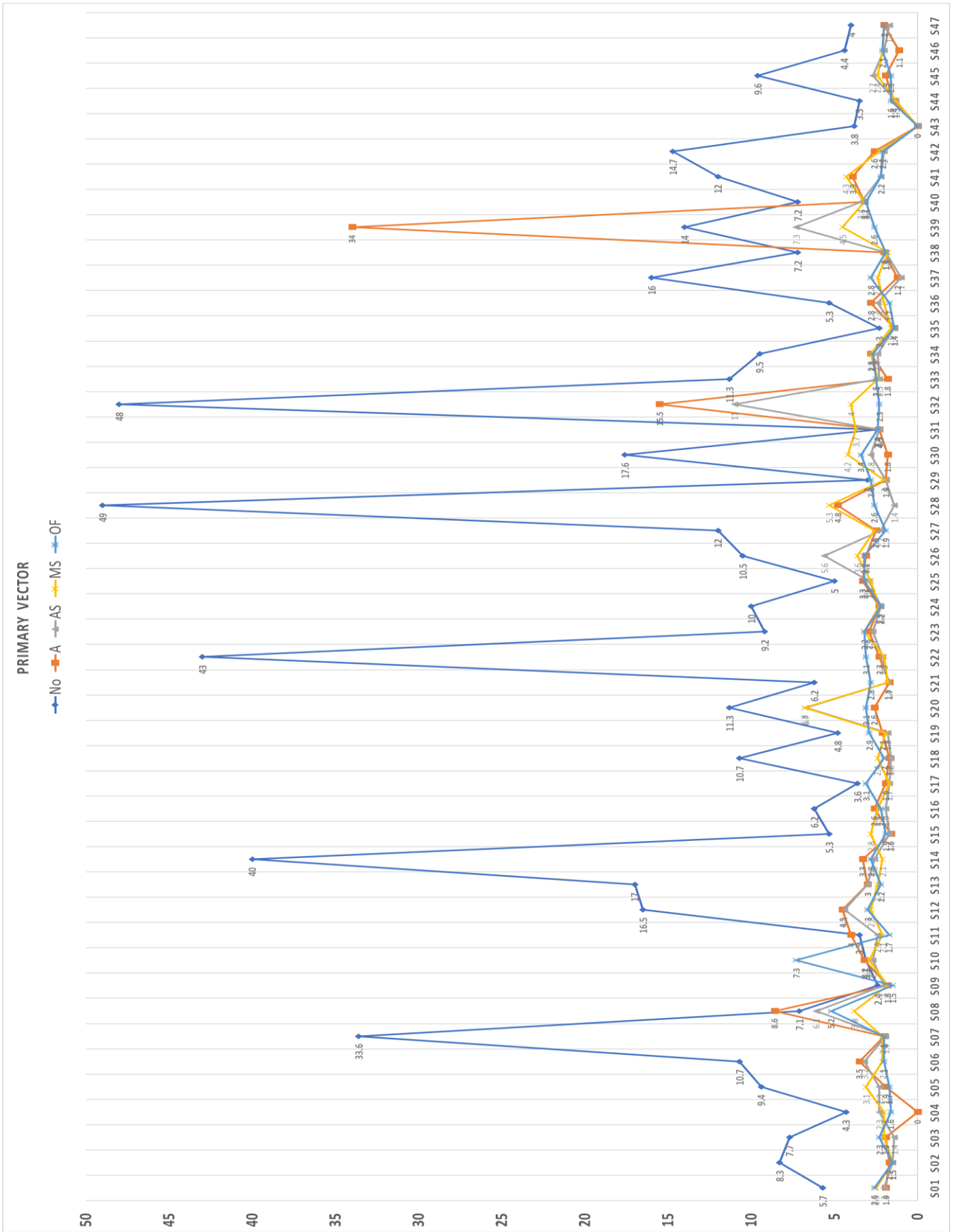


Figure 46 R:T ratios on the individual scale for the primary vector. The R:T ratios are plotted on the y-axis against the individual study ID. No refers to no pacing, A, AS, MS, and OF refers to Apical, apical septum, mid septum, and outflow tract pacing respectively.

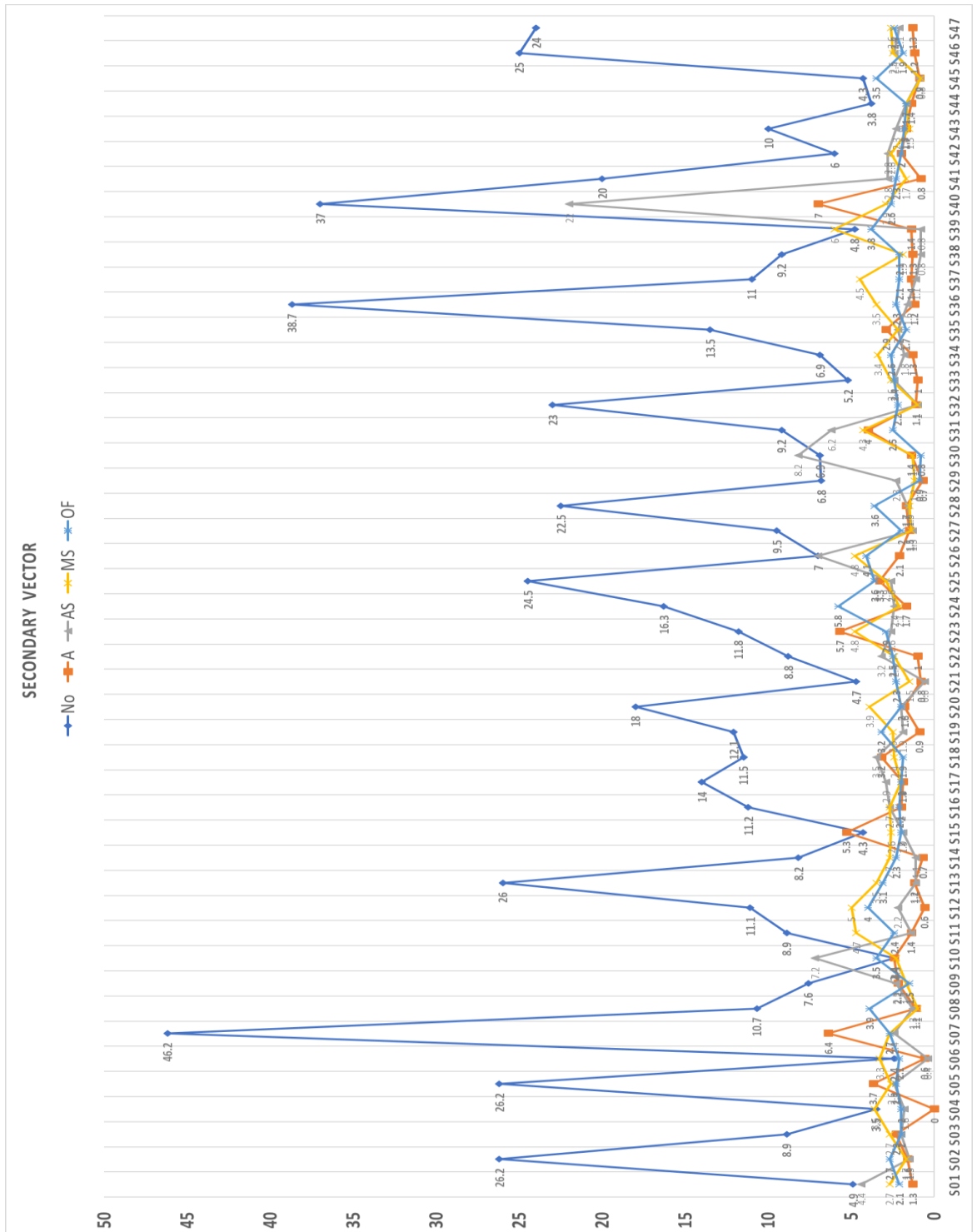


Figure 47 R:T ratios on the individual scale for the secondary vector. The R:T ratios are plotted on the y-axis against the individual study ID. No refers to no pacing, A, AS, MS, and OF refers to Apical, apical septum, mid septum, and outflow tract pacing respectively.

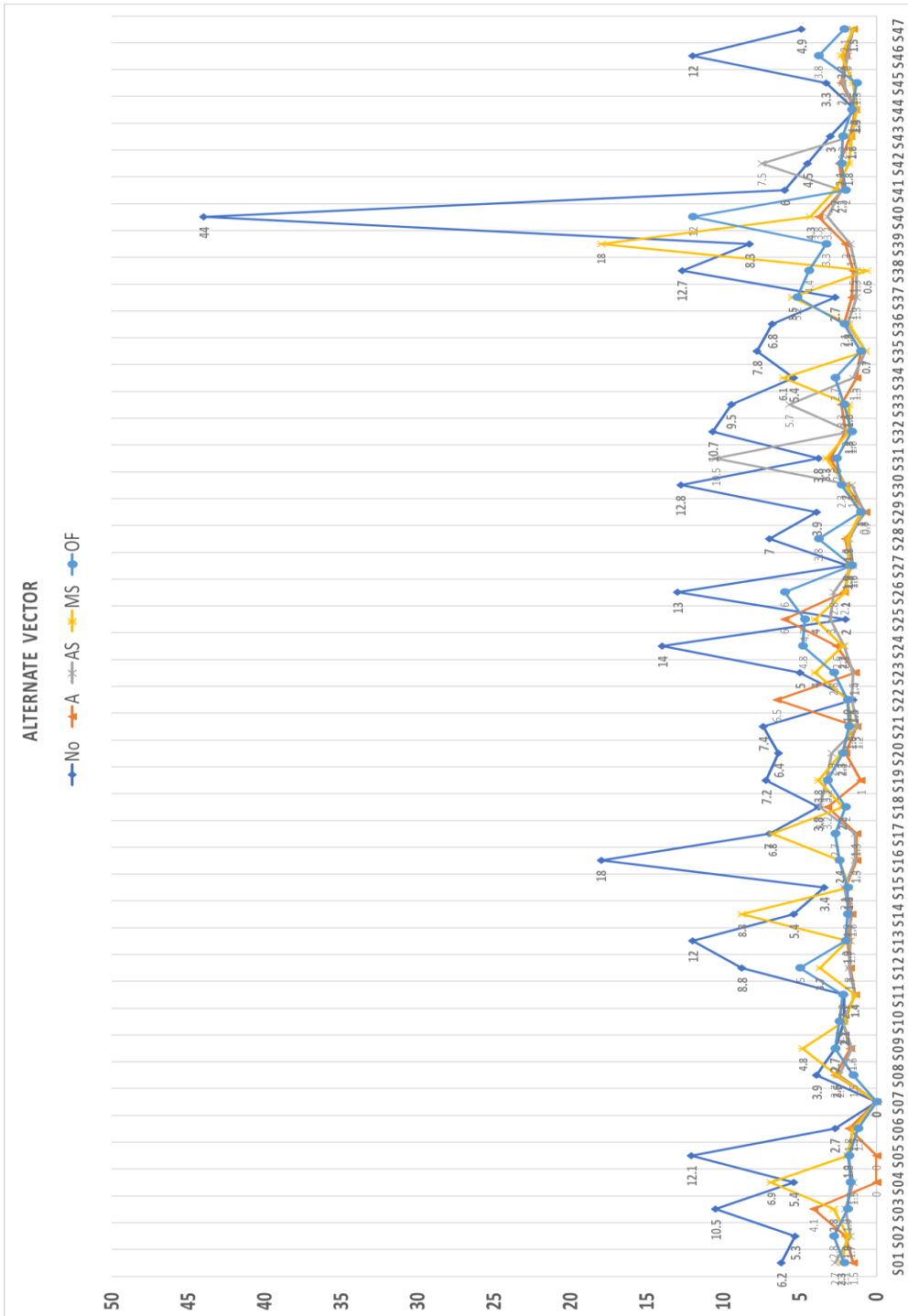


Figure 48 R:T ratios on the individual scale for the alternate vector. The R:T ratios are plotted on the y-axis against the individual study ID. No refers to no pacing, A, AS, MS, and OF refers to Apical, apical septum, mid septum, and outflow tract pacing respectively.

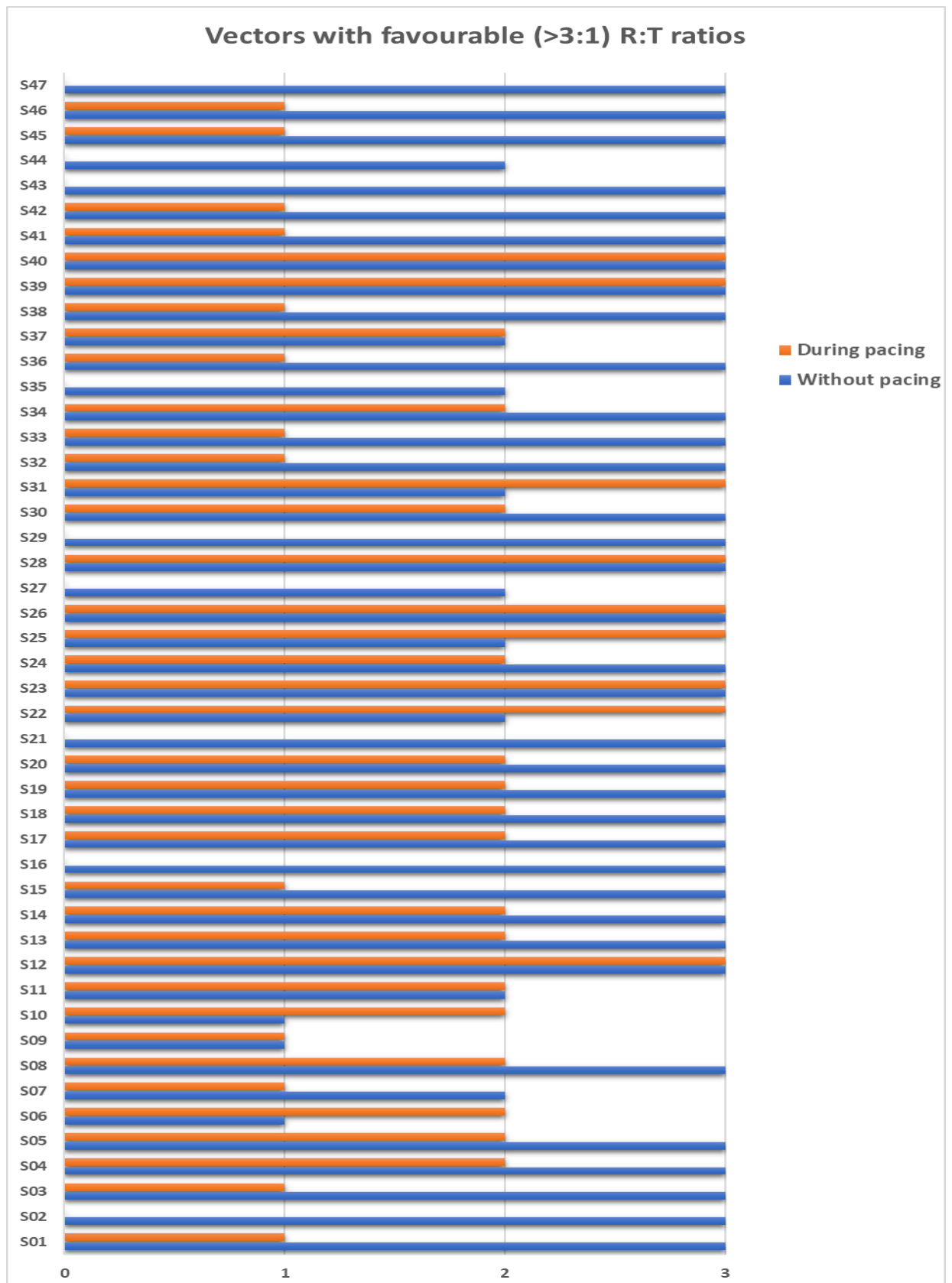


Figure 49 Vectors with favourable R:T ratios on the individual scale. The study ID is plotted on the y-axis against the number of favourable R:T ratios on the x-axis.

## 7.5 Discussion

### 7.5.1 Clinical relevance

The effect of pacing on the sensing process of the S-ICD is not well studied and the effect of pacing specifically on the R:T ratio as perceived by the S-ICD is not currently known. Changes in the R wave and T wave amplitudes can lead to changes in the R:T ratio which is vital to the sensing mechanism of the S-ICD. It is important to note that even in the modular CRM system, there is only unidirectional communication from the S-ICD to the LP (to deliver ATP therapy) and not vice versa. As such, the S-ICD will not know if pacing is instigated by the LP and will still rely on the sensed electrograms for rhythm discrimination.

In this study, I was particularly interested in the changes associated with R:T ratios because of pacing as well as changing the location of pacing. R:T ratio was chosen specifically as the parameter to be analysed because of the crucial role of the R:T ratio in the sensing mechanism of the S-ICD and its subsequent determination of S-ICD eligibility and TWO events. Even though the patient would have previously passed the S-ICD screening, it is possible that QRS double counting or T wave oversensing could occur during paced rhythm. In this case there is a potential risk of inappropriate shock due to oversensing of paced rhythm. This may be particularly relevant in certain pacing circumstances. For example, a patient programmed with hysteresis may see a rapid jump from 45bpm to 90bpm. If there were TWO, this may produce a perceived sudden onset of a heart rate of 180bpm which may be within the detection zone of the programming of the S-ICD. Aside from few sporadic cases published as case reports,<sup>154,155</sup> I am not aware of any studies that looked specifically into the cohort of patients who have leadless pacemakers in situ who would be deemed eligible for an S-ICD if they develop an indication for one.

### 7.5.2 Pacemaker position effect on ECG signals

Current practices favour implanting the leadless pacemaker into the trabeculated septal wall and avoid the right ventricular free wall or the right ventricular apex, this is to minimise the perceived risk of perforation. Leadless pacemaker registries have demonstrated wide variation in the implantation sites of leadless pacemakers.<sup>156</sup> Further data analysis demonstrated no variation in the short and intermediate term performance of the leadless pacemakers regardless of the



implantation site.<sup>158,159</sup> As such, there is no preference in the leadless pacemaker deployment location as long as the thinner right ventricular free wall is avoided.

While pacing is known to be associated with ECG morphological changes, the effect of changing the pacing location on certain morphological aspects of the ECG is not well studied. The specific locations for pacing that were chosen for the study were based on the leadless pacemakers' implant locations reported in the registries.<sup>156</sup> My aim was to identify the most favourable location that would either lead to a minimal effect on the ECG morphology and R:T ratios or even if associated with significant changes, still maintain a favourable R:T ratio from a S-ICD perspective. Similarly, sub-optimal pacing positions could also be identified and thus better avoided if S-ICDs and LPs were to be used concomitantly.

### 7.5.3 Data analysis

I have demonstrated through this study that first; pacing caused significant changes in the ECG morphology, particularly in the R:T ratios when looked at from an S-ICD perspective. In some cases, as demonstrated in Table 38, R:T ratios dropped to 1:1 or even below once pacing was instigated. This is quite significant as TWO will most likely be an issue at these low ratios. Second, pacing site also had an impact on the morphological changes associated with pacing, and R:T ratios perceived by all the S-ICD vectors changed with changing the pacing site, see Figure 50. Pacing, regardless of the pacing site, in general had a detrimental effect on the R:T ratio perceived by the S-ICD vectors. This is clearly demonstrated as the median R:T ratios in all three vectors and across all the pacing sites has fallen below 3:1 once pacing was instigated. Perhaps this is not surprising as ventricular pacing results in abnormal depolarisation and subsequently abnormal repolarisation which are represented as QRS complexes and T-waves respectively on the ECG signals. When a pacing stimulus is delivered in the right ventricular apex, the activation starts in the right ventricle and spreads towards the left ventricle. This results in ECG signals similar to those seen during left bundle branch block (LBBB). While pacing closer to the right ventricular septum allows the pacing impulses to enter the conduction system with subsequent faster conduction of impulses, resulting in shorter QRS durations. However, regardless of the pacing location, the subsequent ECG signals that are produced by pacing are characteristically different to those without pacing, see Figure 50. These changes are significant enough to compellingly alter the R:T ratios.

Most (89%) of the recorded vectors had a favourable R:T ratio (>3:1) prior to pacing in the cohort of recruited patients. This high percentage drastically falls once pacing is initiated, the average percentage of favourable R:T ratios in all vectors at all pacing locations once pacing was instigated was only 21%.

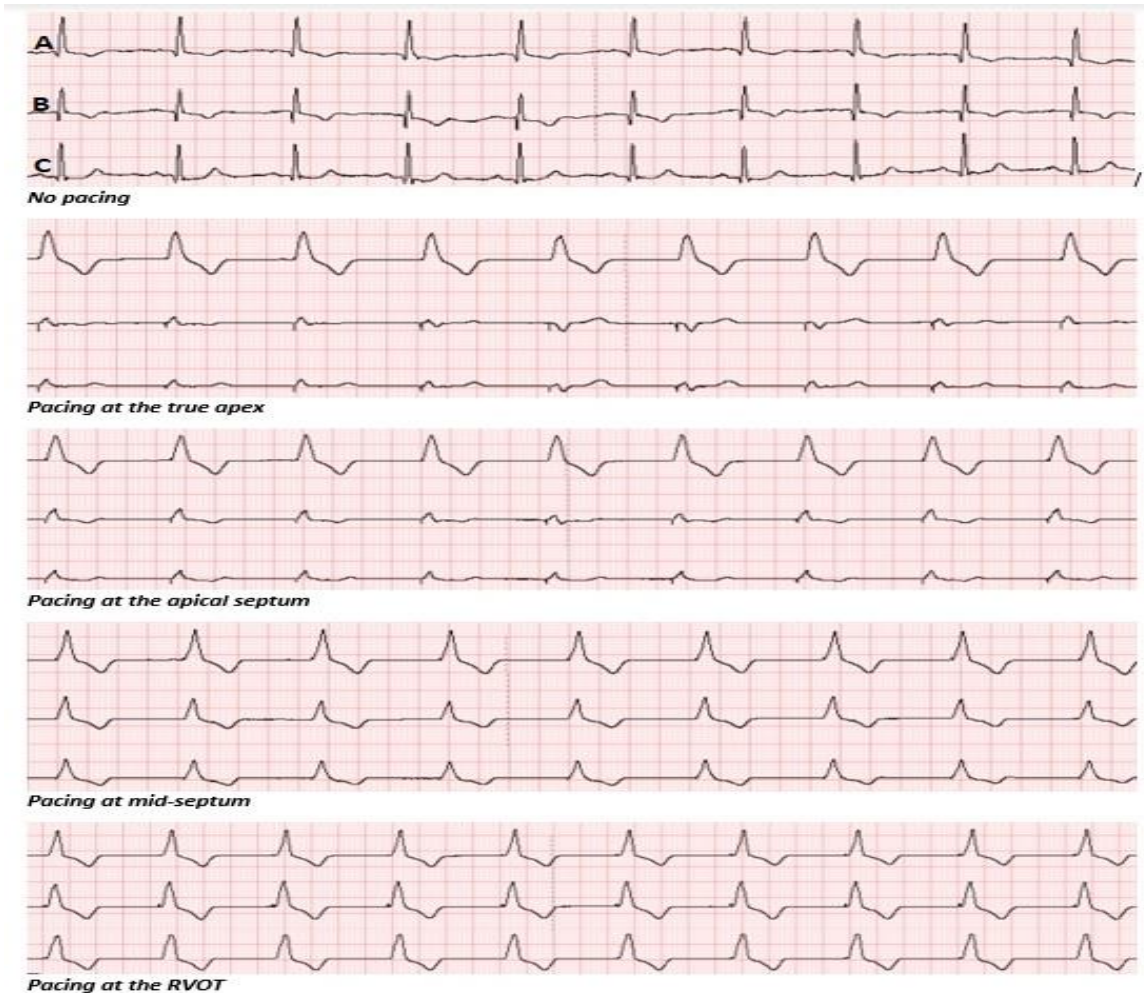


Figure 50 An example of the effect of pacing as well as changing the pacing site on the morphology of the Holter traces corresponding to the S-ICD vectors. A, B, and C correspond to primary, alternate, and secondary vectors respectively.

However, and despite the detrimental effect of pacing on the R:T ratio, favourable R:T ratios (>3:1) were recorded during pacing in all 3 vectors and at all the pacing locations, albeit significantly less prevalent than in the “no pacing” traces. In fact, most (81%) of the patients recruited in the study had at least one vector that exhibited favourable R:T ratio during pacing at at least one pacing location. This means that even if the percentage of the favourable R:T ratios during pacing is overall significantly less when looking at all vectors, the remainder favourable vectors are distributed in a way that allows 81% of the patients in the cohort to have at least one favourable/suitable vector which is enough to pass the screening. However, none of the vectors,

and none of the four different pacing locations were consistently favourable (or statistically better) from the R:T ratio perspective.

When it comes to implanting a leadless pacemaker into a patient with an existing S-ICD, there is no “one size fits all”. The choice of implantation location of the leadless pacemaker as well as the choice of vector programming for the S-ICD must be tailored to each individual patient. Even in the absence of a favourable R:T ratio across all vectors and pacing locations, implanting a leadless pacemaker into a patient with an S-ICD while minimising the risk of inadvertent interaction is theoretically possible in most patients.

Furthermore, careful individualised programming of both devices is paramount. For example, the upper limit of the pacing rate of a pacemaker as well as the therapy threshold heart rate of an S-ICD should be both set- if possible- in a way that even if the pacing rate is inappropriately double counted, still wouldn't exceed the therapy rate threshold for the concomitant S-ICD. This ought to reduce the risk of inappropriate shocks due to TWO because of pacing.

#### **7.5.4 Limitations**

This study had several limitations. First, the relatively lower number of recruited patients might have hindered the ability to identify a statistically significant difference in the R:T ratio between different pacing sites. Second, none of the patients recruited for the study had either or were candidates for an S-ICD or pacemaker therapy, although the same principles should still apply for them. Third, the presence of both devices (S-ICDs and leadless pacemakers) was mimicked using a Holter device with its leads placed to mimic S-ICD vectors and a standard pacing catheter was used as a surrogate of a leadless pacemaker. This could be relevant, particularly due to the different pacing parameters between the pacing catheter (2 milliseconds in this study) versus that of the leadless pacemaker (0.24 milliseconds). Consequently, the paced QRS from the catheter could be potentially different from the paced QRS from the leadless pacemaker. However, exclusively recruiting patients with S-ICDs who develop a pacing indication for the study would appear to be an unjustified time-consuming process and likely to yield a lower number of recruited patients to the study even at a tertiary referral centre of this calibre specialised in implanting both S-ICDs and leadless pacemakers. In addition, most of the patients in the study had underlying structurally normal hearts. In real-life, there are a lot of patients with S-ICDs with apparently structurally normal hearts, such as patients with underlying channelopathies. However, a lot of S-ICD patients have underlying cardiomyopathies of various etiologies which can affect the results, for example, the voltage and duration of a paced QRS is not the same in healthy

tissue vs scar tissue. There was a significant difference in the R:T ratio between both groups in this study. However, larger studies involving wider cohort of patients with various underlying etiologies are needed to consolidate the findings. R:T ratio of 3:1 that was used as the threshold of eligibility for this study is based on the screening threshold cut-off of the S-ICD, based on manufacturer recommendations for screening allowing for a safety margin. There is no evidence that lower R:T ratios would inevitably lead to adverse clinical events. In real-life, R:T ratio might need to fall way below the proposed ratio of 3:1 for TWO to occur, however, this needs to be studied further. In this study, the effect of pacing only on the R:T ratio was assessed and not on other parameters such as QRS duration and QT interval, which could also potentially affect the S-ICD eligibility. However, as previously mentioned, the R:T ratio parameter was chosen for this study as a simple, easily measured parameter based on the integral role of the R:T ratio in the S-ICD sensing mechanism and determinability of S-ICD eligibility. In addition, the cut-offs at which other parameters such as QRS or QT durations would fail the S-ICD screening is not known. Further work is needed before the proposed personalised approach towards device therapy be applied in clinical practice.

## 7.6 Conclusion

Extravascular and leadless devices may represent the future of cardiac device therapy. They have consistently demonstrated reliable performance and high safety profile avoiding the complications associated with the traditional transvenous lead-reliant devices. It is inevitable that we will see more and more patients in whom we will be tempted to utilise concomitant leadless pacemakers and S-ICDs for their pacing and defibrillator protection indications rather than implanting the traditional TV-ICDs. I have demonstrated through this study that pacing, regardless of the pacing site, in general had a detrimental effect on the R:T ratio perceived by the S-ICD vectors, significantly lowering the percentages of favourable R:T ratios once pacing is instigated. However, the study also demonstrated that, at least theoretically, it is feasible in most patients to concomitantly utilise both devices if we adopt a personalised devices therapy approach. Implantation procedure for the devices as well as the devices programming needs to be tailored for every individual patient.

## Chapter 8 Conclusion

### 8.1 Summary of findings

Most “real-life” patients referred for S-ICD therapy are likely to be deemed S-ICD eligible following current screening practices. Certain patient characteristics such as gender, BMI, and underlying cardiac aetiologies can impact the S-ICD screening outcomes. (Chapter 2)

R:T (or T:R) ratio, one of the integral components of the S-ICD sensing mechanism and a main determinant of S-ICD eligibility, is significantly lower (higher T:R) in heart failure, ACHD and HCM patients when compared to patients with structurally normal hearts. It also has the tendency to significantly fluctuate overtime, particularly in patients with heart failure and ACHD. This poses a theoretical risk for TWO and inappropriate shocks in patients who have S-ICDS fitted in after being found S-ICD eligible following the current screening practices. (Chapter 3)

The adoption of novel deep learning methods approaches for data analysis for S-ICD screening to determine patient eligibility for S-ICD implantation as well as guide vector selection in S-ICD eligible patients seems promising. Utilising these methods could enable more accurate and efficient screening methods. (Chapter 3, Chapter 4)

Slightly changing the R:T (or T:R) ratio cut-off for eligibility can have a huge impact on the S-ICD eligibility rates. The current screening parameters need to be revisited if the concept of prolonged screening for S-ICD eligibility, utilising machine learning methods, is to be adopted. (Chapter 5)

There is a variation in the implantation sites for leadless pacemakers. Regardless of the deployment site, the rate of complications associated with leadless pacemaker implantations are low in experienced operators. The variation in the implantation site of the pacemakers didn't have any negative effect on the performance of the devices. (Chapter 6)

Leadless pacing, regardless of the pacing site, had a detrimental effect on the R:T (T:R) ratio perceived by a concomitant S-ICD device, significantly lowering the percentages of favourable ratios once pacing is instigated. However, it is theoretically feasible in most patients to concomitantly utilise leadless pacemakers and S-ICDs if a personalised devices therapy approach is adopted. Implantation procedure for the devices as well as the devices programming needs to be tailored for every individual patient. (Chapter 7)

## 8.2 Clinical implications

In addition to any academic interest in the work presented in this thesis, there are potential tangible clinical implications to the findings presented in this work. Perhaps the first practical application that comes to mind is utilising the proposed prolonged screening methods to help select the most stable S-ICD vector in patients with multiple eligible vectors, thus reducing the risk of TWO and inappropriate shocks. Furthermore, the adoption of the principles and technologies proposed in this work facilitates the acquiring of significantly more detailed ECG signals for each individual patient in an efficient yet a precise process. This information can facilitate a more refined and individualised risk assessments for device therapy and in turn promotes shared informed decision making between the physicians and their patients. Finally, using S-ICD screening approaches proposed in this work can potentially alter the outcome for some patients who were previously deemed ineligible for S-ICD therapy using traditional screening methods. This can be achieved after careful consideration and weighing the individualised risk of inappropriate shocks vs benefits of advanced device therapy for each individual patient.

## 8.3 Summary of limitations

The limitations that are relevant to each of the studies presented in this thesis were described in previous chapters. However, with regards to the overall work, there are few limitations that warrant further discussion.

First of all, despite being a key component in the S-ICD sensing process, and a major determinant of S-ICD eligibility, R:T or T:R ratio is not the only parameter and other factors that play a role in the S-ICD sensing process such as QRS duration and QT interval, which could also potentially affect the S-ICD eligibility were not examined in this thesis. However, as previously mentioned, the R:T or T:R ratio was chosen as a simple, easily measured parameter based on its integral role in the S-ICD sensing mechanism and determinability of S-ICD eligibility, while the eligibility cut-offs for other parameters such as QRS duration or QT intervals are not readily known.

Moreover, the proposed methodology also does not consider the impact of the relatively newer S-ICD sensing algorithms, i.e., SMART PASS, that are integrated into the S-ICD that can help it differentiate between R and T waves based on other characteristics rather than just their

amplitudes. Further maturation of the deep learning methods tools could facilitate the incorporation of software such as SMART PASS into the proposed screening methodology.

R:T ratio of 3:1 (T:R of 1:3) that was used as the threshold of eligibility is based on the screening threshold cut-off of the S-ICD, based on manufacturer recommendations for screening, allowing for a safety margin. However, there is no evidence that lower R:T ratios would inevitably lead to adverse clinical events. In real-life, R:T ratio might need to fall way below the proposed ratio of 3:1 for TWO to occur, however, this needs to be studied further.

At last, it is also important to note that – while theoretically relevant - there is no evidence that the fluctuations in the ratio between R and T wave amplitudes would inevitably lead to adverse clinical outcomes such as TWO and inappropriate shocks. Further experimental work is needed to consolidate the findings presented in this thesis and to determine their clinical relevance.

## **8.4 Proposed further work**

### **8.4.1 Application of the deep learning tool in clinical practice**

I have demonstrated in this thesis, that R:T or T:R ratio – an integral component of the S-ICD sensing mechanism and a major determinant of S-ICD eligibility- is dynamic. This was evident when ECG signals were acquired over much longer durations than the standard S-ICD screening practices. I have also introduced a state-of-the-art deep learning tool that is capable of tracking ECG signals corresponding to S-ICD vectors. I have demonstrated that this tool could be used to track R:T or T:R ratios of S-ICD vectors accurately and efficiently. I have introduced a new term, – favourable ratio time (FRT), to assess and compare S-ICD vectors from the R:T or T:R ratios perspective. However, the FRT cut-off for vector eligibility is not known. In addition -while theoretically relevant- there is no clinical evidence that vectors with worse FRT would inevitably correlate with higher rates of adverse clinical events in the form of TWO and inappropriate shocks. These questions need to be addressed prior to considering applying the proposed deep learning tool in clinical practice for patients (as well as individual vectors) selection for S-ICD therapy.

One way to address these questions, is through a prospective study where patients referred for S-ICD therapy are randomised into two groups; one group receives standard care of S-ICD screening, while the other group receives S-ICD screening through the proposed screening methodology utilising the deep learning tool. This study will likely require a large cohort and a

follow-up period of many years. The proposed end points of the study would include the rates of TWO and inappropriate shocks in both groups.

Furthermore, a retrospective study is a feasible option, where the FRT of patients who have experienced inappropriate S-ICD shock therapy due to TWO are compared to a control group. This could be particularly helpful in determining the cut-off FRT for S-ICD eligibility.

#### **8.4.2 Personalised devices therapy**

Leadless pacemakers and S-ICDs are becoming a more favourable choice to cover for pacing and defibrillator protection indications in comparison to transvenous devices. I have demonstrated in this thesis that, at least theoretically, it is feasible in most patients to concomitantly utilise both devices if a personalised devices therapy approach is adopted. Further work needs to be done before this can be translated into clinical practice.

A prospective study where patients referred for devices therapy are randomised into two groups; one group receives standard of care, where leadless pacemakers' implantation sites in S-ICD patients are decided at the discretion of the operator. The other group receives a more personalised approach, where the effect of pacing at different sites on the R:T ratios as perceived by the S-ICD vectors is examined first in each individual patient before the leadless pacemaker implantation site is determined. This is done in addition to revisiting the S-ICD vector programming choice (primary, alternate, or secondary) if needed. This study will also likely require a large cohort of patients and long-term follow-up. The rates of (pacemaker mediated) TWO and inappropriate shocks can be then compared in both groups.

### **8.5 Summary**

Artificial Intelligence and deep-learning methods can be an invaluable resource to facilitate informed decision making with regards to patient selection for these advanced device therapies as well as optimisation of device programming. Adopting a personalised device therapy approach allows most patients to benefit from these advanced devices therapies without compromising on patients' safety.

S-ICDs and leadless pacemakers may represent the future of cardiac device therapy. They have consistently demonstrated reliable performance and high safety profile while avoiding the



complications associated with the transvenous devices. However, not everyone is deemed suitable for these advanced devices therapy. In addition, inappropriate shock therapy, a common complication associated with S-ICD therapy, is associated with increased morbidity as well as overall mortality.

This work has demonstrated that the understanding of how the ECG signals behave, in different underlying disease processes, in the context of S-ICD, can be further refined. Adopting newer technologies can allow efficient and accurate computation of ECG signal processing. This in turn, can further refine the process of patient selection and management of advanced device therapy.

## Appendix A

### A.1 Publications arising from work in this thesis

#### A.1.1 Abstracts presented

- M Elrefai, C Menexi, P Roberts, Leadless pacemakers: where is the device? EP Europace, Volume 23, Issue Supplement\_3, May 2021, euab116.375, <https://doi.org/10.1093/europace/euab116.375>
- C Menexi, M Elrefai, M Abouelasaad, P Roberts, Leadless pacemakers: does location matter? EP Europace, Volume 23, Issue Supplement\_3, May 2021, euab116.376, <https://doi.org/10.1093/europace/euab116.376>
- Abstract 10370: Personalised Approach is the Key When it Comes to Pacing a Patient with an S-ICD. Circulation. 2021;144: A10370. [https://www.ahajournals.org/doi/10.1161/circ.144.suppl\\_1.10370](https://www.ahajournals.org/doi/10.1161/circ.144.suppl_1.10370)
- Abstract 9203: Role of Artificial Intelligence and Utilisation of Deep Learning Methods in Screening for Subcutaneous Implantable Cardioverter Defibrillator Eligibility. Circulation. 2021;144: A9203. [https://www.ahajournals.org/doi/10.1161/circ.144.suppl\\_1.9203](https://www.ahajournals.org/doi/10.1161/circ.144.suppl_1.9203)
- Eligibility for the subcutaneous implantable cardiac defibrillator therapy using standard screening practice – our experience. European Journal of Arrhythmia & Electrophysiology. 2021;7(Suppl. 1): abstr67. <https://www.touchcardio.com/devices/journal-articles/67-eligibility-for-the-subcutaneous-implantable-cardiac-defibrillator-therapy-using-standard-screening-practice-our-experience/>
- M Elrefai, M Abouelasaad, I Conibear, B Wiles, A Dunn, S Coniglio, A Zemkoho, P Roberts, The use of artificial intelligence and deep learning methods in subcutaneous implantable cardioverter defibrillator screening to optimise selection in special patient populations, EP Europace, Volume 24, Issue Supplement\_1, May 2022, euac053.448, <https://doi.org/10.1093/europace/euac053.448>
- M Elrefai, M Abouelasaad, A Dunn, S Coniglio, A Zemkoho, B Wiles, P Roberts, Eligibility for subcutaneous implantable cardiac defibrillator utilising artificial intelligence and deep learning methods for prolonged screening: where is the cut-off, EP Europace, Volume 24, Issue Supplement\_1, May 2022, euac053.447, <https://doi.org/10.1093/europace/euac053.447>

### A.1.2 Peer-reviewed published manuscripts

- Anthony J. Dunn, Mohamed H. ElRefai, Paul R. Roberts, Stefano Coniglio, Benedict M. Wiles, Alain B. Zemkoho, Deep learning methods for screening patients' S-ICD implantation eligibility, *Artificial Intelligence in Medicine*, Volume 119,2021,102139, ISSN 0933-3657, <https://doi.org/10.1016/j.artmed.2021.102139>.
- ElRefai, M., Abouelasaad, M., Menexi, C. et al. Impact of right ventricular pacing site on the subcutaneous ICD sensing—a step towards personalised device therapy? *J Interv Card Electrophysiol* (2022). <https://doi.org/10.1007/s10840-022-01218-9>
- ElRefai, M., Abouelasaad, M., Wiles, B.M. et al. Deep learning-based insights on T:R ratio behaviour during prolonged screening for S-ICD eligibility. *J Interv Card Electrophysiol* (2022). <https://doi.org/10.1007/s10840-022-01245-6>
- ElRefai M, Menexi C, Abouelasaad M, Tsoi V, Roberts PR. Insights on subcutaneous implantable cardiac defibrillator eligibility using standard screening practices. *J Interv Card Electrophysiol*. 2022 Dec 16. doi: 10.1007/s10840-022-01453-0. Epub ahead of print. PMID: 36525169.
- ElRefai M, Abouelasaad M, Wiles BM, Dunn AJ, Coniglio S, Zemkoho AB, Morgan JM, Roberts PR. Role of deep learning methods in screening for subcutaneous implantable cardioverter defibrillator in heart failure. *Ann Noninvasive Electrocardiol*. 2022 Dec 16:e13028. doi: 10.1111/anec.13028. Epub ahead of print. PMID: 36524869.

## **Appendix B**

### **B.1 Research Governance, Monitoring, Ethics and Research and Development (R&D) approval**

All the studies in this thesis were performed with approval from the relevant research authorities. All studies were conducted in accordance with the Research Governance Framework for Health and Social Care (2005), Good Clinical Practice and their relevant updates.

Adverse events were recorded in accordance with research related adverse event reporting policy. All studies were monitored and audited in accordance with standard procedures. All the studies related documents were made available on request for monitoring and audit by the sponsor, relevant Research and Ethics Committees (REC) or other licensing bodies.

#### **B.1.1 Approaching Participants:**

Participants were directly approached by an appropriately trained member of the research team. All the participants were directly approached at outpatient departments when they came in for routine follow up or when they were admitted to the hospital for other causes. All the studies were introduced through patient information sheets and verbal explanations. Participants did not receive any payment for taking part.

Efforts were made to maximise the duration of time the participants had available to decide on whether to take part in the research. To this extent, in some instances, I have elected to send patient information sheets to patients prior to attending at outpatient departments.

#### **B.1.2 Data handling and record keeping**

Data was collected and retained in accordance with the Data Protection Act 1998 and updates. All documents (paper and electronic) were retained in a secure location during and after the studies have finished. All essential documents and source data, including any medical records where the

entries related to the research have been made will be retained for a minimum period of 3 years following the end of the corresponding study.

Each participant's name, date of birth, hospital number and the assigned study number were kept on the investigator's password protected NHS desktop computer.

## Bibliography

1. Mensah GA, Roth GA, Fuster V. The Global Burden of Cardiovascular Diseases and Risk Factors: 2020 and Beyond. *J Am Coll Cardiol.* 2019;74(20):2529-2532. doi:10.1016/j.jacc.2019.10.009
2. Berdowski J, Berg RA, Tijssen JGP, Koster RW. Global incidences of out-of-hospital cardiac arrest and survival rates: Systematic review of 67 prospective studies. *Resuscitation.* 2010;81(11):1479-1487. doi:10.1016/j.resuscitation.2010.08.006
3. Adabag AS, Luepker R v., Roger VL, Gersh BJ. Sudden cardiac death: Epidemiology and risk factors. *Nat Rev Cardiol.* 2010;7(4):216-225. doi:10.1038/nrcardio.2010.3
4. R M. Global public health problem of sudden cardiac death. *J Electrocardiol.* 2007;40(6 Suppl). doi:10.1016/J.JELECTROCARD.2007.06.023
5. de Vreede-Swagemakers JJM, Gorgels APM, Dubois-Arbouw WI, et al. Out-of-hospital cardiac arrest in the 1990s: A population-based study in the Maastricht area on incidence, characteristics and survival. *J Am Coll Cardiol.* 1997;30(6):1500-1505. doi:10.1016/S0735-1097(97)00355-0
6. Cupples, L. A., Gagnon, D. R. & Kannel, W. B. Long- and short-term risk of sudden coronary death. *Circulation* 85 (1 Suppl.), I11–I18 (1992).
7. Jouven, X. et al. Diabetes, glucose level, and risk of sudden cardiac death. *Eur. Heart J.* 26, 2142–2147 (2005).
8. Goldenberg, I. et al. Current smoking, smoking cessation, and the risk of sudden cardiac death in patients with coronary artery disease. *Arch. Intern. Med.* 163, 2301–2305 (2003).
9. Jouven, X., Desnos, M., Guerot, C. & Ducimetière, P. Predicting sudden death in the population: the Paris Prospective Study I. *Circulation* 99, 1978–1983 (1999).
10. Myerburg, R. & Castellanos, A. in *Braunwald's Heart Disease. A Textbook of Cardiovascular Medicine* 8th edn (eds Libby, P., Bonow, R. O., Mann, D. L. & Zipes, D. P.) 933–974 (Saunders, Philadelphia, 2007).
11. Kannel, W. B., Plehn, J. F. & Cupples, L. A. Cardiac failure and sudden death in the Framingham study. *Am. Heart J.* 115, 869–875 (1988).

12. J B, RA B, JG T, RW K. Global incidences of out-of-hospital cardiac arrest and survival rates: Systematic review of 67 prospective studies. *Resuscitation*. 2010;81(11):1479-1487. doi:10.1016/J.RESUSCITATION.2010.08.006
13. Pell JP, Sirel JM, Marsden AK, et al. Presentation, management, and outcome of out of hospital cardiopulmonary arrest: comparison by underlying aetiology. *Heart* 2003;89:839-42.
14. Berdowski J, Berg RA, Tijssen JG, et al. Global incidences of out-of-hospital cardiac arrest and survival rates: Systematic review of 67 prospective studies. *Resuscitation* 2010;81:1479-87.
15. Hazinski, M. F. et al. Lay rescuer automated external defibrillator ("public access defibrillation") programs: lessons learned from an international multicenter trial: Advisory statement from the American Heart Association Emergency Cardiovascular Committ.
16. Priori SG, Blomström-Lundqvist C, Mazzanti A, et al. 2015 ESC Guidelines for the management of patients with ventricular arrhythmias and the prevention of sudden cardiac death: The Task Force for the Management of Patients with Ventricular Arrhythmias and.
17. Bardy GH, Lee KL, Mark DB, et al. Amiodarone or an implantable cardioverter-defibrillator for congestive heart failure. *The New England journal of medicine* 2005;352:225-37.
18. Moss AJ, Zareba W, Hall WJ, et al. Prophylactic implantation of a defibrillator in patients with myocardial infarction and reduced ejection fraction. *The New England journal of medicine* 2002;346:877-83.
19. Kuck KH, Cappato R, Siebels J, et al. Randomized comparison of antiarrhythmic drug therapy with implantable defibrillators in patients resuscitated from cardiac arrest : the Cardiac Arrest Study Hamburg (CASH). *Circulation* 2000;102:748-54.
20. Connolly SJ, Gent M, Roberts RS, et al. Canadian implantable defibrillator study (CIDS) : a randomized trial of the implantable cardioverter defibrillator against amiodarone. *Circulation* 2000;101:1297-302.
21. Kleeman T, Becker R, Doenges K et al. Annual rate of transvenous defibrillation lead defects in implantable cardioverter defibrillators over a period of >10 years. *Circulation* 2007;115:2474-80.

22. Kirkfeldt RE, Johansen JB, Nohr EA, Jorgensen OD, Nielsen JC. Complications after cardiac implantable electronic device implantations: an analysis of a complete, nationwide cohort in Denmark. *Eur Heart J*. 2014;35(18):1186-1194. doi:10.1093/EURHEARTJ/EHT511
23. Bardy GH, Smith WM, Hood MA, et al. An entirely subcutaneous implantable cardioverter-defibrillator. *N Engl J Med* 2010;363:36-44.
24. Grace AA, Hood MA, Smith WM, et al. Evaluation of four distinct subcutaneous implantable defibrillator (S-ICD) lead systems in humans. *Heart Rhythm* 2006;Vol. 3:S128-S9.
25. Burke MC, Gold MR, Knight BP et al. Safety and Efficacy of the Totally Subcutaneous Implantable Defibrillator: 2-Year Results From a Pooled Analysis of the IDE Study and EFFORTLESS Registry. *Journal of the American College of Cardiology* 2015;65:1605-15.
26. Gold MR, Theuns DA, Knight BP, et al. Head-to-head comparison of arrhythmia discrimination performance of subcutaneous and transvenous ICD arrhythmia detection algorithms: The START study. *J Cardiovasc Electrophysiol*. 2012;23(4):359-366. doi:10.1111/j.1540-8167.2011.02199.x
27. Theuns DAMJ, Brouwer TF, Jones PW, et al. Prospective blinded evaluation of a novel sensing methodology designed to reduce inappropriate shocks by the subcutaneous implantable cardioverter-defibrillator. *Heart Rhythm*. 2018;15(10):1515-1522. doi:10.1016/J.HRTHM.2018.05.011
28. Al-Ghamdi B. Subcutaneous Implantable Cardioverter Defibrillators: An Overview of Implantation Techniques and Clinical Outcomes. *Curr Cardiol Rev*. 2019;15(1):38. doi:10.2174/1573403X14666180716164740
29. Chang SC, Patton KK, Robinson MR, Poole JE, Prutkin JM. Subcutaneous ICD screening with the Boston Scientific ZOOM programmer versus a 12-lead ECG machine. *Pacing and Clinical Electrophysiology*. 2018;41(5):511-516. doi:10.1111/PACE.13314
30. Daubert JP, Zareba W, Cannom DS, et al. Inappropriate implantable cardioverter-defibrillator shocks in MADIT II: frequency, mechanisms, predictors and survival impact. *JACC* 2008;51:1357-65. No Title.
31. Kooiman KM, Knops RE, Olde Nordkamp L, Wilde AAM, de Groot JR. Inappropriate subcutaneous implantable cardioverter-defibrillator shocks due to T-wave oversensing can



- be prevented: implications for management. *Heart Rhythm*. 2014;11(3):426-434.  
doi:10.1016/J.HRTHM.2013.12.007
32. Francia P, Adduci C, Palano F, et al. Eligibility for the Subcutaneous Implantable Cardioverter-Defibrillator in Patients With Hypertrophic Cardiomyopathy. *J Cardiovasc Electrophysiol*. 2015;26(8):893-899. doi:10.1111/JCE.12714
  33. Afzal MR, Evenson C, Badin A, et al. Role of exercise electrocardiogram to screen for T-wave oversensing after implantation of subcutaneous implantable cardioverter-defibrillator. *Heart Rhythm*. 2017;14(10):1436-1439. doi:10.1016/J.HRTHM.2017.06.022
  34. Srinivasan NT, Patel KH, Qamar K, et al. Disease Severity and Exercise Testing Reduce Subcutaneous Implantable Cardioverter-Defibrillator Left Sternal ECG Screening Success in Hypertrophic Cardiomyopathy. *Circ Arrhythm Electrophysiol*. 2017;10(4).  
doi:10.1161/CIRCEP.117.004801
  35. Dayal N, Jacon P, Venier S, Dugenet F, Carabelli A, Defaye P. P910Insight into screening results and post-implantation exercise testing in recipients of a subcutaneous Implantable cardioverter defibrillator. *EP Europace*. 2018;20(suppl\_1):i175-i175.  
doi:10.1093/EUROPACE/EUY015.511
  36. Tachibana M, Nishii N, Morita H, et al. Exercise stress test reveals ineligibility for subcutaneous implantable cardioverter defibrillator in patients with Brugada syndrome. *J Cardiovasc Electrophysiol*. 2017;28(12):1454-1459. doi:10.1111/JCE.13315
  37. Garside H, Leyva F, Hudsmith L, Marshall H, de Bono J. Eligibility for subcutaneous implantable cardioverter defibrillators in the adult congenital heart disease population. *PACE - Pacing and Clinical Electrophysiology*. 2019;42(1):65-70. doi:10.1111/pace.13537
  38. Świerżyńska E, Sterliński M, Syska P, Sadowski K, Szumowski Ł. Use of an exercise test to enhance sensing vector assessment and prevent inadequate subcutaneous implantable cardioverter-defibrillator discharges. *J Electrocardiol*. 2021;67:73-76.  
doi:10.1016/J.JELECTROCARD.2021.05.013
  39. Aydin A, Hartel F, Schluter M, et al. Shock Efficacy of Subcutaneous Implantable Cardioverter-Defibrillator for Prevention of Sudden Cardiac Death: Initial Multicenter Experience. *Circulation: Arrhythmia and Electrophysiology* 2012;5:913-9.

40. Jarman JWE, Lascelles K, Wong T, et al. Clinical experience of entirely subcutaneous implantable cardioverter-defibrillators in children and adults: cause for caution. *European Heart Journal* 2012;33:1351-9.
41. Dabiri Abkenari L, Theuns DA, Valk SD, et al. Clinical experience with a novel subcutaneous implantable defibrillator system in a single center. *Clin Res Cardiol* 2011;100:737-44.
42. Olde Nordkamp LRA, Dabiri Abkenari L, Boersma LVA, et al. The Entirely Subcutaneous Implantable Cardioverter-Defibrillator. *Journal of the American College of Cardiology* 2012;60:1933.
43. Burke MC, Gold MR, Knight BP et al. Safety and Efficacy of the Totally Subcutaneous Implantable Defibrillator: 2-Year Results From a Pooled Analysis of the IDE Study and EFFORTLESS Registry. *Journal of the American College of Cardiology* 2015;65:1605-15.
44. Bardy GH, Smith WM, Hood MA, et al. An entirely subcutaneous implantable cardioverter-defibrillator. *N Engl J Med* 2010;363:36-44.
45. Kamp NJ, Al-Khatib SM. The subcutaneous implantable cardioverter-defibrillator in review. *Am Heart J*. 2019;217:131-139. doi:10.1016/j.ahj.2019.08.010
46. Knops RE, Nordkamp LRAO, Delnoy PPHM, et al. Subcutaneous or Transvenous Defibrillator Therapy. <https://doi.org/10.1056/NEJMoa1915932>. 2020;383(6):526-536. doi:10.1056/NEJMoa1915932
47. Gold MR, Lambiase PD, El-Chami MF, et al. Primary Results From the Understanding Outcomes With the S-ICD in Primary Prevention Patients With Low Ejection Fraction (UNTOUCHED) Trial. *Circulation*. 2021;143(1):7-17. doi:10.1161/CIRCULATIONAHA.120.048728
48. Al-Khatib SM, Stevenson WG, Ackerman MJ, et al. *2017 AHA/ACC/HRS Guideline for Management of Patients With Ventricular Arrhythmias and the Prevention of Sudden Cardiac Death: Executive Summary*. Vol 138.; 2018. doi:10.1161/CIR.0000000000000548
49. Quast AFBE, Brouwer TF, Tjong FVY, Wilde AAM, Knops RE. Clinical parameters to optimize patient selection for subcutaneous and transvenous implantable defibrillator therapy. *PACE - Pacing and Clinical Electrophysiology*. 2018;41(8):990-995. doi:10.1111/pace.13411
50. Chaudhry SP, Stewart GC. Advanced Heart Failure: Prevalence, Natural History, and Prognosis. *Heart Fail Clin*. 2016;12(3):323-333. doi:10.1016/j.hfc.2016.03.001

51. Ponikowski P, Voors A. 2016 Esc guidelines for the diagnosis and treatment of acute and chronic heart failure: The Task Force for the diagnosis and treatment of acute and chronic heart failure of the European society of cardiology (ESC): Developed with the special contribution . *Russian Journal of Cardiology*. 2017;141(1):7-81. doi:10.15829/1560-4071-2017-1-7-81
52. Ayyadurai P, Alkhawam H, Saad M, et al. An update on the CardioMEMS pulmonary artery pressure sensor: <https://doi.org/10.1177/1753944719826826>. 2019;13. doi:10.1177/1753944719826826
53. AP M, U D, G F, et al. EURObservational Research Programme: the Heart Failure Pilot Survey (ESC-HF Pilot). *Eur J Heart Fail*. 2010;12(10):1076-1084. doi:10.1093/EURJHF/HFQ154
54. Knops RE, Olde Nordkamp LRA, Delnoy PPHM, et al. Subcutaneous or Transvenous Defibrillator Therapy. *New England Journal of Medicine*. 2020;383(6):526-536. doi:10.1056/nejmoa1915932
55. S G, G C, M B, R G. Long-Term Outcomes Following Transvenous Lead Extraction. *Pacing Clin Electrophysiol*. 2016;39(4):345-351. doi:10.1111/PACE.12812
56. Boersma L, Barr C, Knops R, et al. Implant and Midterm Outcomes of the Subcutaneous Implantable Cardioverter-Defibrillator Registry: The EFFORTLESS Study. *J Am Coll Cardiol*. 2017;70(7):830-841. doi:10.1016/j.jacc.2017.06.040
57. Kamp NJ, Al-Khatib SM. The subcutaneous implantable cardioverter-defibrillator in review. *Am Heart J*. 2019;217:131-139. doi:10.1016/j.ahj.2019.08.010
58. Madias JE. QTc interval in patients with changing edematous states: Implications on interpreting repeat QTc interval measurements in patients with anasarca of varying etiology and those undergoing hemodialysis. *PACE - Pacing and Clinical Electrophysiology*. 2005;28(1):54-61. doi:10.1111/j.1540-8159.2005.09384.x
59. Madias JE, Bazaz R, Agarwal H, Win M, Medepalli L. Anasarca-mediated attenuation of the amplitude of electrocardiogram complexes: A description of a heretofore unrecognized phenomenon. *J Am Coll Cardiol*. 2001;38(3):756-764. doi:10.1016/S0735-1097(01)01429-2
60. Al-Zaiti SS, Runco KN, Carey MG. Increased T wave complexity can indicate subclinical myocardial ischemia in asymptomatic adults. *J Electrocardiol*. 2011;44(6):684-688. doi:10.1016/j.jelectrocard.2011.07.017

61. Assanelli D, di Castelnuovo A, Rago L, et al. T-wave axis deviation and left ventricular hypertrophy interaction in diabetes and hypertension. *J Electrocardiol*. 2013;46(6):487-491. doi:10.1016/j.jelectrocard.2013.08.002
62. Hasan MA, Abbott D, Baumert M. Relation between beat-to-beat QT interval variability and T-wave amplitude in healthy subjects. *Ann Noninvasive Electrocardiol* 2012;17(3):195-203.
63. Walker BD, Krahn AD, Klein GJ, Skanes AC, Yee R. Drug induced QT prolongation: Lessons from congenital and acquired long QT syndromes. *Curr Drug Targets Cardiovasc Haematol Disord*. 2003;3(4):327-335. doi:10.2174/1568006033481393
64. Fosbøl EL, Seibæk M, Brendorp B, Torp-Pedersen C, Køber L. Prognostic Importance of Change in QRS Duration Over Time Associated With Left Ventricular Dysfunction in Patients With Congestive Heart Failure: The DIAMOND Study. *J Card Fail*. 2008;14(10):850-855. doi:10.1016/J.CARDFAIL.2008.07.238
65. Baumgartner H, de Backer J, Babu-Narayan S v., et al. 2020 ESC Guidelines for the management of adult congenital heart disease. *Eur Heart J*. 2021;42(6):563-645. doi:10.1093/eurheartj/ehaa554
66. Koyak Z, Harris L, de Groot JR, et al. Sudden cardiac death in adult congenital heart disease. *Circulation*. 2012;126(16):1944-1954. doi:10.1161/CIRCULATIONAHA.112.104786
67. Lundqvist CB, Potpara TS, Malmborg H. Supraventricular Arrhythmias in Patients with Adult Congenital Heart Disease. *Arrhythm Electrophysiol Rev*. 2017;6(2):42. doi:10.15420/AER.2016:29:3
68. Vehmeijer JT, Brouwer TF, Limpens J, et al. Implantable cardioverter-defibrillators in adults with congenital heart disease: A systematic review and meta-analysis. *Eur Heart J*. 2016;37(18):1439-1448. doi:10.1093/eurheartj/ehv735
69. D'Souza BA, Epstein AE, Garcia FC, et al. Outcomes in Patients With Congenital Heart Disease Receiving the Subcutaneous Implantable-Cardioverter Defibrillator: Results From a Pooled Analysis From the IDE Study and the EFFORTLESS S-ICD Registry. *JACC Clin Electrophysiol*. 2016;2(5):615-622. doi:10.1016/j.jacep.2016.02.008
70. P A, J O, O C, et al. The Role of Conventional and Right-Sided ECG Screening for Subcutaneous ICD in a Tetralogy of Fallot Population. *Pacing Clin Electrophysiol*. 2017;40(2):145-153. doi:10.1111/PACE.13017

71. Wang L, Javadekar N, Rajagopalan A, et al. Eligibility for subcutaneous implantable cardioverter-defibrillator in congenital heart disease. *Heart Rhythm*. 2020;17(5):860-869. doi:10.1016/j.hrthm.2020.01.016
72. Sen-Chowdhry S, Jacoby D, Moon JC, McKenna WJ. Update on hypertrophic cardiomyopathy and a guide to the guidelines. *Nat Rev Cardiol*. 2016;13(11):651-675. doi:10.1038/nrcardio.2016.140
73. O'Mahony C, Jichi F, Pavlou M, et al. A novel clinical risk prediction model for sudden cardiac death in hypertrophic cardiomyopathy (HCM Risk-SCD). *Eur Heart J*. 2014;35(30):2010-2020. doi:10.1093/eurheartj/eh439
74. Zamorano JL, Anastasakis A, Borger MA, et al. 2014 ESC guidelines on diagnosis and management of hypertrophic cardiomyopathy: The task force for the diagnosis and management of hypertrophic cardiomyopathy of the European Society of Cardiology (ESC). *Eur Heart J*. 2014;35(39):2733-2779. doi:10.1093/eurheartj/ehu284
75. Lambiase PD, Eckardt L, Theuns DA, et al. Evaluation of subcutaneous implantable cardioverter-defibrillator performance in patients with ion channelopathies from the EFFORTLESS cohort and comparison with a meta-analysis of transvenous ICD outcomes. *Heart Rhythm O2*. 2020;1(5):326. doi:10.1016/J.HROO.2020.10.002
76. Lambiase PD, Gold MR, Hood M, et al. Evaluation of subcutaneous ICD early performance in hypertrophic cardiomyopathy from the pooled EFFORTLESS and IDE cohorts. *Heart Rhythm*. 2016;13(5):1066-1074. doi:10.1016/j.hrthm.2016.01.001
77. LRA ON, JLF W, KM K, et al. Which patients are not suitable for a subcutaneous ICD: incidence and predictors of failed QRS-T-wave morphology screening. *J Cardiovasc Electrophysiol*. 2014;25(5):494-499. doi:10.1111/JCE.12343
78. Maurizi N, Olivotto I, Olde Nordkamp LRA, et al. Prevalence of subcutaneous implantable cardioverter-defibrillator candidacy based on template ECG screening in patients with hypertrophic cardiomyopathy. *Heart Rhythm*. 2016;13(2):457-463. doi:10.1016/j.hrthm.2015.09.007
79. Francia P, Ziacchi M, de Filippo P, et al. Subcutaneous implantable cardioverter defibrillator eligibility according to a novel automated screening tool and agreement with the standard manual electrocardiographic morphology tool. *Journal of Interventional Cardiac Electrophysiology*. 2018;52(1):61-67. doi:10.1007/s10840-018-0326-2

80. NT S, KH P, K Q, et al. Disease Severity and Exercise Testing Reduce Subcutaneous Implantable Cardioverter-Defibrillator Left Sternal ECG Screening Success in Hypertrophic Cardiomyopathy. *Circ Arrhythm Electrophysiol.* 2017;10(4). doi:10.1161/CIRCEP.117.004801
81. Srinivasan NT, Patel KH, Qamar K, et al. Disease Severity and Exercise Testing Reduce Subcutaneous Implantable Cardioverter-Defibrillator Left Sternal ECG Screening Success in Hypertrophic Cardiomyopathy. *Circ Arrhythm Electrophysiol.* 2017;10(4):1-10. doi:10.1161/CIRCEP.117.004801
82. Lambiase PD, Theuns DA, Murgatroyd F, et al. Subcutaneous implantable cardioverter-defibrillators: long-term results of the EFFORTLESS study. *Eur Heart J.* 2022;43(21):2037-2050. doi:10.1093/EURHEARTJ/EHAB921
83. McKenna WJ, Borggrefe M, England D, Deanfield J, Oakley CM, Goodwin JF. The natural history of left ventricular hypertrophy in hypertrophic cardiomyopathy: An electrocardiographic study. *Circulation.* 1982;66(6 I):1233-1240. doi:10.1161/01.CIR.66.6.1233
84. Zorzi A, Elmaghawry M, Rigato I, et al. Exercise-induced normalization of right precordial negative T waves in arrhythmogenic right ventricular cardiomyopathy. *American Journal of Cardiology.* 2013;112(3):411-415. doi:10.1016/j.amjcard.2013.03.048
85. Udo EO, Zuithoff NPA, Hemel NM, van Cock CC, de Hendriks T, Doevendans PA et al. Incidence and predictors of short- and long-term complications in pacemaker therapy: the FOLLOWPACE study. *Heart Rhythm* 2012;9:728–35.
86. Kirkfeldt RE, Johansen JB, Nohr EA, Jørgensen OD, Nielsen JC. Complications after cardiac implantable electronic device implantations: an analysis of a complete, nationwide cohort in Denmark. *Eur Heart J* 2014;35:1186–94.
87. Hauser RG, Hayes DL, Kallinen LM, Cannom DS, Epstein AE, Almquist AK et al. Clinical experience with pacemaker pulse generators and transvenous leads: an 8-year prospective multicenter study. *Heart Rhythm* 2007;4:154–60.
88. (Reddy VY, Knops RE, Sperzel J, Miller MA, Petru J, Simon J, et al. Permanent leadless cardiac pacing: results of the LEADLESS trial. *Circulation.* 2014;129(14):1466–71. <https://doi.org/10.1161/CIRCULATIONAHA.113.006987>).

89. Steinwender C, Lercher P, Schukro C, et al. State of the art: leadless ventricular pacing. *Journal of Interventional Cardiac Electrophysiology*. Published online 2019:27-37. doi:10.1007/s10840-019-00680-2
90. Bhatia N, El-Chami M. Leadless pacemakers: A contemporary review. *Journal of Geriatric Cardiology*. 2018;15(4):249-253. doi:10.11909/j.issn.1671-5411.2018.04.002
91. Reddy VY, Knops RE, Sperzel J, et al. Permanent leadless cardiac pacing: Results of the LEADLESS trial. *Circulation*. 2014;129(14):1466-1471. doi:10.1161/CIRCULATIONAHA.113.006987
92. Reddy VY, Exner D v., Cantillon DJ, et al. Percutaneous implantation of an entirely intracardiac leadless pacemaker. *New England Journal of Medicine*. 2015;373(12):1125-1135. doi:10.1056/NEJMoa1507192
93. A worldwide experience of the management of battery failures and chronic device retrieval of the Nanostim leadless pacemaker - Heart Rhythm. Accessed March 8, 2020. [https://www.heartrhythmjournal.com/article/S1547-5271\(17\)30846-9/fulltext](https://www.heartrhythmjournal.com/article/S1547-5271(17)30846-9/fulltext)
94. Reynolds D, Duray GZ, Omar R, et al. A Leadless Intracardiac Transcatheter Pacing System. *New England Journal of Medicine*. 2016;374(6):533-541. doi:10.1056/NEJMoa1511643
95. El-Chami MF, Al-Samadi F, Clementy N, et al. Updated performance of the Micra transcatheter pacemaker in the real-world setting: A comparison to the investigational study and a transvenous historical control. *Heart Rhythm*. 2018;15(12):1800-1807. doi:10.1016/j.hrthm.2018.08.005
96. Steinwender C, Lercher P, Schukro C, et al. State of the art: leadless ventricular pacing: A national expert consensus of the Austrian Society of Cardiology. *Journal of Interventional Cardiac Electrophysiology*. 2020;57(1):27-37. doi:10.1007/s10840-019-00680-2
97. Kempa M, Mitkowski P, Kowalski O, Sterliński M, Przybylski A, Kaźmierczak J. Expert opinion of the Working Group on Leadless Pacing appointed by the National Consultant in Cardiology and the Board of the Heart Rhythm Section of the Polish Cardiac Society. *Kardiol Pol*. Published online April 29, 2021. doi:10.33963/kp.15982
98. Boveda S, Marijon E, Lenarczyk R, et al. Factors influencing the use of leadless or transvenous pacemakers: results of the European Heart Rhythm Association Prospective Survey. *EP Europace*. Published online 2020:1-7. doi:10.1093/europace/euz357

99. Ip JE, Wu MS, Kennel PJ, et al. Eligibility of Pacemaker Patients for Subcutaneous Implantable Cardioverter Defibrillators. *J Cardiovasc Electrophysiol*. 2017;28(5):544-548. doi:10.1111/jce.13182
100. Friedrich S, Groß S, Kö Nig IR, et al. Applications of artificial intelligence/machine learning approaches in cardiovascular medicine: a systematic review with recommendations. *European Heart Journal - Digital Health*. 2021;2(3):424-436. doi:10.1093/EHJDH/ZTAB054
101. Machine learning, explained | MIT Sloan. Accessed January 4, 2023. <https://mitsloan.mit.edu/ideas-made-to-matter/machine-learning-explained>
102. Bahri M, Ashino R, Vaillancourt R. Convolution theorems for quaternion fourier transform: Properties and applications. *Abstract and Applied Analysis*. 2013;2013. doi:10.1155/2013/162769
103. Hempstead EL. Bernard Gersh and Paul Friedman on the future of artificial intelligence in cardiology. *Eur Heart J*. Published online June 8, 2022. doi:10.1093/EURHEARTJ/EHAC269
104. Fan X, Yao Q, Cai Y, Miao F, Sun F, Li Y. Multiscaled Fusion of Deep Convolutional Neural Networks for Screening Atrial Fibrillation from Single Lead Short ECG Recordings. *IEEE J Biomed Health Inform*. 2018;22(6):1744-1753. doi:10.1109/JBHI.2018.2858789
105. Kiranyaz S, Ince T, Gabbouj M. Real-Time Patient-Specific ECG Classification by 1-D Convolutional Neural Networks. *IEEE Trans Biomed Eng*. 2016;63(3):664-675. doi:10.1109/TBME.2015.2468589
106. Pourbabaee B, Roshtkhari MJ, Khorasani K. Deep Convolutional Neural Networks and Learning ECG Features for Screening Paroxysmal Atrial Fibrillation Patients. *IEEE Trans Syst Man Cybern Syst*. 2018;48(12):2095-2104. doi:10.1109/TSMC.2017.2705582
107. Zhang J, Liu A, Gao M, Chen X, Zhang X, Chen X. ECG-based multi-class arrhythmia detection using spatio-temporal attention-based convolutional recurrent neural network. *Artif Intell Med*. 2020;106:101856. doi:10.1016/J.ARTMED.2020.101856
108. Lih OS, Jahmunah V, San TR, et al. Comprehensive electrocardiographic diagnosis based on deep learning. *Artif Intell Med*. 2020;103:101789. doi:10.1016/J.ARTMED.2019.101789
109. Liu W, Zhang M, Zhang Y, et al. Real-Time Multilead Convolutional Neural Network for Myocardial Infarction Detection. *IEEE J Biomed Health Inform*. 2018;22(5):1434-1444. doi:10.1109/JBHI.2017.2771768



110. Miao F, Wen B, Hu Z, et al. Continuous blood pressure measurement from one-channel electrocardiogram signal using deep-learning techniques. *Artif Intell Med*. 2020;108:101919. doi:10.1016/J.ARTMED.2020.101919
111. Sangaiah AK, Arumugam M, Bian G bin. An intelligent learning approach for improving ECG signal classification and arrhythmia analysis. *Artif Intell Med*. 2020;103:101788. doi:10.1016/J.ARTMED.2019.101788
112. TjongFVY, BrouwerTF, KooimanKM, SmedingL, KoopB, SoltisB, ShurosA, WildeAAM, BurkeMC, KnopsRE (2016) Communicating Antitachycardia pacing-enabled leadless pacemaker and subcutaneous implantable defibrillator. *J Am Coll Cardiol* 67(15):1865–1866.
113. Tjong FVY, Koop BE. The modular cardiac rhythm management system: the EMPOWER leadless pacemaker and the EMBLEM subcutaneous ICD. *Herzschrittmachertherapie und Elektrophysiologie*. 2018;29(4):355-361. doi:10.1007/s00399-018-0602-y
114. Effectiveness of the EMPOWER™ Modular Pacing System and EMBLEM™ Subcutaneous ICD to Communicate Antitachycardia Pacing - Full Text View - ClinicalTrials.gov. Accessed June 10, 2022. <https://clinicaltrials.gov/ct2/show/NCT04798768>
115. Maurizi N, Olivotto I, Olde Nordkamp LRA, et al. Prevalence of subcutaneous implantable cardioverter-defibrillator candidacy based on template ECG screening in patients with hypertrophic cardiomyopathy. *Heart Rhythm*. 2016;13(2):457-463. doi:10.1016/J.HRTHM.2015.09.007
116. Srinivasan NT, Patel KH, Qamar K, et al. Disease Severity and Exercise Testing Reduce Subcutaneous Implantable Cardioverter-Defibrillator Left Sternal ECG Screening Success in Hypertrophic Cardiomyopathy. *Circ Arrhythm Electrophysiol*. 2017;10(4). doi:10.1161/CIRCEP.117.004801
117. Francia P, Ziacchi M, de Filippo P, et al. Subcutaneous implantable cardioverter defibrillator eligibility according to a novel automated screening tool and agreement with the standard manual electrocardiographic morphology tool. *Journal of Interventional Cardiac Electrophysiology* 2018 52:1. 2018;52(1):61-67. doi:10.1007/S10840-018-0326-2
118. Groh CA, Sharma S, Pelchovitz DJ, et al. Use of an electrocardiographic screening tool to determine candidacy for a subcutaneous implantable cardioverter-defibrillator. *Heart Rhythm*. 2014;11(8):1361-1366. doi:10.1016/J.HRTHM.2014.04.025

119. Rudic B, Tulumen ; E, Fastenrath ; F, et al. P917Evaluation of a new automated screening tool for the assessment of the eligibility for a subcutaneous implantable-cardioverter defibrillator. *EP Europace*. 2018;20(suppl\_1):i177-i178. doi:10.1093/EUROPACE/EUY015.518
120. Randles DA, Hawkins NM, Shaw M, Patwala AY, Pettit SJ, Wright DJ. How many patients fulfil the surface electrocardiogram criteria for subcutaneous implantable cardioverter-defibrillator implantation? *EP Europace*. 2014;16(7):1015-1021. doi:10.1093/EUROPACE/EUT370
121. Olde Nordkamp LRA, Warnars JLF, Kooiman KM, et al. Which Patients Are Not Suitable for a Subcutaneous ICD: Incidence and Predictors of Failed QRS-T-Wave Morphology Screening. *J Cardiovasc Electrophysiol*. 2014;25(5):494-499. doi:10.1111/JCE.12343
122. Alonso P, Osca J, Cano O, et al. The Role of Conventional and Right-Sided ECG Screening for Subcutaneous ICD in a Tetralogy of Fallot Population. *Pacing Clin Electrophysiol*. 2017;40(2):145-153. doi:10.1111/PACE.13017
123. Fan X, Yao Q, Cai Y, Miao F, Sun F, Li Y. Multiscaled Fusion of Deep Convolutional Neural Networks for Screening Atrial Fibrillation from Single Lead Short ECG Recordings. *IEEE J Biomed Health Inform*. 2018;22(6):1744-1753. doi:10.1109/JBHI.2018.2858789
124. Pourbabaee B, Roshtkhari MJ, Khorasani K. Deep Convolutional Neural Networks and Learning ECG Features for Screening Paroxysmal Atrial Fibrillation Patients. *IEEE Trans Syst Man Cybern Syst*. 2018;48(12):2095-2104. doi:10.1109/TSMC.2017.2705582
125. Identification of ECG Arrhythmias Using Phase Space Reconstruction | Proceedings of the 5th European Conference on Principles of Data Mining and Knowledge Discovery. Accessed June 14, 2021. <https://dl.acm.org/doi/10.5555/645805.670008>
126. Rocha T, Paredes S, de Carvalho P, Henriques J, Antunes M. Phase space reconstruction approach for ventricular arrhythmias characterization. In: *Proceedings of the 30th Annual International Conference of the IEEE Engineering in Medicine and Biology Society, EMBS'08 - "Personalized Healthcare through Technology."* Vol 2008. IEEE Computer Society; 2008:5470-5473. doi:10.1109/iembs.2008.4650452
127. Classification methodology of CVD with localized feature analysis using Phase Space Reconstruction targeting personalized remote health monitoring | IEEE Conference Publication | IEEE Xplore. Accessed June 14, 2021. <https://ieeexplore.ieee.org/abstract/document/7868773>

128. Vemishetty N, Gunukula RL, Acharyya A, Puddu PE, Das S, Maharatna K. Phase Space Reconstruction Based CVD Classifier Using Localized Features. *Sci Rep.* 2019;9(1):1-18. doi:10.1038/s41598-019-51061-8
129. Zhang J, Liu A, Gao M, Chen X, Zhang X, Chen X. ECG-based multi-class arrhythmia detection using spatio-temporal attention-based convolutional recurrent neural network. *Artif Intell Med.* 2020;106. doi:10.1016/j.artmed.2020.101856
130. Lih OS, Jahmunah V, San TR, et al. Comprehensive electrocardiographic diagnosis based on deep learning. *Artif Intell Med.* 2020;103. doi:10.1016/j.artmed.2019.101789
131. Cho Y, Kwon J myoung, Kim KH, et al. Artificial intelligence algorithm for detecting myocardial infarction using six-lead electrocardiography. *Scientific Reports 2020 10:1.* 2020;10(1):1-10. doi:10.1038/s41598-020-77599-6
132. Jo YY, Cho Y, Lee SY, et al. Explainable artificial intelligence to detect atrial fibrillation using electrocardiogram. *Int J Cardiol.* 2021;328:104-110. doi:10.1016/J.IJCARD.2020.11.053
133. Zhu H, Cheng C, Yin H, et al. Automatic multilabel electrocardiogram diagnosis of heart rhythm or conduction abnormalities with deep learning: a cohort study. *Lancet Digit Health.* 2020;2(7):e348-e357. doi:10.1016/S2589-7500(20)30107-2
134. Wiles BM, Morgan JM, Allavattam V, ElRefai M, Roberts PR. S-ICD screening revisited: do passing vectors sometimes fail? *Pacing and Clinical Electrophysiology.* Published online December 26, 2021. doi:10.1111/PACE.14424
135. Dunn AJ, ElRefai MH, Roberts PR, Coniglio S, Wiles BM, Zemkoho AB. Deep learning methods for screening patients' S-ICD implantation eligibility. *Artif Intell Med.* 2021;119:102139. doi:10.1016/J.ARTMED.2021.102139
136. Daubert JP, Zareba W, Cannom DS, et al. Inappropriate implantable cardioverter-defibrillator shocks in MADIT II: frequency, mechanisms, predictors, and survival impact. *J Am Coll Cardiol.* 2008;51(14):1357-1365. doi:10.1016/J.JACC.2007.09.073
137. Rocha T, Paredes S, de Carvalho P, Henriques J, Antunes M. Phase space reconstruction approach for ventricular arrhythmias characterization. *Proceedings of the 30th Annual International Conference of the IEEE Engineering in Medicine and Biology Society, EMBS'08 - "Personalized Healthcare through Technology."* Published online 2008:5470-5473. doi:10.1109/IEMBS.2008.4650452

138. Lee JW, Kim KS, Lee B, Lee B, Lee MH. A real time QRS detection using delay-coordinate mapping for the microcontroller implementation. *Ann Biomed Eng.* 2002;30(9):1140-1151. doi:10.1114/1.1523030
139. Hauser RG, Hayes DL, Kallinen LM, et al. Clinical experience with pacemaker pulse generators and transvenous leads: An 8-year prospective multicenter study. *Heart Rhythm.* 2007;4(2):154-160. doi:10.1016/j.hrthm.2006.10.009
140. Kirkfeldt RE, Johansen JB, Nohr EA, Jorgensen OD, Nielsen JC. Complications after cardiac implantable electronic device implantations: An analysis of a complete, nationwide cohort in Denmark. *Eur Heart J.* 2014;35(18):1186-1194. doi:10.1093/eurheartj/eh511
141. Udo EO, Zuithoff NPA, Van Hemel NM, et al. Incidence and predictors of short- and long-term complications in pacemaker therapy: The FOLLOWPACE study. *Heart Rhythm.* 2012;9(5):728-735. doi:10.1016/j.hrthm.2011.12.014
142. El-Chami MF, Clementy N, Garweg C, et al. Leadless Pacemaker Implantation in Hemodialysis Patients: Experience With the Micra Transcatheter Pacemaker. *JACC Clin Electrophysiol.* 2019;5(2):162-170. doi:10.1016/j.jacep.2018.12.008
143. Rordorf R, Savastano S, Bontempi L, et al. Leadless pacing in cardiac transplant recipients: Primary results of a multicenter case experience. *J Electrocardiol.* 2020;60:33-35. doi:10.1016/j.jelectrocard.2020.03.010
144. Reynolds D, Duray GZ, Omar R, et al. A Leadless Intracardiac Transcatheter Pacing System. *New England Journal of Medicine.* 2016;374(6):533-541. doi:10.1056/nejmoa1511643
145. El-Chami MF, Al-Samadi F, Clementy N, et al. Updated performance of the Micra transcatheter pacemaker in the real-world setting: A comparison to the investigational study and a transvenous historical control. *Heart Rhythm.* 2018;15(12):1800-1807. doi:10.1016/j.hrthm.2018.08.005
146. Roberts PR, Clementy N, al Samadi F, et al. A leadless pacemaker in the real-world setting: The Micra Transcatheter Pacing System Post-Approval Registry. *Heart Rhythm.* 2017;14(9):1375-1379. doi:10.1016/j.hrthm.2017.05.017
147. Pang BJ, Joshi SB, Lui EH, et al. Validation of conventional fluoroscopic and ecg criteria for right ventricular pacemaker lead position using cardiac computed tomography. *PACE - Pacing and Clinical Electrophysiology.* 2014;37(4):495-504. doi:10.1111/pace.12301

148. Reynolds D, Duray GZ, Omar R, et al. A Leadless Intracardiac Transcatheter Pacing System. *New England Journal of Medicine*. 2016;374(6):533-541. doi:10.1056/nejmoa1511643
149. Garweg C, Vandenberk B, Foulon S, Haemers P, Ector J, Willems R. Leadless pacing with Micra TPS: A comparison between right ventricular outflow tract, mid-septal, and apical implant sites. *J Cardiovasc Electrophysiol*. 2019;30(10):2002-2011. doi:10.1111/jce.14083
150. Bongiorno MG, della Tommasina V, Barletta V, et al. Feasibility and long-term effectiveness of a non-apical Micra pacemaker implantation in a referral centre for lead extraction. *Europace*. 2019;21(1):114-120. doi:10.1093/europace/euy116
151. Hauser RG, Hayes DL, Kallinen LM, et al. Clinical experience with pacemaker pulse generators and transvenous leads: an 8-year prospective multicenter study. *Heart Rhythm*. 2007;4(2):154-160. doi:10.1016/J.HRTHM.2006.10.009
152. Udo EO, Zuithoff NPA, van Hemel NM, et al. Incidence and predictors of short- and long-term complications in pacemaker therapy: the FOLLOWPACE study. *Heart Rhythm*. 2012;9(5):728-735. doi:10.1016/J.HRTHM.2011.12.014
153. El-Chami MF, Al-Samadi F, Clementy N, et al. Updated performance of the Micra transcatheter pacemaker in the real-world setting: A comparison to the investigational study and a transvenous historical control. *Heart Rhythm*. 2018;15(12):1800-1807. doi:10.1016/J.HRTHM.2018.08.005
154. Mondésert B, Dubuc M, Khairy P, Guerra PG, Gosselin G, Thibault B. Combination of a leadless pacemaker and subcutaneous defibrillator: First in-human report. *HeartRhythm Case Rep*. 2015;1(6):469-471. doi:10.1016/J.HRCR.2015.07.009
155. Ng JB, Chua K, Teo WS. Simultaneous leadless pacemaker and subcutaneous implantable cardioverter-defibrillator implantation—When vascular options have run out. *J Arrhythm*. 2019;35(1):136. doi:10.1002/JOA3.12140
156. Roberts PR, Clementy N, Samadi F al, et al. A leadless pacemaker in the real-world setting: The Micra Transcatheter Pacing System Post-Approval Registry. *Heart Rhythm*. 2017;14(9):1375-1379. doi:10.1016/J.HRTHM.2017.05.017
157. Randles DA, Hawkins NM, Shaw M, Patwala AY, Pettit SJ, Wright DJ. How many patients fulfil the surface electrocardiogram criteria for subcutaneous implantable cardioverter-defibrillator implantation? *EP Europace*. 2014;16(7):1015-1021. doi:10.1093/EUROPACE/EUT370

158. Bongiorno MG, della Tommasina V, Barletta V, et al. Feasibility and long-term effectiveness of a non-apical Micra pacemaker implantation in a referral centre for lead extraction. *EP Europace*. 2019;21(1):114-120. doi:10.1093/EUROPACE/EUY116
159. Garweg C, Vandenberg B, Foulon S, Haemers P, Ector J, Willems R. Leadless pacing with Micra TPS: A comparison between right ventricular outflow tract, mid-septal, and apical implant sites. *J Cardiovasc Electrophysiol*. 2019;30(10):2002-2011. doi:10.1111/JCE.14083